University of Nottingham

UK | CHINA | MALAYSIA

FORMULATION SYSTEM WITH ENHANCED PERFORMANCE VIA PARTICLE AGGLOMERATION FOR DRY POWDER INHALATION

Thesis submitted to the University of Nottingham for the degree of Doctor of Philosophy, July 2024.

Qingzhen Zhang

Student ID：20415966

Supervised by

First Supervisor: Philip Hall

Second Supervisor: Zheng Wang

Third Supervisor: Jason Li

Signature: Qingzhen Zhang

Date: July 29, 2024

Formulation system with enhanced performance via particle agglomeration for dry powder inhalation

Abstract

Dry powder inhalation (DPI) offers a valuable method for delivering medication directly to the lungs for respiratory diseases. Compared to oral administration, DPIs provide a faster onset of action due to targeted delivery and achieve higher drug concentrations within the lungs while minimising systemic exposure. Carrier-based DPIs, the most prevalent formulation type, often exhibit a limited fine-particle fraction (FPF), hindering their effectiveness. Spherical agglomerate formulations present a promising solution. These agglomerates, formed by the cohesiveness of micronised drug particles and a small amount of fine lactose, possess improved flowability compared with micronised powders. Additionally, their pellet-like morphology facilitates disintegration into primary particles during inhalation, owing to their lower mechanical strength.

This thesis delves into strategies to enhance the aerodynamic performance of DPIs through particle agglomeration. Following a foundational overview of DPIs and their working principles, this study explored the critical relationship between device design, formulation characteristics, and characterisation methods to achieve optimal performance. A comprehensive review examined the various strategies employed to improve aerosol performance using particle agglomeration. By elucidating the mechanisms underlying these strategies, this thesis aims to contribute to the development of more effective DPI formulations for targeted pulmonary drug delivery.

Acknowledgments

I would like to express my sincere gratitude to my supervisor, Prof. Zheng Wang, for his invaluable guidance and mentorship during this research project. His willingness to share his expertise and constant encouragement were instrumental in the successful completion of this work.

I am also grateful to Prof. Philip Hall and Dr. Jason Li for their insightful advice and support during my research. Their contributions significantly enhanced the project quality.

My appreciation extends to Dr. Kaiqi Shi for his continued support and helpful suggestions throughout my study.

Finally, I would like to express my deepest gratitude to my family for their unwavering love and encouragement. Their constant support has been a source of immense strength and inspiration throughout my academic journey.

Content

List of Tables

List of Figures

Abbreviations

ACN	Acetonitrile
API	Active pharmaceutical ingredient
BET	Brunauer Emmett Teller
COPD	Chronic obstructive pulmonary disease
DPI	Dry powder inhaler
DSC	Differential scanning calorimetry
DVS	Dynamic vapor sorption
ED	Emitted dose
FPD	Fine particle dose
FPF	Fine particle fraction
HPLC	High pressure liquid chromatography
IGC	Inverse Gas chromatography
MgSt	Magnesium stearate
NGI	Next generation pharmaceutical impactor
Ph. Eur.	European pharmacopoeia
PSD	Particle size distribution
q3	Volume based size distribution
RD	Relative deagglomeration
RH	Relative humidity
rpm	Rounds per minute
RSD	Relative standard deviation
SD	Standard deviation
UV	Ultraviolet

XRPD	X-ray powder diffraction
$\Delta m/\Delta t$	Mass change per time change

Chapter 1: INTRODUCTION

Pulmonary drug delivery has demonstrated significant potential for treating both localized lung infections and systemic diseases. To achieve optimal therapeutic effects, drug particles must possess an aerodynamic diameter within the 1-5 µm range to successfully navigate the lung's conducting airways and reach the target respiratory region. However, the inherent cohesiveness and adhesiveness of these fine particles often impede efficient aerosol formation. A common strategy to address this challenge involves blending micronized drug particles with larger carrier particles, typically comprising 98.5% of the formulation by weight. This approach enhances powder flowability and facilitates dispersion during inhalation.

The expanded use of Dry Powder Inhalers (DPIs) in the treatment of lung infections and systematic disease has led to the development of new techniques for high-efficiency of delivery and deposition. However high doses with higher carrier amounts would result in an increased powder volume that is inconveniently bulky for multidose inhalers and may result in several adverse effects as throat irritation and coughing. Formulation system via particle agglomeration is a suitable technique to produce good flowing agglomerates which are not only stable enough to allow handling and dosing but also are soft enough to be deagglomerated and get dispersed during inhalation utilising a suitable inhaler, such as Turbuhaler®.

In this study, we propose to produce engineered agglomerates with micronized API and fine lactose as binder excipients in the Turbuhaler to disperse drug particles while maintaining the internal resistance at a medium level (typically 4Kpa). The advances in agglomerate formulation systems will open an opportunity for the formulation and delivery of more complex and labile drugs like biopharmaceuticals in the future pharmaceutical industry.

The central objective of the research is to improve the dose delivery and lung deposition efficiency by properly designing and characterizing an agglomerate

formulation, fabricating a set of preparation apparatuses, and investigating the interactive mechanism between active pharmaceutical ingredients and fine lactose.

The structure of this thesis is listed as follows:

Chapter 1 Introduction and Objectives

This chapter introduces the general research aim and potential result.

Chapter 2 Literature review

This chapter reviews the related literature on fine particle agglomeration research including the background, mechanism of agglomerate formation and deagglomeration, and recent advancement in fine particle agglomeration and preparation methods.

Chapter 3 Methodology

This chapter describes the materials used in the research. Characterisation techniques for sample and agglomerate, as well as performance evaluation approaches for prepared agglomerate formulation are discussed.

Chapter 4: Formulation Study of fine lactose attributes for particle agglomeration via vibration

Preparation of fine lactose is essential to ensure agglomerate formulation suitable for various dose strengths and facilitate dosing and deagglomeration. Fine lactose powder with favourable aerodynamic properties is featured with a narrow size range, suitable cohesion attributes and particle shape factors. This brings challenges to the fine lactose powder preparation process.

In this work, the fluidized bed opposed jet mill was operated with controlled milling pressure, loading speed and the classifier speed to produce micronized particles with uniform particle shapes and narrow. The inhaled fine lactose particles were fluidized and suspended by up-flowing gas with well-controlled humidity and temperature for re-crystallization of amorphous surface to reduce

powder adhesion and cohesion.

Dry powder inhalers (DPI) agglomerate formulations were prepared by mixing the micronized budesonide and melatonin particles with fine lactose particles and characterized using Next Generation Impactor (NGI) to develop an initial “road map” to provide more information for pharmaceutical industry.

Chapter 5: Study of mixing effect on drug Adhesion and Dispersion for particle agglomeration

In this chapter, air jet mixing and high shear mixing method were used to obtain homogeneous mixture prior to agglomeration, the candidate compounds of budesonide and melatonin were used in the study.

For high shear mixing, the high mixing speed would input sufficient energy to break down the cohesive aggregate in the mixture, the blades in the mixer would help to distribute the API and fine lactose to achieve uniformity. The mixing speed and mixing time were studied to investigate the effect on homogeneity and agglomerate formulation aerodynamic behaviour.

For air jet mixing, a compressed air is used in this process to accelerate the particles speed and leads to particles-particles and particles instrument wall collisions and impactions, which in turns lead to the breakage of the cohesive aggregate into to a smaller size. After the dispersion of the aggregate, the cohesive fine particles would be uniformly mixed. The effect of inlet air pressure, feeding pressure and feeding speed were studied on the content uniformity and the attributes of final agglomerate formulation were studied.

Chapter 6: Continuous particle agglomeration via vibration and mechanical dry coating technique for enhanced aerodynamic performance

Vibration technique were applied and optimized for particle agglomeration to enhance the aerodynamic performance. The production of agglomerate formulation of budesonide and melatonin were carried out with ultrasonic vibration and resonant acoustic mixing, respectively.

Compared to the established standard procedure in chapter 4, these methods offer the advantage of being a continuous process with improved fine particle delivery efficiency. The influence of production parameters such as ultrasonic power, vibration intensity for pre-agglomeration with acoustic mixer, as well as the mechanical dry coating on formulation morphology and the aerodynamic behaviour of the produced spherical agglomerates are also discussed.

Chapter 7: General conclusion and future work

This chapter will summarize the key findings from this work and propose directions of future work.

.

Chapter 2 Literature Review

2.1 Introduction

Dry powder inhalation (DPI) effectively delivers pharmaceutical components in aerosol form to treat respiratory diseases (Ivanova et al., 2013). Compared to the oral dose form, DPI is characterised by rapid action and empowers higher drug concentrations only in the lung tissue because lungs served as action site with large surface area, abundant blood supply, high permeability, low enzymatic activity and ability to avoid first-pass metabolism(Shahin and Chablani, 2023). Carrier-based DPI is the most widely used formulation consisting of large carrier particles and micro-sized drugs. However, the fine particle fraction (FPF) of carrier-based DPI formulations can only achieve 20-30% (Benke et al., 2020). The particle agglomerate formulation system takes advantage of the cohesiveness of micronized drug particles and fine lactose to enable a higher dosing amount, which provides an alternative solution to realize a higher FPF. Soft agglomerates have a morphological appearance of pellets with improved flowability compared to the micronized powders themselves; they can easily disintegrate into primary particles owing to their lower mechanical strength during inhalation and can achieve an FPF of up to 50%(Hoe et al., 2011).

To obtain an in-depth understanding of how to enhance the aerodynamic performance of DPI via particle agglomeration, literature related to strategies to enhance aerosol performance via particle agglomeration is reviewed. The following sections begin with general information on dry powder inhalation and its working principle, followed by the formulation design, characterisation methods, and mechanism behind the improvement.

- **General principles of DPIs:** This section will explain how DPIs work, focusing on the importance of particle size and inhalation airflow in delivering medication to the lungs.
- **Formulation design for agglomeration:** We'll explore how to design DPI formulations that encourage the formation of beneficial agglomerates,

optimizing particle size distribution and interactions between drug and carrier particles.

- **Characterization methods for agglomerates:** Techniques to analyze the size, morphology, and stability of these agglomerates will be discussed, ensuring their suitability for efficient drug delivery.
- **Mechanisms of performance improvement:** This section will specifically address how particle agglomeration impacts the deposition of medication in the desired regions of the lungs. We'll explore mechanisms such as improved de-aggregation upon inhalation, increased inertial impaction, and reduced excipient influence.

2.1 Dry powder inhalation Delivery

2.1.1 Deposition of drug particles in the respiratory tract

The human respiratory system consists of two main sections: conducting and respiratory zones (Patwa and Shah, 2015). The conducting zone includes the upper airways, from the trachea to the terminal bronchioles and mucociliary clearance (MCC). As shown in Figure 2.1, the respiratory zone, comprising the respiratory bronchioles, alveolar ducts, and alveoli, can provide rapid gaseous exchange (Bustamante-Marin and Ostrowski, 2017). Particles deposited in conducting airways will be removed using MCC (Agnew et al., 1986). Controlling particle deposition in the targeted region for inhaled drug delivery is a challenging task for DPIs. The deposition pattern within the respiratory tract determines the efficacy of inhaled therapy (Labiris and Dolovich, 2003).

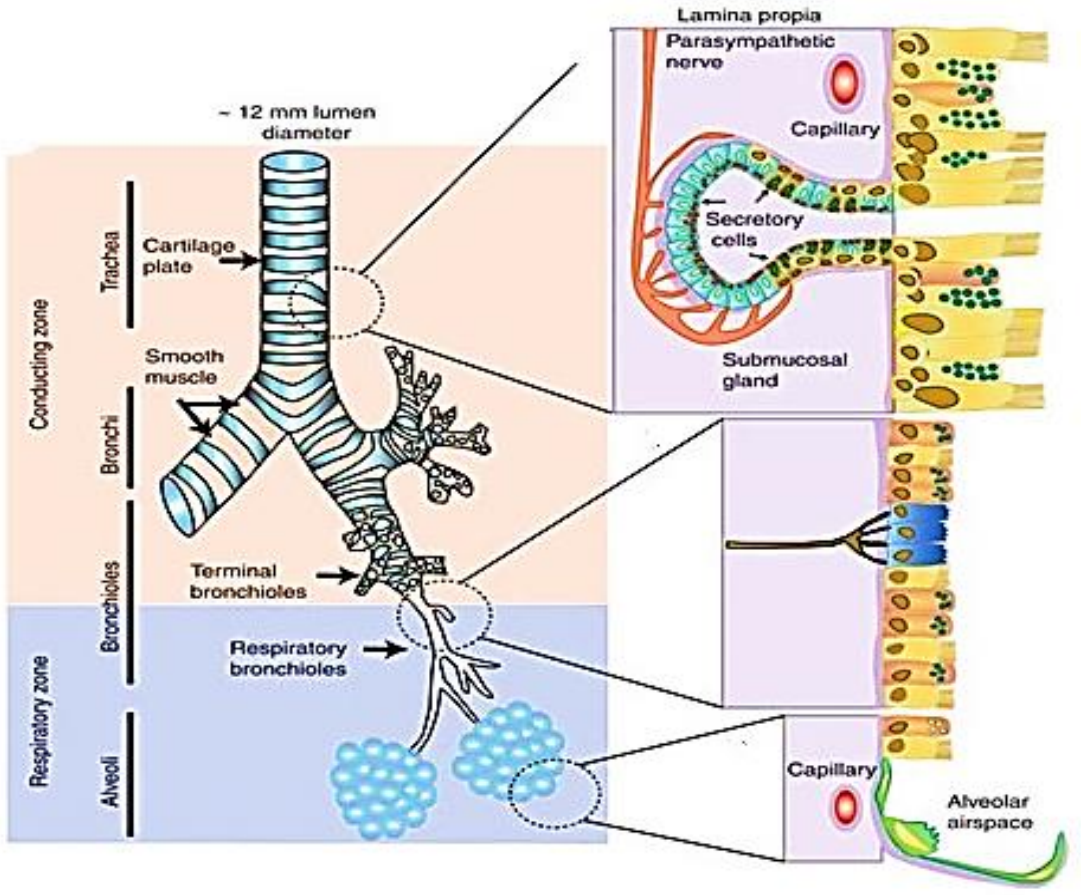

Figure 2. 1 Schematic representation of the airway epithelium(Bustamante-Marin and Ostrowski, 2017)

Aerodynamic Diameter (d_{ae}) represents the deposition pattern of drug particles in the lungs. This was related to the four parameters defined in Equation. (1), and can be defined as the diameter of a spherical particle with a unit density that reaches the same falling speed (Hassan and Lau, 2010):

$$d_{ae} = d_g\sqrt{\rho_p / \rho_0 x} \qquad \text{Equation. (1)}$$

where dae is the aerodynamic diameter (μm),

d_g represents the cut-off particle diameter (μm),

ρ_p and ρ_0 indicate the true density of the particle and the air(g/cm^3), respectively,

x represents the shape factor which can be expressed as the ratio of the drag force of an inhaled particle to the drag force of an equivalent volume of spherical particles (typically in the range 1 to 2).(Hassan and Lau, 2009)

The particle deposition mechanism in the conducting and lower respiratory zones is illustrated in Figure 2.2 The particle deposition pattern is dominated by inertial impaction, sedimentation, and Brownian diffusion.

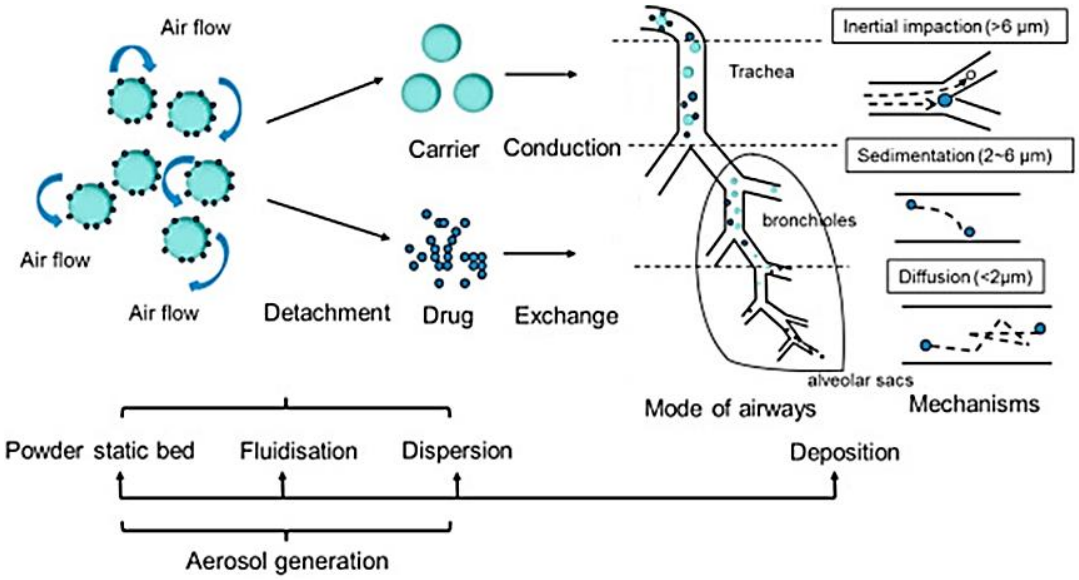

Figure 2. 2 Mechanism of aerosol particle separation in the respiratory tract (Peng et al., 2016)

- **Inertial impaction**: Particle sizes more than 6μm, they would impact the airway walls and make it difficult to change motion with airflow. Inertial impaction dominates when particle size increases (Jaafar-Maalej et al., 2009).
- **Sedimentation**: For smaller articles(2~6μm) that require longer retention times to result in clinical effects, sedimentation as the deposition manner plays an important role in the upper airways (a natural passage for air to enter and exit the lungs).
- This principle has a significant effect on clinical trials. When taking an inhalation product, have a deep breath and hold for a few seconds would enhance the particle residence period and increase deposition (Tsuda et al., 2013).
- **Diffusion:** Brownian motion is important for small particle (<2 μm) deposition and occurs in small airways where airflow is negligible(Lee et al., 2009).

Different clearance mechanisms in each section of the respiratory system dominate the particle positioning and retention time of particles in dry powder formulations. Deposition patterns within the respiratory tract can be strategically utilized to achieve different desired clinical effects in inhaled therapies.

Targeting Specific Regions:

- **Lower Respiratory Tract (LRT) Targeting:** For diseases affecting the lower airways, such as asthma and COPD (Chronic Obstructive Pulmonary Disease), the goal is to deliver medication to the bronchiolar and alveolar regions(Zhang et al., 2023). Particles sized between 2-5 μm are ideal for this purpose. These particles can reach the target site where they can interact with the inflamed or diseased tissues, leading to bronchodilation (relaxation of airways), reduced inflammation, or other therapeutic effects.
- **Upper Respiratory Tract (URT) Targeting:** For localized conditions like allergic rhinitis (hay fever) or laryngitis, medication needs to reach the upper airways (ET and TB regions). Here, larger particles (around 5-10 μm) can be beneficial(Ortigoza et al., 2023). They deposit in the nasal cavity, throat, and larger airways, providing a localized effect to address symptoms like congestion, runny nose, or irritation.

Controlled Release:

- **Rapid Onset of Action:** For conditions requiring immediate relief, such as acute asthma attacks, medications formulated with larger, porous particles can be used(Wegener et al., 1992). These particles deposit in the upper airways where they dissolve quickly, leading to a rapid onset of action (within minutes).
- **Sustained Release:** For chronic conditions requiring long-lasting medication delivery, controlled-release formulations can be employed. These formulations may use biodegradable carriers or other techniques to slowly release the drug over an extended period (hours or even days) after deposition in the lower airways(Pulivendala et al., 2020).

Deposition patterns are a crucial consideration in inhaled therapy design. By

strategically manipulating particle size and formulation, we can achieve targeted drug delivery to specific regions within the respiratory tract. This allows for optimized treatment of various respiratory conditions, maximizing therapeutic benefits while minimizing side effects. Therefore, the desired clinical effects can be achieved using different deposition patterns.

2.1.2 The application of dry powder respiratory delivery

Pulmonary drug delivery is a successful method of lung therapy, particularly in patients with obstructive pulmonary disease (A.L. Adjei, 1996a). Furthermore, it has shown great potential for the treatment of local lung infections and systemic diseases (Lavorini et al., 2017). DPI has the advantage of being low-cost and easy to operate, with superior formulation stability over solutions or suspensions (Todo et al., 2001).

DPI contains a powder formulation and works with a device that is normally composed of micronised drugs (<5 μm in diameter) and a larger carrier lactose(range from 30-90 to μm) (Zeng et al., 2000b, Kaialy et al., 2011b). The drug particles are dispersed by the patient's breath through the device, as shown in Figure. 2.3. The formulation is typically either manually filled in a capsule or pre-packed in a reservoir-based device (Qualicaps, 2016). The patient takes a deep breathing-in action and holds breath for 5-10 seconds after putting the mouthpiece into their mouth to ensure the medication reaches the lung. Inhaled drug particles with different aerodynamic particle sizes will deposit in different regions of the respiratory tract. A single inhalation can deliver a dose typically of less than tens or hundreds of milligrams.

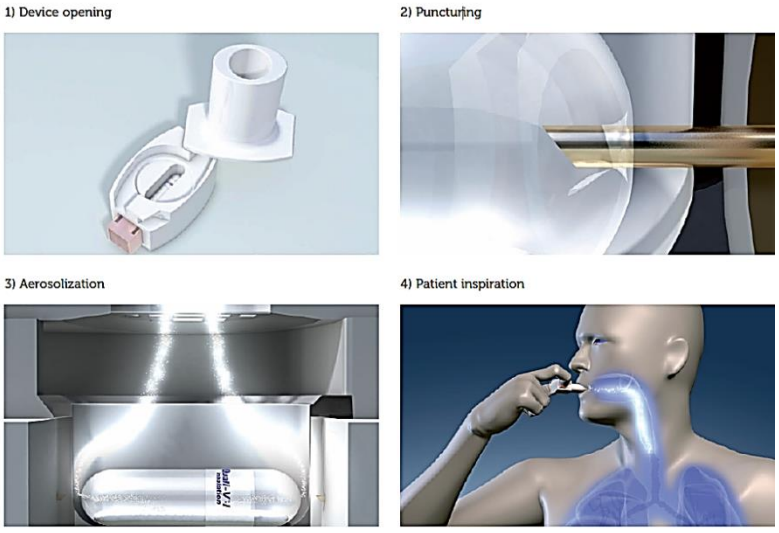

Figure 2. 3 Principle of the dry powder inhalation (DPI) operation (Qualicaps, 2016).

The extended use of DPI for systematic disease has accelerated the research and development of new techniques for enhanced aerosol performance and high-dose loading respiratory drug delivery. However, high drug doses with corresponding carrier amounts would result in an increased powder volume, which is inconvenient to manufacture and may lead to adverse effects such as throat irritation and coughing (Son YJ, 2021b).

To solve these problems, engineered particles or novel formulations and devices with fewer carriers or additives, such as lactose or magnesium stearate combined with the designed device, have been studied to introduce more effective turbulent flow and collision to disperse drug particles while maintaining internal resistance at a medium level. (Kaialy and Nokhodchi, 2013)

2.1.3 Formulation approach for dry powder inhalation

2.1.3.1 Carrier based dry powder inhalation

To ensure the delivery of particles to the central and peripheral pulmonary regions, the aerodynamic diameter of the particles must be between 1 and 5 μm (He and Novosselov, 2017). However, fine particles tend to stick together (due to cohesion force) or to any surface (due to adhesion force) and can easily form agglomerations due to high surface energy; therefore, it is challenging to handle when administered to patients and may exhibit poor de-agglomeration properties. The conventional application of coarse particles as carriers to deliver fine drug

particles is widely used to form ordered mixtures with micronised drug particles (Fig. 2.4). The carrier particles enhance flowability and result in reproducible dose metering (Fussell et al., 2014).

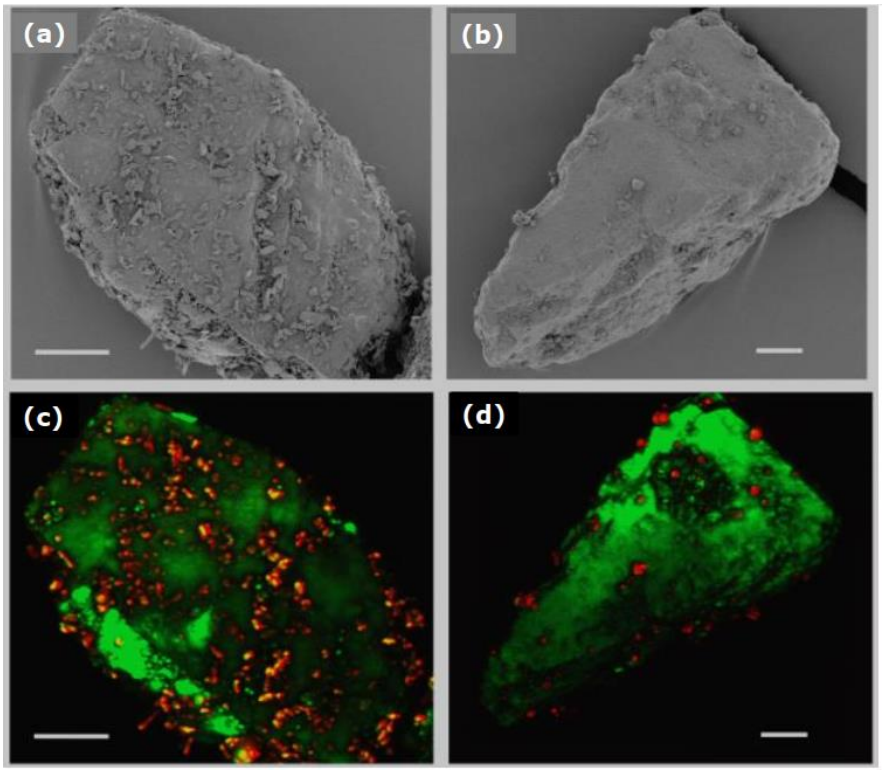

Figure 2. 4 Typical Scanning electron microscopy (SEM) images (a,b) and anti-Stokes scattering microscopy images (red dots represent API) and (green part represent lactose carrier) (c,d)(Fussell et al., 2014)

The dispersion mechanism for carrier-based inhalation formulations can be illustrated by the following process: a) powder fluidisation in the airflow, b) primary drug particles detached, and c) agglomerates dispersed into individual pharmaceutical particles. Particles within the range of 1-5 μm were deposited in the lungs, and larger particles were deposited in the mouth or/and throat (see Figure.2.5). The cohesive/adhesive and expelling forces resulting from the inhaled airflow dominate the extent of dispersion. (Grasmeijer et al., 2015)

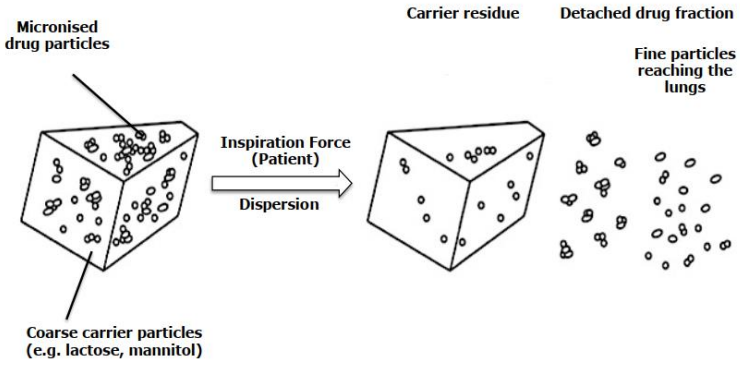

Figure 2. 5 Schematic of DPI adhesive mixtures.

The cohesive and adhesive forces should be kept balanced between the lactose carrier and drug to facilitate aerosolisation. Atomic Force Microscope (AFM) is usually used to detect the cohesive-adhesive balance (CAB) between particles (Weiss, 2015). Factors that influence aerosolisation include the carrier size distribution, carrier surface morphology, and physicochemical properties of both the drug and carrier particles.

As a few micro-grams administration was sufficient for the treatment of asthma and COPD due to highly potent APIs, the addition of coarse carrier particles dilutes these APIs and optimizes flowability and deagglomeration However for higher dose delivery and fine particle deposition efficiency requirements with systematic disease, higher carrier amount would result in an increased powder volume that is inconvenient to meter and decrease the fine particle deposition and may result in several adverse effects as throat irritation and coughing(Son YJ, 2021a).

Carrier-based formulations are primarily suited for low-dose drug delivery due to their inherent limitations in drug loading capacity. Typical drug-to-carrier ratios of 1:67.5 to 1:99, as reported by Guenette et al. (2009), underscore this constraint. The physicochemical properties of the carrier, often lactose, significantly impact formulation performance. Optimal formulation necessitates a delicate balance between drug-carrier interactions and the dispersion forces generated during inhalation. Excessive drug-carrier adhesion can hinder drug detachment, resulting in suboptimal lung deposition, a recognized limitation of many DPIs (Smith and Parry-Billings, 2003).

2.1.3.2 Formulation systems via particle agglomeration

Formulation systems via particle agglomeration can be applied as an alternative way to solve the problem and are successfully employed in many commercial products such as the Turbuhaler® marketed by AstraZeneca but are not as commonly used as carrier-based formulation, the formation process and difference between carrier based dry powder inhalation is illustrated in Fig2.6. It can be used to formulate active ingredients alone or in combination with less lactose (Chan et al., 2014).

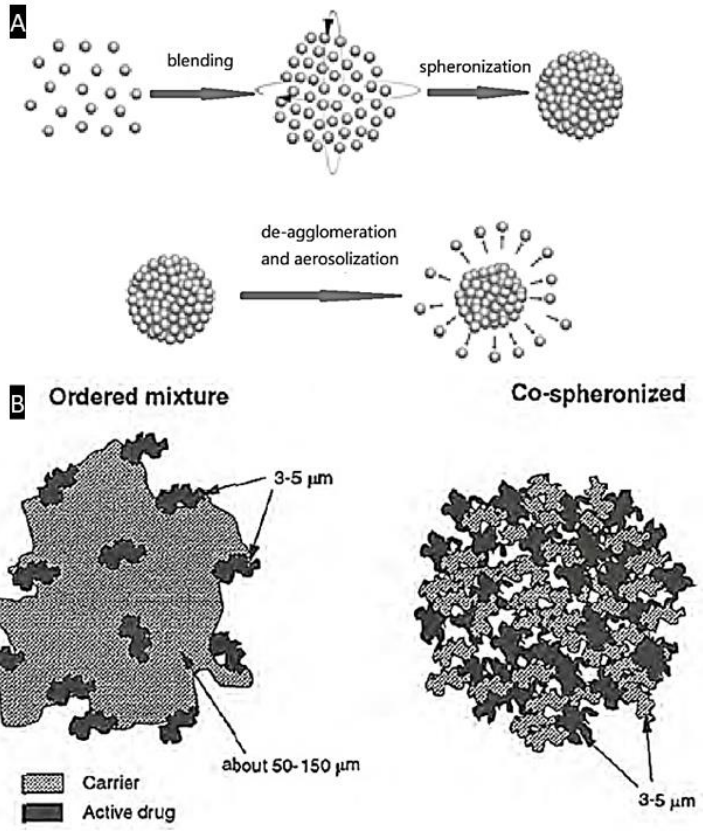

Figure 2. 6 Illustration of the formation of agglomerate and deagglomeration (A) and diagram of an ordered mixture of carrier-based and agglomerate formulation (B)(ZHENG, 2012)

Fine drug particles present significant formulation challenges due to their inherent physicochemical properties. Their low density, cohesiveness resulting from strong van der Waals forces, and tendency to agglomerate during storage and handling contribute to poor powder flowability(Kamranian Marnani et al., 2019). These characteristics complicate powder processing, metering, and

ultimately, efficient delivery to the respiratory tract. Agglomerate formation further exacerbates these issues, as they often exhibit larger particle sizes, hindering penetration into the bronchial region(Le et al., 2012). Precise metering of the desired drug dose is also compromised by the inconsistent size distribution of these agglomerates. To address these challenges, various techniques have been explored to improve powder flowability while maintaining suitable deagglomeration properties(Sahni et al., 2011). These include controlled agglomeration processes, such as vibration, agitation, or rolling, to produce agglomerates with desired characteristics for efficient inhalation(Dunst et al., 2018).

Agglomerates show good flowability compared to micronised powder during manufacturing because of their larger size and spherical shape. Interparticle interactions facilitate the cohesion of particles in the absence of binding agents. Mechanical interlocking and van der Waals forces dominate the agglomerates along with the capillary force. The cohesiveness increased when the primary particles were smaller. This is because the van der Waals forces linearly decrease with a reduced particle radius, but the gravitational forces decrease in proportion to the square of the particle radius. (Gonda, 2004)

For example, the commercial Pulmicort® contains budesonide with only fine lactose. Symbicort® contains formoterol fumarate and budesonide as active ingredients, with a small percentage of lactose. The formulation can be prepared using a controlled agglomeration procedure, including mixing and spheronization. The agglomerates are sufficiently stable for handling and metering during manufacture, at the same time soft enough to deagglomerate when inhaled by the patient. Agglomerates can be formed using only an active pharmaceutical ingredient (API) and fewer ingredients, which are suitable for high-dose inhalation products.

In this study, candidate compounds are formulated via particle agglomeration, and studies through Design of Experiments (DOE) and Principal Component Analysis (PCA) will be performed to investigate the factors and key parameters which influence the aerosol performance (such as fine particle fraction and

emitted dose uniformity) of the particle agglomeration system. In addition, an insight into the underlying relationship between in vitro characterisation and in vivo performance is expected.

2.2 Dry Powder Inhalation Devices

Devices combined with the formulation were designed to deliver pharmaceutical components that contribute to clinical effects via the lungs. Three generations of devices are available for DPI use (Fig.2.7).

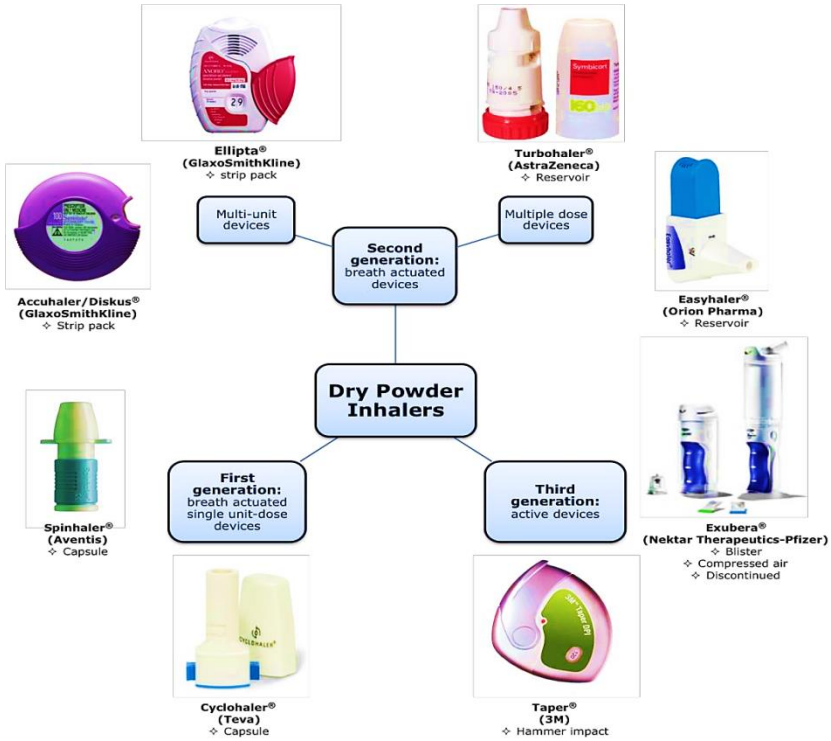

Figure 2. 7 Dry powder inhalation devices for different formulation types

First-generation devices are used for a single unit dose. The capsule is filled into the device before inhalation and the powder is aspirated and discarded after use. The Spinhaler® is an example of this category (Bundgaard et al., 1982) and is a DPI device designed for sodium cromoglicate inhalation products. The capsule is filled into the device before the patient operates the device by sliding a cam, and two needles penetrate through the capsule to release the mixture. The capsule spins and vibrates when the patient inhales through the mouthpiece, dispersing the powder into fine particles. New single unit-dose devices such as the HandiHaler® from Boehringer-Ingelheim and Aerolizer® from Novartis are commonly used in the market. Previously, hard gelatin capsules were popular,

but there was a risk of inhaled capsule fragments and poor capsule emptying owing to their fragile properties. Hydroxypropyl methylcellulose (HPMC) capsules have been widely used in this type of DPI because of their lower water content compared to gelatin capsules (Chong et al., 2016). Moreover, HPMC capsules tend to generate fewer fragments than gelatin capsules at extremely low relative humidity.

Second-generation devices include multiple-dose inhalation devices and multi-unit dose devices. The first type is dose metered in a reservoir that contains powder, known as reservoir-based devices. The second type of device pre-metered the dose using blisters or disks and disperse the individual doses.

Turbuhaler® (AstraZeneca) for the administration of formoterol and terbutaline is a popular type of multiple-dose DPIs in the market, and the formulation is formed by the cohesive force of the micronised drug and lactose particles (Haikarainen et al., 2017).Clickhaler® from Innovata Biomed, Easyhaler® from Orion Pharma, and Novolizer® from ASTA Medica are other commercially available reservoir devices. These devices have the advantage of minimising the flow dependence that occurs in Turbohaler®. For reservoir devices, such as Turbuhaler®, attention must be paid to avoid moisture, which can be achieved by including a desiccant and a protective cap.

Diskhaler® and Accuhaler/Diskus® are typically multi-unit DPI, the individual doses applied to blisters assembled on a disk. Upon actuation, the blister is pierced by a needle, and the powder is dispersed by airflow and detached from the carrier as the patient inhaled. Diskhaler® was replaced by Accuhaler/Diskus® in the late 1990s for a larger capacity. The newly designed Accuhaler/Diskus® has the advantage of holding 60 doses in a double-foil strip. Ellipta® (GlaxoSmithKline) is recently developed as a multi-unit device that can incorporate 30 doses and was easily operated for nearly all ages of patients. (Grant et al., 2015).

Third-generation devices employ energy from electrical or mechanical power, which enables force-independent respiratory dosing with precision and reproducibility(de Boer et al., 2017). Moreover, active devices can play an

important role in the delivery of systemic effects because they can deposit more pharmaceutical fine particles into the lungs.

2.3 Considerations on development of agglomerate formulation

2.3.1 Interparticle Interactions

When considering cohesive mixtures in agglomerate formulations, the study of the interactions between fine lactose and drug particles is of great importance for a good understanding of the processes that determine the performance of the agglomerate formulation. One of the most problematic aspects is the presence of interparticle forces that prevent disaggregation of the agglomerate formulation, thus compromising the efficiency of drug delivery into the lungs. These interparticle interactions result from both drug-drug particle cohesion and adhesion between the lactose-drug particles. As shown in Fig 2.8, there are mainly four types of interaction forces due to the physical and chemical properties of fine particles: (i): van der Waals forces (ii): electrostatic, (iii): capillary forces, (iv): specific (acid-base) interaction forces and hydrogen bonding(Hickey et al., 2007).

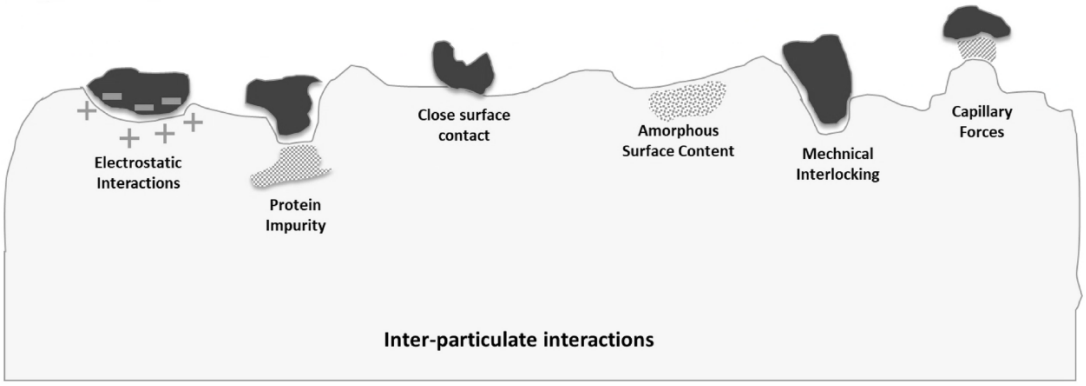

Figure 2. 8 Schematic of interparticle interactions between lactose-drug particles(Yang et al., 2023)

In agglomerate formulations, the similar size between a micronised drug particle and a lactose particle allows the consideration of their interaction (adhesion) as that between two individual particles. Van der Waals and electrical forces are proportional to the diameter of the micronised drug particles and fine lactose and vary with their distances and contact area. Capillary forces are affected by the

surface tension of the liquid between the particles(Pilcer et al., 2012).

Van der Waals forces are the predominant interparticle interactions influencing the cohesive properties of fine powders. These weak attractive forces, arising from transient fluctuations in electron distribution, are significantly affected by particle surface topography. Rougher surfaces with pronounced asperities can increase interparticle distance, thereby reducing the strength of these interactions(Gu et al., 2016).

Capillary forces contribute significantly to powder cohesion. These forces arise from the formation of liquid bridges due to adsorbed moisture at particle contact points. The intensity of capillary forces is influenced by both particle surface characteristics (e.g., roughness) and environmental humidity(Young et al., 2004).

Electrostatic interactions can be attractive or repulsive depending on whether they involve particles with opposite or the same charge. An electrostatic charge is a type of contact electrification produced by triboelectrification(Mort, 2003). Certain materials become charged after a brief collision or a strong frictional contact. Triboelectrification occurs primarily during manufacturing processes, such as mixing and handling, but it may also occur during the fluidization of the powder bed within the inhaler unit. Electrostatic interactions are related to the formation and maintenance of binder mixtures, separation of drug particles from carriers, and their deposition in the respiratory tract(Naik et al., 2016). In addition, they can be strongly affected by the relative humidity. During storage, high relative humidity conditions may lead to reduced electrostatic interactions because the formation of a water layer around the particles enhances the surface conductivity and facilitates the dissipation of charges. However, these conditions favor capillary coagulation and stronger capillary interactions(Ghori and Conway, 2018).

Amorphous drugs lack the crystalline structure of their counterparts. This altered structure can influence their surface properties and potentially lead to weak acid-base interactions. This can occur due to the presence of unpaired electrons or the arrangement of functional groups on the drug's surface.

The aforementioned adhesive and cohesive forces between particles pose

significant challenges to efficient aerosol generation. Ideally, the inhalational airflow should generate sufficient inertial, lift, drag, friction, and shear forces to overcome these interparticle attractions and facilitate drug particle detachment. However, the intricate and heterogeneous nature of powder systems renders the independent control of these individual forces highly complex.

2.3.2 Mechanical strength of agglomerate formulation

The dispersion performance of the agglomerate formulation depends dominantly on the agglomerate strength resulting from the strong van der Waals forces between fine particles (< 5μm). To improve the agglomerate formulation performance, a balance of agglomerate strength should be maintained to meet the manufacturing purpose and not hinder the dispersion of fine particles.

The mechanical strength of the agglomerate formulation can be predicted by the Kendall and Stainton theory using Equation (1) which is suggested to be the total interparticle bond strength across the fracture surface.

$$\sigma = 15.6\left(\frac{\varphi^4 w}{d}\right) \qquad (1)$$

where, d is the particle diameter, φ is the packing fraction (volume of particles/volume of aggregates) and W (J/m²) is the work of adhesion or cohesion of particles. In general, the deagglomeration of powders decreases as the strength of the agglomerates increases(Das et al., 2013). It is difficult to disperse agglomerates as the tensile strength increases. Controlling the particle size distribution, surface energy, and porosity of the agglomerate according to Rumpf model theory would contribute to a better balance between aerosol performance and mechanical strength. Investigations have been conducted to find the effect of physical characteristics (size and shape) of cohesive fine particles on agglomerate strength distributions in understanding de-agglomeration of cohesive materials.(Das et al., 2012) Strategies to decrease agglomerate strength relate to reducing packing fraction, work of cohesion and increasing the fine particle size. In previous study, the agglomerate strength changes with various lactose size and shape although cohesion force remained relatively constant between the powder samples.(Das et al., 2013)

However, cohesive powders consist of particles of varying sizes and a distribution of surface energies; therefore, the work of cohesion of powders is represented by a distribution(Das et al., 2011). The packing fraction also varies across the powder bed. As all three parameters–particle size, work of cohesion, and packing fraction–have distributions in real interactive powder systems, the tensile strength of a powder will have a distribution, and de-agglomeration will be related to tensile strength distributions rather than average values.

The size and shape parameters of the cohesive lactose and/or drug fraction significantly influence the structure of the powder bed, ultimately impacting deagglomeration behavior. For instance, the presence of a significant fraction of fine particles can increase interparticle forces and lead to the formation of dense, cohesive agglomerates. Conversely, a larger proportion of coarser particles may result in a more loosely packed powder bed with reduced interparticle interactions.

Furthermore, particle shape plays a critical role. Irregularly shaped particles can create complex packing arrangements, leading to variations in local void spaces and interparticle contact points within the powder bed. This heterogeneity in particle packing can significantly influence the flowability of the powder and the ease with which agglomerates can be deagglomerated.

Understanding these intricate relationships between particle size, shape, and powder bed structure is crucial for optimizing the design of DPI formulations. By carefully selecting excipients with appropriate size and shape characteristics, and by controlling the particle size distribution of the API, it is possible to engineer powder beds with improved flowability and deagglomeration properties, ultimately enhancing the delivery efficiency of the inhaled drug(Adi et al., 2011b).

2.4 Strategies to enhance aerosol performance for DPIs

Although the formulation of DPI seems simple, it is essential to consider technological and scientific challenges to enhance pulmonary deposition and delivery efficiency. Dry powder delivery to the lungs consists of two key steps:

powder fluidisation and deagglomeration (Fig. 2.9). Powder fluidisation (which often occurs in a device) is a process in which airflow mobilises the bulk powder to form a “fluid” gas with a loose agglomerate. Powder deagglomeration is a process by which agglomerates are dispersed into individual particles via inhalation.

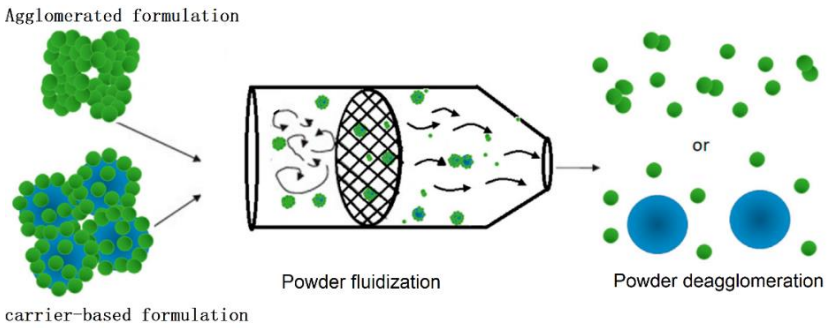

Figure 2. 9 Schematics of aerosol delivery mechanisms for dry powder inhalations (DPIs) (Zheng et al., 2021)

Efforts to improve energy translation and efficiency have focused on modifying or changing the physicochemical properties of both the API and excipient, application of novel formulation systems, and modifications in device design (Weers and Miller, 2015).

2.4.1 Modification of the API to enhance pulmonary deposition

The size of drug particles should be within 1-5μm to achieve efficient respiratory delivery. The conventional method for producing inhalable particles involves high-energy jet milling of a large crystalline starting material (Loh et al., 2015). However, high-energy input generates irregular particle morphologies and amorphous regions, as shown in Fig2.10. Such regions can be highly unstable and may result in spontaneous re-crystallisation in elevated humidity environments, where water vapour acts as a plasticiser to lower the glass transition of the material to ambient temperature (Fang et al., 2020).

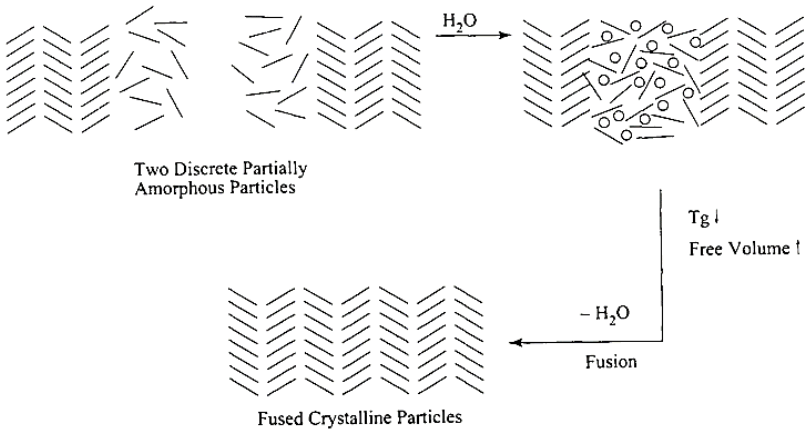

Figure 2. 10 Schematic of mechanically induced molecular surface damage (amorphous regions) and recrystallisation(Ward and Schultz, 1995b).

Owing to the large surface area of these micronised particles, the instability of the surface amorphous regions may lead to moisture-induced amorphous-to-crystalline conversion, which causes interparticle fusion and agglomeration of individual particles(Kulasinski et al., 2014). Previous particle size reduction efforts may be cancelled out, and the particle size distribution and particle deposition in the lungs will be greatly affected. Consequently, more attention has been paid to particle engineering to reduce surface instability and to develop a new method for the measurement of amorphous content at low levels in DPI products (Shah et al., 2006).

Several methods for preparing inhalable drug particles have improved the aerosol properties. Both antisolvent precipitation crystallisation and spray drying of drugs can yield APIs that meet the inhalable size range(Weers and Miller, 2015). The purpose of engineering the starting material is to change and improve its particle size, shape, crystallisation habits, density, porosity, and other properties (Mirza et al., 2009).

2.4.2 Modification of Lacoste to enhance aerodynamic performance

A series of approaches have been studied to achieve optimum performance characteristics of a DPI product from the lactose alteration aspect which mainly consists of altering the surface morphology, particle shape, and size. Efforts have been made to facilitate adequate flow (for processing and dosing) and excellent

deagglomeration attributes of dry powder formulations (Faulhammer et al., 2015). The morphology of the lactose has a great effect on efficient mixing and aerosolisation for DPI formulation because the adhesive force between the micron-sized API and fine lacoste should maintain a balance to ensure liberation (Mangal et al., 2019b). There are several approaches to improve drug aerosolisation during inhalation:(1) modifying or altering the particle roughness to decrease the contact area between the API and carrier (Peng et al., 2016) and (2) reducing the surface energy of the carrier surface (Tsuda and Venkata, 2016).

The roughness of the carrier surface can significantly affect the degree of interparticle adhesion and lead to changes in the drug delivery efficiency (Flament et al., 2004). Carrier surface roughness affects drug dispersion by the following forces: drag and lift force, shear and friction force, and inertial forces, to facilitate drug detachment (Fig 2.11).

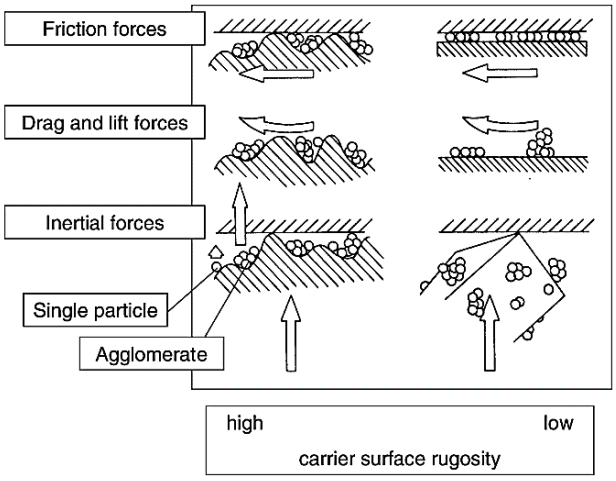

Figure 2. 11 Schematic of the separation forces regarding carrier surface roughness(de Boer et al., 2003)

In inhalation mixtures with relatively smooth surfaces of fine particles, drag and lift forces may play a dominant role in the separation aspect as drug particles slide or roll on the carrier surface before detachment (de Boer et al., 2003). When the roughness is equal to or larger than that of the drug particles, the inertial force has a more significant effect, and the drag and lift forces affect the motion of the particles in the surface crack.

Carrier shape modification is also a useful way of improving fine particle deposition; particle adhesion can be affected by different carrier shapes (Das et

al., 2013). Irregularly shaped particles have high adhesion properties owing to more interactions between the particles(Sarangi et al., 2021). The crystal shape can be modified by changing the recrystallisation solvent (Chen et al., 2008). Polar crystal faces absorb polar solvents and vice versa (Maghsoodi, 2015). The crystal morphology can be modified by predicting which axis the crystal will grow and by changing the solvent n accordingly.

Maghsoodi (2015) showed that lower ER carriers can produce a higher delivery efficiency. The force between the particles is inversely proportional to the distance between them, which in turn depends partly on the shape of the particles. The increase in the distance between particles caused by the change in particle shape reduces the force between particles, so that the drug can be better separated from the carrier and improve the aerosol performance.

2.4.3 Ternary component to improve aerosolisation performance

A strategy that has been frequently reported to have a positive effect on the aerosolisation performance of adhesive mixtures is the addition of fines (fine lactose particles of a similar size to that of the drug) to the formulation, thus obtaining a ternary mixture(Grasmeijer et al., 2014). Formulations containing an increased percentage of fines (to a certain extent) and/or fines with a reduced size generally resulted in improved FPFs. However, the presence of larger carrier particles remains essential, and excessive amounts of fines negatively affect powder flowability, mixing homogeneity, and long-term stability (especially under conditions of high RH)(Dahmash and Mohammed, 2015).

The addition of a ternary excipient can significantly improve powder dispersion based on the principle of “force control agents” to minimise the cohesive force (Begat et al., 2009a). This mechanism can be explained by two principal hypotheses: (1)The active-sites hypothesis suggested that high-energy sites on particle surfaces can be filled by fine particles, resulting in a lower energy status(Louey and Stewart, 2002). High-energy sites can be formed by the presence of amorphous regions from the micronization process or by different crystalline face orientations and other surface defects. (2) The agglomerate hypothesis proposed that the agglomerate structures of drug particles and

excipient fines formed by preparation are sufficiently loose and can deagglomerate easily compared to drug crystals alone(Grasmeijer et al., 2014). There is an obvious improvement in the fine particle fraction (FPF) to 73.72% and 71.87% for a carrier-based system with salbutamol sulphate crystals coated with force control agents (leucine and lecithin), respectively (Begat et al., 2005).

The agglomerate formulation system can also take advantage of this strategy to enhance aerosol performance. To ensure an agglomerate formulation for more compounds that require high-dose delivery or lower deposition in the mouth, co-milling or mixing with tertiary components as force control agents can be used to reduce inter-particle forces(Begat et al., 2009b). Lau et al. investigated the effect of adding magnesium stearate to the agglomerate formulation and found improved aerosol performance in beclomethasone dipropionate with an increased emitted dose from 71.3% to 84.5% containing 5% magnesium stearate (Lau et al., 2017b). The term of "dual excipient platform " was used to illustrate the application of force control agents in the formulation (Shur et al., 2016).

2.4.4 Improvement in Device Design

Device design characteristics can significantly influence the performance of the DPI product (Berkenfeld et al., 2015). The basic functions of the device are (1) facilitating operation by the patient and (2) providing a container for preparation (Chan et al., 2014).

There are previous reports on device design optimisation to improve the performance of the formulation, for example, airflow and aerosol generation modification by incorporating gauzes and meshes (Leung et al., 2016). A vortex-type assembling device(Vectura's Aspirair®) utilising a compressed air reservoir with a breath sensor was applied to aerosolise the powder (Tobyn et al., 2004). The modified device from Britannia Pharmaceuticals with a venturi powered by pressurised air or a CO_2 canister can deliver high dose (25–250 mg) formulations (Price R, 2004). Nektar's pulmonary inhaler, with a holding chamber to coordinate breathing, can facilitate powder aerosolisation and generate a standing aerosolised cloud via pressurised gas (Muchão and Silva Filho, 2010).

In addition, improved aerodynamic performance can be achieved by the aid of

computational fluid dynamics (CFD) for the optimisation of inhalation devices. Coates et al. studied the Aerolizer® systematically to improve aerosol performance through optimisation of the mouthpiece and internal grid (Coates et al., 2005). Chen et al.(Chen et al., 2013) modified the Seretide® Accuhaler (Glaxo Group Ltd.) device with a channel design. Zhou et al. used CFD-discrete element method (CFD-DEM) technology to simulate particle flow and particle agglomeration from a rotating capsule and proposed a scheme to modify the inlet size and mouthpiece length of the device, which significantly improved the FPF (Zhou et al., 2013b).

By addressing these challenges and employing a combination of these strategies, researchers can develop DPIs that offer superior pulmonary drug delivery efficiency and targeted medication deposition. This will ultimately lead to improved patient outcomes and a more effective approach to managing respiratory diseases.

2.4.5 Key comparisons and Considerations:

While the formulation of DPIs appears straightforward, optimizing pulmonary deposition and delivery efficiency presents significant challenges. Successful DPI delivery hinges on two critical steps: powder fluidization and deagglomeration. Fluidization, often facilitated within the device, involves the mobilization of the bulk powder by airflow, creating a "fluid" state. Deagglomeration, crucial for effective drug delivery, is the process of breaking down agglomerates into individual particles during inhalation.

Efforts to enhance DPI performance have focused on modifying the physicochemical properties of both the API and excipient, exploring novel formulation systems, and refining device design.

Compared to traditional high-energy jet milling, which often results in particles with irregular morphologies and a significant proportion of amorphous regions, advanced techniques offer several advantages as summarized in Table 2-1:

Table 2-1 Advantages and Disadvantages of particle production techniques

Technique	**Particle Size & Morphology**	**Crystallinity**	**Amorphous Content**	**FPF**	**Advantages**	**Disadvantages**
Jet Milling	Irregular, broad size distribution	High risk of amorphous phase formation	High	Moderate-to-low	High throughput, scalable	High energy input, potential for particle damage, limited control over particle properties
Antisolvent Precipitation	Narrow size distribution, spherical or near-spherical	High crystallinity	Low	High (e.g., 55% for budesonide(Adami et al., 2022)	Precise control over particle size and shape, minimizes amorphous phases	Potential for solvent residues, scalability challenges
Spray Drying	Controlled particle size and morphology (porous particles possible), narrow size distribution (e.g., GMD 2-4 µm) (Louey et al., 2004)	High crystallinity	Low	High (e.g., >50% for salbutamol(Louey et al., 2004)	Versatile, allows for encapsulation, can produce porous particles	Potential for particle aggregation during drying, may require optimization for heat-sensitive drugs

These advanced techniques can minimize the formation of amorphous regions, which are prone to moisture-induced recrystallization and subsequent particle agglomeration, leading to a more stable and predictable drug delivery.

Furthermore, optimizing excipient selection, employing surface modification techniques, and developing controlled agglomeration processes are crucial for improving powder flowability, deagglomeration, and overall formulation performance.

Finally, advancements in device design, such as optimizing airflow patterns and incorporating patient-centric features, are essential for maximizing drug delivery to the lungs.

In conclusion, a multi-faceted approach involving particle engineering, formulation optimization, and device innovation is necessary to overcome the challenges associated with DPI formulation and deliver effective and consistent pulmonary drug delivery.

2.5 Identifying Gaps in the Literature

Despite significant advancements in dry powder inhalation (DPI) formulations, several critical research gaps remain, particularly in the mechanistic understanding of agglomeration processes, comprehensive characterization of agglomerates, long-term stability assessment, clinical translation, and the standardization of characterization techniques, which collectively hinder the optimization and predictability of DPI performance for enhanced therapeutic outcomes.

Limited Focus on Mechanistic Understanding: While existing research has explored various agglomeration techniques, there is a lack of in-depth mechanistic understanding of how specific processing parameters (e.g., vibration frequency, amplitude, coating material) influence agglomerate formation and subsequent deagglomeration behavior.

Lack of Comprehensive Characterization: Many studies may not fully characterize the agglomerates, focusing primarily on size distribution while neglecting other critical properties such as porosity, density, and surface morphology, which significantly impact aerodynamic performance.

Insufficient Investigation of Long-Term Stability: Studies often focus on short-term stability assessments. There is a need for more comprehensive studies investigating the long-term stability of agglomerates under various environmental conditions (e.g., humidity, temperature) and their impact on drug delivery.

Limited Clinical Translation: While preclinical studies demonstrate promising results, there is often a gap in translating these findings into clinically relevant outcomes. More studies are needed to investigate the correlation between in vitro and in vivo performance, including clinical studies to assess the efficacy and safety of agglomerated formulations in human subjects.

Lack of Standardized Characterization Techniques: The lack of standardized methods for characterizing agglomerate properties (e.g., porosity, surface area, mechanical strength) hinders the comparability of results across different studies.

Addressing these gaps through this thesis will contribute significantly to:

Developing a deeper understanding of the agglomeration process: By investigating the underlying mechanisms and their influence on agglomerate properties.

Optimizing agglomeration techniques: By identifying and refining parameters for achieving desired agglomerate characteristics.

Improving the predictability of formulation performance: By establishing stronger correlations between in vitro and in vivo data.

Developing more robust and stable formulations: By addressing the challenges of long-term stability and ensuring consistent drug delivery.

By addressing these critical gaps, this research will contribute to the development of more effective and reliable DPI formulations for improved patient outcomes.

Chapter 3 Methodology

3.1 Materials

3.1.1 Melatonin

Melatonin, also known as N-acetyl-5-methoxytryptamine, is a naturally occurring hormone produced by the pineal gland (Liu et al., 2019). This off-white powder plays a key role in regulating sleep-wake cycles (Mannino et al., 2021). Melatonin's unique chemical structure (shown in Figure 3.1), defined by the formula $C_{13}H_{16}N_2O_2$ with a molecular weight of 232.28 g/mol and a density of 1.175 g/cm³, grants it an interesting property: high solubility in both lipids (fats) and water. This dual-natured solubility allows melatonin to move effortlessly between cell membranes and various fluids throughout the body, ensuring that it reaches wherever needed. The core structure of melatonin is an indole chemical scaffold, further functionalized with a 3-amide group and a 5-alkoxygroup, contributing to its special characteristics.

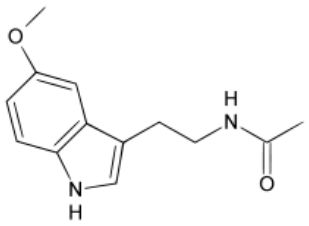

Figure 3.1 Chemical structure of Melatonin

Oral administration of melatonin resulted in low and variable bioavailability due to first-pass hepatic metabolism; Lane and Moss estimated a low oral bioavailability of less than 10% through an experimental study (Lane and Moss, 1985). The pharmaceutical grade melatonin used in this study was purchased from Saikang (Saikang pharmaceutical, China)

3.1.2 Budesonide

Budesonide is a medication that belongs to the class of corticosteroids. Chemically, it is designated as (RS)-11β,16α,17,21-tetrahydroxypregna-1,4-diene-3,20 dione cyclic 16,17-acetal with butyraldehyde (see Figure 3.2 for the

structural formula). It exists as a mixture of two slightly different molecular forms (22R and 22S) and has an empirical formula of $C_{25}H_{34}O_6$ with a molecular weight of 430.5. The pharmaceutical grade budesonide used in this study (purity: 99.8%) was purchased from Humanwell Healthcare (Group) Co., Ltd, Hunan, China.

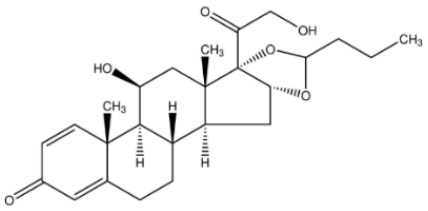

Figure 3. 2 Chemical structure of Budesonide

Clinical Applications

Budesonide is classified as a second-generation glucocorticoid, meaning that it offers a more targeted anti-inflammatory effect compared to earlier corticosteroids. This translates to lower systemic absorption, minimising side effects, while still being effective for treating respiratory conditions, such as asthma and rhinitis, as well as inflammatory bowel disease.

Commercial Availability

Pulmicort® is a well-known brand name for budesonide, particularly the inhaled form used for long-term management of asthma and chronic obstructive pulmonary disease (COPD).

3.1.3 Lactose

Lactose remains one of the most important excipients in pharmaceutical technology, and often plays a decisive role in powder inhalation. The structural formula of the monohydrate is shown in Figure 3.3. Lactose is chemically known as O-ß-D-galactopyranosyl-(1-4)-ß-D-glucose, with the molecular formula $C_{12}H_{22}O_{11}$ (342.3 g/mol) (Majd and Nickerson, 1976).

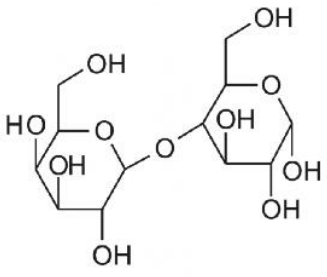

Figure 3. 3 Chemical structure of lactose

Fine lactose of various grades was used as an auxiliary substance in this work, which was used as a filler in soft spherical agglomerates and co-agglomerates with drug particles. InhaLac® 70 (Meggle GmbH, Wasserburg, Germany) was initially used after air jet milling for the agglomerate formulation, followed by LH300 (DFE Pharma, Netherlands) and InhaLac® 500. In subsequent trials, different shapes with various lactose morphologies were prepared via the antisolvent method.

3.1.4 Magnesium stearate

Magnesium stearate (MgSt), chemically known as $Mg(C_{18}H_{35}O_2)_2$, has a molar mass of 591.27 g/mol. It is a slightly water-soluble material (4 mg/mL at 25°C)(Haware et al., 2018). MgSt reduces friction during inhalation and is already used in commercial inhalation products such as Foradil®, NEXThaler®, and Breezhaler® (Shur et al., 2016). The addition of MgSt to the mixture of the interacting inhalation powder negatively affects its aggregation, thus improving the fine particle fraction (FPF)(Jetzer et al., 2018a). MgSt forms a thin layer on irregularly filled carrier particles, resulting in reduced surface roughness (Das et al., 2011). The adhesion between the substrate and API was reduced because of less mechanical entanglement or active site saturation on the substrate.

In this study, MgSt was used as the force-control agent. The aim was to investigate whether the agglomeration behaviour of the agglomerates could be influenced by the application of MgSt in different ways.

Pharmaceutical grade MgSt was purchased from PETER GREVEN(Netherlands).

3.2 Inhaler device

Turbuhaler®

Pulmicort Turbuhaler® (AstraZeneca GmbH, Wedel, Germany) is a widely used inhaler for delivering medication to the lungs. It uses a unique approach based on agglomerated particles (Berkenfeld et al., 2015). As shown in Figure 3.4, this passive multi-dose dry powder inhaler (DPI) features a tubular reservoir filled with medication in the form of these agglomerates.

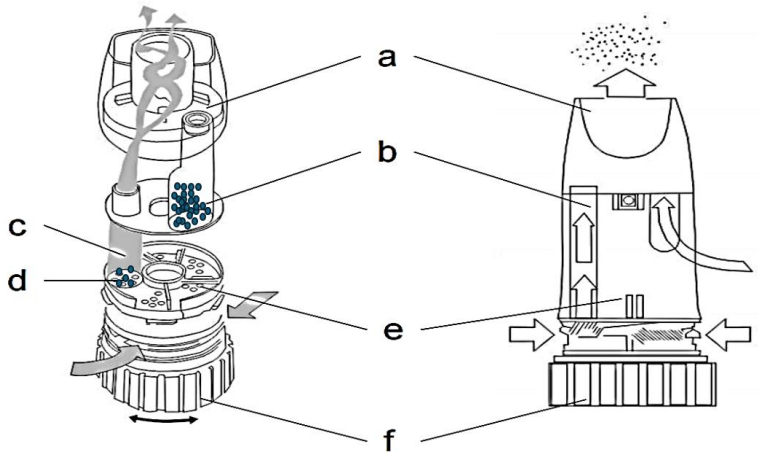

Figure 3. 4 Schematic of the Turbuhaler ® in disassembled form (left) and cross section (right): a) mouthpiece with spiral channel, b) reservoir for agglomerate, c) inhalation channel, d) dosing openings on dosing disc, e) scraper, f) dosing wheel(Wetterlin, 1988)

Volumetric Dosing Mechanism

Pulmicort Turbuhaler® employs a volumetric dosing principle. Turning the dosing wheel at the bottom of the inhaler rotates the dosing disc by one position. This action dispenses a single dose of the agglomerate formulation from the reservoir into designated openings. Simultaneously, another dose was positioned in the inhalation channel for subsequent use.

Inhalation Process and Dispersion

During inhalation, air enters through the slots above the dosing wheel and travels downwards towards the openings containing the medication. This airflow propels the agglomerates upwards into the mouthpiece. Within the mouthpiece, the airflow splits and transforms into a vortex within the spiral channel. This vortex generates a strong shear force that effectively disperses agglomerates into smaller particles for efficient lung delivery.

Refilling with Self-made Agglomerates

For research purposes, inhalers can be refilled with custom-made spherical agglomerates. This process involves:

1. Removing the mouthpiece.
2. Tweezers are used to open the reservoir by removing the blue cap.
3. Emptying the original commercial formulation and cleaning any residual particles with compressed air.
4. Filling the reservoir with a self-made agglomerate batch.
5. The reservoir was closed with a blue cap and the mouthpiece was reattached.

3.3 Methods

This chapter describes the manufacturing and analytical methods used in this thesis, including the apparatus and working principles. Some important definitions and calculation methods are also introduced after the corresponding equipment.

3.3.1 Manufacturing methods

3.3.1.1 Air jet milling

Air jet milling is a well-established technique for reducing the particle size, particularly for the creation of inhalable medications. This study employed two types of air jet mill: a spiral jet mill and a fluidised bed jet mill (Figure 3.5).

Spiral Jet Milling: Power through Collision

In spiral jet milling, particle size reduction occurs primarily through collisions between particles and between particles and the mill walls (Djokić et al., 2014). Figure 3.5A depicts a schematic of a spiral jet mill. It consists of a grinding chamber, air inlet channel, feed channel, venturi system, collection container, and other components. The powders were drawn from the feed funnel using a high-speed air vacuum generated at the nozzle through the Venturi system. This intense airflow accelerated the particles, causing them to collide with each other and with the mill walls. Centrifugal forces within the chamber keep larger

particles in the outer area until they are broken down. Smaller particles migrated towards the centre and were directed toward the cyclone separator for collection. While effective for micronisation (grinding to a micrometre size), spiral jet mills have limitations. Oversized feed particles can clog the hopper and lead to variations in the particle size distribution.

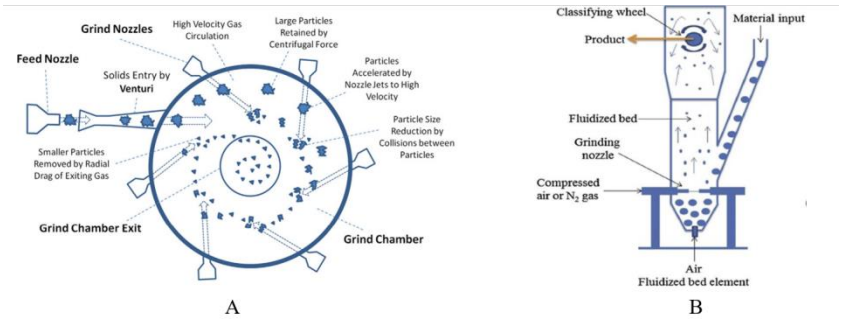

Figure 3. 5 Schematic of the spiral jet mill (A)(MacDonald et al., 2016) and fluidized-bed jet-mill (B)(Tidke. et al., 2021)

Fluidized-Bed Jet Milling: Precise Control

This study also utilised a fluidised bed jet mill, as illustrated in Figure 3.5B. This type of mill has two distinct sections: the lower grinding section houses a chamber with three nozzles positioned radially within the walls; and the upper section acts as a centrifugal forced vortex air classifier, which is responsible for controlling the particle size (Kou et al., 2017). This two-stage process allows for steeper particle size distribution and precise control of the final particle size.

The material enters through a special inlet and is entrained by the high-velocity gas streams generated by the nozzles. Particle size reduction occurred because of collisions within the gas stream. A key advantage of a fluidised bed jet mill is its ability to precisely control the particle size distribution. The rotational speed of the upper classifier wheel determined the maximum particle size. By increasing the speed, a greater force was exerted on the particles, causing larger particles to be rejected and recirculating back to the grinding zone.

To optimise the particle size of lactose and the active pharmaceutical ingredient (API), this study investigated the milling pressure, classifier speed, and feeding speed. A spiral jet mill was also used for mixing the powder mixtures in this study. A low milling pressure of 1 bar was used to prevent the product from

being ejected through the feed funnel.

3.3.1.2 Powder conditioning

Micronisation, a process of reducing particle size, can introduce challenges for the use of lactose monohydrate in drug formulations.

Amorphous Formation and Stability Issues

Micronisation can create small amorphous domains on the surface of lactose particles (Janssen et al., 2023a). This is problematic because amorphous lactose is hygroscopic, meaning that it readily absorbs moisture from the environment. This moisture absorption can lead to the following:

- **Fusing and Agglomeration:** The absorbed moisture can cause the micronized particles to stick together, forming larger clusters and compromising the desired particle size distribution (Huppertz and Gazi, 2016). This is a significant issue for applications that require long-term physical stability.
- **Reduced aerosolization performance:** The presence of these small amorphous fractions can negatively affect the interaction between lactose and the drug, thereby hindering the ability of the drug to disperse effectively when inhaled (Depasquale et al., 2015).

Overcoming Stability Issues

A vapour-driven conversion process can be employed to address these challenges and ensure long-term stability. This involves conditioning milled lactose before mixing it with the drug.

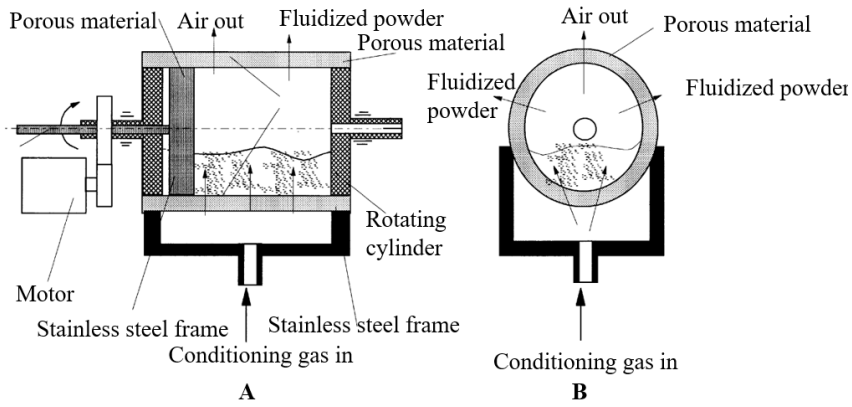

Figure 3. 6 Cross sectional view (A) and side view(B) of rotating fluidized bed

Conditioning Process using rotating fluidised bed

The conditioning process utilises a self-assembled rotating fluidised bed (Figure 3.6) and involves the following steps(Brodka-Pfeiffer et al., 2003):

1. **Material Introduction:** Milled lactose was introduced into a rotating fluidised bed, where it was suspended in a fluidised state.
2. **Exposure to Conditioning Gas:** A humidified gas stream was introduced to the bed, exposing lactose particles to controlled levels of moisture.
3. **Residence time and optimisation:** The lactose particles remained in contact with the conditioning gas for a predetermined amount of time, with the rotating speed of the bed being optimised for efficient conditioning.
4. **Separation and Collection:** Finally, the conditioned lactose particles were separated from the gas stream and collected.

Crystallisation through controlled vapour exposure

The key principle behind this conditioning process is the conversion of the amorphous phase on the lactose surface back to the crystalline form(Stankovic-Brandl et al., 2021). This crystallisation typically occurs rapidly when the amorphous material is exposed to vapour levels that exceed its glass transition temperature (Tg) by approximately 20°C (Lechuga-Ballesteros et al., 2002). The glass transition temperature itself is influenced by the amount of solvent present

in the amorphous material, a phenomenon known as plasticisation. By carefully controlling the vapour concentration of the solvent surrounding lactose particles, the conditioning process can be precisely tailored to obtain optimal results.

3.3.1.3 High shear mixing process.

CYCLOMIX IM-0.1/1 (HOSOKAWA MICRO B. Japan) is a high-shear impact mixer designed for the efficient blending of powders, as shown in Figure 3.7. It features a conical mixing vessel equipped with a central paddle rotor that can rotate at speeds up to 30 m/s. This high-speed rotation generates centrifugal forces that propel the product mixture towards the vessel wall.

The conical shape of the vessel guides the product upward. A cover positioned at the top directed the mixture back towards the centre of the mixer. Finally, an impact blade at the top efficiently disperses any cohesive powder, ensuring a high degree of uniformity and homogeneity throughout the blend, even within ultrashort mixing cycles. High shear mixing can exert significant influence on agglomerate size distribution. By applying intense mixing energy, the process can effectively break down larger, irregularly shaped agglomerates into smaller, more uniform particles. This controlled deagglomeration contributes to a narrower particle size distribution, which is crucial for achieving consistent and accurate dosing behaviours during drug delivery.

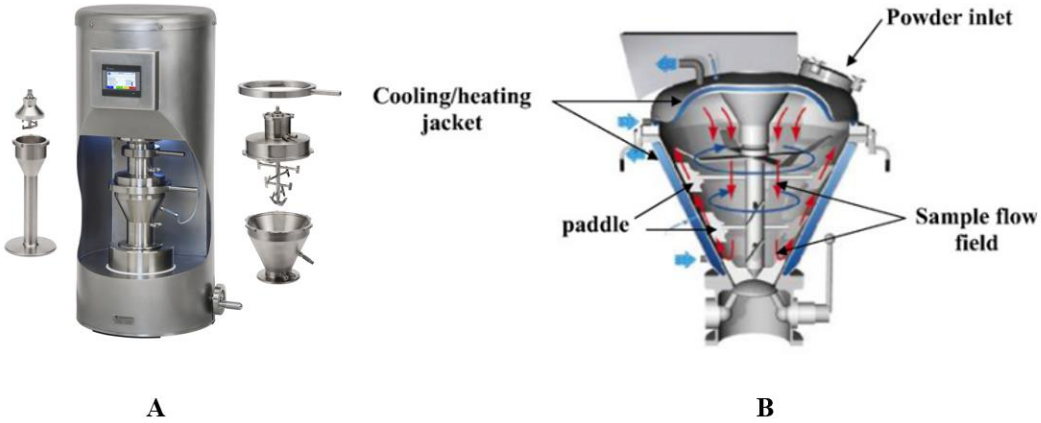

Figure 3. 7 Image(A) and schematic diagram(B) of the Cyclomix high-shear mixer(Ouabbas et al., 2009).

Investigating Mixing Parameters

In this study, we sought to enhance the consistency of drug content and overall aerosol performance of the formulation. To attain this objective, two critical mixing parameters were modified:

1. **Mixing Speed:** By varying the speed of the rotor to control the intensity of the shear forces applied to the mixture.
2. **Mixing Time:** The total duration of the mixing process was also a variable, allowing for the optimisation of the blending efficiency.

Maintaining Consistency: Sieving Before and After mixing

To ensure consistent starting conditions and eliminate any pre-existing agglomerates, all materials were sieved both before and after the blending process using Cyclomix.

3.3.1.4 Intensive mechanical dry coating

Fine powders often exhibit high inter-particle cohesion, indicating that the particles tend to stick together. This can lead to issues such as poor mixing, handling difficulties, and problems during the manufacturing process (Pfeffer et al., 2001, Yang et al., 2019, Yang et al., 2015).

Mechanical Dry Coating as a Solution

Mechanical dry coating has emerged as a promising technique for addressing these challenges. This modifies the surface characteristics of the powder particles, reducing their intrinsic cohesiveness and improving their flowability(Jallo et al., 2011). By decreasing interparticle forces, such as van der Waals forces and electrostatic interactions, surface modification techniques can enhance powder dispersibility(Hirschberg et al., 2019). This reduced surface energy contributes to superior deagglomeration and dispersion within the inhaler, leading to a higher proportion of respirable particles reaching the target site in the lungs.

Conventional dry coating systems

There are two main types of mechanical dry coating systems, distinguished by the blade geometry of the processing unit. Both systems involve a "press head" that compresses the powder against the inner wall of the chamber (Quinlan et al.,

2015).

Working Mechanism of Dry Coating

The mechanical dry coating process applies intense shear and compression forces to both the core (host) and coating (guest) particles. This is achieved through a combination of impaction and compression, as the particles are forced between the edge of the press head and the chamber wall. This action served two purposes:

1. **Breaking Up Agglomerates:** The high-speed rotation disrupts the existing agglomerates of the cohesive host particles, exposing their individual surfaces for coating.
2. **Reducing Inter-particle Attraction:** By increasing the distance between the host particles or reducing their contact area, dry coating effectively reduces the attractive forces that cause them to cling together.

Experimental Setup:

In this study, a mortar grinder (MG100, Beijing Grinder Instrument Co., LTD) was employed for the mechanical dry coating of drug powders with magnesium stearate (MgSt). This grinder features a rotating cylindrical chamber and press head similar to that of the Nanocular® system. It operates at speeds ranging from 100 to 2000 rpm, generating the required shear and compression forces (Figure 3.8).

Coating Process:

1. **Pre-mixing:** Fine lactose samples (approximately 100 g) were first blended with a predetermined amount of MgSt (the coating material) in a cyclomixer (IM-0.1/1, HOSOKAWA MICRO B.V.) at a predefined speed and duration.
2. **Dry Coating:** The premixed powder mixture was then transferred to the cylindrical chamber of the grinder. The coating process was carried out at an optimised speed and duration to ensure the effective deposition of MgSt onto lactose particles (Zhou et al., 2010b).

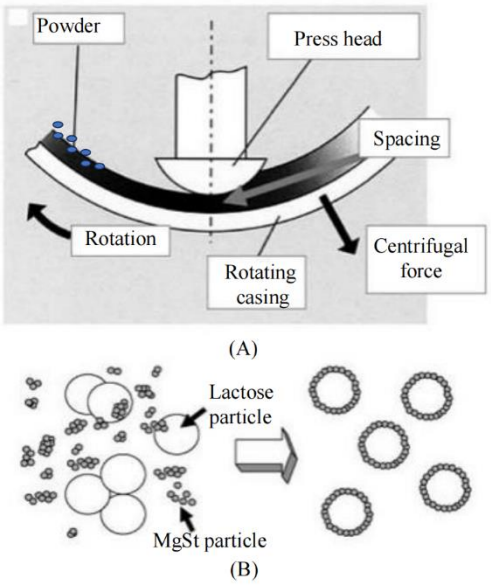

Figure 3. 8 Schematic of mechanical dry coating in a rotating device (A), guest particles coated and bonded onto the surfaces of host particles (B)(Rojas et al., 2010).

3.3.1.5 Agglomerate production with ultrasonic vibration

This method utilises the inherent cohesive properties of micronized particles(Abhijit Kadam1*, 2017), which are activated by vibration (Zeng et al., 2000a), the manufacture steps were listed as followed:

1. **Pre-agglomeration with Vibration:** First, a mixture of the drug and fine lactose was fed through a vibration feeder (BF-09, Suzhou Huilide Machine Co., Ltd.). This vibration causes the particles to clump together, forming the initial agglomerates. The power supply for the vibration feeder was precisely controlled at 160V and 80 Hz using a variable-frequency digital controller (SDVC31-M, Nanjing CUH Science & Technology Co., Ltd).
2. **Smoothing and Strengthening in Rotary Drum:** The pre-agglomerates were then transferred to a rotary drum agglomerator (Wenling Aoli Machinery Co. Ltd.), with a diameter of 30 cm. Inside the drum, the agglomerates were smoothed and strengthened as they tumbled at a predetermined speed and for a predetermined duration.
3. **Ultrasonic Enhancement (Optional):** For additional strengthening, the bottom of the rotary drum can be submerged in an ultrasonic cleaner

(Shenzhen Yujie Cleaning Equipment Co., Ltd.) during the tumbling process. The specific power input for the ultrasonic cleaner can be adjusted to obtain optimal results (Figure 3.9).

The specific voltage and frequency for stable powder agglomeration will vary significantly depending on several factors:

Powder Properties:

1.Particle size and distribution: Fine powders may require lower voltages and frequencies compared to coarser powders.

2.Material properties: Dielectric constant, conductivity, and particle shape all influence how the powder interacts with the applied electric field.

3.Cohesiveness: Cohesive powders may require higher voltages or specific frequency ranges to overcome interparticle forces and facilitate agglomeration.

This approach leveraged the combined effects of vibration, tumbling, and optional ultrasonic treatment to create well-formed and robust drug-loaded agglomerates.

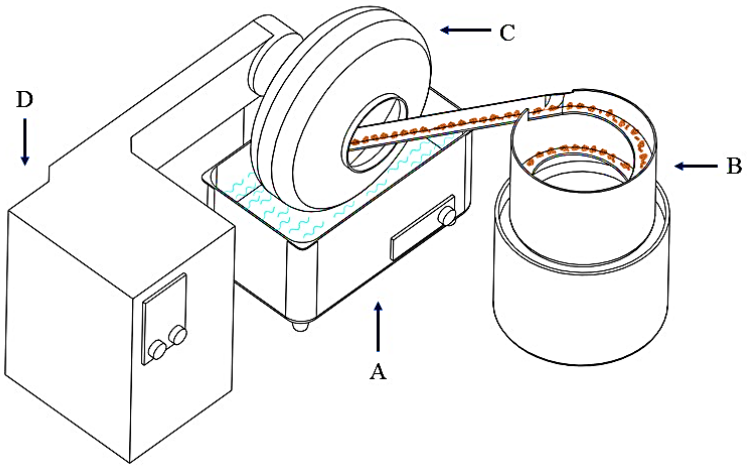

Figure 3. 9 Schematic of agglomeration apparatus, A represents the ultrasonic cleaner, B is the vibration bowl feeder, C and D represent the drum agglomerator and controller unit

3.3.1.6 Agglomerate production with resonant Acoustic Mixing

Resonant Acoustic Mixing (RAM) technology offers a unique approach to mixing powders, as shown in Figure 3. 10. It utilises the vertical reciprocating

movement of springs to generate short-amplitude, high-frequency (60 Hz) acoustic pressure waves (Osorio et al., 2016) which create two key effects within the mixing vessel:

1. **Micro-mixing Zones:** The acoustic waves induce the formation of micro-mixing zones throughout the entire vessel. These zones promote intimate contact between the particles at the microscopic level.
2. **Bulk Material Movement:** In addition to the micro-mixing, the acoustic waves also facilitate the bulk movement of the entire material within the vessel. This bulk flow is essential for efficient mixing and agglomeration, particularly for fine particles.

Pre-agglomeration with RAM

In this study, a Resonant Acoustic Mixer (Ramixers G500, Shenzhen Ramixers Technology Co., LTD) was employed for the pre-agglomeration of the powder mixture before the spheroidization process. Acoustic mixing was operated at an acceleration of 9.8 m/s^2 (equivalent to gravitational acceleration) for a predetermined mixing time to achieve the desired level of pre-agglomeration.

Spheroidization Process

After pre-agglomeration with RAM, the powder mixture was transferred to a rotary drum apparatus (RO-TAP® test sieve shaker, RX-29, HAVER & BOECKER OHG, Germany) for spheroidization. This device uses a combination of sieves (500 µm and 350 µm meshes) to obtain different fractions of agglomerates.

The powder mixture was forced through these sieves by a tapping motion and horizontal circular movement within the rotary drum. This tapping motion and rotation of the drum together contribute to the formation of spherical agglomerates. The specific speed of this eccentric oscillation within the drum was predetermined to achieve optimal spheroidization.

Combined Approach for Efficient Agglomeration

By combining RAM for pre-agglomeration and the subsequent spheroidization process in a rotary drum, this method offers a potentially efficient approach for

creating well-formed spherical agglomerates from powder mixtures.

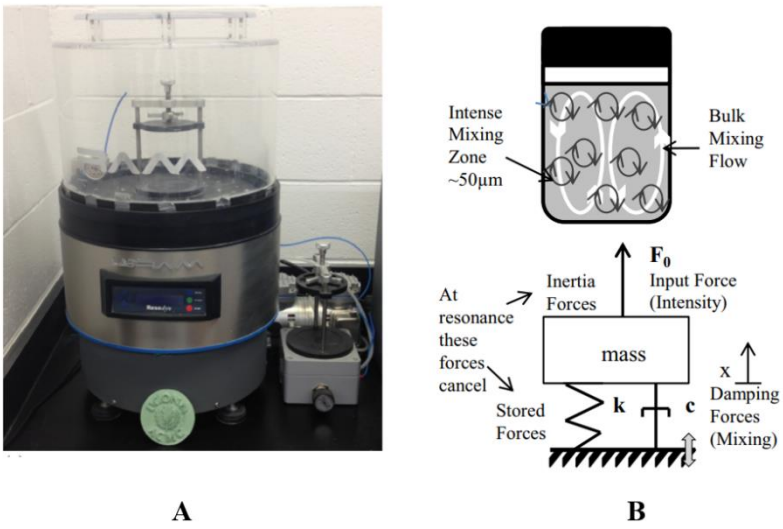

Figure 3. 10 A) The laboratory scale resonant acoustic mixer and B) the schematic of RAM technology (Vandenberg and Wille, 2018)

3.3.2 Analytical methods

The conventional approach for assessing DPI safety and efficacy relies on clinical studies that incorporate pharmacokinetic (PK) and pharmacodynamic (PD) evaluations (Nugent et al., 2018).

- **PK studies** measure how the drug moves through the body, with the aim of demonstrating bioequivalence (similar absorption profiles) between the new DPI and a reference product.
- **PD studies** assess the effects of drugs on the body, with the aim of establishing equivalence in terms of efficacy and clinical outcomes.

However, this approach has several challenges.

1. **Dose Detection:** The minimal dose amounts used in DPIs can make it difficult to accurately measure drug absorption using standard PK methods.
2. **Subject Variability:** Differences in airway anatomy among subjects can lead to variations in how the drug is delivered and absorbed, potentially confounding the results (Tomlinson et al., 2005).
3. **Cost and Time:** Clinical trials are expensive and time-consuming, making them less suitable for early R&D stages.

Alternative Strategies for Early R&D

Given these limitations, this study emphasises the importance of thorough characterisation of the active pharmaceutical ingredient (API) and excipients used in the DPI formulation, along with in vitro (laboratory-based) evaluations. This two-pronged approach can provide valuable data for optimising the DPI design and formulation before progressing to clinical trials.

Focus Areas:

1. **API and carrier characterisation**
    - The factors influencing the aerodynamic performance of the drug, such as particle size, polymorphism (crystal form), and crystal habit (shape), were investigated for the API.
    - For the carrier material (usually lactose), bulk properties such as density, size distribution, and mechanical strength were evaluated, along with their impact on the final aerodynamic particle size distribution of the DPI formulation.
2. **In Vitro Evaluation:** The passage mentions that various in vitro techniques will be discussed later, likely focusing on methods that simulate drug delivery to the lungs and assessing factors such as particle deposition and dispersion.

By implementing these alternative strategies, valuable insights into the safety and efficacy of DPI formulations during the early stages of R&D have been obtained, paving the way for more informed and efficient clinical trials in the development process.

3.3.2.1 Laser Diffraction size measurement

Laser diffraction is a widely used technique for measuring the particle size distribution (Merkus, 2009). The working principle is illustrated in Figure 3.11, and it is based on the following parameters:

Light Source: A monochromatic laser beam (single colour) was directed at the powder sample in a parallel path.

Particle Interaction: Laser light interacts with particles in three ways.

Reflection: Some light bounces off the particles.

Absorption: Some light is absorbed by the particles.

Diffraction: Light bends slightly as it passes around the edges of the particles.

Diffraction Angle and Particle Size: The angle at which light diffracts is inversely proportional to the particle size (smaller particles cause larger diffraction angles) (Eshel et al., 2004).

Signal Analysis: A Fourier lens transforms diffracted light signals into measurable patterns, which can then be analysed using software to determine the particle size distribution.

Two types of distributions can be reported:

The volume-based distribution (q_3) represents the total volume of particles within a certain size range.

The number-based distribution (q_1) represents the number of particles within a certain size range.

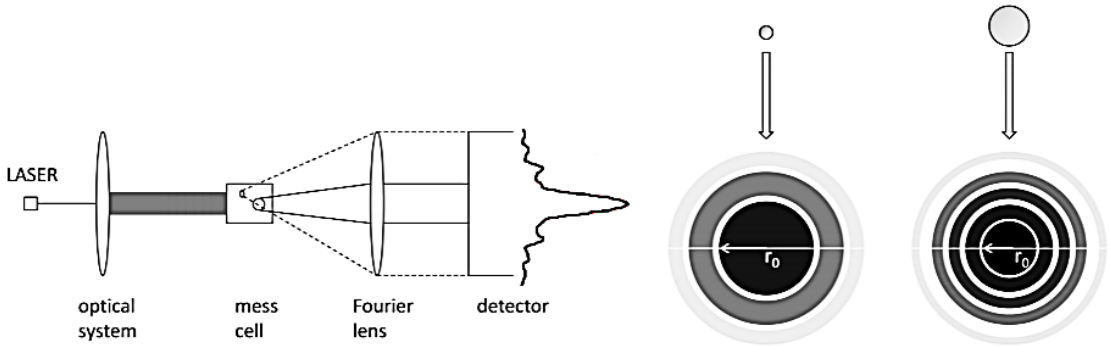

Figure 3. 11 The principle of Laser Diffraction testing(Heinson et al., 2014)

Measurement Setup in This Study

- **Laser Diffractometer:** The instrument used for this study was the HELOS laser diffractometer (Sympathec GmbH, Germany).
- **Software:** The data were analysed using PAQXOS® software (Sympathec GmbH, Germany).
- **Sample Feeding:** A vibrating chute feeder (VIBRI) ensured a continuous flow of powder into the measurement zone.
- **Dry Dispersion:** The RODOS dry dispersion system (Sympathec GmbH, Germany) was used to separate the individual particles within the powder

sample.

Optimizing Dispersion Pressure

The critical aspect of dry dispersion is to achieve the optimal separation of particles without breaking them down (comminution). To determine the optimal pressure, the pressure was gradually increased from 0.5 bar to 6 bar during the first measurement of a new material. The optimum pressure was identified as the point at which the measured particle-size distribution remained constant with increasing pressure.

Reporting Particle Size Distribution

The particle size distribution was characterised using three key parameters (D_{10}, D_{50}, and D_{90}):

- **D_{10}** represents the diameter at which 10% of the particles (by volume) are smaller than this size.
- **D_{50}** represents the median diameter, where 50% of the particles are smaller and 50% are larger.
- **D_{90}** represents the diameter at which 90% of the particles (by volume) are smaller than this size.

The reported particle size data represent the average of three measurements with the standard deviation (SD).

3.3.2.2 Scanning Electron Microscopy

Scanning Electron Microscopy (SEM) was used to investigate the morphology (shape and structure) and elemental composition of magnesium stearate within the samples.

High-Resolution Imaging with Electrons: Unveiling Surface Details

SEM is a powerful technique for acquiring high-resolution images of a sample's surface. In contrast to conventional light microscopy, SEM employs a focused beam of electrons to generate images (Homma, 2001).

Core Principles of SEM

As shown in Figure 3.12, an electron gun positioned at the top of the microscope

served as the electron beam source. the entire microscope chamber was maintained under a high vacuum to enable the uninhibited movement of the electron beam without gaseous interference. For beam focusing, a series of electromagnetic fields and lenses within the microscope column precisely focus and direct the electron beam towards the sample area of interest. The interaction of the electron beam with the sample surface leads to the ejection of electrons and X-rays from the sample atoms. Dedicated detectors within the SEM capture the ejected electrons and X-rays. The collected signals were then processed to generate a detailed image on a screen under vacuum conditions.

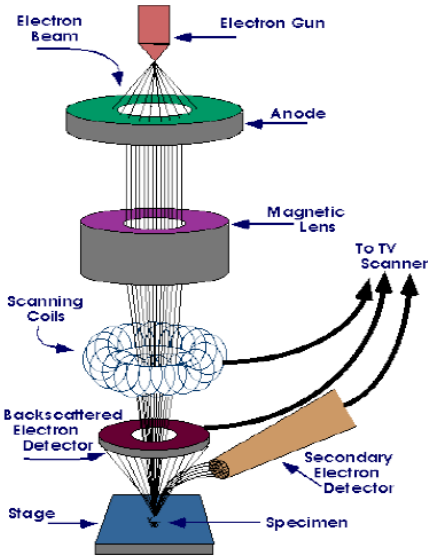

Figure 3. 12 Schematic working principle of SEM(Shawky, 2016)

Sample Preparation for SEM Analysis

Biological samples typically lack sufficient electrical conductivity to achieve clear SEM imaging. To address this, a thin layer of conductive material, such as gold, was sputter-coated onto the sample surface before analysis. This sputter coating (DII-29030SCTR) facilitated the flow of electrons across the sample and minimised image distortion due to electrical charging.

SEM Configuration and Analysis Parameters in this Study

Microscope: Scan Electron Microscope (SEM, JCM-7000; JEOL, Japan)

Analytical Technique: Energy Dispersive X-ray Analysis (EDX)

Tailored Analysis for Different Sample Types:

Primary Particles: These were examined at an acceleration voltage of 15 kV and magnifications ranging from 100x to 5000x. The higher voltage setting provides superior resolution for scrutinising the fine details of the individual particles.

Spherical Agglomerates: Owing to their larger size, they were analysed at a lower voltage of 5 kV to prevent potential sample damage. The magnification range employed was also 250x to 5000x.

Synergistic Approach: Combining Imaging and Spectroscopy

SEM imaging provided valuable morphological information regarding the shape and texture of magnesium stearate particles and agglomerates. Additionally, EDX analysis, employed concurrently with SEM, facilitated the identification of the elemental constituents within magnesium stearate, verifying its presence in the mixture.

3.3.2.3. Digital microscope

A digital microscope (ZML-310, Mengxin, China) with a high resolution of 3664 × 2748 pixels was used to capture light microscope images of the agglomerates at 50x magnification. This magnification level provides detailed visual information regarding the overall shape and texture of the agglomerates.

Beyond Size: Image Analysis for Shape Characterization

While laser diffraction primarily focuses on measuring the particle size based on the projected area, digital microscopy coupled with image analysis offers additional insights into the particle shape. The image analysis software utilises the projected area of each particle in the image as the primary measurement parameter.

Extracting Shape Information from 2D Data

Area Equivalent Circle Diameter: This parameter provides an estimate of the size of agglomerate particles. The software calculated a circle with the same area as the projected area of each particle. The diameter of this equivalent circle was measured as shown in Figure 3.13 and Equation 1.

Sphericity: This parameter quantifies how closely a particle resembles a perfect sphere. It is calculated as the ratio of the perimeter of the equivalent circle (PEQPC) to the actual perimeter of the particle (Preal) as shown in Figure 3.14 and Equation 2. Sphericity values ranged from 0 to 1. A value closer to 1 indicates a more spherical shape, whereas a value closer to 0 suggests a more irregular shape. The rationale behind using the equivalent circle perimeter as the reference is that it represents the smallest possible perimeter for a given projected area.

$$x_{EQpC} = 2\sqrt{A / \pi} \qquad \text{(Equation 1)}$$

x_{EQpC} represents the diameter of the area equivalent circle, μm.

A is the area of the area equivalent circle, μm².

Figure 3. 13 Schematic of diameters derived from the equivalent circle(Li et al., 2005).

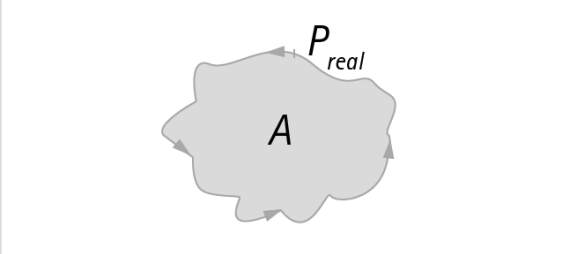

Figure 3. 14 Schematic of sphericity derived from the equivalent circle (P = perimeter, A = area)(Li et al., 2005)

$$S = \frac{P_{EQPC}}{P_{real}} = \frac{2\sqrt{\pi \times A}}{P_{real}} \qquad \text{(Equation 2)}$$

By incorporating image analysis, this study goes beyond simple size determination and delves deeper into the shape characteristics of agglomerates. This additional information provides a more comprehensive understanding of the overall morphology of particles.

3.3.2.4. Particle topography study with AFM

Atomic Force Microscopy (AFM) was used to investigate the surface topography of lactose samples in this study. Understanding surface roughness is crucial, as it can influence the aerosolization efficiency of drugs delivered through dry powder inhalers (DPIs).

AFM: Unveiling Surface Details at the Nanoscale

AFM is a powerful tool for acquiring high-resolution, three-dimensional images of a sample's surface at the nanoscale as shown in Figure 3.15. It provides valuable information about surface features, such as roughness, texture, and topography, all in a non-destructive manner (Arnold, 2014).

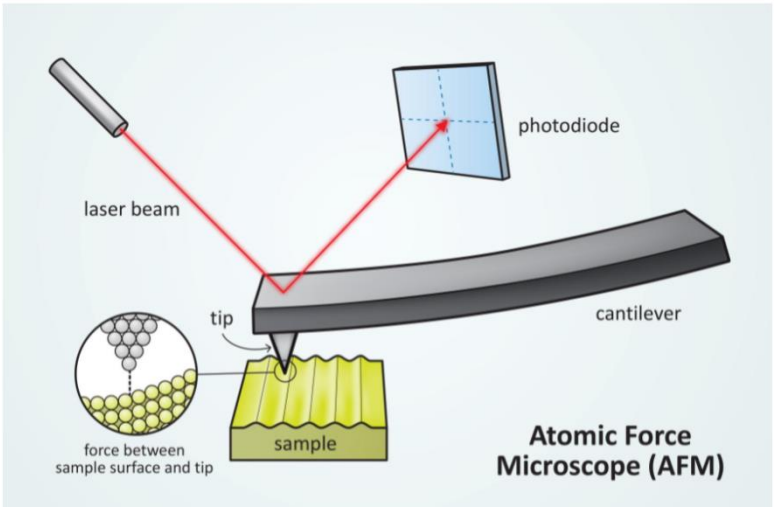

Figure 3. 15 Schematic of working principle of AFM(Marti, 1999)

Core Principles of AFM:

- **Sharp Probe:** An incredibly sharp tip, typically crafted from silicon or silicon nitride, was attached to a flexible cantilever arm.
- **Scanning Pattern:** The AFM system meticulously scans the sample surface in a raster pattern, akin to how a printer scans a document.
- **Precise Tip-Surface Interaction:** During scan, the tip interacts with the sample surface, causing the cantilever to deflect accordingly.
- **Deflection Detection:** A highly sensitive photodetector monitors these cantilever deflections.

- **Image Formation:** AFM software translates the recorded tip movements and positions into a three-dimensional topographic image of the scanned surface.

AFM Configuration and Measurement Parameters in this Study

Microscope: Bruker ICON AFM (Bruker Nano, Inc, Germany)

Sample Preparation and Imaging: The lactose samples were secured on sticky carbon tabs for AFM analysis. A high aspect ratio silicon probe was used to achieve optimal resolution during scanning. The tapping mode was utilised, which is a common technique for minimising tip-sample contact forces and preventing damage to delicate samples. A scan rate of 1 Hz was employed to ensure a sufficiently detailed capture. Each sample was scanned across an area of 3×3 μm².

Surface Roughness Analysis

Image analysis software was used to calculate the average roughness (Ra) of the lactose surfaces according to Equation 3.

$$Ra = \frac{1}{L_x L_y} \int_0^{L_y} \int_0^{L_x} f(x,y) dx \, dy \qquad \text{Equation 3}$$

where $f(x,y)$ is the surface relative to the centre plane and Lx and Ly are the dimensions of the surface.

By analysing the surface roughness obtained through AFM, researchers can gain insights into the potential aerosolization efficiency of lactose carriers, particularly when combined with drug particles.

3.3.2.5. Aerodynamic particle size distribution

The Next Generation Impactor (NGI) was used to assess the potential pulmonary deposition of drugs delivered via dry powder inhalers (DPIs) (Abdo et al., 2020). A critical aspect of DPI development lies in ensuring optimal deposition of the drug within the lungs. In vitro lung deposition assessment methods offer valuable insights into the behaviour of inhaled particles within the respiratory system(Ammari et al., 2019). The primary mechanism by which drug particles

(APIs) are deposited within the lungs is inertial impaction. Larger and heavier particles possess greater inertia, which causes them to deviate more significantly from the airflow path and impact the airways. Cascade impactors, such as NGI, are designed to leverage this principle for in vitro testing.

Working principle of NGI: Mimicking Lung Deposition In Vitro

NGI is a well-established cascade impactor commonly used for the evaluation of inhalation products. Its design incorporates multiple stages that progressively collect particles of varying sizes as the airflow carrying the particles traverses the instrument as shown in Figure 3.16.

The higher stages within the NGI possess larger collection plates specifically designed to capture particles with greater inertia (typically larger and heavier). As airflow progresses through the NGI, the subsequent stages with progressively smaller collection areas target finer particles with less inertia(Khalili et al., 2018).The remaining particles that fail to impact earlier stages are collected by a final filter at the end of the NGI.

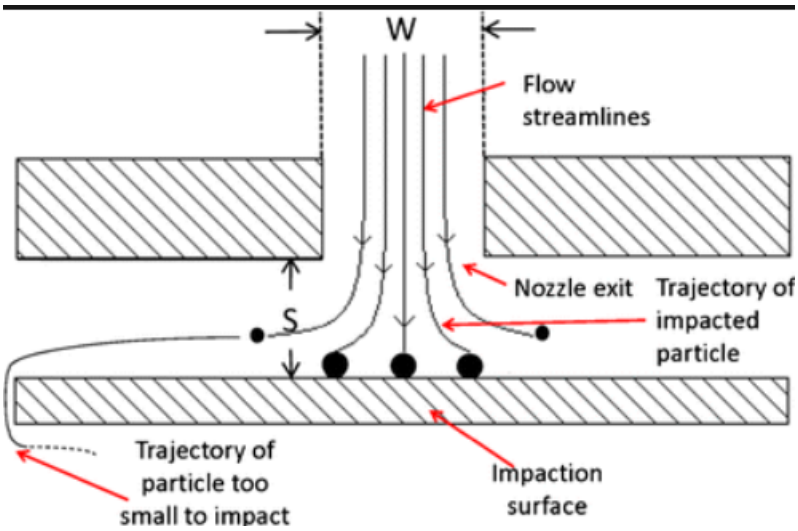

Figure 3. 16 Principle of cascade impactor operation(Nichols et al., 2013)

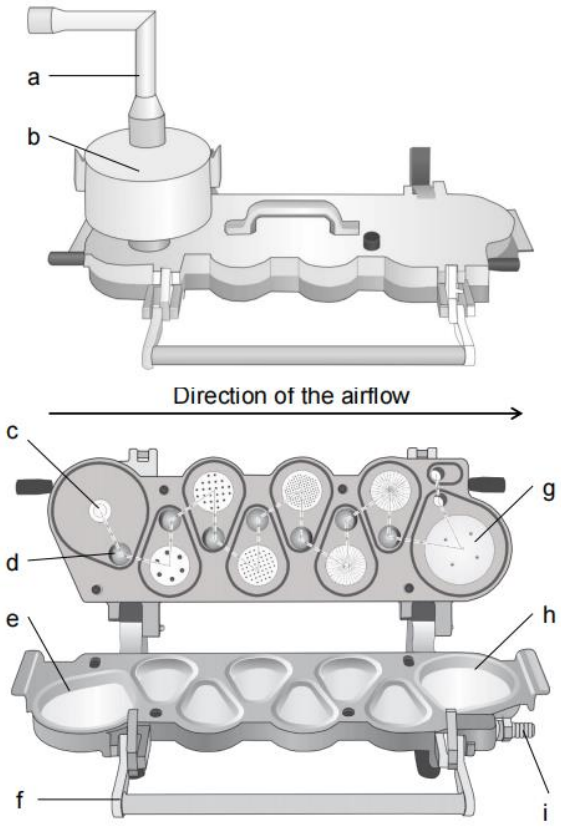

Figure 3. 17 Schematic of the closed (top) and open (bottom) state of NG, the dashed line represents how the air is passed through each section: a) induction port, b) pre-separator, c) stage 1, d) outlet opening of stage 1, e) collection cup of stage 1, f) locking holder, g) micro orifice collector (MOC), h) collection cup of MOC, i) connection to vacuum pump (Reproduced from Copley, 2008)

NGI Configuration and Operation in the Present Study

- **NGI Model:** Next Generation Impactor (NGI, Copley Scientific, Nottingham, UK)
- **Number of Stages:** 7 (as illustrated in Figure 3.17)
- **Operational Airflow Rate:** Adjustable from 30 L/min to 90 L/min, suitable for testing dry powder inhalation.

Operational Procedure:

1. **DPI Connection and Dose Release:** The DPI is connected to a designated port on the NGI. A predetermined dose was released from DPI upon activation.
2. **Airflow Initiation:** A solenoid valve was activated to initiate airflow through the NGI for a predetermined duration.
3. **Sample Collection:** Following the airflow cycle, the NGI was disassembled, and each component (including the induction port, pre-

separator, stages 1-7, and the micro-orifice collector) was rinsed with a suitable solvent to collect the deposited drug particles.

4. **Drug Quantification:** The collected samples from each stage were then analysed using High-Performance Liquid Chromatography (HPLC) to determine the mass of the deposited drug at each stage.

Data Analysis and Calculations

- Software (CITDAS 3.0, Copley Scientific Limited, Nottingham, UK) was employed to calculate the key parameters based on the collected mass data(Mitchell and Nagel, 2004):
- **Fine Particle Dose (FPD):** The mass of drug particles with a diameter less than a specific size (typically 5 μm).
- **Fine Particle Fraction (FPF):** The ratio of the FPD to the nominal dose emitted from the DPI, expressed as a percentage.
- **Geometric Standard Deviation (GSD):** A measure of the width of the particle size distribution.
- **Mass Median Aerodynamic Diameter (MMAD):** The diameter at which half of the drug mass resides in particles with smaller diameters and the other half resides in particles with larger diameters.

By analysing these parameters, researchers can gain valuable insights into the efficiency of DPI in delivering drug particles within a size range suitable for optimal lung deposition, paving the way for improved DPI formulations.

3.3.2.6 In-vitro dissolution for dry powder formulation

Although aerodynamic particle size distribution is critical for understanding the inhalability of a DPI formulation, it might not be sufficient to predict its effectiveness in vivo(May et al., 2014). For instance, two formulations with similar aerodynamic properties can exhibit different pharmacokinetic (PK) profiles, indicating that the drug is absorbed into the bloodstream at different rates(Floroiu et al., 2018).

Dissolution: A Key Determinant for Drug Absorption

For poorly soluble drugs, the rate of dissolution is a critical factor influencing DPI performance. Dissolution refers to the process in which a drug substance dissolves in a solvent (usually aqueous solutions mimicking biological fluids). This dissolution step is essential for the drug to be absorbed by epithelial cells in the lungs and to exert its therapeutic effect.

In Vitro Dissolution Testing: A Valuable Tool

In vitro dissolution testing offers a valuable method for assessing and comparing drug release rates from various DPI formulations during early development stages. By incorporating this method, researchers can gain insights into potential formulation differences that might not be apparent solely from evaluating aerodynamic properties.

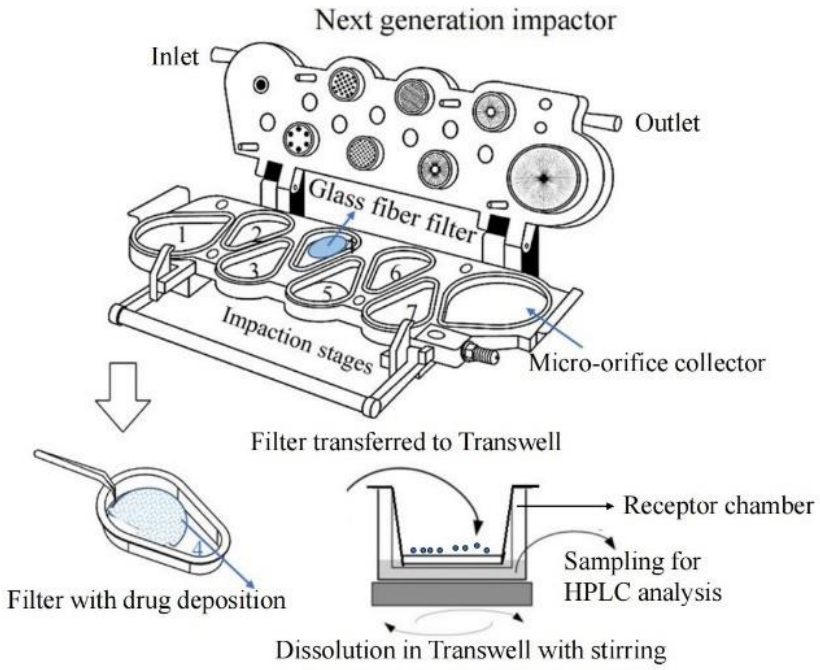

Figure 3. 18 The schematic of dissolution apparatus for DPI

The Setup: A Transwell Dissolution Apparatus

The study employed a Transwell dissolution apparatus specifically designed to evaluate inhaled products (Figure 3.18). This apparatus consists of two main compartments:

- **Upper Donor Compartment:** This compartment houses a filter (typically made of glass fibre) that serves as the donor membrane. The

DPI formulation containing the drug was placed on the filter.

- **Lower Receptor Compartment:** This compartment contains dissolution medium, which mimics the fluids present in the lungs.

The Dissolution Process

1. **Sample Collection:** Drug particles were first aerosolised from a DPI using a NGI operated at an airflow rate of 60 L/min. Particles deposited at a specific stage of the NGI were collected for the dissolution test.
2. **Diffusion Membrane:** The collected particles were placed onto the glass fibre filter within the donor compartment, essentially transforming the filter into a diffusion membrane separating the drug formulation from the dissolution medium(Sonvico et al., 2021).
3. **Dissolution Initiation:** The dissolution process begins when the dissolution medium comes into contact with the drug particles on the filter.
4. **Sample Collection at Intervals:** At predetermined time points, aliquots of the dissolution medium were withdrawn for analysis.

Dissolution Medium and Considerations

- The intrinsic solubility of a drug (its inherent ability to dissolve in a solvent) is a crucial factor when selecting the dissolution medium and test conditions.
- For poorly soluble drugs, surfactants are often added to the dissolution medium to enhance drug solubility and ensure adequate drug release during testing.

By analysing the drug concentration in the collected medium samples at different time points, researchers can establish the dissolution profiles of various DPI formulations(Eriksson et al., 2020).

3.3.2.7 Dynamic Vapor Sorption

Maintaining consistent quality across multiple production batches is a critical aspect of dry powder inhaler (DPI) manufacturing. This consistency

encompasses both the homogeneity of the formulation and its overall performance in delivering the medication to the lungs. Several factors can influence batch-to-batch variability, including:

- **Physicochemical Properties:** The inherent characteristics of the active pharmaceutical ingredient (API) and excipient materials employed in the formulation can significantly impact stability and performance.
- **Manufacturing Processes:** The specific methods and procedures used during DPI production can introduce variations if not controlled meticulously.
- **Environmental Conditions:** Fluctuations in humidity and temperature throughout the manufacturing process, handling, and storage can adversely affect the DPI stability.

Amorphous Materials and the Challenge of Moisture Sensitivity

Drug formulations containing amorphous APIs, which lack a well-defined crystalline structure, are particularly susceptible to moisture absorption compared with their crystalline counterparts(Lau et al., 2017a). This increased moisture uptake can potentially lead to physical and chemical instability within the DPI formulation, thereby compromising its efficacy and safety.

Dynamic Vapor Sorption (DVS): Characterizing Moisture Sorption Behavior

DVS has emerged as a valuable technique to investigate the hygroscopic properties of DPI formulations. It provides quantitative data on a material's propensity to absorb and desorb water vapour when exposed to controlled changes in relative humidity (RH) using the following actionable strategies:

- **Understanding Moisture Sensitivity:** DVS data provide essential information regarding the sensitivity of DPI formulations to moisture. This is particularly crucial for formulations containing amorphous drugs to identify potential stability concerns.
- **Informing Packaging Design:** By understanding the moisture sorption

behaviour of a DPI formulation, appropriate packaging materials with superior barrier properties can be selected(Simon et al., 2016). This selection process minimises moisture ingress from the external environment, thereby maintaining the product stability throughout its shelf life.

- **Optimising Manufacturing and Storage Conditions:** DVS data can guide the establishment of optimal humidity and temperature conditions throughout the entire DPI lifecycle, encompassing manufacturing, handling, storage, and ultimately patient use.

DVS Instrumentation and Measurement Process for DPI Characterization

- **DVS Apparatus:** The DVS Resolution instrument (Surface Measurement Systems Ltd., London, UK) is a commonly employed tool for this application, as shown in Figure 3.19.
- **Sample Preparation:** A small sample (typically 10-20 mg) was precisely weighed and placed on the sample pan of the instrument.
- **Gravimetric Detection:** A high-precision microbalance within the DVS apparatus meticulously measures minute changes in sample mass (accuracy: 0.01 μg, noise level: < 0.3 μg) as the sample absorbs or desorbs water vapour. This gravimetric approach provides highly sensitive detection of moisture sorption phenomena.
- **Controlled Humidity Environment:** The DVS system precisely regulated RH within the measurement chamber. This meticulous control was achieved by carefully mixing nitrogen streams with predetermined RH values (typically ranging from 0% to 100%).
- **Temperature Regulation:** The entire DVS unit was meticulously maintained within a climate chamber at a constant temperature (e.g. 25°C) to ensure consistent and reproducible measurement conditions.
- **Reference Disk for Accuracy:** The DVS incorporates a reference disk to account for any potential moisture adsorption by the sample pan. By

meticulously comparing the mass changes of the sample pan with those of the reference pan, researchers can isolate the true moisture sorption behaviour of the DPI formulation, enhancing the accuracy of the analysis.

The data obtained from the DVS analysis plays a critical role in predicting how a DPI formulation might respond to various humidity conditions encountered throughout its lifecycle. This information is instrumental in formulating, packaging, and storing DPIs to ensure consistent performance, optimal patient outcomes, and overall product safety(Systems, 2022).

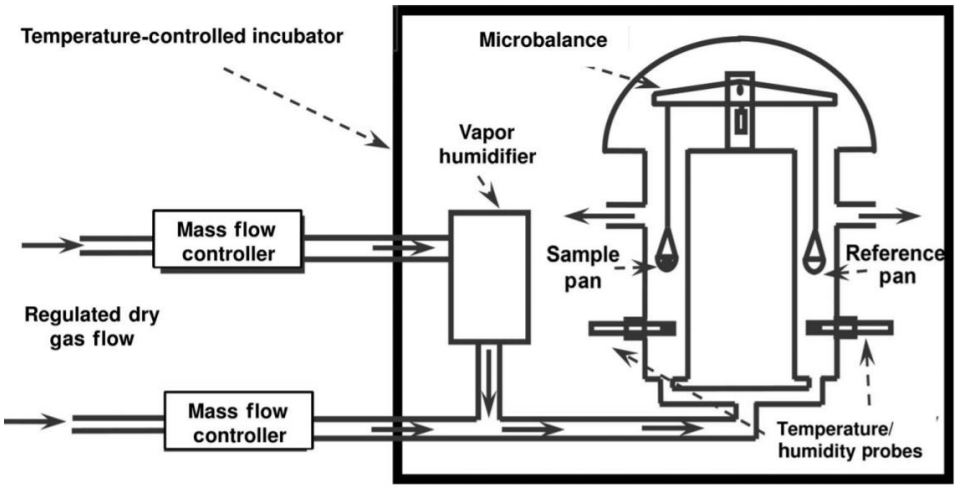

Figure 3. 19 Schematic of the DVS instrument.

3.3.2.8 X-Ray Diffraction

Particle size is critical for successful DPI delivery, and the API must be between 1 to 5μm in diameter to reach the lung. Therefore, pharmaceutical materials are usually crushed and ground before formulation. Grinding has the potential to change the physical form of a material, which changes the surface energy of the material, thus affecting its cohesion and adhesion. Therefore, it is necessary to quantitatively analyse the amorphous content (Hoppentocht et al., 2014).

X-ray diffraction is commonly used in the clinical field with invisible electromagnetic energy beams to produce images of internal tissues, and its application has been extended to the pharmaceutical industry for the characterisation of crystallinity. The sample was placed at the centre of the X-ray beam, and diffraction occurred. Parameter 2θ, as shown in Figure 3.20, can be

understood as the angle of X-ray radiation after refraction, the Y-axis corresponds to the intensity of parameter 2θ (Ivanisevic et al.). Crystalline materials exhibit sharp peaks in their images. X-ray powder diffraction (XRPD) was used to characterise the crystallinity and amorphous states. The crystal structure information was obtained from the X-ray diffraction pattern. The amorphous samples did not exhibit obvious diffraction patterns but only background signals.

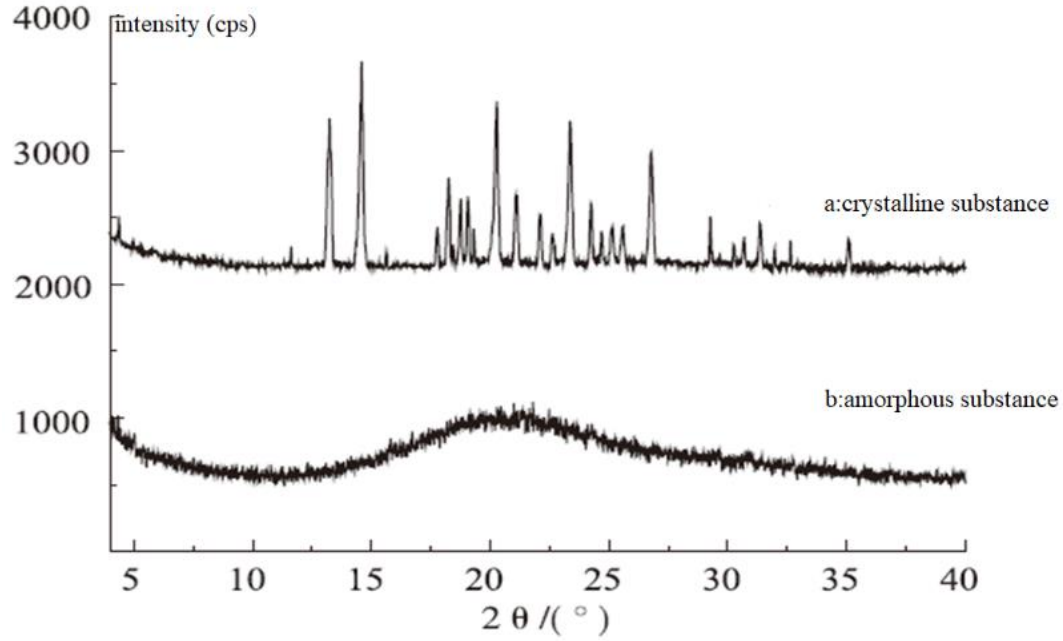

Figure 3. 20 XRPD pattern of a crystalline substance and amorphous sample (Thakral et al., 2018)

3.3.2.9 Inverse Gas Chromatography

The efficiency of drug delivery via DPIs is significantly influenced by the surface energy of the powder formulation(Das et al., 2009). The surface energy dictates the force required to create a new unit area of the surface and can be affected by the physical state of the drug substance. Notably, micronisation, which reduces the size of drug particles, can induce a transition from an amorphous (less ordered) to a crystalline (highly ordered) state(Mohammadi-Jam and Waters, 2014). This transition can alter the surface energy of the particles, thereby affecting their interaction with other particles and the carrier lactose typically used in DPIs(Brum and Burnett, 2011).

Measurements of Surface Energy with Inverse Gas Chromatography (IGC)

IGC has emerged as a prominent technique for investigating the surface energy of materials employed in DPI formulations as shown in Figure 3.21. This analytical method offers a multifaceted approach, providing valuable insights into several physicochemical properties that influence the DPI performance.

- **Intermolecular Interactions:** The IGC elucidates the energetic interactions between the surface of the DPI material and the surrounding molecules. This knowledge is crucial for optimising how drug particles interact with each other and with the carrier lactose, ultimately impacting the flowability and dispersion within the DPI.
- **BET Surface Area Quantification:** IGC can determine the BET surface area, which refers to the total surface area of the particles. This parameter significantly influences how easily the particles disperse and flow within a DPI device.
- **Understanding Cohesion and Adhesion:** IGC helps quantify the interparticulate forces governing cohesion (particle clumping) and adhesion (sticking to surfaces). Minimising these forces is essential to ensure optimal aerosolization from the DPI.
- **Glass Transition Temperature (Tg) Determination:** IGC can assist in determining the Tg, a critical parameter for understanding a material's physical state (amorphous or crystalline) and its potential stability during storage.
- **Surface Energy Heterogeneity Detection:** IGC can detect variations in surface energy across different regions of a particle's surface. This information is crucial for formulating strategies to achieve uniform particle behaviour and optimise aerosolization performance.

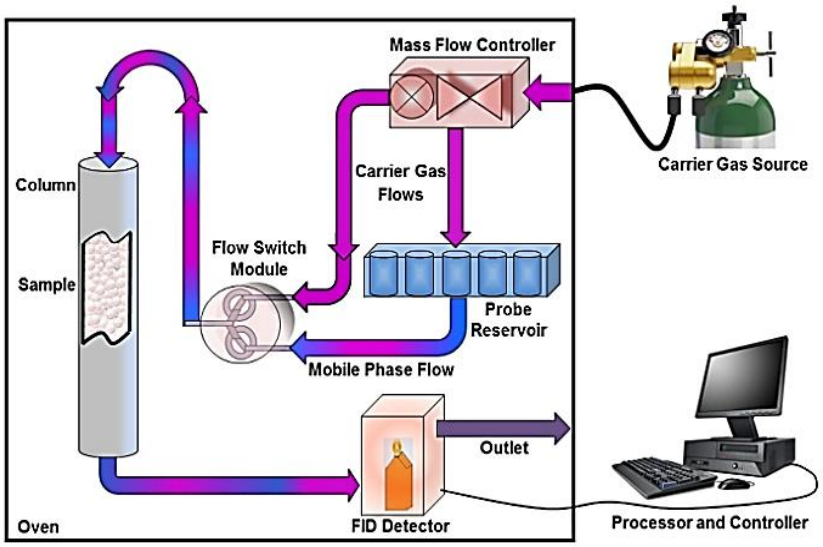

Figure 3. 20 Schematic of a typical inverse gas chromatography (IGC) analyzer(Mohammadi-Jam and Waters, 2014)

The IGC apparatus (SEA, Surface Measurement Systems, London, UK) was used in this study and consisted of the following parts.

- **Column Oven with Gas Flow Control:** This component precisely regulated the temperature and gas flow throughout the analysis.
- **Sample Introduction:** The DPI material under investigation was packed in a column.
- **Probe Molecules and Carrier Gas:** A series of different gas molecules (probe molecules) was introduced into the column using a carrier gas. The interaction between these probes and the sample surface revealed information regarding the surface energy.
- **Signal Detection and Software Analysis:** A detector captured the signals generated during the experiment. Dedicated software (Version 1.2.4.0, Surface Measurement Systems Ltd, London, UK) was used to interpret these signals and provide surface energy data.

Surface Free Energy: The Core Concept

Surface free energy (γ), denoted by the symbol $\gamma(mJ/m^2)$, represents the energetic cost associated with creating a new unit area of surface. It can be further decomposed into two primary components(Puri et al., 2019):

- **Dispersive (Non-polar) Component (γ^d):** This component arises from London dispersion forces, which is a type of weak intermolecular interaction.
- **Polar Component (γ^{sp}):** This component originates from specific interactions such as hydrogen bonding and acid-base interactions. These interactions are typically stronger than the dispersion forces.

The total surface free energy (γ) can be calculated using Equation 4, which incorporates both dispersive and polar components.

$$\gamma = \gamma^d + \gamma^{sp} \qquad \text{(Equation 4)}$$

Determining the Dispersive Component (γ^d):

1. **Sample Preparation:** The DPI material was loaded into specially treated glass columns and equilibrated under controlled conditions (303 K and 0% RH) to ensure consistency.
2. **Alkane Probe Molecules:** A series of alkane molecules with varying chain lengths was injected into the column. The strength of the interaction between these probes and the sample surface is influenced by the dispersive component of the surface energy.
3. **Schultz Plot Analysis:** A linear relationship was established by plotting the adsorption free enthalpy ($\Delta_{ads}G^d$) of the alkane probes versus their corresponding molar surface area. The slope of this plot (as shown in Equation 5) was used to calculate the dispersive component of the surface energy (γ_s^d).

$$\Delta_{ads}G^d = RT \ln VN = 2N.a.\sqrt{\gamma_s^d}.\sqrt{\gamma_l^d} + C \qquad \text{Equation 5}$$

where γ_s^d is the surface dispersive free energy of the solid (mJ/m^2), and γ_l^d is the dispersion surface free energy of the liquid (probe) (mJ/m^2), a is the cross-sectional area of the alkane molecule(m^2), C is the constant, R is the gas constant (8.314 J K^{-1} mol^{-1}), T is absolute temperature (K), VN is the retention volume of the probe molecule (mL) (Davies et al., 2005).

Estimating the Polar Component (γ^{sp}):

1. **Acid-Base Probe Approach:** The specific component (γ^{sp}) is estimated using the concept of donor-acceptor parameters(mJ/m^2). This approach involves employing a pair of probe molecules, one with an acidic character and the other with a basic character (e.g. ethyl acetate and dichloromethane), as shown in Figure 3.22.
2. **van Oss-Good-Chaudhury Method:** The specific free energy changes of adsorption (ΔGads) for these probe molecules are analyzed using the van Oss-Good-Chaudhury approach (Equation 6) to calculate the base parameter (γ_s^+) and the acid parameter (γ_s^-) of the sample surface.

$$\gamma_s^{sp} = 2\sqrt{\gamma_s^+ \gamma_s^-} \qquad \text{Equation 6}$$

These parameters (γ_s^- and γ_s^+) were calculated using Equation 7 to estimate the specific component (γ_s^{sp}) of the surface energy (mJ/m^2) (Rudawska and Jacniacka, 2018).

$$-\Delta_{a\,ds}G^{ab} = 2N.a.\left(\sqrt{\gamma_s^+ \gamma_s^-} + \sqrt{\gamma_s^- \gamma_s^+}\right) \qquad \text{Equation 7}$$

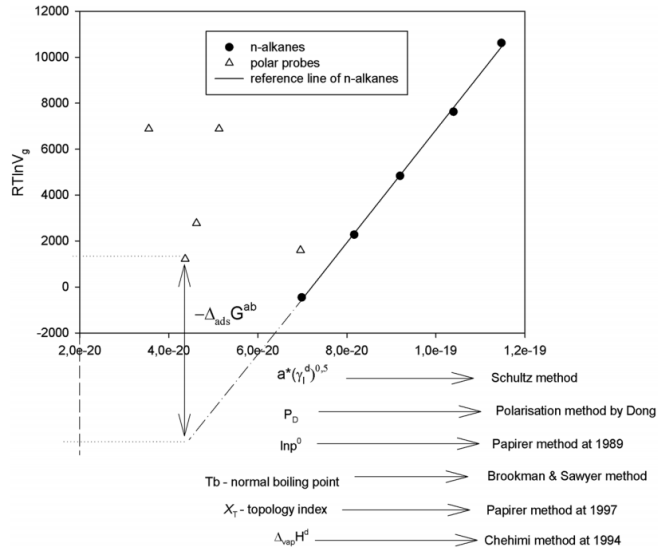

Figure 3. 21 Determination of the specific free enthalpy of adsorption(Kondor et al., 2015)

3.3.2.10 Mechanical strength measurement

A micromanipulation technique for assessing the mechanical strength of

individual soft agglomerates was employed in dry powder inhaler (DPI) formulations(Zhang et al., 2022, Du et al., 2017).

The Rationale for Studying Mechanical Strength

Soft agglomerates, which are desirable for flowability in automated DPI manufacturing, must possess a specific balance of mechanical characteristics.

- **Optimal Flowability:** They should flow readily for smooth, large-scale filling processes.
- **Controlled Mechanical Strength:** They require sufficient strength to withstand the rigors of production, transport, and storage without fragmentation.
- **Dispersibility upon Inhalation:** During inhalation, they must efficiently disintegrate into respirable particles that are suitable for deep lung deposition.

Micromanipulation: A Method for Precise Measurement

Micromanipulation offers a highly accurate method of quantifying the mechanical strength of individual soft agglomerates. This technique involves compressing these particles between two parallel surfaces and meticulously recording the resulting force versus displacement data(Zhang et al., 2022).

Experimental Setup and Instrumentation

The experimental setup (as depicted in Figures 3.23 and 3.24) comprises several key components:

- **Micromanipulation Rig:** This apparatus features a glass slide where individual particles are positioned for testing. A dedicated probe is used to compress the particles.
- **Force Transducer:** This instrument (Model 406A, Aurora Scientific Inc., Canada) measures the applied compression force and converts it into a corresponding voltage signal.
- **Data Acquisition System:** A computer equipped with a PC-30D data acquisition board (Amplicon Liveline, Brighton, UK) captured the

voltage signal generated by the force transducer.

- **Microscope and Camera:** These tools facilitate the visualisation and accurate size measurement of the agglomerates.

Measurement Process

1. **Sample Preparation:** Agglomerates were sieved to achieve a specific size range (355–500 µm). Twenty particles were randomly selected for testing.
2. **Particle Positioning:** A single agglomerate was meticulously placed on a glass slide and manoeuvred close to the compression probe using a micromanipulator.
3. **Compression and Data Acquisition:** The probe compressed the particles at a predetermined speed. Simultaneously, the force transducer measured the force and transmitted the corresponding voltage signal, which was captured by the data acquisition system.
4. **Particle Diameter Measurement:** The diameters of the compressed particles were measured using high-resolution microscope images.

Data Analysis and Strength Parameters

The raw data (voltage vs. displacement) were analysed using specialised software (Micro-Particle Strength Analysis Software, v2.1.x). This analysis identifies critical points on the curve and calculates various parameters that quantify the mechanical strength of the soft agglomerates:

- **Rupture Force (FR):** This value signifies the maximum force required to rupture a particle.
- **Fractional Deformation at Rupture (δ_r):** This parameter expresses the degree of deformation experienced by a particle relative to its initial size at the point of rupture.
- **Nominal Rupture Stress (σ_γ):** This value indicates the internal stress acting on a particle at the moment of rupture.
- **Rupture Tension (T_r):** This value represents the tensile force per unit

cross-sectional area at the rupture point.

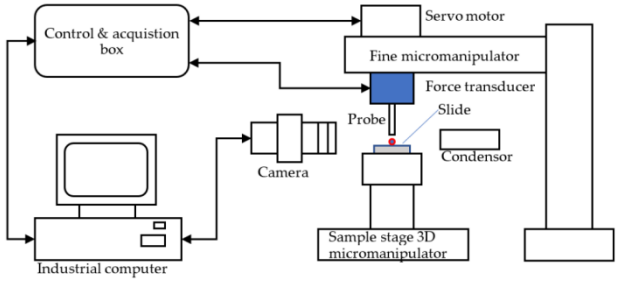

Figure 3. 22 Schematic diagram of the micromanipulation rig(Zhang et al., 2022)

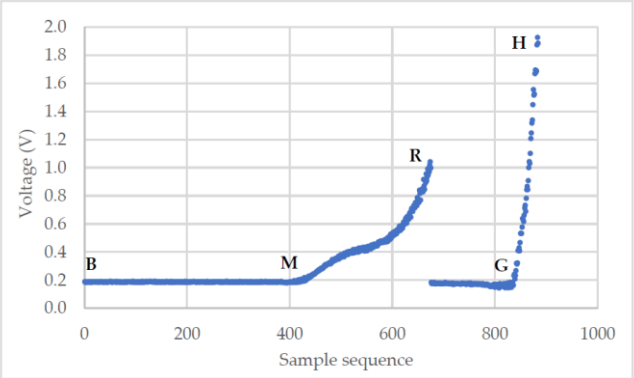

Figure 3. 23 Curve of voltage versus sampling sequence from compression of single agglomerate particles(Zhang et al., 2022)

Equations 8 to 11 detail the calculations used to determine these strength parameters based on the measured data and various constants or predetermined factors, such as compression speed, sampling time, and force transducer properties.

$$FR = s(v_r - v_B) \quad \text{(Equation 8)}$$

$$\delta_r = vT_s(r - m) - C * FR \quad \text{(Equation 9)}$$

$$\sigma_\gamma = \frac{4FR}{\pi D^2} \quad \text{(Equation 10)}$$

$$T_r = \frac{FR}{D} \quad \text{(Equation 11)}$$

where m (m) is the starting point index, r (m) is the rupture point index, v_r (V) is the voltage corresponding to rupture, v_B (V) is the average voltage of the baseline, v (m/s) is the compression speed, T_s (s) is the sampling time, s (NV^{-1}) is the sensitivity of the force transducer, C (mN^{-1}) is the compliance of the force transducer, D (m) is the initial diameter of the single microparticle.

Controlled Conditions and Considerations for Analysis

- The measurements were performed under controlled temperature conditions (20 ± 2 °C) to ensure consistent and reliable results.
- Rupture tension (TR) is considered the most size-independent parameter for comparing the mechanical strength of agglomerates with slight variations in the diameter.

By employing micromanipulation and analysing the obtained data, researchers can gain valuable insights into the mechanical properties of soft agglomerates used in DPIs. This knowledge is instrumental in optimising the DPI formulation design, enabling efficient manufacturing processes, and ultimately ensuring successful inhalation therapy.

3.3.2.11 Deagglomeration behaviours of agglomerates individually

Deagglomeration refers to the breakdown of larger particles into smaller, more inhalable particles when exposed to forces within the inhaler device.

Investigating Deagglomeration with Laser Diffraction

Dry dispersion laser diffraction, a well-established technique (Jaffari et al., 2013), was employed to assess the deagglomeration behaviour of spherical agglomerates. The experimental setup and analysis are as follows.

Sample Preparation and Measurement:

- **Sample Loading:** 5 mg of the soft agglomerate was loaded into a specialised testing tube using a laser diffraction instrument (Sympatec HELOS/RODOS, Sympathec GmbH, Germany).
- **Dispersion Pressure Variation:** A range of dispersion pressures (0.2 to 4.0 bar) was manually applied during the measurement. This simulates the shear forces experienced by agglomerates within the inhaler device.
- **Measurement Control:** The laser diffraction measurement commenced with an R2 lens (0.45–87.5 µm) when the optical concentration (a measure of particle presence in the laser beam) surpassed 0.5% and

automatically stopped when it fell below 0.3%. This ensures a reliable measurement range.

- **Triplicate Measurements:** For each dispersion pressure, the measurement was repeated three times to ensure data accuracy.

Degree of Deagglomeration (DA) calculation

Equation 12 was used to calculate the DA at each applied dispersion pressure. This equation considers the following:

- D_{50}**:** The median particle size (D_{50}) represents the size at which half the particles are larger and the other half are smaller. This value was measured at each dispersion pressure.
- **DH:** This value represents the D_{50} obtained at the highest pressure (4 bar), signifying a state of complete deagglomeration.

A lower DA value indicates a greater extent of deagglomeration, indicating that the dispersion pressure effectively breaks down the agglomerates into finer particles.

$$\mathrm{DA} = \frac{\mathrm{DH}}{\mathrm{D_x}} \qquad Equation\ 12$$

D_x is the median particle size (µm) at each dispersion pressure (0.2–4.0 bar), and DH is expressed as the D_{50} value measured (µm) at 4 bar (full deagglomeration)

Data Presentation:

The DA values calculated at different dispersion pressures were plotted against the corresponding pressures. This plot visually depicts the deagglomeration behaviour of the soft agglomerate formulation, revealing how effectively the particles disperse under increasing shear forces.

3.3.2.12 Deagglomeration behaviours of agglomerates in Turbuhaler®

The flow titration method was used to investigate the cohesive properties of soft agglomerates used in dry powder inhalers (DPIs) (Behara et al., 2011). Cohesiveness refers to the interparticle forces that cause these particles to adhere

to each other, potentially hindering their dispersion within an inhaler device during inhalation.

Flow Titration: Mimicking Inhalation Airflow

The flow titration method offers a controlled environment to simulate the airflow experienced by particles during inhalation from a DPI. The experimental setup and analysis were as followed:

Instrumental Configuration:

- **INHALER™ Adapter (Sympatec GmbH, Germany):** This interface seamlessly connected the DPI device to a laser diffraction instrument (Sympatec HELOS). To mimic the workings of the human mouth, the INHALER™ adapter is intended to acquire particle size distribution data that closely mirror the aerodynamic diameter distribution observed during actual inhalation from the DPI.
- **Laser Diffraction Instrument (Sympatec HELOS):** This instrument plays a critical role in measuring the size distribution of aerosolised particles.

Measurement Process:

1. **Sample Preparation:** A precisely weighed amount of spherical agglomerates (approximately 150 mg) was loaded into a Turbuhaler® DPI device.
2. **Varied Flow Rates:** The DPI device was connected to the INHALER™ adapter in a horizontal position. A series of airflow rates (30, 45, 60, 90, and 120 L/min) was applied to simulate the inhalation process.
3. **Real-Time Particle Size Distribution:** During each flow rate application, the instrument captured rapid particle size distribution measurements (100 measurements per second) over a 5-second period. The R2 lens on the instrument enables the analysis of particles within the size range of 0.45-87.5 µm, ensuring the capture of the relevant particle fraction for efficient lung deposition.

Analysis of Deagglomeration behaviour:

- **Relative Deagglomeration:** This parameter quantifies the extent of particle breakdown within the aerosolised agglomerate. It is calculated as the ratio of the cumulative particle size distribution for aerosolised particles smaller than 5 µm to the corresponding value for the entire particle population within the DPI in the same size range.
- **Flow Rate Profiles:** The relative de-agglomeration values obtained at different flow rates are plotted to create a profile that visually depicts the influence of airflow on particle dispersion.
- **Sigmoidal Equation Fitting:** A non-linear least squares regression analysis was performed to fit the de-agglomeration profile to a three-parameter sigmoidal equation (Equation 13).

$$y = \frac{a}{1 + e^{(-(x-x_0)/b)}} \qquad Equation\ 13$$

- **a** represents the maximum achievable relative de-agglomeration (%), signifying the greatest degree of particle breakdown attainable under the applied flow conditions.
- x_0 represents the specific airflow rate (L/min) at which 50% of the maximum de-agglomeration occurs. This value provides valuable insights into the flow rate required to achieve half the optimal particle dispersion for efficient drug delivery.
- **b:** represents the difference in airflow rate (L/min) between the points where 75% and 25% of the maximum de-agglomeration occur. This parameter reflects the sensitivity of de-agglomeration to changes in airflow rate. A lower b value indicates a more pronounced airflow effect on particle dispersion.

3.3.2.13 Fine particle dispersion of agglomerate in Turbuhaler®

A modified laser diffraction instrument (Sympatec HELOS) was used to investigate the real-time release profiles of fine particles from spherical

agglomerates during inhalation of a Turbuhaler® DPI(Zhang et al., 2020).

Mimicking the Human Respiratory Tract

The experimental setup incorporated several key components to simulate the human respiratory tract and analyse the dispersion behaviour of spherical agglomerates as shown in Figure 3.25.

- **Modified Sympatec HELOS:** This instrument was equipped with an R2 lens suitable for measuring particles within the size range relevant for lung deposition (0.45-87.5 µm).
- **Inhaler Device Adapter:** This adapter facilitates the connection between the Turbuhaler® DPI and laser diffraction instrument.
- **Artificial Throat:** This component mimics the human throat, where larger particles with higher inertia tend to impact and become trapped.
- **Pre-separator:** This element simulates bronchial bifurcation within the lungs, where fine particles with lower inertia can successfully pass through.

Measurement Process and Data Acquisition:

1. **Triggering Measurements:** The laser diffraction measurement commences when the optical concentration (Opc) reaches 1.0% and automatically stops when it falls below 0.5%. This ensured a reliable measurement range that focused on the initial particle release.
2. **Measurement Duration and Sampling:** The measurement lasted for 4 s, with data captured at 100 ms intervals. The airflow rate was maintained at 60 L/min, which mimicked a typical inhalation manoeuvre.
3. **Triplicate Measurements:** Each sample was measured three times to ensure data accuracy.

Data Analysis and Release Profile Generation:

PAQXOS® software was used to analyse the acquired data. The amount of particles released within each 100 ms time interval was calculated by the software using Equations 14 and 15.

$$R = C_{opt} \times dQ_3 \qquad Equation\ 14$$

$$dQ_3 = Q_3(D_{i1}) - Q_3(D_{i2}) \qquad Equation\ 15$$

where dQ_3 represents the volume percentage of particles within a specific size range (%). $Q_3(D_{i1})$ represents the ratio of the total volume of particles that are smaller than D_i to the total volume of all particles. D_i (µm) represents the instantaneous particle size measured at each 100 ms interval within the 4-second duration.

The analysis focused on capturing the particle fraction between D10 of budesonide (around 0.5 µm) and D_{90} of lactose (around 7 µm). This size range encompasses the respirable size range for efficient drug delivery to the lungs.

Visualisation of the Release Profile

Origin 2023b software was used to plot the release amount (R) against time (t). This graph visually depicts the real-time profile of fine particle release from spherical agglomerates during Turbuhaler® actuation.

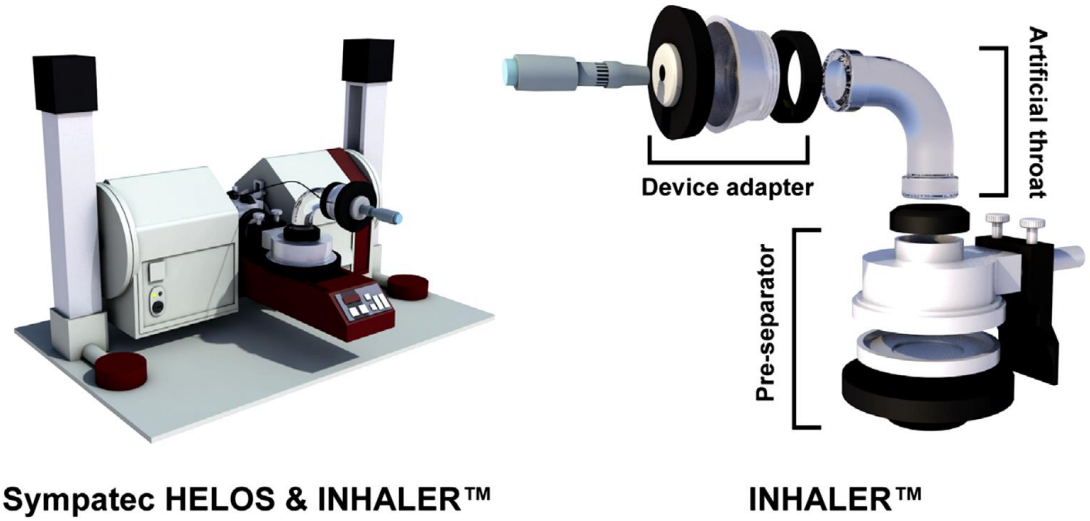

Figure 3. 24 Schematic diagram of Sympatec HELOS & INHALER™.(Zhang et al., 2020)

3.4 Statistical analysis

Statistical analyses were performed to evaluate the experimental data. Descriptive statistics including mean and standard deviation (SD) were calculated using Microsoft Excel 365 (Microsoft Corporation, Redmond, WA, USA). All experiments were performed in triplicates or more to ensure data

reliability. For comparative analysis between two groups, Student's t-test was conducted using SPSS software (IBM SPSS Statistics, Version 28.0). A significance level of $p < 0.05$ was set to indicate statistically significant differences between the groups. This threshold indicates a probability of less than 5% that the observed difference occurred through random chance.

Chapter4.Formulation Study of fine lactose attributes for particle agglomeration via vibration

4.1 Introduction

Agglomerate formulations, typically ranging from 100 to 500 μm in size, offer a versatile approach for improving the delivery efficiency and aerodynamic performance of inhaled medications (Ikegami et al., 2003). They differ from carrier-based dry powder formulations in that the agglomerates are the active ingredients (Figure 4.1). These agglomerates were formed using spheronization techniques, leveraging the inherent cohesive forces of micronised drug particles and fine lactose. The drug to lactose ratio can be adjusted flexibly to meet specific needs. Agglomerate formulations have several advantages:

- **Enhanced deagglomeration efficiency:** Compared to high-shear blends, the cohesive force between particles in agglomerates is weaker, which translates to high de-agglomeration efficiency during inhalation, allowing for better drug delivery to the lungs. However, the agglomerates maintained sufficient stability for handling and dosing during manufacturing.
- **High dose delivery:** Larger agglomerates simplify the manufacturing process, particularly for high-dose medications.
- **Improved inhaler compatibility:** Agglomerates are well-suited for use with specific inhaler devices such as Turbuhaler®. These inhalers generate sufficient turbulence to effectively de-agglomerate and disperse particles, facilitating deep lung deposition (Russo et al., 2004).

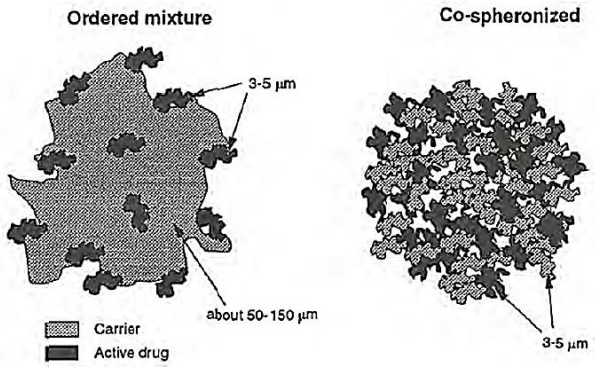

Figure 4. 1 Diagram of an ordered mixture of carrier-based and agglomerate formulation(ZHENG, 2012)

To ensure an agglomerate formulation suitable for various dose strengths, incorporation of extra fine lactose with stable physicochemical properties and negligible cytotoxicity in agglomerate formulations should be considered and optimised for particle agglomeration formulations for inhalation(Lamešić et al., 2017). Research on the production of fine lactose as a diluter is essential to facilitate dosing and deagglomeration. Achieving optimal aerodynamic properties using fine lactose powder for inhalation formulations presents several challenges. First, there is a balance between the three key particle characteristics:

- **Narrow size range:** This ensures uniform aerosolization for efficient drug delivery to the lungs.
- **Suitable cohesion:** Balanced cohesive forces are necessary for efficient deagglomeration during inhalation.
- **Favourable particle shape:** Specific shapes can enhance packing and de-agglomeration behaviour.

Second, deagglomeration efficiency directly influences the performance of inhalation formulations. The agglomerate strength, determined by the particle diameter, packing fraction (ratio of particle volume to total aggregate volume), and work of adhesion/cohesion, plays a crucial role. Real powders exhibit heterogeneity, leading to a distribution of these factors, and consequently, a range of agglomerate strengths within the formulation(Adi et al., 2011a). Agglomerates containing a higher proportion of smaller particles are typically more difficult to aerosolise because of stronger interparticle forces than those with larger cohesive

particles. The presence of a higher proportion of cohesive intermediate-sized lactose particles can promote the formation of loosely packed agglomerates that are readily aerosolised. Third, the particle shape plays a role, and the particle orientation and contact area with other particles influence the packing fraction and interaction forces, impacting the de-agglomeration efficiency(Hassan and Lau, 2009).

Future research should investigate how fine particle properties interact with the manufacturing processes. Establishing a correlation between agglomerate formulation characteristics and aerodynamic performance would accelerate the formulation screening process for inhalation applications. This could potentially lead to the development of fine lactose with optimised properties that creates more open-packed powder beds within the agglomerates, facilitating easier de-agglomeration and improved drug delivery.

Another hurdle in developing stable agglomerate formulations for inhalation is the potential deterioration of dispersion owing to the sticking and caking properties of fine lactose particles(Janssen et al., 2023b). This issue often arises from the presence of an amorphous lactose layer formed during the micronisation process used to reduce the particle size.

Micronisation and formation of amorphous lactose

Micronisation is a high-energy process that can induce changes in the crystallinity of a material. During micronisation, the crystalline structures on the particle surfaces are disrupted, leading to the formation of amorphous regions. While only small amounts of amorphous material are typically produced during lactose micronisation for inhalation applications, these trace quantities can significantly affect the physical stability of the powder (Ward and Schultz, 1995a).

Effect of Amorphous Lactose:

Amorphous lactose is hygroscopic, meaning it readily absorbs moisture from the environment(Listiohadi et al., 2005). Compared to crystalline lactose, amorphous

lactose can absorb up to 100 times more free moisture during storage. The absorbed water acts as a plasticiser, reducing the glass transition temperature (Tg) of the amorphous material. Above its Tg, amorphous lactose becomes rubbery and its viscosity decreases(Joardder et al., 2024). This allows the previously solid glass-like material to flow, collapse, and potentially crystallise.

Uncontrolled recrystallisation and particle growth

Problematic uncontrolled particle growth can occur during storage if the recrystallisation of micronised lactose proceeds haphazardly(Badal et al., 2017). This growth can generate particle fractions outside the desired respirable range (less than 5 μm) for inhalation applications. Additionally, these larger particles can become trapped within aggregates, leading to their deposition in the mouth or throat during inhalation, thereby hindering their intended pulmonary delivery.

Strategies for mitigating amorphous lactose issues:

To minimise the formation of amorphous surfaces, controlled humidity exposure can be employed to induce crystallisation. In an amorphous powder bed, water absorption initially occurs faster than the rate of the water vapour supply, preventing immediate surface saturation. However, over time, the central layers eventually acquire sufficient moisture content to reduce the driving force for further moisture transport. This can lead to a scenario in which the adsorption rate exceeds the transport rate, resulting in surface saturation and subsequent crystallisation. The expulsion of water from the surface creates a rapid vapour supply that can further saturate and crystallise the inner layers (Buckton & Darcy, 1995). However, maintaining a delicate balance is crucial for achieving crystallisation without the formation of unwanted solid bridges owing to the oversaturation of the lactose surface with water.

This study investigated methods to produce micronised lactose particles with a controlled size distribution and shape suitable for inhalation formulations as follows:

- **Micronisation with a controlled process:** A fluidised bed opposed jet

mill was employed to obtain micronised particles with reduced variability in size and shape.

- **Recrystallisation of amorphous lactose:** The inhaled fine lactose particles were fluidised and suspended in a rotating fluidised bed. The up-flowing gas with precisely controlled humidity and temperature facilitated the recrystallisation of amorphous surfaces on the particles. The rotating bed and porous housing design improved the gas exposure to lactose and minimised powder adhesion to the walls.
- **Optimisation of agglomerate properties:** An orthogonal design experiment was conducted to analyse the impact of factors, such as fine lactose size, sieve size, vibration voltage, and frequency, on the resulting agglomerate size, morphology, and mechanical strength.
- **Formulation and characterisation:** Dry powder inhaler (DPI) agglomerate formulations were prepared by mixing micronised budesonide and melatonin particles with optimised fine lactose. Next Generation Impactor (NGI) analysis was used to characterise the formulations.

4.2 Method

4.2.1. Production of fine lactose using air jet mill

Lactose powder was micronised using a fluidised bed opposed jet mill (model 100 AFG; Hosokawa Micron Corporation, Osaka, Japan). The process began by directly loading lactose into the mill chamber and initiating grinding in the automatic mode. A rotating classifier wheel separates the particles by size. Only fine particles with lower inertia pass through the vanes, whereas larger particles are rejected and recirculated back to the grinding zone for further size reduction. A constant airflow maintained by a blower at the mill outlet conveys fine particles that pass through the classifier to the collection cyclone. Within the

cyclone, micronised lactose particles were separated from the air stream and collected in a designated product bin. Finally, any exceptionally fine particles that escaped the cyclone were captured by a filter bag at the end.

Initial investigations focused on the impact of varying the micronisation pressure (0.3-0.8 MPa) on the particle size distribution. Subsequently, during the optimisation phase, three different load levels (200, 300, and 400 g/min) and rotational speeds (10000, 20000 and 30000 rpm) for the classifier wheel were investigated. Nine experimental runs were conducted, with particle size and shape analyses performed on the obtained products.

4.2.2. Preparation of different shaped lactose

Three distinct lactose morphologies (needle-shaped N-Lac, plate-shaped P-Lac, and tomahawk-shaped T-Lac) were prepared using an antisolvent crystallisation method with rapid precipitation as previously reported(Bund and Pandit, 2007).

Crystallisation Process:

- 0.25 g/mL α-lactose monohydrate solution (20 mL) was prepared in distilled water at 80 °C. The solution was then gradually cooled to 5-10 °C at a rate of 5 °C/min.
- During cooling, ethanol was pumped into the solution at a predetermined flow rate and maintained at 10 °C with 300 W of ultrasonic power applied throughout the addition period.
- Specific ethanol addition parameters to induce varying recrystallisation patterns were used for each lactose shape:
    - N-Lac: 2 mL/min for 30 minutes
    - P-Lac: 6 mL/min for 10 minutes
    - T-Lac: 10 mL/min for 3 minutes
- The obtained lactose crystals were filtered using a vacuum filter, dried at 40 °C in an oven, and sieved through a 1 mm sieve.
- Prior to formulation preparation, the recrystallized lactose underwent micronisation with an air jet mill (details in Section 4.2.1).

4.2.3 Moisture induced conditioning of lactose amorphous surface.

To enhance the physicochemical stability of micronised powders, a conditioning step is often employed. This process targets the conversion of amorphous regions into crystalline structures under a controlled relative humidity and temperature.

Mechanism of controlled humidity and temperature during re-crystallization:

Conditioning can be achieved through controlled moisture adsorption and temperature manipulation. By carefully managing moisture content, the glass transition temperature (Tg) of amorphous materials in the formulation could be lowered(Ebnesajjad, 2016). This, in turn, increases the molecular mobility when the surrounding temperature is set above Tg.

However, this increased mobility creates a double-edged sword. While it facilitates a desired recrystallisation process, uncontrolled recrystallisation can lead to several challenges. Excessive particle growth can occur, pushing particles beyond the optimal size range (0.5-5 μm) for efficient inhalation and potentially hindering their ability to reach the lungs.

Additionally, solid bridging might form between lactose carrier particles due to uncontrolled crystal growth. These bridges can negatively impact the flowability of the powder, hindering its proper dispersion during inhalation. Therefore, precise control of both moisture adsorption and temperature during conditioning is essential to achieve optimal particle properties for effective DPI function.

Investigation of the optimal conditioning parameters

This study systematically investigates the influence of conditioning parameters on micronised lactose (as detailed in Section 4.2.1) to identify the optimal settings for:

1.Rapid and complete conversion of amorphous material to crystalline form.

2.Minimised particle growth.

3.Reduced surface energy.

Experimental Design:

Micronised lactose was subjected to various conditioning settings in a rotating fluidised bed (refer to Section 3.3.1.2). The temperature was fixed at 25°C to reflect the typical manufacturing conditions. The relative humidity was varied between 40% and 70%, with durations of 8 h and 24 h, respectively (Figure 4.2).

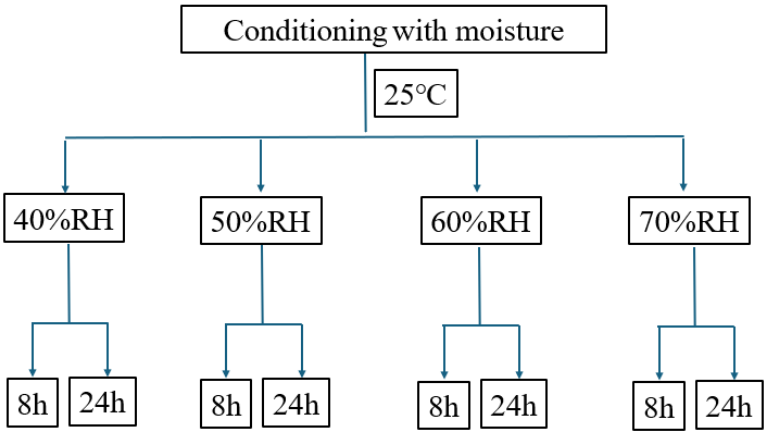

Figure 4. 2 Systematic evaluation of conditioning parameters for micronised lactose

4.2.4. Packing fraction distributions

By pouring 15 g of binary mixture of powders slowly into a 50 ml measuring cylinder, the tapped volume for each powder was determined in triplicate over 1024 taps in 5 min with an automatic tapper (AUTOTAP™, Quantachrome Instruments, Boynton Beach, FL, USA). By normalising the weight to the true density of lactose (1.545 g cc), the true volume or volume of the particles was calculated. The packing fraction was calculated by dividing the true volume by the tapped volume for each time interval.

4.2.5. Mean Particle Diameter and Particle Shape

The particle size distribution of the materials was determined by laser diffractometry. This method employed a Sympatec HELOS laser diffraction instrument (Sympatec GmbH, Clausthal-Zellerfield, Germany) as mentioned in Section 3.3.2.1.

The Scanning Electron Microscopy (SEM) and Microscopy were used to characterise the shape and size of the recrystallised large particles and micronised

particles as illustrated in Section 3.3.2.2 and Section 3.3.2.3, respectively.

4.2.6. Performance evaluation of a vibratory bowl feeder

The vibratory bowel feeder uses electromagnetic vibrations converted into mechanical movements to facilitate the agglomeration of fine lactose particles. These particles move in small jumps along an inclined track due to vibrations generated by leaf springs operating at various voltage and frequency settings (Kadam, 2017). This rolling motion encourages the adhesion of fine lactose particles, forming agglomerates of specific sizes and mechanical strengths.

Performance evaluation was conducted by varying the operational voltage and working frequency. Approximately 50 g of micronised fine lactose was deposited in a bowl after sieving. Two key aspects are evaluated:

- **Production rate:** This refers to the time taken to obtain agglomerates within the desired size range (200-500 μm) exiting the feeder bowl, along with the percentage of total agglomerates within this range (yield).
- **Powder movement behaviour:** The phenomenon of powder movement on the feeder during vibration was observed visually.

A graphical analysis was performed using a one-factor-at-a-time approach. The operating voltage was set to a constant value (e.g., 150V) while varying the frequency. Three readings were recorded for each frequency, and the average was calculated to determine the final feed rate. The process was repeated for different voltage settings while maintaining a constant frequency.

4.2.7. Production of agglomerates by vibration

Fine lactose required sufficient cohesive and adhesive properties to achieve consistent drug delivery through spherical agglomerates. Both the milled API (active pharmaceutical ingredient) and fine lactose were sieved using a 355 μm sieve to eliminate clusters and ensure uniform powder consistency. The sieved API and lactose were then mixed in a Turbula® mixer for 10 min at 42 rpm to obtain a homogeneous mixture. After mixing, the mixture was sieved again to remove any larger particles before being processed in a vibration bowl feeder.

This feeder likely facilitated the formation of the initial pre-agglomerate structures. The pre-agglomerates were then transferred to a rotating agglomerator (as shown in Figure 4.3) for final smoothing and shaping into spherical structures. The finished spherical agglomerate formulations were collected in sealed containers with a desiccant to minimise moisture absorption and ensure stability before further analysis.

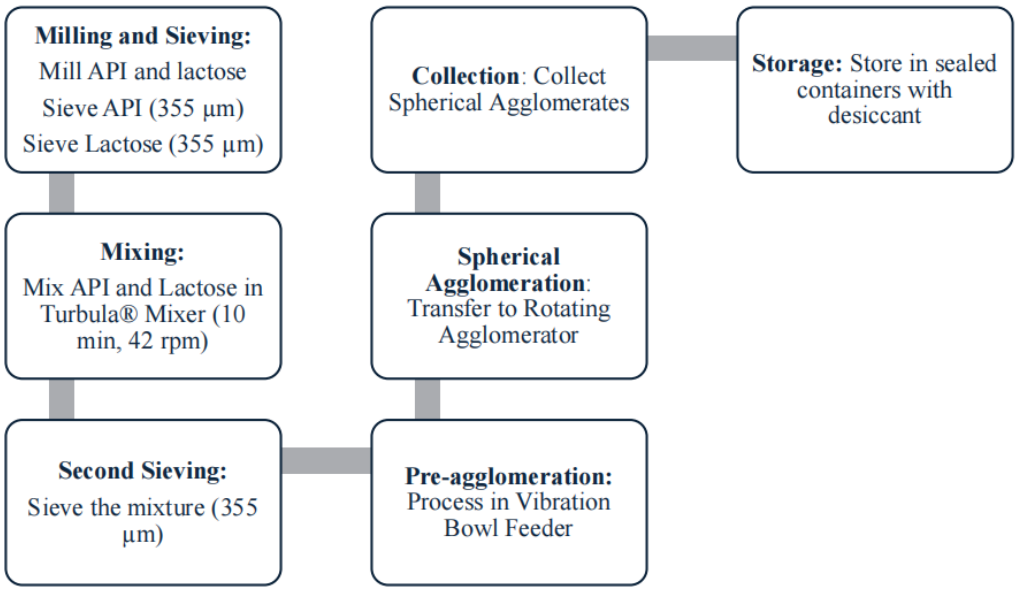

Figure 4. 3 Flow diagram for particle agglomerationprocess

4.2.8 Micromanipulation for Agglomerate Strength Measurement

The micromanipulation technique was employed to measure the mechanical properties of the agglomerates as described in Section 3.3.2.10 (Zhang et al., 2009).

Data Analysis:

30 agglomerate particles were randomly selected from each sample for compression at room temperature.

From the recorded force-displacement curve, the following parameters were determined:

- **Rupture Force**: The maximum force applied before the agglomerate ruptures.
- **Deformation at Rupture**: The change in diameter of the agglomerate at

the point of rupture.

- **Rupture Tension**: Calculated as the rupture force divided by the diameter of the agglomerate.

The data were then analysed using Micro-Particle Strength Analysis Software (v2.1.x, Micromanipulation and Microencapsulation Research Group (μCAP), School of Chemical Engineering, University of Birmingham, UK).

4.2.9. In Vitro Aerodynamic Assessment

A Next Generation Impactor (NGI) equipped with a United States Pharmacopoeia (USP) induction port was used to evaluate the aerosolization properties of the powder formulations. This section details the methodology employed:

Materials and Preparation:

- **Powder Collection Cups:** To minimise particle bouncing during testing, the collection cups were pre-coated with a 0.5% (w/v) silicone oil solution in n-hexane before each run.
- **Sample Loading:** Each Turbuhaler device (Symbicort Turbuhaler®, AstraZeneca) was filled with a precisely weighed dose of 150 mg of the agglomerate formulation (with a tolerance of ± 15 mg). The device was then connected to the NGI using an adapter.

NGI settings and operations:

- **Airflow Rate:** A constant airflow rate of 60 L/min (with a tolerance of ± 5 L/min) was maintained throughout the test using an HCP5 pump (Copley Scientific, MN, USA). The airflow was monitored using a DFM 2000 flow meter (Copley Scientific, MN, USA) and sustained for 4 s.
- **Sample Collection:** Following aerosolisation, the powder deposited on each stage of the impactor was collected using a mobile phase solvent (acetonitrile/water, 60:40).

Data Analysis:

- **Emitted Dose (ED):** Three Turbuhaler devices were aerosolised from

each powder mixture. The emitted dose (ED) for each capsule was determined by calculating the difference between the initial drug loaded and the amount remaining in the device and adapter after testing.

- **Fine Particle Fraction (FPF):** The FPF represents the percentage by mass of drug particles within the emitted dose with an aerodynamic diameter of less than 5 μm. This value was calculated relative to the total mass of recovered drug.

4.2.10. Mechanism study of De-agglomeration Behavior

The flow titration method, which measures the particle size distribution at a sequence of different flow rates, was applied to characterise the effect of lactose shape on the deagglomeration behaviour of agglomerates (Behara et al., 2011).

Equipment and Setup:

- **Inhaler Adapter (INHALER™):** This device (Sympatec GmbH, Clausthal-Zellerfeld, Germany) acts as an interface between the Sympatec HELOS analyzer and the inhaler. It can be configured to accommodate different inhalation devices.
- **Sympatec HELOS:** This laser diffraction instrument was used to measure particle size distribution. Measurements were initiated upon reaching the minimum optical concentration of 0.5%. An R2 lens with a size range of 0.45-87.5 μm was used to analyse the inhaled particle size distribution.
- **Test Setup:**
    - Approximately 150 mg of the agglomerates was loaded into a Turbuhaler® device.
    - The Turbuhaler® was then connected to the INHALER™ adapter in a horizontal position.

Measurement Process:

- **Airflow Rates:** The de-agglomeration behavior was evaluated at airflow rates ranging from 30 L/min to 120 L/min, mimicking the peak inhalation

flow rates reported for humans (20-160 L/min) (Baloira et al., 2021, Hua et al., 2021)

- **Real-Time Measurements:** Rapid, real-time measurements were conducted at each airflow rate, capturing 100 measurements per second over a 5-second period.
- **Measurement Replicates:** The measurements at each airflow rate were repeated three times for better accuracy.

Data normalisation and analysis

- **Particle size distribution variation:** Because the particle size distribution can vary depending on the formulation, a normalisation step was employed. The fraction of particles smaller than 5 μm after dispersion was normalised against the corresponding value obtained from the RODOS module, which represents 100% deagglomeration.
- **Selection of Measurement:** Cumulative proportion below 5 μm was chosen for analysis, as it is relevant for lower respiratory tract deposition.
- **Relative De-agglomeration Calculation:** The relative de-agglomeration (%) was calculated using the following formula (Equation. 1) based on the average of three measurements for each flow rate and the corresponding standard deviations (SD).

$$R=\frac{FI}{FR}\times 100\% \qquad \text{Equation. 1}$$

where R represented the relative de-agglomeration, %,

FI: particle fraction <5.0 μm from the INHALER™ module at various flow rate,

FR: particle fraction <5.0μm from the RODOS module

4.2.11. Determination of Surface Roughness

AFM imaging of the lactose samples was used to characterise the surface roughness. Following a previously described method in Section 3.3.2.4 (Islam et al., 2005), lactose particles were sprinkled onto silicon wafers. The surface morphology of these particles was then analyzed using tapping mode AFM in air

at ambient temperature and humidity.

Bruker ICON AFM (Bruker Nano, Inc., Germany) was used for the analysis. Before measurement, the samples were placed on carbon sticky tabs. High-resolution images were captured over 3 × 3 μm² areas using the tapping mode with a scan rate of 1 Hz and a high aspect ratio silicon probe. Image analysis software (Simulator, Leica Microsystem) was then used to determine the average roughness and root mean square (RMS) roughness (Rq) of the particles.

4.3. RESULTS

4.3.1 Micronisation Process

In addition to the powder packing fraction (ratio of tapped density to true density), the particle size and shape factor play a crucial role in determining the suitability of a powder for particle agglomeration. Only when micronised with a specific starting lactose powder and micronisation process can the obtained fine particles produce spherical agglomerates with the desired size distribution and mechanical strength for dosing and dispersion.

Therefore, coarse lactose was micronised using various micronisation parameters and analysed for particle size distribution, surface area, circularity, hygroscopicity, density, and surface energy. These data were utilised to elucidate the diverse aerodynamic behaviours exhibited by the resulting spherical agglomerates in the subsequent chapters.

The chosen pressures (3 bar, 5 bar, and 8 bar) were selected based on preliminary investigations and represent a range encompassing typical operating conditions for this type of micronization process. These pressures were chosen to explore the effect of increasing process energy on particle size reduction while considering potential factors such as equipment limitations and the risk of particle degradation.

4.3.1.1 Effects of Varying micronisation pressure

Particle size distribution

The particle size distribution data presented in Table 4.1 reveals a clear correlation between the classifying speed and particle size. Higher classifying speeds resulted in a statistically significant decrease in particle size, whereas the micronisation pressure itself appeared to have a minimal impact within the tested range. However, manipulating the micronisation process at high pressures can generate ultrafine materials. As the pressure increased, the proportion of particles smaller than 2 μm also increased. Interestingly, the span value of the size distribution also changed, decreasing from 4.66 at 8 bar to 4.16 at 3 bar(10000rpm). This indicates more rapid generation of ultrafine particles at higher micronisation pressures.

Table 4. 1 Size distribution and production speed results for jet milled coarse particles.

Grinding pressure/ bar	Classifier speed/rpm	Particle size distribution/μm			span	Production speed/(g/min)
		D10	D50	D90		
3	10000	2.73±0.23	8.00±1.18	35.97±4.96	4.16	127.10
	30000	1.20±0.03	3.57±0.08	7.74±0.35	1.83	32.43
5	10000	2.58±0.08	7.51±0.46	35.42±2.95	4.37	135.06
	30000	0.87±0.03	3.18±0.12	7.25±1.14	2.01	47.11
8	10000	2.28±0.12	6.22±1.09	31.24±3.02	4.66	154.20
	30000	0.74±0.11	3.07±0.07	7.17±0.15	2.09	64.45

Two mechanisms contributed to the observed particle size reduction during micronisation.

1. Effect of Classification Speed

A higher rotational speed of the classifying wheel translates into a stronger centrifugal force. This force acts against the movement of particles through the wheel vanes. Only smaller and lighter lactose particles can overcome this force and be directed towards the product collection bin.

2. Effect of Grinding Pressure

Increasing the grinding pressure (GP) within the micronisation chamber significantly affects the particle size. At higher air pressures, the velocity of particle-particle collisions increases. This enhanced collision energy promotes fracturing of coarse particles through a mechanism known as brittle fracture. Brittle fracture involves the propagation of cracks within the particle structure,

ultimately leading to fragmentation and reduction in the median particle size.

Thermal and structural analysis

The PXRD data (Figure. 4.4) revealed no significant changes in the crystalline structure of lactose monohydrate following micronisation in any batch. This suggests that the micronisation process did not induce the transformation from monohydrate to anhydrous lactose. However, the DSC analysis (Figure. 4.5) for micronised batches processed at 8 bar presented an interesting observation. Two distinct dehydration peaks were identified, indicating the potential presence of different water environments within lactose particles.

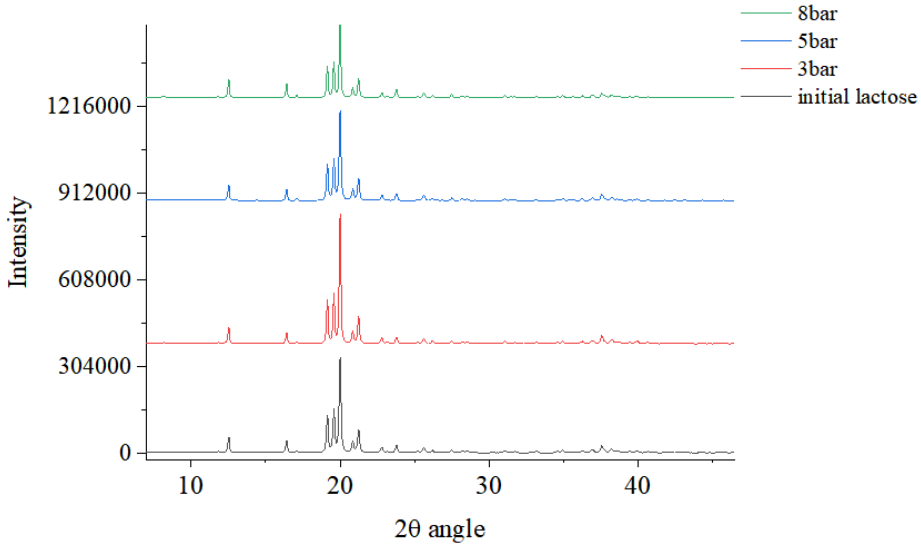

Figure 4. 4 X-ray powder diffractometry of lactose at different micronisation pressures.

The endothermic transition observed in the DSC data for all samples between 140-145°C aligns with the loss of water molecules incorporated within the lactose monohydrate crystal structure, as previously reported(GombÁs et al., 2002). This dehydration event corresponds to the removal of water molecules, which are essential for maintaining the monohydrate form.

Furthermore, the melting and decomposition of lactose monohydrate were observed in the range of 214-217°C, which is consistent with previous findings(Garnier et al., 2008).

Interestingly, the DSC data for micronised batches processed at 5 bar and higher pressures displayed additional exothermic transitions between 170-180°C. The

nature of these exothermic events requires further investigation. However, the broad dehydration endotherms observed at 140-145°C in these batches suggest a potential interaction between the micronisation process and water molecules within the lactose particles.

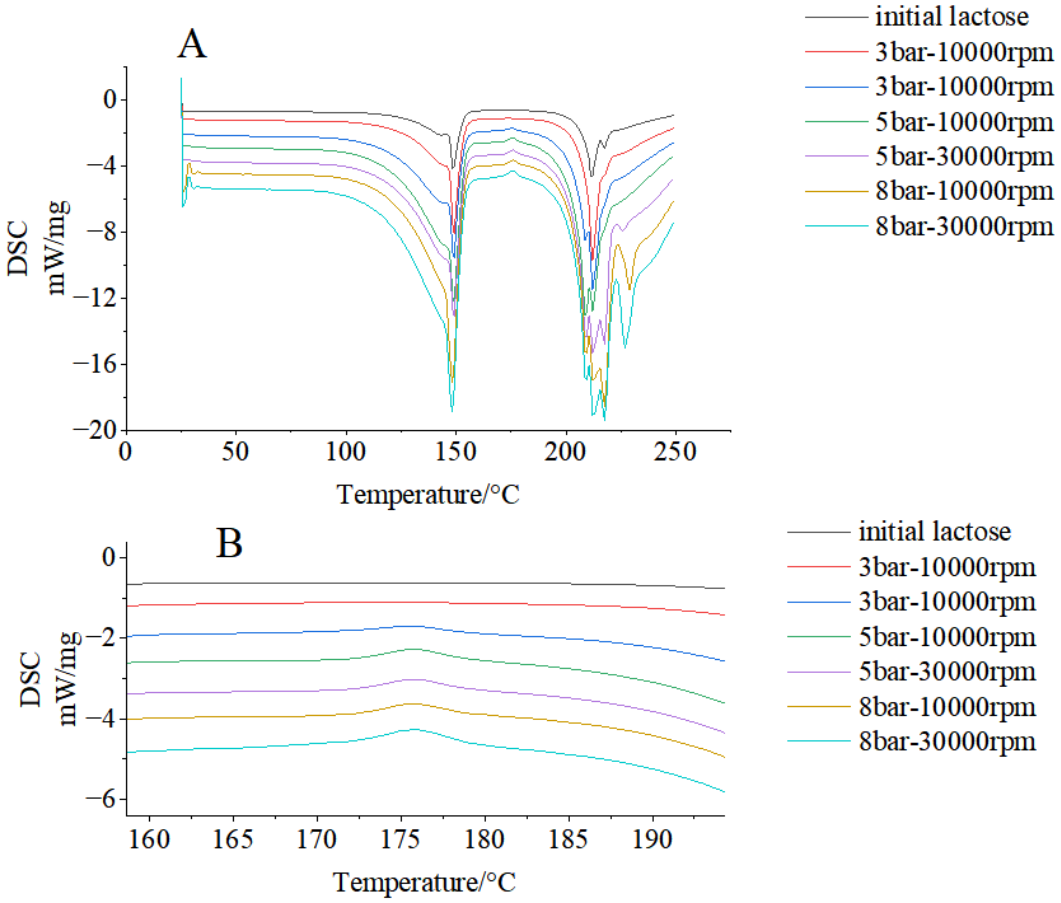

Figure 4. 5 Differential Scanning Calorimetry (DSC) traces of micronised lactose as compared to the starting material at various pressures. (A show the full DSC thermogram, B focuses on the region between 160 and 190 °C for a magnified view)

The exothermic peaks observed in the DSC data of micronised lactose at high pressures likely indicate recrystallisation of amorphous lactose monohydrate(Listiohadi et al., 2009). This suggests that micronisation, particularly at higher pressures, disrupts the crystal structure of lactose monohydrate. Interestingly, the micronised batches processed at 3 bar exhibited negligible exothermic events. This implies that these samples experienced minimal fracturing compared with the unmicronised starting material. Therefore,

to investigate the effects of varying the rotational speed on the particle size and shape while minimising disruption to the crystal structure, further studies were conducted using a micronisation pressure of 3 bar.

4.3.1.2. Effects of Varying Rotational Speed on size and shape

The classifier wheel speed plays a significant role in shaping the size distribution of micronised lactose particles as shown in Table 4. 2. However, its effectiveness can be influenced by the processing load. Lower feed loads seem to benefit more from the increased speed in terms of both size and shape control.

Reduced Variation at Lower Feed Loads: Increasing the classifier wheel speed from 10,000 rpm to 30,000 rpm generally led to a decrease in the "span value" for particle size distribution and shape descriptors. This was observed for the feed loads of 200 g/min (A1-A3) and 300 g/min (B1-B3) This signifies a narrower distribution of particle sizes and shapes, which is believed to facilitate the formation of micronised particles with a more uniform mechanical strength profile for successful de-agglomeration.

Limited Improvement at High Feed Loads: The trend of improvement with increased speed did not hold true for the higher feed load of 400 g/min (C1-C3). The circularity and aspect ratio (indicators of roundness and elongation, respectively) did not show significant improvement despite increasing the speed from 10,000 to 30,000 rpm. This suggests a potential limitation of the classifier wheel at high processing loads.

Smoother particle morphology: Unmilled lactose exhibited the lowest circularity and highest aspect ratio values, signifying a less spherical and more elongated shape compared to micronised particles. Micronisation effectively transforms the particles into a smoother and rounder morphology owing to the abrasive forces experienced during the processing.

Speed and Shape Relationship: The impact of the classifier wheel speed on the shape descriptors was more pronounced at lower feed loads (200 g/min and 300 g/min) than at higher loads (400 g/min). This suggests that higher speeds are

more effective for shaping particles at lower processing volumes.

Balancing Speed and Size Distribution: While 20,000 rpm speed with a 200 g/min feed load (A2/A3) resulted in a narrower size distribution than 10,000 rpm, the particle shapes remained similar. Conversely, using a 400 g/min feed load (C1/C2/C3) demonstrated reduced classifier wheel efficiency in terms of size distribution improvement at higher speeds without affecting the final particle shapes.

Table 4. 2 Descriptive statistics of the shape and size descriptors for the unmilled and micronised lactose

Batch No.	Feed load(g/min)	Classifier Speed (rpm)	Particle size/μm			Span	Circularity	Aspect ratio
			D10	D50	D90			
Unmilled lactose			8.52±0.16	37.74±0.25	177.24±0.38	4.47	0.62±0.28	1.51±0.63
A1	200	10000	2.58±0.08	7.51±0.46	35.42±2.95	4.37	0.81±0.17	1.41±0.25
A2	200	20000	1.60±0.09	4.73±0.26	13.93±2.40	2.61	0.85±0.09	1.38±0.12
A3	200	30000	1.87±0.03	3.18±0.12	8.25±1.14	2.01	0.87±0.04	1.39±0.22
B1	300	10000	2.28±0.12	8.22±1.09	31.24±9.02	3.52	0.84±0.17	1.42±0.05
B2	300	20000	1.75±0.03	4.50±0.13	12.42±3.36	2.37	0.85±0.11	1.41±0.07
B3	300	30000	1.28±0.10	3.28±0.08	6.39±0.17	1.56	0.87±0.05	1.38±0.04
C1	400	10000	2.58±0.08	7.21±0.41	33.62±2.39	4.13	0.83±0.28	1.53±0.16
C2	400	20000	1.44±0.02	3.64±0.06	11.82±0.46	3.40	0.85±0.30	1.49±0.13
C3	400	30000	0.52±0.01	3.15±0.10	7.58±0.42	2.24	0.84±0.32	1.46±0.15

The improved classification efficiency of the fluid bed jet mill relies on the increased centrifugal force exerted on micronised particles at higher classifier wheel speeds, enabling lactose intake with a narrower size distribution. This narrower size distribution contributed to the reduced variation in the particle shapes. However, when operating at a high feed load of 400 g/min, more particles were propelled against the rotating classifier wheel, resulting in insufficient micronised particles exiting the milling chamber. Furthermore, the increased feed load of unmilled lactose resulted in a higher frequency of interparticle and particle-wall collisions within the processing equipment. This increased collision frequency led to the formation of irregularly shaped agglomerates with a wider size distribution, as evidenced by the lack of a significant reduction in the span values of shape descriptorsIt is crucial to note that particle morphology significantly influences lung deposition. Studies have

shown that spherical particles with smooth surfaces exhibit improved aerodynamic behavior and enhanced deposition in the target regions of the lungs (e.g.,: previous study demonstrated the impact of spherical particles on lung deposition(Lv et al., 2024)). In contrast, irregular or needle-shaped particles may exhibit increased deposition in the upper airways, potentially leading to adverse effects (e.g., Gao et al. (2020) demonstrated the negative impact of irregular particle shapes on lung deposition).

This observation highlights the importance of controlling particle morphology during the agglomeration process to achieve optimal lung deposition and minimize the risk of adverse effects.

4.3.1.3. Milling lactose with different initial shape

While adjusting the feed load and classifier wheel speed of the fluid bed jet mill can effectively control the particle size of micronised lactose within the capabilities of the machine, it only marginally improved sphericity and reduced elongation compared to the unmilled starting material.

However, the success of deagglomeration of these micronised lactose formulations depends heavily on their packing fraction. This packing fraction can be significantly influenced by various particle shape parameters even for powders with similar particle size distributions. Therefore, a deeper understanding of the impact of the particle shape on aerosolization, deposition, and de-agglomeration behaviour is crucial. By identifying and tailoring these relevant shape properties, the aerosolization performance of the final agglomerate formulations can be optimised.

Solid-state characterization

X-ray diffraction (PXRD) analysis confirmed that all lactose samples, regardless of their shape after recrystallisation, exhibited a predominantly crystalline structure, as shown in Figure 4.6. Similarly, Karl Fischer titration revealed no significant differences in water content between the samples, as shown in Table 4.3.

These findings suggest that recrystallisation resulted in predominantly crystalline lactose particles with a consistent water content (close to the theoretical value of lactose monohydrate). Consequently, the solid-state properties of the particles are unlikely to significantly influence their inhalation performance compared to the initial lactose samples.

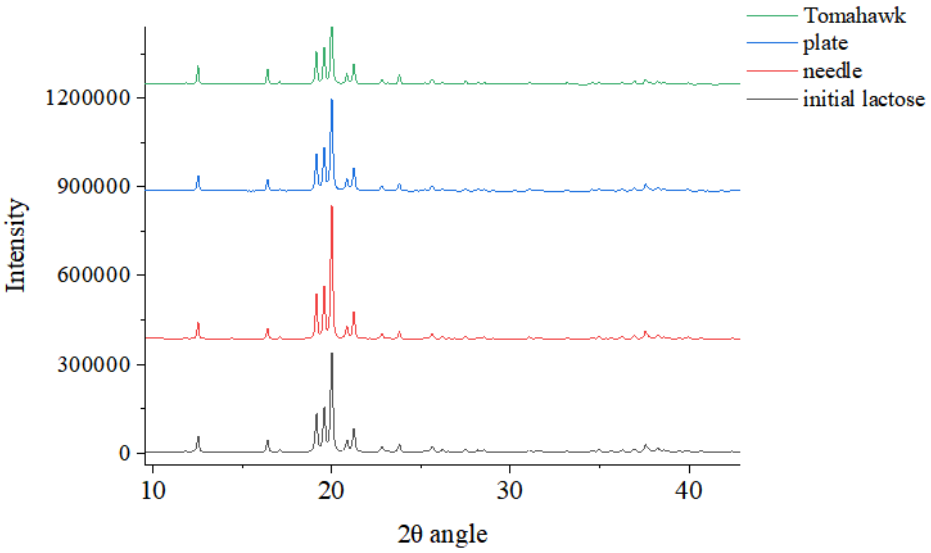

Figure 4. 6 X-ray diffraction (PXRD) results of different shape of lactose

Table 4. 3 Water content of the different shaped recrystallized lactose by Karl-Fischer titration

Shape	Water content/%
Lactose	5.24±0.02
Needle	5.25±0.04
Tomahawk	5.24±0.01
Plate	5.26±0.04

Lactose Particle Characteristics

Laser diffraction, a common technique used in this study to measure the particle size, can be misleading for irregularly shaped particles. These particles, like the ones studied here (plate-shaped, needle-shaped, and tomahawk-shaped), have varying dimensions (length, width, height), and their orientation during the laser measurement significantly impacts the results, as shown in Figure 4.7. To overcome this limitation, this study combined laser diffraction with microscopy

to obtain a more comprehensive understanding of particle size distribution. Microscopy allows for direct observation of the particle shapes and dimensions.

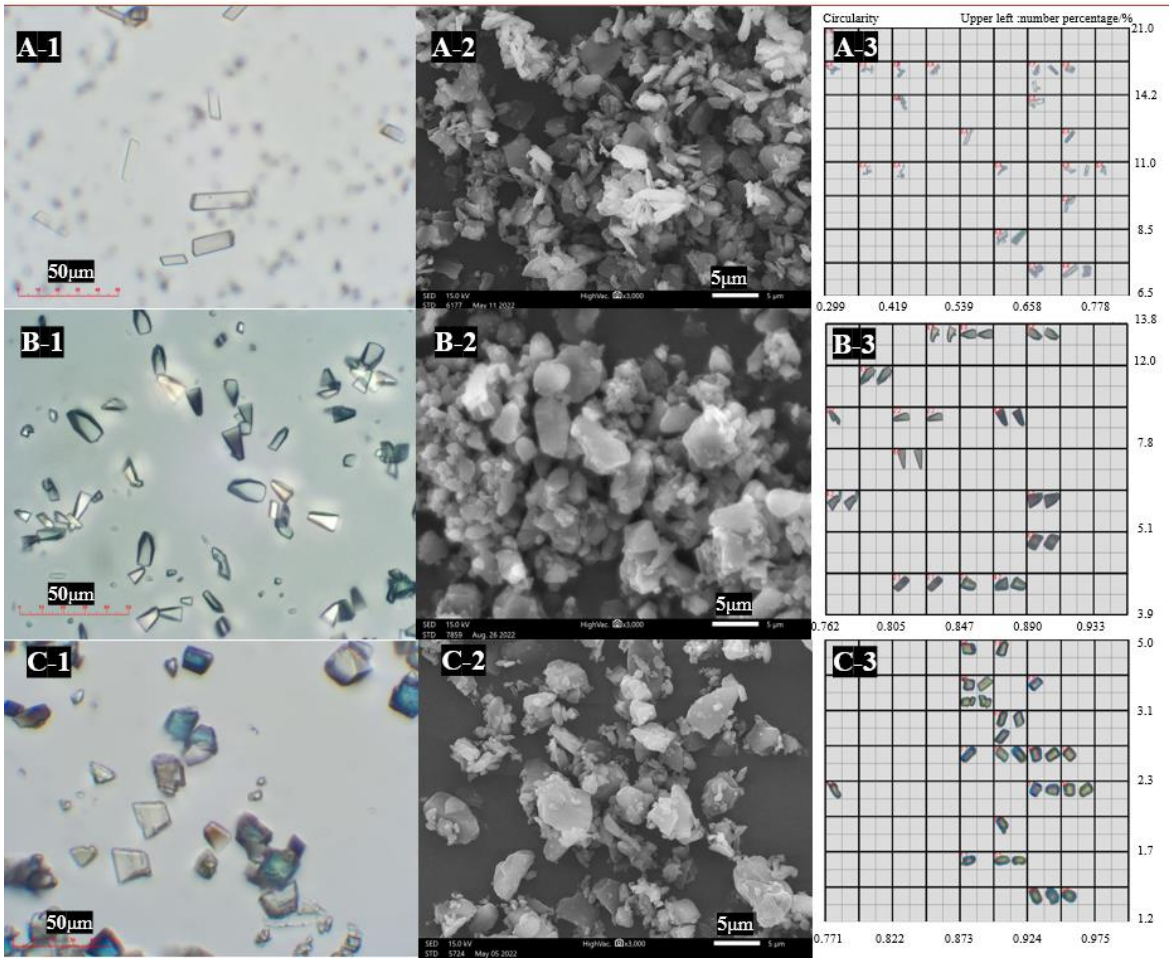

Figure 4. 7 Optical images of different shape lactose before (A1, B1 and C1) and after micronisation (A2, B2 and C2) and shape analysis of crystallized lactose (A3, B3 and C3) (A: needle lactose, B: tomahawk lactose and C: plate lactose)

The combined approach proved to be valuable for each particle type:

- **Plate-Shaped Lactose:** Interestingly, the laser diffraction measurement (D50%(laser) = 18.5 µm) aligned reasonably well with the average length observed using microscopy (D50(optical) = 14.2 µm), as shown in Table 4.4. This suggests that in this specific case, the laser diffraction measurement might have coincidentally captured a dimension close to the actual side length of the plate-shaped particles.
- **Needle-Shaped Lactose:** Laser diffraction yielded a D50 of 11.6 µm, which significantly underestimated the size compared with microscopy observations. Most particles had a length exceeding 20 µm and a width of

approximately 2 μm. This discrepancy arises because laser light can capture a combination of both the length and width of these elongated particles during the measurement. Therefore, the study adopted the D50(optical) of 24.1 μm, reflecting the length observed through microscopy, for a more accurate representation.

- **Tomahawk-Shaped Lactose:** Both laser diffraction and optical measurement yielded similar size distributions, but the laser diffraction measurement consistently gave a larger size. This is because the irregular surfaces of these particles cause additional light diffraction, leading to an overestimation of the particle size. Therefore, the optical image measurement results were used as the characteristic sizes.

Table 4. 4 Size properties of different shape particles

Shape	D50 (laser)/ μm	D50 (optical)/μm
tomahawk	15.9±0.07	13.2±0.13
plate	18.5±0.11	14.2±0.08
needle	11.6±0.10	24.1±0.06

By combining these two techniques, this study provides a more comprehensive picture of the particle size distribution for all non-spherical lactose particles. This approach highlights the importance of considering particle shape for the accurate characterisation of materials that deviate from perfect spheres.

Effect of micronisation on bulk property of lactose

Micronisation and Lactose Particle Shape

Micronisation significantly improved the sphericity (roundness) of all three lactose samples, as reflected by the increased mean circularity values (Figure 4.8). However, the initial particle shapes were largely preserved despite micronisation. Needle-shaped lactose particles remained significantly less circular compared to plate and Tomahawk shapes, indicating that micronisation was not entirely effective in transforming their elongated form.

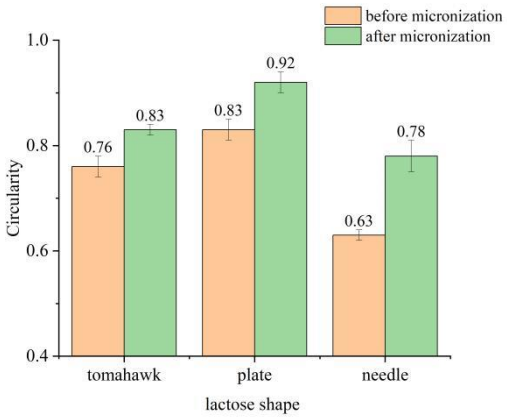

Figure 4. 8 Change in circularity before and after micronisation for different lactose shapes

Density and Packing Implications

Furthermore, differences in the density properties of micronised lactose powders suggest variations in their internal structures (cohesive matrix). These structural differences may influence the packing of the powders during particle agglomeration. Consequently, the needle-shaped lactose, with a higher packing fraction (25.78 ± 0.41), as shown in Table 4.5, is expected to form a more consolidated powder bed compared to plate lactose.

Table 4. 5 Characteristic size and shape factors of different shape lactose after micronisation

Shape	D50 (μm)	span	ρbulk (g/cm^3, n=0)	ρtap (g/cm^3, n=2,500)	packing fraction
tomahawk	3.15±0.10	1.68	0.25±0.01	0.33±0.02	22.81±1.07
plate	3.37±0.07	1.78	0.25±0.04	0.34±0.01	23.60±0.11
needle	3.18±0.12	2.01	0.23±0.03	0.37±0.01	25.78±0.41

Agglomerate strength and mechanism of deagglomeration.

We hypothesised that the varied shapes of lactose particles would result in different structures of the cohesive powder bed after agglomeration, leading to variations in de-agglomeration behaviour. To elucidate this mechanism, an experiment was designed to investigate the influence of lactose shape on both the agglomerate strength and relative deagglomeration.

Table 4. 6 Summary results of agglomerate density and mechanical property

	Density/ (g/cm^3)	Rupture force / (mN)	Rupture Deformation/ (%)	Rupture Tension/(μN/μm)
tomahawk	0.28±0.01	1.94±0.26	3.13±1.19	0.0020±0.0010
plate	0.31±0.00	2.51±0.71	5.96±2.15	0.0048±0.0029
needle	0.35±0.03	4.46±0.56	6.35±1.00	0.0070±0.0016
Turbuhaler®	0.34±0.00	1.83±0.83	4.33±1.27	0.0037±0.0014

The agglomerate strength was characterised using a compression method, as shown in Table 4.6, because the rupture behaviour of agglomerates under compaction is highly sensitive to their microstructure. All the agglomerate formulations exhibited rupture deformations within 10%, suggesting that they could be classified as elastic particles (Paul et al., 2014). The rupture tension and force of needle-shaped lactose agglomerates were approximately twofold those of Tomahawk and plate-shaped lactose agglomerates, indicating a more elastic nature and lower susceptibility to de-agglomeration.

These mechanical properties demonstrate the overall mechanical stability of all the obtained agglomerated particles, which are suitable for pharmaceutical manufacturing. This stability can be further confirmed by comparing the rupture force with values determined for agglomerate particles in commercially available Turbuhaler® devices (e.g., PULMICORT® Turbuhaler®, AstraZeneca AB, Södertälje, Sweden).

The aerosolised particle size distribution and deagglomeration profiles were evaluated to elucidate the relationship between the lactose shape and aerodynamic behaviour. As shown in Table 4.7, needle-shaped lactose formulations exhibited a broader size distribution of aerosolised particles than the plate and tomahawk shapes. This aligns with the de-agglomeration behaviour observed in Figure 4.9. At the lowest flow rate (30 L/min), there was a minimal difference in de-agglomeration for all the formulations. However, as the flow rate increased, the plate and Tomahawk lactose formulations underwent greater de-agglomeration than the needle formulation. Notably, within the flow rate range of

up to 60 L/min, the de-agglomeration profiles of the plate and Tomahawk formulations were statistically similar. The maximum percent relative de-agglomeration achieved was 81.8%, 88.3%, and 96.3% for needle, plate, and Tomahawk lactose formulations, respectively.

Table 4. 7 The aerosolized particle size distribution of agglomerate formulation from Turbuhaler at varied flow rate

Agglomerate formulation	D_{10} / μm	D_{50} / μm	D_{90} / μm
needle-30L/min	2.58±0.08	8.22±1.09	35.42±2.95
needle-45L/min	1.60±0.09	4.73±0.26	14.55±2.01
needle-60L/min	1.38±0.10	3.96±0.18	9.08±0.78
needle-90L/min	1.20±0.03	3.57±0.08	7.74±0.35
needle-120L/min	1.14±0.11	3.37±0.07	7.17±0.15
Tomahawk--30L/min	2.28±0.12	7.51±0.46	25.97±4.96
Tomahawk--45L/min	1.65±0.03	4.50±0.13	13.93±2.40
Tomahawk--60L/min	1.44±0.02	3.64±0.06	7.82±0.46
Tomahawk--90L/min	1.28±0.10	3.18±0.08	6.39±0.17
Tomahawk--120L/min	1.28±0.01	3.15±0.10	6.58±0.42
plate-30L/min	2.43±0.23	8.00±1.18	31.24±9.02
plate-45L/min	1.24±0.07	4.34±0.05	14.42±3.36
plate-60L/min	0.99±0.11	3.42±0.11	8.34±1.08
plate-90L/min	0.87±0.03	3.18±0.12	7.25±1.14
plate-120L/min	1.02±0.23	3.17±0.35	14.09±14.87

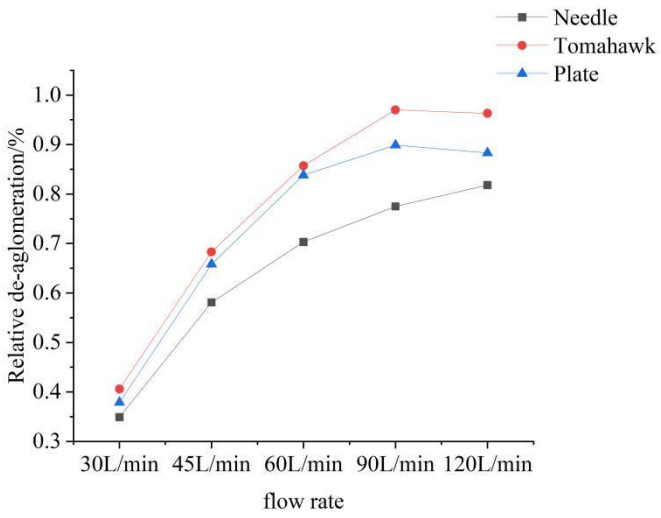

Figure 4. 9 The percent relative de-agglomeration profiles versus air flow rate for the aerosolised plume of agglomerate formulation with different shaped lactose dispersed from Turbuhaler.

These findings demonstrate the significant influence of particle shape on de-agglomeration behaviour. Careful selection of the initial lactose shape can be employed to optimise the de-agglomeration performance of the final formulation.

Among the investigated shapes, tomahawk-shaped lactose particles exhibited superior de-agglomeration, and consequently, improved aerosolisation. Therefore, the utilisation of tomahawk-shaped lactose is a promising strategy for enhancing the delivery efficiency of dry powder inhalation formulations.

4.3.2 Conditioning with Moisture

Micronised lactose often has an amorphous layer on its surface, which exhibits a higher water vapour sorption capacity than the crystalline state. This is due to the increased surface free energy and/or surface area of amorphous materials. However, this presents a storage challenge. When stored at high temperature and humidity, the amorphous parts of micronised lactose undergo a transition to a crystalline state. This recrystallisation significantly reduced the water sorption capacity. When adjusting humidity during conditioning (preparing lactose for use), it is crucial to consider interparticle bridging. During recrystallisation, bridges can form between amorphous surfaces. These bridges can create an unsuitable surface morphology that negatively affects the interaction between the fine lactose and drug particles within the formulation. Therefore, for stable formulations, it is essential to recover the amorphous portion back to a crystalline state to prevent the amorphous portion of fine lactose from recrystallising during storage and prevent particle bonding simultaneously.

Table 4. 8 Study of particle growth on the relative humidity during conditioning

Condition parameter	Particle size distribution /μm		
	<10%	<50%	<90%
Micronised lactose	0.93±0.11	2.89±0.11	6.19±0.02
40% RH 8h	1.05±0.11	2.97±0.06	6.42±0.27
40% RH 12h	1.06±0.13	3.02±0.16	6.22±0.02
50% RH 8h	1.02±0.08	3.06±0.02	6.48±0.05
50% RH 12h	1.20±0.09	3.13±0.06	6.68±0.14
60% RH 8h	1.17±0.02	3.09±0.08	6.47±0.05
60% RH 12h	1.24±0.02	3.38±0.08	8.04±0.04
70% RH 8h	1.49±0.04	3.73±0.12	9.21±0.23
70% RH 12h	1.61±0.04	4.16±0.13	11.57±0.23

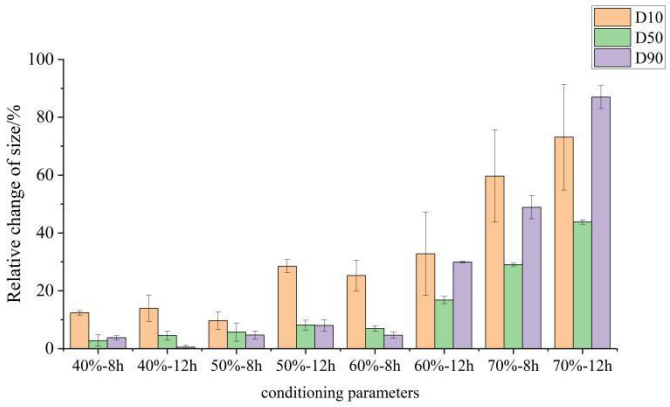

Figure 4. 10 Relative change in particle size distribution at varied condition parameters

By employing DVS analysis, it was determined that a relative humidity below 40% at 25 °C is inadequate for achieving complete recrystallisation of amorphous fine lactose within a 24-hour timeframe, as evidenced by the mass loss observed above 60% RH due to excess water desorption during crystallisation (Figure 4.11).

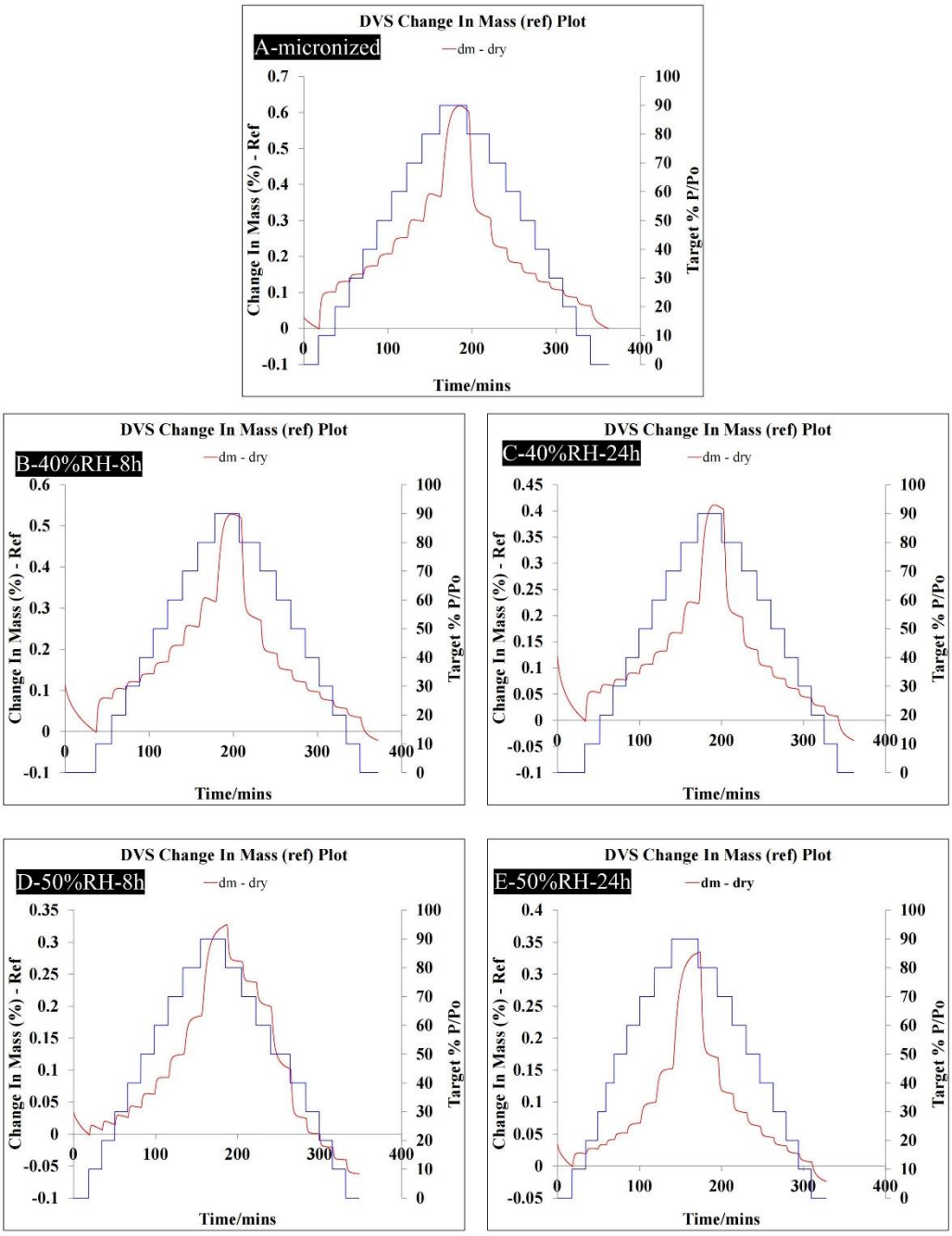

Figure 4. 11 DVS profile of micronised lactose at different condition parameters

A distinct trend towards enhanced particle growth was observed with an increase in relative humidity (Table 4.8). For example, the relative change in D50 increased from 2.7% at 40% RH(8h) to 15.0% at 29.1% RH(8h). A less pronounced impact on particle growth was noted with an elevation in the conditioning temperature from 40% RH(8h) to 50% RH(8h) while maintaining a constant temperature of 25 °C. Significant changes in the particle size distribution were observed after exposure to RH above 70 %.

The partially amorphous powder sample underwent complete conversion into crystalline material after conditioning for 12 h at 50 %RH; extending the duration of the conditioning process did not yield any additional effects, as indicated by the DVS profile. The most rapid conditioning occurred at 70 %RH, where a stable and entirely crystalline product was obtained after just eight hours of treatment but was accompanied by the largest increase in particle size. Thus, it can be concluded that the final stage of the conditioning process was reached before eight hours.

Maintaining a relative humidity (RH) of at least 50% is crucial to achieve lactose recrystallisation within 24 h because this humidity level has a minimal impact on particle size. The extent of agglomeration depends on the amount of amorphous lactose (influenced by the micronisation energy) and the conditions used during conditioning and storage. Unconditioned lactose carries the risk of uncontrolled recrystallisation. This could happen at any point after milling, during formulation for dry powder inhalers, or even after product manufacturing, potentially affecting the stability of the product in the hands of the patient.

Further analysis of the IGC data (Table 4.9) indicated that the dispersive surface energy of the lactose particles remained relatively unchanged after the moisture conditioning process compared to that of the starting micronised materials. However, the specific surface energy of the conditioned batches decreased significantly compared to the initial values, particularly when the conditioning humidity exceeded 50% relative humidity (RH). This decrease in specific surface energy can be attributed to two factors.

1. **Milling Effect:** The initial milling process itself might have disrupted the crystal structure of the lactose particles, creating imperfections on their surfaces. These imperfections could contribute to the higher initial specific surface energy.
2. **Moisture-Induced Surface Changes:** The decrease in the specific surface energy observed for conditioned batches (particularly at 50% RH

and above) suggests a change in the surface chemistry of the particles. The use of tetrahydrofuran (THF) as a probe indicates that the particle surface may have become more acidic. This could be due to the increased exposure of hydroxyl groups on the surface, potentially caused by moisture-induced rearrangement.

The influence of particle surface energy on agglomerate behavior is a critical factor. High surface energy can lead to strong interparticle forces, such as van der Waals forces and electrostatic interactions, which can promote excessive agglomeration. This can result in the formation of large, dense agglomerates that are difficult to deagglomerate during inhalation, leading to reduced fine particle fraction (FPF) and potentially decreased lung deposition.

Table 4. 9 Dispersive and specific surface energy for starting micronised and conditioned batches of lactose.

Samples	Dispersive energy (mJ/m2)	specific energy in tetrahydrofuran (kJ/mol)	specific energy in chloroform (kJ/mol)
Initial	44.2±0.6	7.31±0.35	1.99±0.01
40%RH-8h	44.3±2.2	7.36±0.29	2.01±0.15
40%RH-24h	42.7±2.0	7.42±0.41	1.88±0.02
50%RH-8h	43.6±0.3	7.03±0.17	1.83±0.12
50%RH-24h	43.8±1.6	6.19±0.02	1.85±0.17
60%RH-8h	46.2±3.7	5.45±0.28	1.94±0.08
60%RH-24h	44.2±0.6	5.05±0.09	1.78±0.06
70%RH-8h	44.2±0.6	5.09±0.41	1.84±0.13
70%RH-24h	44.2±0.6	5.16±0.33	1.75±0.05

The AFM images revealed qualitative differences in the roughness of fine lactose under various conditions. Morphological changes were observed, with large spines beginning to form on the surface (Figure 4.12 A1, A2), which gradually became smoother until surface dissolution occurred after more than 8 h at 70% RH (25 °C). Increasing the relative humidity to 40% from the initially micronised lactose immediately resulted in changes in surface morphology. Fig4.12 C1 and C2 show that although large spines were still present in the cross section, their depth decreased from approximately 34 nm to approximately 27 nm, as shown in Table 4.10.

Table 4. 10 Mean roughness parameters of micronised lactose after various conditions.

Samples	Mean Ra(nm±SD)	Mean Rq(nm±SD)
Initial	34.79±19.65	42.22±21.09
40%RH-8h	27.65±14.35	23.77±12.09
40%RH-24h	18.55±9.55	28.812±2.30
50%RH-8h	3.49±1.16	1.59±1.25
50%RH-24h	1.65±0.54	2.99±0.38
60%RH-8h	1.10±0.43	1.53±0.22
60%RH-24h	1.37±0.16	1.83±0.45
70%RH-8h	16.46±13.65	13.77±10.09
70%RH-24h	12.46±13.65	14.25±12.11

Observations of surface morphology after exposure to varying relative humidity (RH) levels are described. At 50% and 60% RH, the surface became smoother than the initial state, but needle-like spines were still visible. However, exposure to 70% RH resulted in the formation of irregularly shaped bumps, which created a pattern of regular roughness. These findings highlight the significant influence of fine lactose surface roughness on the contact area and separation distance between the drug and lactose particles, ultimately affecting the performance of DPI formulations. Therefore, these variations should be considered during the subsequent aerodynamic analysis.

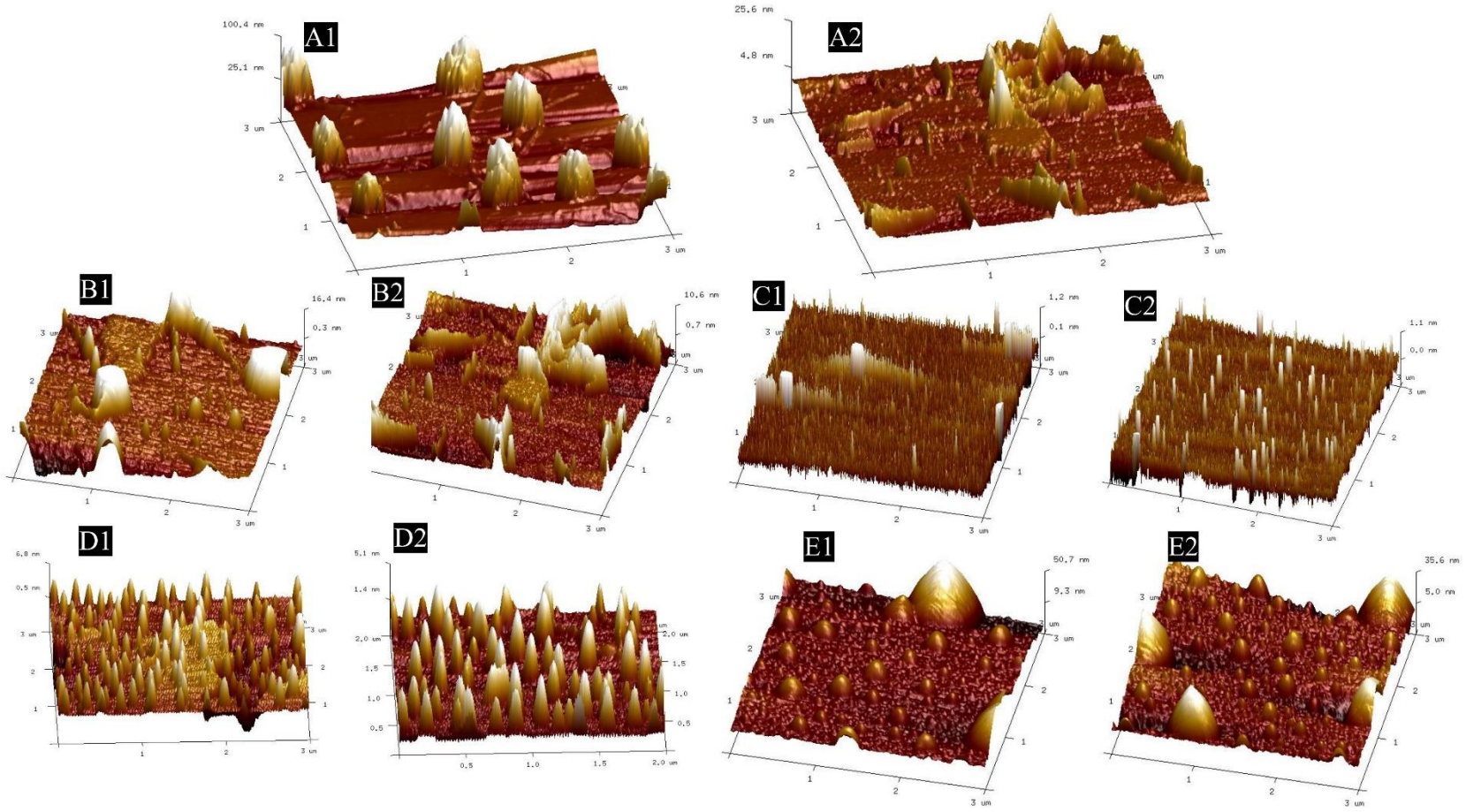

Figure 4. 12 Representative Tapping Mode AFM images of randomly selected 3 μm × 3 μm square areas of the surface of the micronised lactose after conditioning (A1 and A2 represent the initial micronised lactose; B, C, and D represent the condition humidity of 40%RH, 50%RH, 60%RH, and 70%RH, respectively).

4.3.3. Production of agglomerates with vibration bowl feeder

4.3.3.1 Initial assessment of Vibratory Bowl Feeder

To determine the working region of the vibration bowl, a performance analysis was performed by changing the operation voltage and working frequency with approximately 50 g of micronised fine lactose in the bowl after sieving. The performance analysis for particle agglomeration was initially performed by changing the operation voltage and working frequency. The operation voltage was set at 180 V and kept constant with respect to the frequency and total weight of agglomerates with size fraction between 200μm and 500μm coming out of the feeder, and the duration was recorded. Subsequently, the voltage was varied, and the same procedure was repeated.

The experimental results presented in Table 4.11 and 4.12 indicate that the powders did not move within the vibration bowl when the voltage was below 150V. However, particle agglomeration occurred within the operational voltage range of 150V to 210V, beyond which only powder transfer out of the vibration bowl was observed. This can be attributed to the force of inertia, which prevents motion at lower voltages. As the voltage increased, the powder movement and particle agglomeration rates also increased. Nevertheless, there was a marginal increase in the particle agglomeration rate after reaching a critical voltage, and the turbulence became excessive above 210 V, leading to powder bouncing and track detachment.

Table 4. 11 Vibration analysis with varied voltage range at fixed working frequency of 160Hz

Experiment No	Voltage/ V	Duration/ min	Size fraction 200-500μm / %	Phenomenon
1	90	9	--	Powder failed to move and no particle agglomeration
2	120	7	--	
3	150	4	86.98	Agglomerates with sufficient mechanical strength to pass the sieve
4	180	6	95.71	
5	210	4	89.63	
6	240	6	--	Powder moved too fast without particle agglomeration

Table 4. 12 Vibration analysis with varied frequency at fixed working voltage of 180V

Experiment No	Frequency /Hz	Duration/ min	Size fraction 200-500μm / %	Phenomenon
1	145	9	12.34	Rarely particle agglomeration
2	155	4	84.89	Agglomerates with sufficient mechanical strength to pass the sieve
4	165	5	85.72	
5	175	8.5	16.14	Rarely particle agglomeration

The maximum rate of particle agglomeration was observed between 155 Hz and 165 Hz, during which particle agglomeration rarely occurred. This can be attributed to the fact that a lower working frequency result in a slower moving speed within the vibration bowl, leading to the breakdown of the formed agglomerates. Conversely, when the working frequency exceeded the critical value, the powders failed to agglomerate before being transferred from the vibration bowl. Therefore, it was found that the optimum working conditions for particle agglomeration are a working voltage range of 150-210V and a working frequency within 155-165 Hz.

4.3.3.2. Optimization study of particle agglomeration with vibration

The average diameter and circularity of the agglomerates as well as the rupture force were selected as evaluation indices in this orthogonal experiment. Table 4.14 and Figure 4.14 illustrate the correlation between the mean values of these evaluation indices and the three analysed factors. It is worth noting that an increase in the working voltage led to a decrease in the agglomerate diameters in this study. This reduction in particle size, particularly within the range of approximately 10μm for fine lactose particles, contributed to improved circularity and reduced rupture force. These effects enhanced dosing performance

by promoting superior flowability and facilitating deagglomeration.

The optical images from the nine experiments in Table 4.13 are presented in Figure 4.13, showcasing a representative image of the sieved lactose after pre-agglomeration and final spheroidisation for each case. These visual observations indicate the successful attainment of agglomerates with a smooth surface and narrow size distribution using 6μm lactose through vibration. In terms of mechanical strength, image (g) from experiment 7 reveals the presence of aggregate fabrics, suggesting failure to withstand collisions during vibration and spheroidisation.

A possible explanation for this phenomenon is as follows. In orthogonal experiments, a comprehensive study was conducted to analyse the effects of different levels of multiple factors. The working voltage affects the vibration power and powder movements in the vibration bowl, whereas the fine lactose size influences the interactive forces between particles, particularly the van der Waals interactions. Compared to smaller fractions, larger lactose particles have a higher tendency to detach from agglomerates during spheroidisation because their weight exceeds the interparticle forces. Consequently, they formed agglomerated particles with a higher degree of aggregation. Therefore, the particle agglomeration process was predominantly influenced by the size distribution of fine lactose.

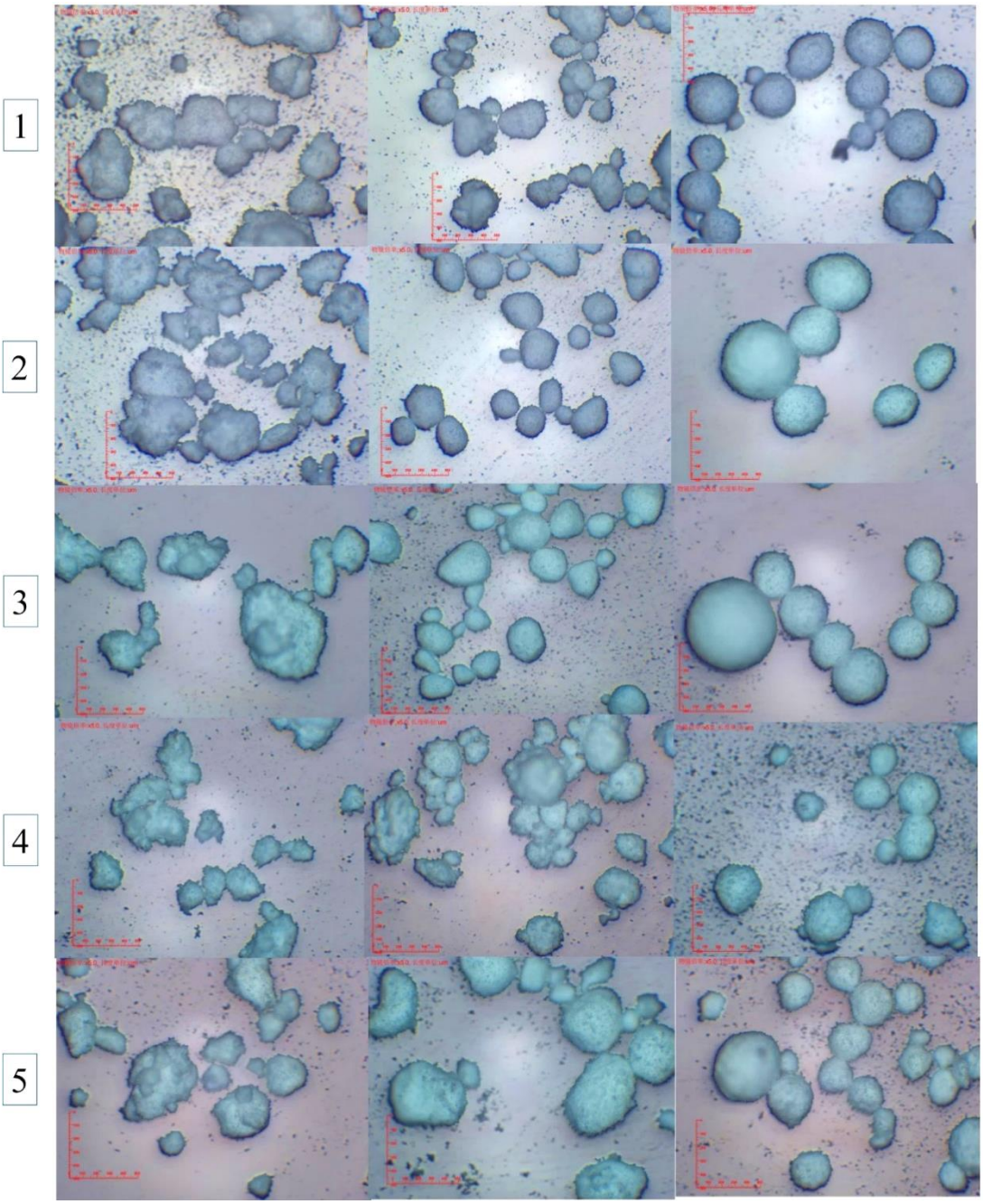

Figure 4. 13 SEM images showing the morphology of particle agglomeration correspond to experiments 1–9, The scale bar in the figure represents 500μm

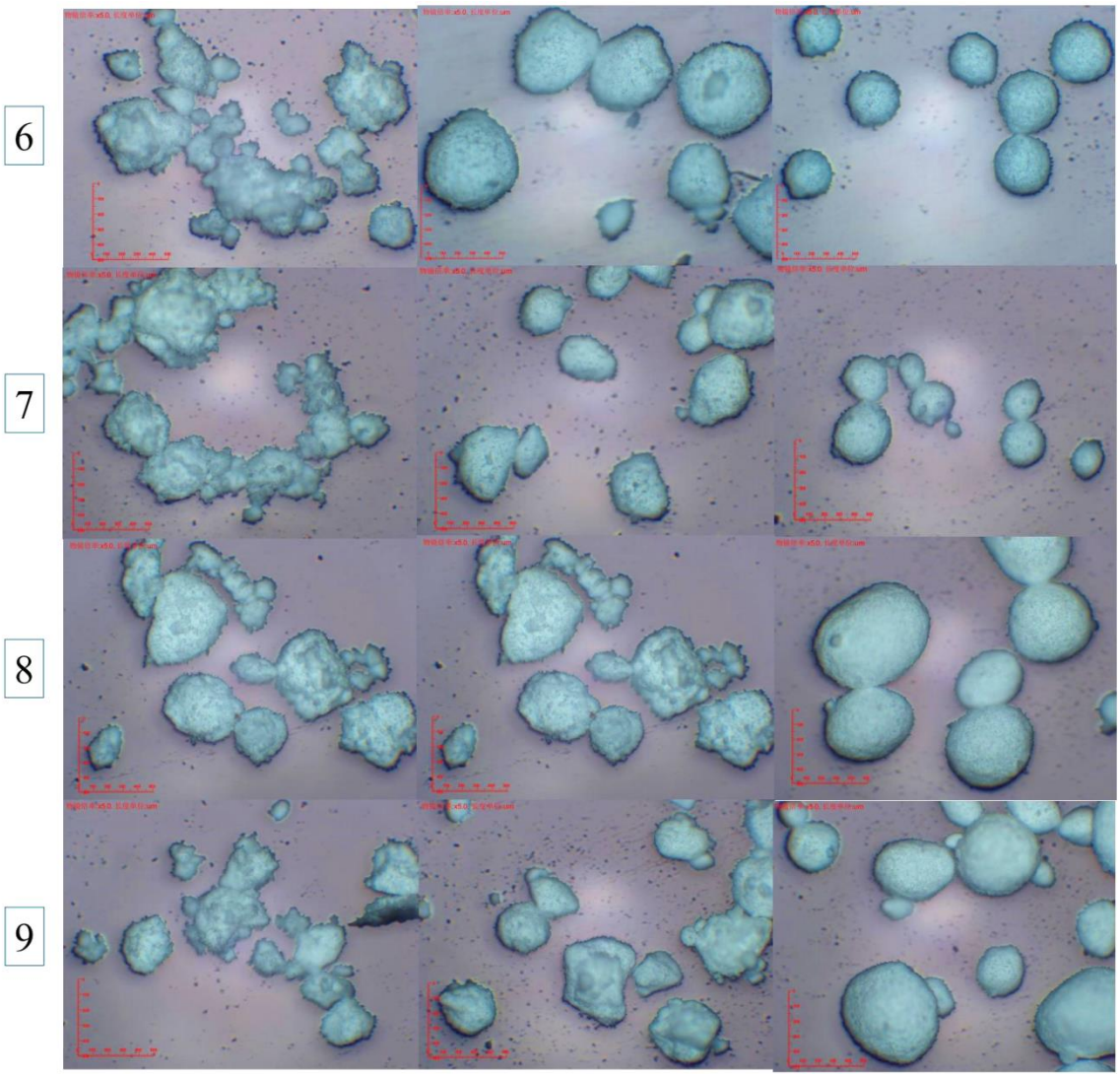

Figure 4. 13-continued. SEM images showing the morphology of particle agglomeration correspond to experiments 1–9, The scale bar in the figure represents 500μm.

Table 4. 13 Results and Analysis of Orthogonal $L_9(3)^4$ Experimental Design

Experiment No.	Lactose size (μm)	Sieve size (μm)	Operation voltage (V)	Operation frequency (Hz)	Agglomerate size/μm	Circularity	Rupture force/μN
1	3.07	200	150	155	586.57±101.47	0.85±0.03	3.43±0.07
2	3.07	450	180	160	437.83±86.43	0.78±0.04	2.88±0.16
3	3.07	600	210	170	541.20±110.69	0.79±0.04	3.14±0.09
4	6.02	200	180	165	368.74±64.24	0.86±0.04	1.44±0.11
5	6.02	450	210	155	405.99±97.92	0.79±0.06	1.51±0.09
6	6.02	600	150	170	469.74±95.41	0.84±0.90	1.85±0.17
7	10.45	200	210	160	446.58±49.56	0.88±0.02	1.23±0.11
8	10.45	450	150	170	526.69±65.31	0.86±0.02	1.51±0.08
9	10.45	600	180	155	536.75±86.11	0.83±0.03	1.29±0.17

Table 4. 14 Correlation analysis of experiment factors with evaluation indexes

		Agglomerate size	Circularity	Rupture force	Convexity
Lactose size	correlation coefficient	0.053	0.949**	-0.949**	0.609
	p	0.893	0.000	0.000	0.082
Sieve size	correlation coefficient	0.053	-0.264	0.053	-0.556
	p	0.893	0.493	0.893	0.120
Working voltage	correlation coefficient	-0.843**	-0.105	-0.105	-0.265
	p	0.004	0.787	0.787	0.491
Working frequency	correlation coefficient	-0.069	0.009	-0.043	0.148
	p	0.859	0.982	0.912	0.704

* p<0.05 ** p<0.01

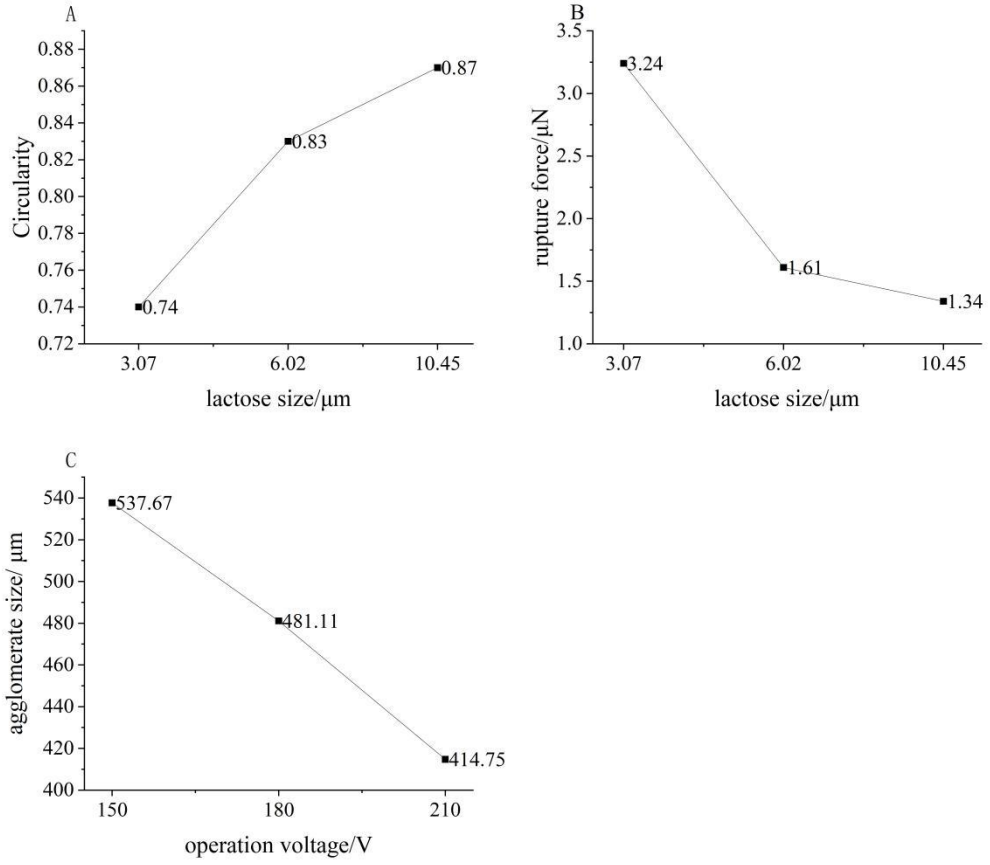

Figure 4. 14 Relationship between average diameter with the three factors and levels.

4.3.4. Aerodynamic performance characterization

To study the aerosolisation performance of the combination formulation of API and the optimised fine lactose, a candidate compound of budesonide and melatonin with varied size distribution was mixed with fine lactose for particle agglomeration, and the interaction between the two components was studied.

The performance of the formulations within the Turbuhaler device was assessed using aerodynamic particle size distribution (APSD) analysis. Table 4.15 reveals a consistent trend across all four samples containing budesonide and melatonin, irrespective of the initial API size. This trend involves an increase in both the fine particle fraction (FPF) and fine particle mass (FPM), followed by a decrease in the median size diameter (D50) of the API. However, a seemingly contradictory observation emerged for the formulations with the smallest API size. These formulations (API size of 0.75 µm for budesonide and 0.62 µm for melatonin) achieved the lowest FPF values. As illustrated in Figure 4.15, this phenomenon can be attributed to enhanced adhesion. Finer API particles exhibit a greater tendency to adhere to fine lactose or other API particles. This adhesion leads to the formation of larger aggregates, which are then deposited within the artificial throat and pre-separator stages of the Turbuhaler device, as shown in Figure 4.15. Consequently, the overall FPF of these formulations decreased.

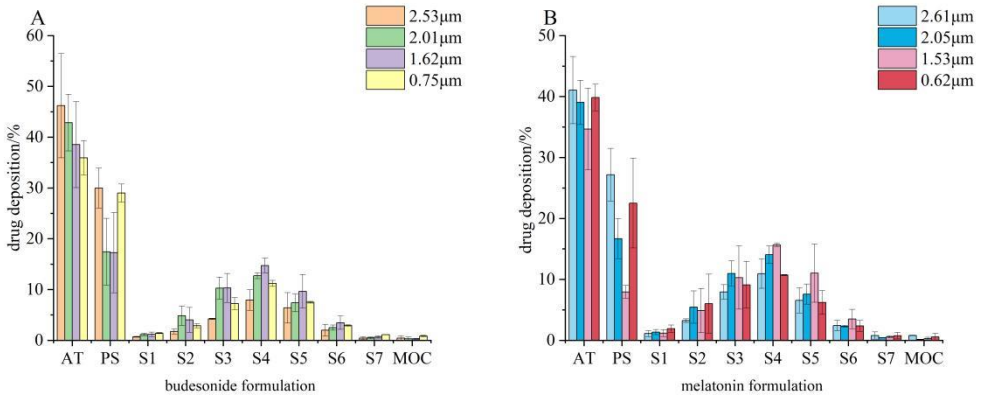

Figure 4. 15 The comparative analysis of the deposition pattern between budesonide (A) and melatonin (B) agglomerate formulations with varied API size

Analysis of the geometric standard deviation (GSD) across varying API particle sizes revealed no discernible trends. This suggests a normal distribution of particle sizes throughout the Turbuhaler device from Stages 1 to 7. The mass median aerodynamic diameter (MMAD) was dependent on the fine particle

fraction (FPF) obtained from the Next Generation Impactor (NGI) analysis, as expected. This confirms the relationship between the initial API particle size and resulting FPF. However, a significant challenge emerged, because the emitted dose of the agglomerate formulations displayed a larger variation for both budesonide and melatonin. This indicates a potential issue in the mixing process. Homogenising cohesive fine materials is notoriously difficult, and this variability warrants further investigation in the next chapter to optimise mixing and achieve consistent emission doses.

Table 4. 15 Summary results of API size effect on aerosolization of agglomerate formulation with budesonide and melatonin

	API size (D50)/μm	ED/%	FPM/μm	FPF/%	MMAD/μm	GSD
Budesonide	2.53	76.1±20.0	24.0±0.3	19.5±6.9	2.8±0.5	1.9±0.0
	2.01	81.2±26.7	46.5±22.6	32.7±2.9	2.9±0.2	1.8±0.1
	1.62	85.1±25.6	55.9±21.4	38.1±0.1	2.6±0.1	1.8±0.0
	0.75	69.4±10.7	30.7±5.7	28.7±2.6	3.0±0.2	1.9±0.1
Melatonin	2.61	86.6±22.0	40.6±8.3	27.9±3.7	2.7±0.5	1.8±0.1
	2.05	85.7±16.1	51.2±18.2	34.4±3.2	3.0±0.3	1.8±0.0
	1.53	82.8±31.0	59.2±28.9	41.0±1.7	2.6±0.1	1.8±0.0
	0.62	78.8±24.0	41.0±20.3	29.5±3.7	3.0±0.2	1.9±0.1

ED = emitted dose; FPM = fine particle dose; FPF = fine particle fraction; GSD = geometric standard deviation; MMAD = mass median aerodynamic diameter; Data are represented as mean ± SD (n = 3).

To assess the impact of conditioned lactose on the stability of the formulations, they were prepared and stored under accelerated conditions (40°C, 75% relative humidity) for 6 months. The aerodynamic performance was evaluated as shown in Figure 4.16. Due to variations observed in the emitted dose, the analysis focused on the deposition percentage in the artificial throat and pre-separator stages, rather than the entire aerodynamic profile.

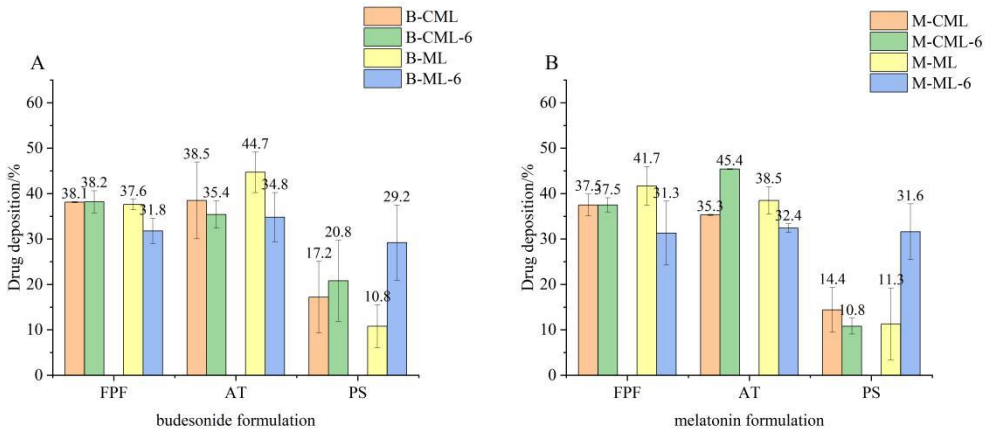

Figure 4. 16 Aerodynamic performance of agglomerate formulation at 0 month and after storage under accelerated conditions (40°C and 75% RH) for 6 months. (ML represent micronised lactose, CML represent conditioned micronised lactose, AT represent artificial throat and PS represent pre-separator stage)

Figure 4.16 compares the aerosolisation performance of agglomerate formulations containing either micronised lactose or conditioned lactose, analysed at the beginning of the study (0 months) and after 6 months of storage under accelerated conditions. The results demonstrated good aerodynamic stability of formulations with conditioned lactose. No statistically significant differences ($p > 0.05$) were observed in the aerosol deposition profiles of these samples at either time point. In contrast, the formulation containing micronised lactose exhibited a decline in the fine particle fraction (FPF) for both budesonide (15.4%) and melatonin (24.9%) after six months of storage. This significant difference in stability highlights the importance of eliminating amorphous materials from the micronised lactose.

Explanation for Stability Difference:

The decrease in the FPF for the micronised lactose formulation can be attributed to particle bonding and the formation of larger particles during storage under accelerated conditions. This phenomenon is likely a result of lactose recrystallisation, which is further supported by the increased deposition observed in the pre-separator stages (Figure 4.16). The influence of moisture on the formulations appeared to be minimal for the formulations with conditioned lactose. The decrease in dispersibility observed in the micronised lactose formulation was more likely related to increased capillary/solid bridging interactions(Janson et al., 2016). This can be explained by the increase in polar surface energy during storage at high humidity, as previously reported(Das et al.,

2009).

4.4 Discussion

Dry powder inhalers (DPIs) are breath-actuated devices that rely on patient inhalation to aerosolise medications for delivery to the lungs. To achieve effective pulmonary deposition, DPIs typically utilise micronised drug particles with aerodynamic diameters of approximately 1-5 μm. These small particles offer a high surface area and maximise interactions within the respiratory tract. However, the dominant interparticle forces governing their behaviour, such as van der Waals and Columbic interactions, can lead to poor flowability and cohesiveness of micronised powders. This presents a challenge in formulating effective DPIs, as these properties can compromise aerosolisation efficiency and, ultimately, drug delivery.

Agglomerate-Based Formulations: A Targeted Solution

Agglomerate-based formulations have emerged as a promising strategy for addressing the limitations of micronised powders in DPIs. This approach involves combining micronised drug particles with a fine excipient, typically lactose, to form larger and more stable agglomerates. During inhalation, turbulence and collisions within the inhaler cause these agglomerates to disintegrate, releasing the encapsulated drug particles for deep lung deposition.

Advantages of Targeted Delivery

A key advantage of agglomerate-based formulations is targeted delivery. Unlike carrier-based systems, where large carrier particles are deposited in the upper airways, agglomerates deliver both the drug and excipient directly to the deep lung, maximising drug efficacy. However, this approach presents some unique challenges:

- **Balancing efficiency and deposition:** Optimising the formulation for a higher fine-particle fraction (FPF) is crucial. FPF refers to the proportion of drug particles within the ideal size range (1-5 μm) for optimal lung deposition. By increasing the FPF, the total amount of excipient inhaled was minimised, thereby improving the overall efficiency and reducing the potential lung burden.
- **Optimising fine lactose properties for superior dispersion:** Optimising the size and shape of the fine lactose particles used as excipients plays a

critical role in deagglomeration during inhalation. Specific characteristics, such as a more spherical or porous lactose structure, can enhance the breakup of agglomerates, leading to a superior dispersion of the active pharmaceutical ingredient (API) for efficient drug delivery.

Fine lactose plays a critical role in forming stable agglomerates with good flowability and deagglomeration characteristics. Effective drug delivery to the deep lungs (alveolar region) requires these agglomerates to break down and disperse into particles smaller than 5 μm. Deagglomeration is influenced by the agglomerate strength, which can be indirectly measured by air shear pressure or mechanical testing. Agglomerate strength is related to the particle diameter, packing fraction (ratio of particle volume to aggregate volume), and work of adhesion or cohesion between particles. However, real powders exhibit heterogeneity with distributions in particle size, work of cohesion, and packing fraction, leading to a distribution of agglomerate strength(Das et al., 2013). While deagglomeration at a specific flow rate might correlate with the average agglomerate strength(Behara et al., 2011), controlled de-agglomeration behaviour across a range of flow rates necessitates appropriate size and shape distribution, along with lower surface energy, for cohesive micronised powders (< 5 μm). To facilitate deagglomeration, controlled feed loads of 200 and 300 g resulted in more spherical and less elongated particles compared to unmilled lactose with fluidised bed opposed jet milling with a classifier wheel speed from 1,000 to 30,000 rpm during controlled milling, which produced less variable particle shapes.

Previous studies have suggested strategies to reduce the agglomerate strength by lowering the packing fraction and work of cohesion. This study supports these findings and finds that lactose particles in the 5-10 μm range with a lower aspect ratio (width/length ratio) are linked to superior agglomerate strength. Tomahawk-shaped particles obtained through the antisolvent method demonstrated better de-agglomeration. Similarly, Das et al. (2013)reported that lactose with a lower aspect ratio (more spherical) influences the packing fraction, resulting in a looser agglomerate structure and improved aerosolisation at low flow rates. Furthermore, moisture-induced recrystallisation on the micronised lactose surface maintained relatively low cohesion. Particle size and shape manipulation

also influenced the packing fraction, contributing to a lower agglomerate strength.

Spherical agglomerate production via vibration:

Previous research has used vibration methods to create soft agglomerates with micronised APIs in a lab-scale batch process (Trofast and Falk, 1996). The mesh size controlled the size of the soft agglomerates during the pre-agglomeration. Later studies explored vibration chutes with a single loudspeaker to minimise inhomogeneous powder movement and reduce the contact between the product and vibrating slide (Etschmann, 2021). However, achieving a narrow size distribution with this method requires repeated rounding processes on the chute, leading to a lower manufacturing capacity and reduced mechanical strength, which are drawbacks for the pharmaceutical industry.

Vibration bowl feeder for efficient agglomeration:

This study employed a vibration bowl feeder combined with a rotating pan to produce soft lactose agglomerates suitable for dispersion using a Turbuhaler device. The vibration bowl feeder offered several advantages:

- Lower particle adhesion to the device surface;
- Higher efficiency, with a yield of over 95%;
- Batch completion times less than 10 min

Optical micrographs of both powder sieving and intact agglomerates revealed control over the spherical agglomerate size by adjusting the sieve mesh size, lactose size, and working voltage. Furthermore, no particle comminution (breaking) was observed after vibration-induced agglomeration, indicating a good stability against mechanical stress. The study observed a trend towards more spherical particles with larger fine lactose (6-10 μm) during the vibration process. This can be attributed to the relatively low surface area of the lactose materials, which decreased the adhesion to the exterior of larger agglomerates. A potential correlation between the size of the agglomerate and the working voltage is also suggested. Other researchers have shown that controlling the agglomerate size fraction within a suitable range result in a higher delivery dose. These findings could potentially be applied to the production of agglomerate formulations.

Interestingly, the agglomerate batch with "API size" exhibited the highest fine particle fraction (FPF) for both budesonide and melatonin. This might seem

counterintuitive, suggesting that FPF is not solely dependent on the hardness. This apparent contradiction arises from the difference in the scale of these properties. Agglomerate hardness is a macroscopic property measured at the size of the entire agglomerate (200-600 μm). Fine particle fraction (FPF), on the other hand, reflects interactions on a much smaller scale (1-2 μm), namely the adhesion between the drug and excipient, and the cohesion between individual drug particles. This distinction is further supported by the results of the inhaled lactose distribution. More API was deposited in the artificial throat and pre-separator stages for all the formulations. This suggests that a higher proportion of the drug adhered to the lactose and was co-deposited early on, likely because all formulations used the same lactose with similar deagglomeration behaviour. While the presence of 20% API increases the agglomerate strength owing to the smaller particle size and higher packing fraction, other factors also come into play. There seems to be a balance between the agglomerate strength (needed for de-agglomeration during inhalation) and interparticle forces (influencing dispersion). This explains why a higher hardness does not directly translate to a lower FPF in this study.

Therefore, this study aimed to achieve controlled size and shape distribution, along with surface modification of lactose for particle agglomeration via vibration. This approach targeted the creation of soft agglomerates with sufficient roundness for good flowability and uniform distribution of agglomerates, ultimately leading to better metering dose consistency. The excellent flowability and uniform distribution observed with the soft agglomerates compared to the micronised API powder make them suitable for automated filling in industrial production settings.

4.5. Conclusions

This study underlines the critical role of fine lactose properties in achieving optimal performance for a dry powder agglomerate formulation:

- **Fine Lactose Control**: The size and shape of the fine lactose particles significantly influence agglomerate formation. Precise control over these attributes is crucial for superior particle agglomeration, leading to the desired dosing behaviour, deagglomeration, and ultimately, efficient fine-particle delivery.

- **Vibration Tailoring**: Vibration parameters can be carefully adjusted to manipulate the size distribution of the agglomerates, thus impacting their dosing function. This knowledge can be used to tailor formulations containing multiple APIs for diverse pharmaceutical applications.
- **Enhanced Stability**: The study highlights the improved stability observed in agglomerate formulations with amorphous lactose surfaces modified to incorporate budesonide and melatonin.

Future Directions

Further exploration is warranted to delve deeper into the complex interactions at play:

- **Mixing and Spheroidisation**: A more detailed investigation is required to understand the combined effects of mixing and spheroidisation processes on agglomerate size, morphology, and deagglomeration behaviour across various drugs and aerosolisation conditions.
- **Mechanism Elucidation**: A deeper understanding of the mechanisms by which lactose and drug fines influence particle agglomeration is crucial for rapid optimisation of DPI performance during development.

Further exploration of these areas, particularly the combined effects of processing and underlying mechanisms, holds the promise of significantly improved control over agglomerate formulation behaviour. This deeper understanding will ultimately pave the way for the development of more effective and efficient inhalation therapies that directly benefit patients who rely on them for optimal health outcomes.

Chapter 5. Study of mixing effect on drug Adhesion and Dispersion for particle agglomeration

5.1 Introduction

The agglomerates are formed by the cohesive force of micronised drug and fine lactose, which consists of van der Waals attraction, capillary forces, electrical forces, and electrostatic forces(Endres et al., 2021), which are less than that of the adhesive force with large carrier lactose; therefore, high deagglomeration efficiency during inhalation could be achieved(Etschmann and Scherliess, 2022). Homogeneity is a technical challenge owing to the similar particle size and cohesiveness of micro-sized drug particles and fine lactose; conventional blade mixing failed to provide sufficient mixing energy input to homogenise the mixture and could produce irregularly sized and compressed clusters in mixtures which are difficult to disperse into fine particles after spheroidisation with vibration(Sankhla et al., 2022). Inappropriate mixing would also result in a larger deviation in drug content uniformity and lower fine particle deposition due to the high interactive force between fine drug particles and lactose (Alyami et al., 2017). Thus, it is of great importance to solve the homogeneity problem and explore the related mechanism of improving aerosolisation performance by agglomeration.

To achieve efficient fine particle deposition, drug-lactose interactions in the formulation and mixing method should be emphasised. First, it is important to maintain a balance between drug and lactose adhesion and the force needed for dispersion(Abiona et al., 2022a). The specific properties of particle size, shape, and surface morphology have been investigated extensively on the cohesive-adhesive balance (CAB) of the drug and lactose which determines the deagglomeration of the formulation and ease of drug detachment from fine lactose(Peng et al., 2016, Zhou et al., 2010d). The improvement in aerosol performance is primarily attributed to the increased frictional and rotational collisions between particles, facilitating the detachment of the API from lactose during aerosolisation (Abiona et al., 2022b). Second, optimisation of the blending method and process parameters can influence the homogeneity of the mixture and fine particle delivery of the DPI formulation (Jones et al., 2010,

Zeng et al., 1999). Compared to low-shear blending, high-shear mixing produces homogenous blends faster and significantly breaks down the aggregates in the mixture to improve the fluidisation characteristics of carrier-based dry powder inhalation products (Jetzer et al., 2018b). However, the high mixing energy input would enhance the adhesion between fine materials to decrease the fine particle deposition owing to particle bonding to form larger ones. To solve this problem, balancing the interaction force of the cohesive mixture after high shear blending with air jet mixing is a highly efficient manufacturing process, which improves fine particle deposition and maintains mixture homogeneity at the same time(Kinnunen et al., 2014). A sufficient mixing effect was achieved to form a uniform mixture and avoid powder clogging in the milling chamber at elevated mixing pressures because the particle collision with the milling chamber wall from the air stream mitigated the particle adhesion from high shear mixing and achieved a uniform mixture morphology(Bungert et al., 2021).

In this chapter, the effects of mixing on drug content uniformity and aerodynamic performance were studied. A series of adhesive mixtures were obtained by air jet mixing (AJM) and high shear mixing (HSM) under various parameters for the preparation of spherical agglomerates. The agglomerate formulation was loaded into a Turbuhaler® device before evaluating the aerodynamic performance with the next-generation impactor (NGI). The dispersibility performance of the agglomerates was studied with relative deagglomeration flow rate profiles using a laser diffraction system. This study aimed to better understand the mechanism of these effects and realise the industrial application of agglomerate formulations in the clinical field.

5.2. Methods

5.2.1. Production of binary mixture

Melatonin and budesonide were micronised using an air jet mill (Aljet J-20, DEC, Switzerland) at 5 bar before blending with micronised lactose (prepared using the process described in Chapter 4). High shear mixing was initially carried out to prepare the binary mixtures (20%w/w APIs, similar dose strength as Pulmicort Turbuhaler®) after the mixture was initially blended with a Turbula® mixer at 16rpm for 15 min and sieved twice with a mesh size of 200μm. For high shear

mixing, the mixing speed and mixing time were set as the influencing factors as shown in Table 5.1. The high shear mixing process utilized a speed range of 300-1200 rpm. This range was selected based on preliminary investigations and literature review, encompassing typical operating speeds for effective mixing of pharmaceutical powders while minimizing the risk of excessive shear-induced degradation.

Table 5. 1 Experimental design for high shear mixing process

Formulation	A1	A2	B1	B2	C1	C2
Mixing speed	300		600		1200	
Time	10	30	10	30	10	30
Mixture name for melatonin	M1	M2	M3	M4	M5	M6
Mixture name for budesonide	B1	B2	B3	B4	B5	B6
Spheroidization	Spheroidization at 60pm at a predetermined time after the optimized mixing condition was confirmed					

Air jet mixing was applied to address the clusters formed during high-shear mixing. This technique utilises three key factors: the feed pressure (A), feed speed (B), and grinding pressure (C). Notably, the grinding pressure serves primarily to prevent powder clogging within the milling chamber, not for particle size reduction (micronisation). For air jet mixing, pressures of 2 bar, 4 bar, and 6 bar were chosen. This range was selected based on prior studies demonstrating that increasing air pressure within this range generally leads to improved particle dispersion and deagglomeration while avoiding excessive particle fragmentation. Therefore, the initial focus was to establish a suitable grinding pressure range that avoids clogging without significantly affecting the particle size.

An L9 (3^4) orthogonal test table, a statistical method for optimising multifactor experiments (detailed in Table 5.2), was used to design the air-jet mixing experiment. This approach enables researchers to efficiently evaluate how these factors influence the effectiveness of air jet mixing in breaking down clusters while maintaining the desired particle size.

Table 5. 2 Factors and Levels for Orthogonal Experimental Design of Air Jet Mixing

	Factors		
Levels	feed pressure (A)/ bar	feeding speed (B) / $g.min^{-1}$	grind pressure (C) / bar
1	2	5	1

2	4	10	2
3	6	20	3

To assess the effect of mixing on both drug loss and fine particle dispersion, two key response data points were initially evaluated.

- **Drug Concentration (Assay):** This measurement reflects the potential influence of mixing on drug particle loss. A margin between the actual drug concentration and 90% of the theoretical value was used as an indicator of the mixing effect. A smaller margin suggests less drug loss during mixing.
- **Fine Particle Fraction (FPF):** This value indicates the influence of mixing on the ability to disperse the drug particles into a respirable size range. A higher FPF indicates a greater proportion of drug particles within a suitable size range for inhalation.

By analysing these two response variables, researchers can gain insights into how the mixing process affects both the quantity and quality of drug particles.

Statistical analysis Method

This study was conducted using the SPSS27.0 statistical software package. The ‘empty" column stands for no design parameter in the analysis.

The "empty" column in a Taguchi experiment essentially represents a control or baseline condition. It signifies a level where no design parameter is applied or altered. This column is incorporated to provide a reference point for comparing the effects of the other levels of the design parameters(Khoei et al., 2002).

Purpose of the Empty Column:

- **Baseline Comparison:** It serves as a benchmark against which the performance of other levels is evaluated. By including an "empty" column, researchers can assess how much variation in the response variable is due to the experimental factors and how much is due to inherent process variability.
- **Error Estimation:** It helps estimate the experimental error, which is crucial for calculating signal-to-noise ratios and determining the significance of the design parameters.
- **Orthogonality:** In Taguchi methods, designs are often orthogonal, meaning that the levels of one factor are equally distributed across the

levels of other factors. The "empty" column helps maintain orthogonality in the design matrix.

One-way analysis of variance (ANOVA) was utilized to evaluate the experimental data, with statistical significance determined at a p-value of less than 0.05.

5.2.2. Preparation of agglomerate formulations

To ensure consistent drug delivery from the Turbuhaler® inhaler, specific approaches were implemented for preparing the agglomerate formulation as follows:

1. **Sieving for Uniformity:** Before the agglomeration process, the mixture (10 g) was passed through a 200 μm sieve to remove any large clusters that could impact dosing consistency.
2. **Pre-agglomeration:** The remaining powder underwent a pre-agglomeration process, which was repeated twice. This involved the use of a vibration bowl feeder set at 160 volts and 80 Hz.
3. **Spheroidisation:** Following pre-agglomeration, irregular particles were further processed in a rotary drum agglomerator at 60 rpm for 10 min to create a more spherical shape.
4. **Targeted Size Distribution:** The dosing unit in a Turbuhaler® relies on a specific volume of particles for consistent delivery(Basheti et al., 2013). Therefore, we aimed to control the size distribution of the final agglomerate. This was achieved by sieving the processed particles with three meshes: 500 μm, 350 μm, and 200 μm.
    - Particles larger than 500 μm were discarded, as they could significantly reduce the delivered dose(TROFAST, 1996b).
    - Particles smaller than 200 μm were excluded from analysis due to the poor flowability.
    - The remaining particles, within the size range of 200-350 μm and 350-500 μm, were collected and weighed. The weight ratio of these two size fractions was targeted to be roughly 1:1, similar to that observed in commercially available Turbuhaler® medications. This specific size distribution helps to ensure consistent filling of

the dosing unit and, consequently, consistent drug delivery.

5. **Storage and filling:** The prepared agglomerates were stored in sealed containers to maintain dryness. For each inhalation device, researchers manually filled a Symbicort Turbuhaler® with approximately 150 mg of the prepared formulation, aiming for a target fill weight within the range of 145-155 mg.

5.2.3 Particle size and morphology analysis

Particle Size Distribution: A HELOS laser diffractometer equipped with a RODOS dry disperser and R2 lens (measuring particles between 0.25/0.45 and 87.5 µm) was used to determine the size distribution of the particles. The disperser was operated at a pressure of 3 bar during measurement. Data are presented as the average of three measurements with standard deviation (SD) included.

Light Microscopy: To visualise the morphology (shape) of the agglomerates, a digital microscope (ZML-310, Mengxin, China) with high resolution (3664×2748 pixels) was used. Images were captured under reflected light with adjusted background illumination to ensure optimal clarity at 5x magnification.

Scanning Electron Microscopy (SEM): For a more detailed examination of the agglomerate morphology, scanning electron microscopy (SEM) (JCM-7000, JEOL, Japan) was employed. To prepare the samples for SEM analysis, a gold sputter coating process was performed using a Smart Coater (DII-29030SCTR) at 0.67 Pa for 2 min with an electrical current of 3 A at 12.5 a distance. SEM images were acquired using an acceleration voltage of 15 kV.

This combined approach provides a comprehensive understanding of the size and shape of agglomerates, which are crucial factors influencing their flow properties and performance within a Turbuhaler® inhaler.

5.2.4 API quantification

To quantify the homogeneity of the mixture, the API content in the samples was determined using high-performance liquid chromatography (HPLC). Acetonitrile: water (40:60, v/v) was used as the eluent. The flow rate was set at 1.0 ml/min and the injection volume was 20 µL. The ultraviolet (UV) detector was set to a wavelength of 240 nm. A Waters Arc™ system (Waters Corp, Milford, USA)

equipped with a C18 column (Waters XBridge® C18 5um 4.6*150 mm) and a C18 column (Waters SPHERISORB 3µm, ODS 4.6×250 mm) was used for melatonin and budesonide quantification, respectively. The results were analysed using Empower ® software (Waters Corp., Milford, USA). All measurements were performed in triplicate.

5.2.5 In vitro aerosolization performance assessment

A Next Generation Impactor (NGI) from Copley Scientific (UK) was used to assess how effectively the formulated agglomerates dispersed as aerosols during inhalation. This instrument simulates the airflow experienced by particles within the respiratory system.

NGI Setup and Analysis:

- **Flow Rate and Air Volume:** The NGI was operated at a controlled air flow rate of 60 liters per minute (L/min) with a tolerance of ±5%. This setting ensured a consistent volume of air (4 liters) passing through the Turbuhaler® inhaler within 4 s, mimicking a typical inhalation manoeuvre.
- **Sample Preparation:** Turbuhaler® was manually filled with the different agglomerate formulations tested.
- **NGI Pre-Coating:** To prevent particles from bouncing and potentially skewing the size distribution results, the NGI stages were pre-treated with a thin layer of a silicone oil solution (0.5% w/v in n-hexane).
- **Sample Collection:** Following aerosolisation, particles deposited within the NGI device, artificial throat, pre-separator, and all impactor stages were carefully rinsed and collected using the same eluent solution employed for HPLC analysis.

Performance Metrics:

- **Emitted Dose (ED):** This value represents the total amount of drug that exits Turbuhaler® during inhalation.
- **Fine Particle Fraction (FPF):** This metric indicates the proportion of drug particles within a size range suitable for deep lung deposition and optimal drug delivery.

Both ED and FPF were calculated after quantifying the collected melatonin and

budesonide contents using the established HPLC method in Section 5.2.4. To ensure data reliability, each sample loading was measured three times. The reported results are presented as average values with the standard deviation (SD) calculated from triplicate measurements.

5.2.6 De-agglomeration characterization

To characterise the cohesive behaviours of the agglomerates, the flow titration method was applied by measuring aerosolisation at a sequence of different flow rates ranging from 30, 45, 60, 90, and 120 L/min (Behara et al., 2011). An inhaler adapter (INHALER™, Sympatec GmbH, Clausthal-Zellerfeld, Germany) was used to interface with Sympatec HELOS as described in section 2.4.1.10 Deagglomeration evaluation.

Measurements at each flow rate were performed manually in 3 replicates. Dispersion data obtained were modeled using a non-linear least square regression analysis in the OriginPro 2022b (OriginLab Corporation, USA)

5.3. Results

5.3.1 Preparation of mixture with high shear mixing

As shown in Table 5.3, budesonide losses were generally higher, particularly at the lower mixing speed of 300 rpm. This was attributed to the thin layer of powder accumulating on the high shear mixer walls over time. The overall API content loss was less than 10% for both drugs, indicating an efficient mixing process with minimal drug sacrifice.

High shear mixing typically led to coarsening of the particle size distribution (larger particles) along with an increase in the fine particle fraction (particles less than 5 µm). This trend is presented in Table 5.3. While the SEM images confirmed the breakdown of larger aggregates during mixing, the process also led to increased adhesion between the fine particles. This phenomenon was more pronounced for budesonide because of its stronger cohesive forces with lactose than with melatonin. Consequently, the D_{90} (particle size where 90% are smaller) for budesonide exhibited a more significant increase after mixing compared to melatonin (D_{90} increase from 6.32 µm to 7.27 µm for budesonide vs. 6.56 µm to 6.92 µm for melatonin). It is important to note that the observed increase in

budesonide particle size may be partially caused by the failure of the laser sizer to fully disperse the strongly bonded budesonide-lactose aggregates.

Despite this potential artefact, the analysis showed that over 80% of the particles in all formulations, except for the mixture produced at 1200 rpm for 30 min, remained smaller than 5 μm. This finding suggests their suitability for use in dry powder inhaler (DPI) formulations.

High shear mixing effectively minimised drug loss while generating a powder mixture with a generally desirable particle size distribution for DPI delivery. However, the potential for increased interparticle adhesion, particularly for budesonide, needs further consideration during the subsequent formulation development stages.

Table 5. 3 Content of budesonide and melatonin formulations after high shear mixing.

Mixing speed /rpm	300		600		1200	
Time /min	10	30	10	30	10	30
Mixture name for melatonin	M1	M2	M3	M4	M5	M6
Mixture name for budesonide	B1	B2	B3	B4	B5	B6
Budesonide /%	93.4±4.6	95.3±2.4	97.8±1.1	99.6±0.5	96.2±2.5	100.5±1.2
Melatonin /%	96.7±1.1	98.4±0.3	99.4±0.4	98.2±0.5	99.6±0.5	99.4±1.6

Table 5. 4 Assay and particle size distribution of mixtures from different mixing approaches

Formulation		Particle size distribution(μm±SD)			
	Mixing process	D_{10}	D_{50}	D_{90}	% <5 μm
Melatonin	M1	0.60±0.01	2.20±0.02	6.56±0.05	83.74±0.34
	M2	0.60±0.01	2.21±0.08	6.74±0.29	81.93±1.95
	M3	0.61±0.01	2.21±0.02	6.74±0.09	81.62±0.56
	M4	0.64±0.03	2.30±0.09	6.98±0.20	79.36±1.03
	M5	0.67±0.01	2.41±0.06	6.84±0.10	80.14±0.43
	M6	0.69±0.01	2.43±0.08	6.92±0.23	78.32±1.32
Budesonide	B1	0.60±0.01	2.23±0.08	6.32±0.23	84.32±1.32
	B2	0.60±0.00	2.28±0.01	6.41±0.03	83.43±0.19
	B3	0.63±0.06	2.22±0.12	6.59±0.23	81.76±1.26
	B4	0.67±0.03	2.32±0.04	6.86±0.28	81.91±1.79
	B5	0.68±0.03	2.39±0.15	7.18±0.21	81.61±1.68
	B6	1.22±0.04	3.27±0.12	7.27±0.12	74.86±1.18

Morphology characterization

Scanning electron microscopy (SEM) was employed to examine the morphology (shape and structure) of the particles within the mixtures after each set of mixing conditions. Representative images are shown in Figure 5.1.

Effect of Mixing Time and Speed

- **Lower Speed (300 rpm):** At a shorter mixing time (10 min), both budesonide and melatonin mixtures displayed coexistence of large aggregates and fine particles. This resulted in visually inhomogeneous mixtures with significant variations in particle size. After 30 min of mixing, the breakdown of larger aggregates into finer particles was observed. However, the budesonide mixture still contained a higher proportion of large aggregates than the melatonin mixture.
- **Higher Speed (1200 rpm):** An increased mixing speed (1200 rpm) resulted in more homogeneous mixtures, particularly after a longer mixing time (30 min). At this higher speed, there were minimal observable differences between budesonide and melatonin mixtures.

  These observations suggest that mixing speed and time have a consistent effect on the morphology of the particles in both mixtures. Longer mixing times and higher speeds promoted the breakdown of larger aggregates into smaller, more desirable fine particles.

.

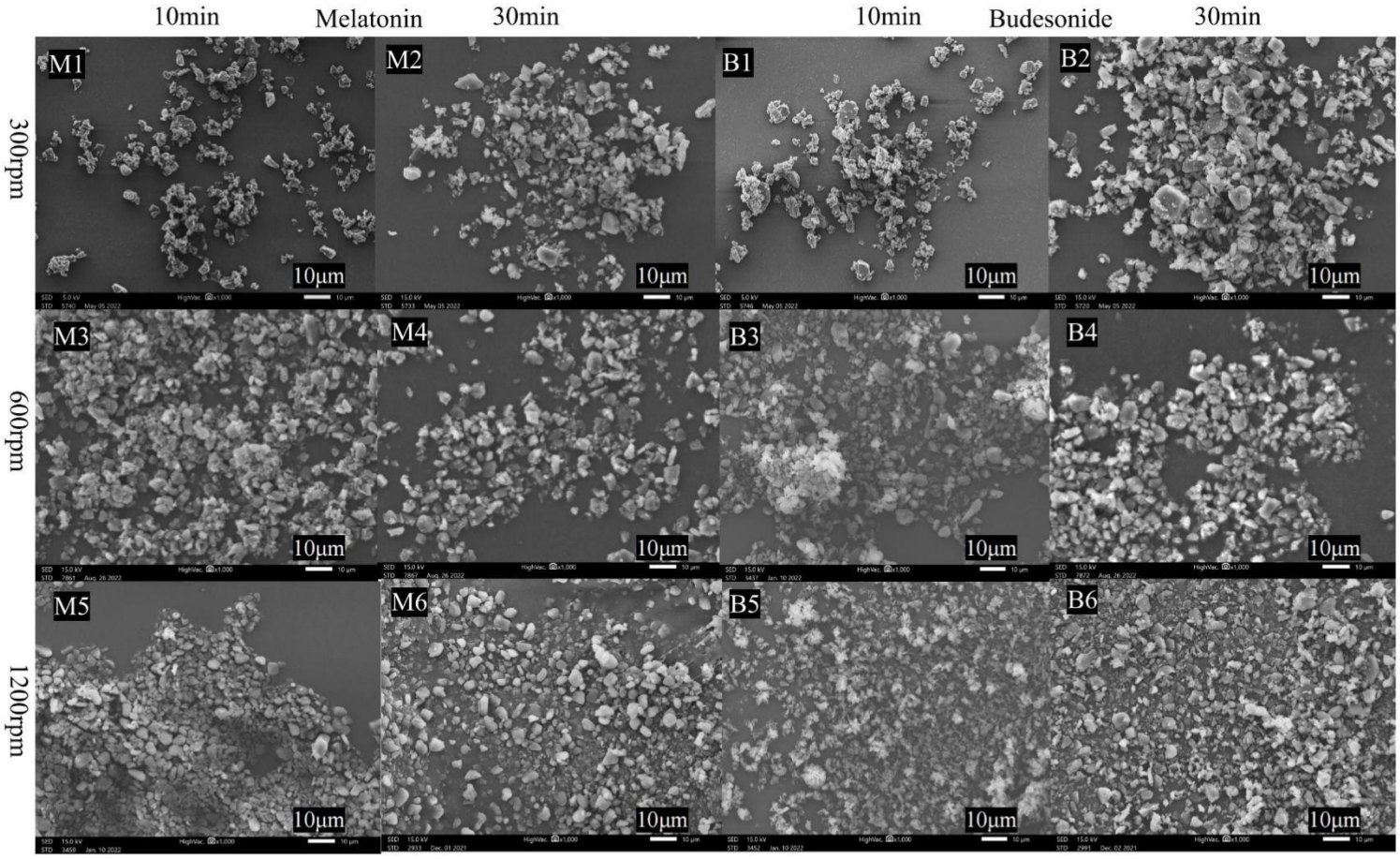

Figure 5. 1 SEM images of melatonin mixture (M1-M6) and budesonide mixture (B1-B6) produced at various high shear mixing speeds and times.

5.3.2 Powder bulk property analysis

The bulk and tapped densities of the mixture showed a similar increasing trend under different mixing conditions for the two formulations, as summarised in Table 3, where the bulk and tapped densities of the mixture gradually increased, followed by an increase in speed and time. This showed that mixing at a higher speed and duration efficiently decreased the porosity of the mixture.

Table 5. 5 Summary of density properties.

Mixing parameter	Budesonide mixture					
	300rpm 10min	600rpm 10min	1200rpm 10min	300rpm 30min	600rpm 30min	1200rpm 30min
Bulk density (g/cm^3)	0.23±0.03	0.23±0.04	0.25±0.01	0.24±0.03	0.25±0.04	0.25±0.01
Tapped density (g/cm^3)	0.33±0.03	0.34±0.01	0.34±0.01	0.33±0.03	0.34±0.01	0.34±0.01
	Melatonin mixture					
Bulk density (g/cm^3)	0.21±0.01	0.21±0.01	0.23±0.02	0.21±0.01	0.23±0.01	0.23±0.02
Tapped density (g/cm^3)	0.30±0.01	0.31±0.02	0.33±0.02	0.30±0.01	0.31±0.02	0.33±0.02

The tapped density was determined after a predetermined number of taps to represent the condensation properties of the powder. Owing to the difference in powder structure, the powder is packed differently during the spheronisation process, resulting in different mechanical strengths, which will, in turn, influence the deagglomeration behaviour of the agglomerate formulation because more impaction force from the agglomerate and device would be required to break up the agglomerate into fine particles to deposit in the deep lung. The higher tapped density of the budesonide powder bed facilitates consolidation better than the lower tapped density of the melatonin mixture; therefore, a higher mechanical strength of agglomerates would be expected for budesonide formulation.

5.3.3 Production of agglomerate formulation

The size distribution of the formulated drug particles is a critical factor that influences the performance of the Turbuhaler® inhaler. Agglomerates exceeding 500μm can significantly hinder consistent dosing by occupying a

disproportionate volume within the metering cavity, which is approximately 1000 µm in diameter (TROFAST, 1996b). To assess the impact of the mixing parameters on the agglomerate size, the weight ratio of particles larger than 500 µm to those smaller than 500 µm was analysed. The results are shown in Figure 5.2.

Influence of Mixing Speed and Time

- **Lower Mixing Speed (300 rpm):** Agglomerates prepared at a lower mixing speed (300 rpm) exhibited a coarser size distribution. More than half (56% and 64%, respectively) of the particles in both budesonide and melatonin formulations exceeded 500 µm. Increasing the mixing time from 10 to 30 min at this speed resulted in a statistically significant reduction in the proportion of large particles (down to 46% for both compounds).
- **Higher Mixing Speeds (600 rpm and 1200 rpm):** As the mixing speed increased to 600 rpm, the weight fraction of particles exceeding 500 µm steadily decreased to around 40% for the melatonin mixture. Extending the mixing duration to 30 min at this speed did not result in any further significant reduction. The budesonide mixture displayed a similar trend, with no substantial change in the large particle fraction (above 500 µm) between the 10-minute and 30-minute mixing times. However, compared with melatonin, the budesonide formulation consistently exhibited a higher proportion of large particles (approximately 10%), with correspondingly smaller fractions of particles below 500 µm. Notably, increasing the mixing speed to 1200 rpm further reduced the large particle fraction (>500 µm) for both mixtures. This reduction was more pronounced for melatonin owing to its inherent cohesive properties, as evidenced by the increased number of clusters observed during subsequent NGI testing.

These findings highlight the importance of mixing speed and time in controlling the resulting agglomerate size distribution. Lower speeds and shorter mixing times led to a higher proportion of large particles, potentially compromising dosing consistency within the Turbuhaler® device. Melatonin exhibited a generally greater decrease in the large particle fraction with increased mixing

intensity compared to budesonide, likely attributable to its more cohesive nature. Careful optimisation of the mixing parameters is therefore essential to achieve the desired size distribution for consistent and efficient drug delivery via Turbuhaler® inhalation.

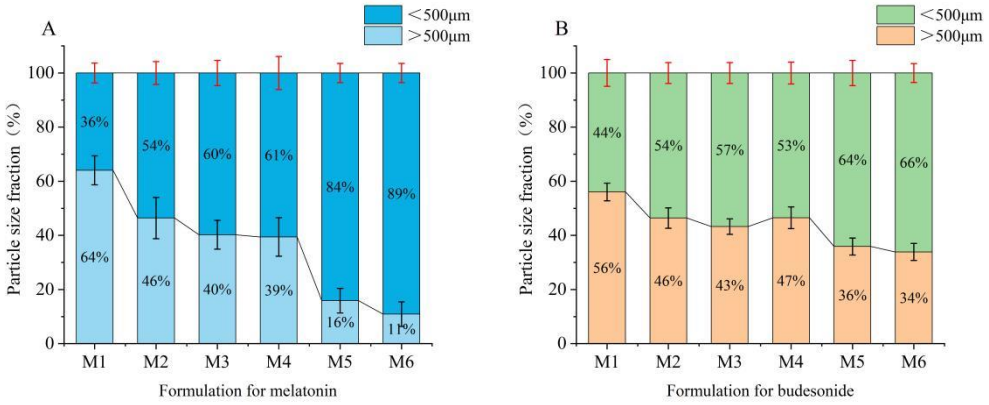

Figure 5. 2 Size fraction of agglomerates based on weight for different mixing processes.

To load the Pulmicort® Turbuhaler® with spherical agglomerates, the mouthpiece needs to be detached, followed by removal of the blue cap that covers the formulation reservoir beneath. The existing spherical agglomerates were then emptied and the device was thoroughly cleaned with compressed air to eliminate any residual fine powders.

The size distribution of the loaded agglomerates plays a crucial role in determining the metered dose dispensed from the Turbuhaler® dosing chamber (illustrated in Figure 5.3). When larger agglomerates prepared at mixing speeds of 300 rpm and 600 rpm were filled into the chamber, a lower drug load was observed. This occurred because the increased size of the agglomerates led to a higher void volume (empty spaces) within the dosing units. Conversely, formulations with smaller agglomerates produced at higher mixing intensities resulted in fewer voids within the dosing chamber. This ensures consistent delivery doses as more agglomerates can be packed into the dosing space. This is because the scraper located on top of the chamber crushes a greater number of smaller agglomerates, allowing them to occupy a larger volume within the dosing hole.

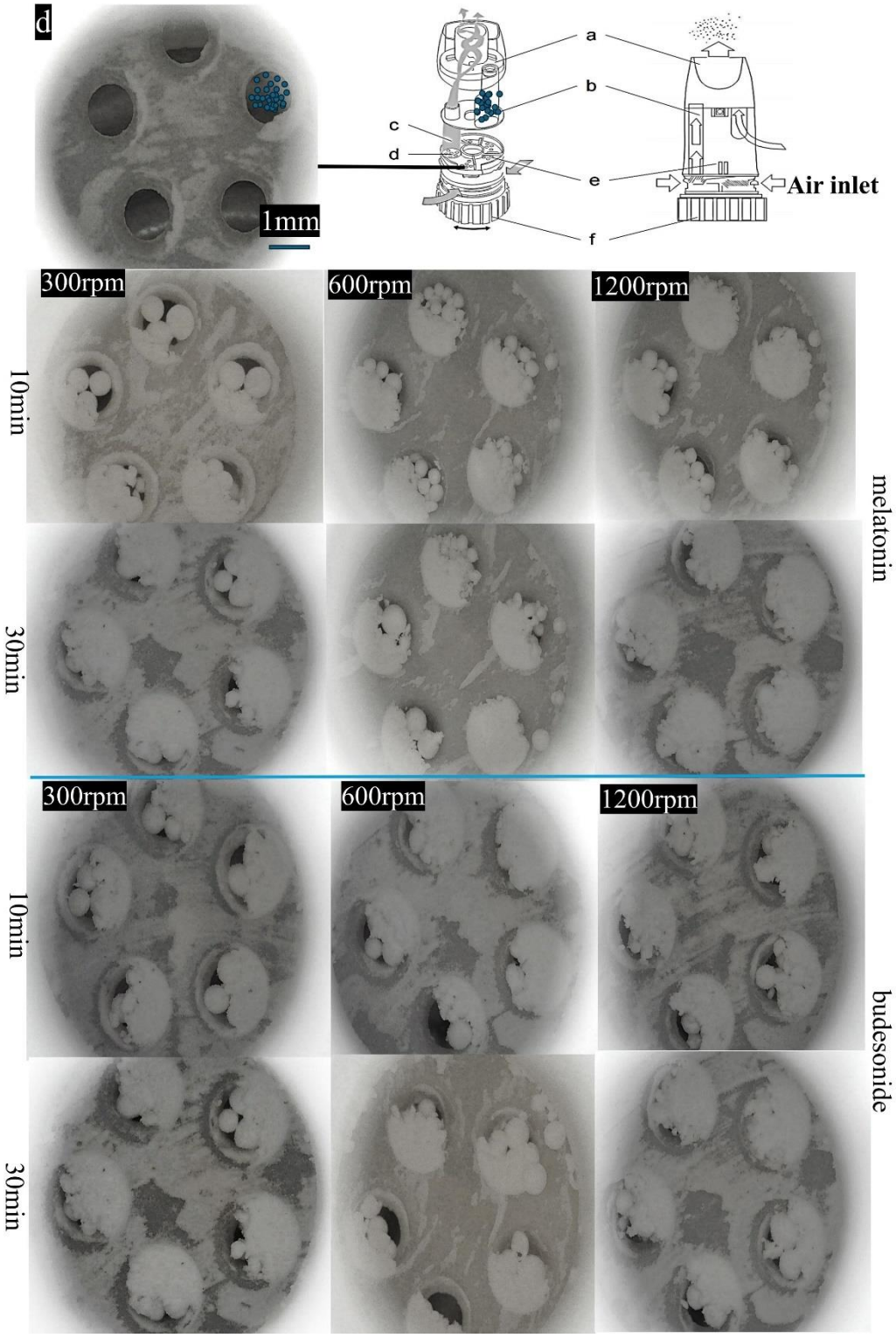

Figure 5. 3 Schematic of the Turbuhaler ® in disassembled form (top-left) and cross-section (top-right): a) mouthpiece with spiral channel, b) reservoir for agglomerate, c) inhalation channel, d) dosing holes after emptying of a dose, e) scraper, f) dosing wheel(Wetterlin, 1988); the bottom images illustrate the dose loading during inhalation.

5.3.4. Aerodynamic assessment

The Turbuhaler® inhaler was designed for agglomerate-based formulations. Agglomerates ensure consistent drug delivery by providing a uniform dosing unit fill with each actuation. Ideally, the dosing unit should be filled with fixed mass of intact agglomerates. However, in reality, a combination of intact and crushed agglomerates typically fills the unit, as shown in Figure 5.4. This study investigated how variations in the agglomerate size distribution affect the filling mass and, consequently, the delivered dose. In addition, the influence of intact and crushed agglomerates on fine-particle deposition was examined.

Impact of Mixing Parameters on Dosing

The delivered dose exhibited a gradual increase in both budesonide and melatonin with increasing mixing speed and duration. At lower mixing speeds (300 and 600 rpm) and a shorter mixing time (10 min), the effective drug (ED) delivery hovered at approximately 55-60%. However, a significant increase in ED was observed for both drugs when a higher mixing speed (1200 rpm) was used for 10 min. This improvement can be attributed to the reduction of voids within the dosing unit due to the use of smaller agglomerates produced by the higher mixing intensity.

Extending the mixing time to 30 min at speeds of 300 and 600 rpm also led to a significant increase in ED compared with the 10-minute mixing time. However, no further improvement was observed with longer mixing times at the highest speed (1200 rpm). Interestingly, for both mixing times (10 and 30 min), the ED values for melatonin formulations showed a more significant improvement with increased mixing speed than budesonide. The ED for melatonin increased from approximately 55.7% to 70.5%, whereas for that budesonide increased from 58.3% to 69.4%. These findings suggest that higher mixing speeds and times generate powder mixtures with more suitable agglomerate size distributions, allowing for better packing within the dosing unit, ultimately leading to a larger delivered dose.

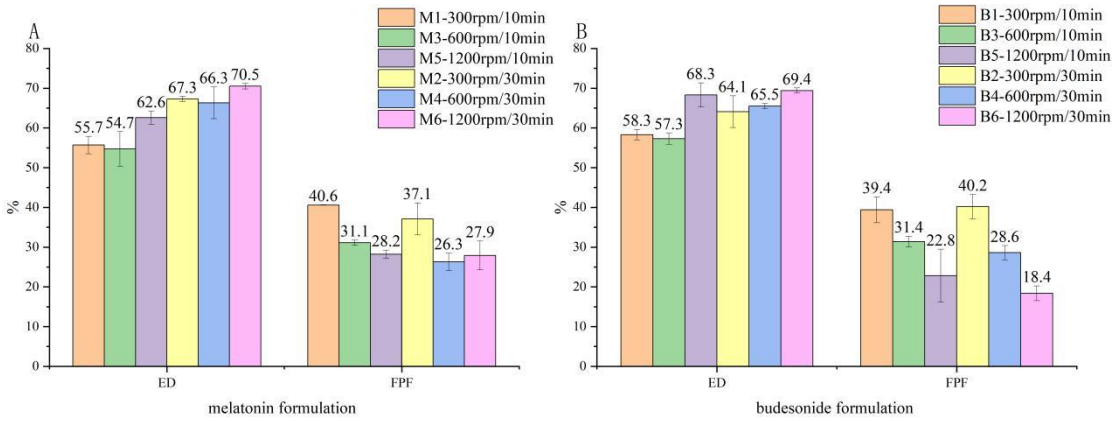

Figure 5. 4 Comparison of ED and FPF of agglomerate formulations

The effects of mixing intensity (speed and time) on the fine particle fraction (FPF) and deagglomeration behaviour of the formulations are listed as follows:

Fine Particle Fraction (FPF): An overall decrease in FPF was observed with increasing mixing intensity for both the budesonide and melatonin formulations. The mixing speed had a more significant influence on FPF compared to mixing time. For instance, the FPF of melatonin decreases from approximately 40% (300 rpm) to nearly 30% (1200 rpm), regardless of the mixing time. Conversely, varying the mixing times at the same speed (10 or 30 min) did not result in substantial FPF differences for the melatonin formulation. The budesonide formulation exhibited a gradual decrease in the FPF with increasing mixing speed, reaching its lowest value (18.4%) at 1200 rpm after 30 min of mixing. Interestingly, no significant change in FPF was observed for budesonide at the different mixing times.

- **Deagglomeration:** The deposition profiles in Figure 5.5 indicate that a higher mixing intensity led to a decrease in the deagglomeration of the spherical agglomerates, which was particularly evident in the pre-separator drug deposition. For example, the amounts of melatonin deposited in the pre-separator at 600 rpm (10 min) and 1200 rpm (10 min) were more than double and triple, respectively, compared to that at 300 rpm (10 min). Similarly, a four-fold increase in pre-separator deposition was observed for the budesonide formulation at 1200 rpm, suggesting poorer deagglomeration behaviour compared to melatonin. While the mixing speed significantly influenced drug deposition in stages 2 and 3 (with an approximate 50% decrease from 300 rpm to 600 rpm), no further

decrease was observed at 1200 rpm.

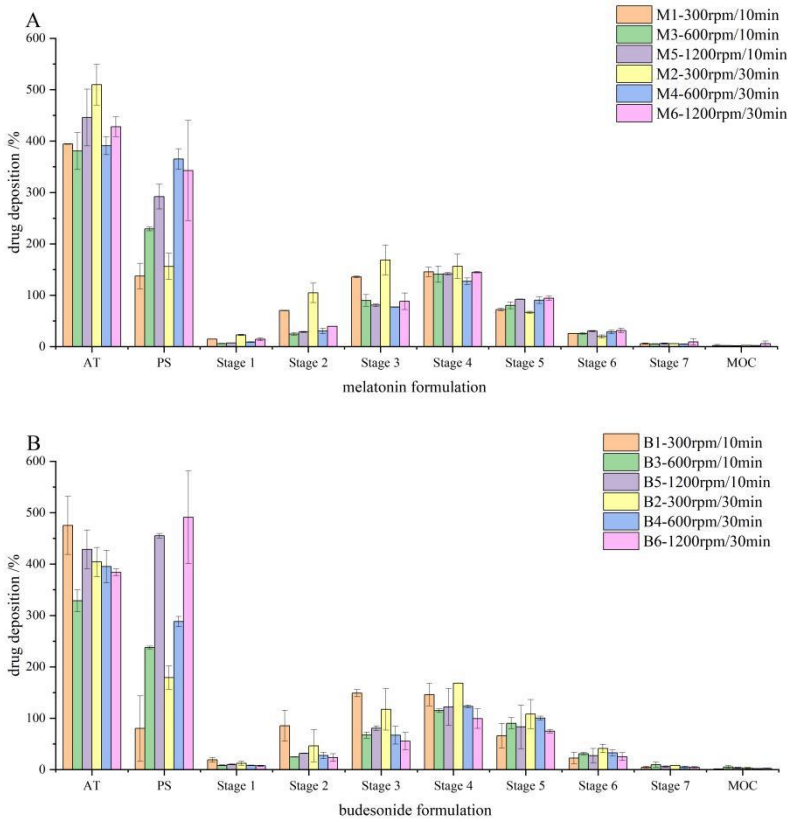

.

Figure 5. 5 Aerodynamic deposition pattern for melatonin (A) and budesonide(B) formulation with high shear mixing (* AT and PS represent the drug deposition at artificial throat and pre-separator, respectively)

Balancing Agglomeration and FPF:

These findings suggest that while high shear mixing effectively breaks down large aggregates into smaller ones, it can also increase the attractive forces between particles, leading to the formation of medium-sized particles that fall outside the ideal inhalable size range. To address this issue and enhance the FPF, mixtures produced at 300 rpm (30 minutes) were chosen for further processing. Air jet mixing, a technique utilising a higher energy input, was employed to further disperse the remaining aggregates and reduce these interparticle forces, ultimately aiming to improve fine particle deposition for efficient drug delivery.

While the mechanistic explanation of de-agglomeration under different mixing conditions is covered, a deeper understanding requires considering the influence of particle orientation and the distribution of surface energy.

- **Particle Orientation:** During mixing, particle collisions occur with

varying orientations. Head-on collisions may result in more effective particle breakage and deagglomeration, while oblique collisions might lead to less efficient deagglomeration or even the formation of larger, more complex agglomerates.

- **Surface Energy Distribution:** Heterogeneity in surface energy across the particle surface can significantly influence interparticle forces. Regions with higher surface energy may exhibit stronger attractive forces, leading to the formation of strong interparticle bonds and hindering deagglomeration. Conversely, regions with lower surface energy may promote easier particle separation.

Furthermore, the interplay between particle orientation, surface energy distribution, and mixing intensity needs to be considered. For example, high shear mixing may disrupt particle orientation, potentially leading to more effective deagglomeration. However, excessive shear forces can also damage particles and alter their surface properties, potentially increasing surface energy and hindering deagglomeration.

5.3.5 Combination of high shear mixing with air-jet mixing

Initial study of mixing pressure

Based on the results obtained from agglomerate dosing in the dose chamber of Turbuhaler® and the aerodynamic behaviour of high shear mixed agglomerate formulations, a significant effect of agglomerate size fraction (>500µm) on reducing dosing load and variation was observed. We compared the impact of air jet mixing alone and in combination with high shear mixing on the bulk properties and aerodynamic deposition of spherical agglomerates.

Additionally, because fine materials tend to clog the milling chamber without grinding pressure, a comparison was made between the size distribution of the initial mixture and after mixing under various ground pressures (ranging from to 1-3 bar) and feed pressure at 6 bar. The D_{50} of all the mixtures was approximately 2µm after mixing within grinding pressure of 3 bar. The particle size was reduced when grind pressure achieved to 4 bar, which was 1.8±0.2µm as shown in Table 5.6. Therefore, the grinding pressure was selected within the range of 1-3 bar in the following study.

Table 5. 6 Particle size distribution of mixtures (Mean ± SD)

Grind	Particle size distribution (μm)		
pressure/bar	D10	D50	D90
0	0.7±0.1	2.4±0.2	6.9±0.2
1	0.7±0.0	2.4±0.1	6.9±0.1
2	0.6±0.0	2.3±0.1	6.6±0.3
3	0.6±0.0	2.2±0.0	6.5±0.2
4	0.5±0.2	1.8±0.2	5.2±0.2

Verification Experiment of air jet mixing

Improper air jet mixing pressure can negatively affect drug concentration owing to variations in the particle size distribution and density of the mixture. Pharmaceutical applications require a drug concentration within 90-110% of its theoretical value (Williams et al., 2002). Therefore, the emitted dose results were excluded from Table 5.7 because of potential fluctuations in drug concentration affecting the delivered dose.

Figure 5.6 depicts the optimal trends for each air jet mixing factor based on the mean values listed in Table 5.7. This analysis aimed to identify the settings that achieved the best overall outcome.

Table 5. 7 The results of orthogonal experiment (n=3)

factors	A FP*	B FS*	C GP*	EMPTY	FPF （melatonin）	ASSAY （melatonin）	FPF （budesonide）	ASSAY （budesonide）
1	6.00	20.00	2.00	1.00	54.04	1.20	52.30	-10.15
2	6.00	20.00	3.00	2.00	57.10	-7.02	55.61	-12.40
3	4.00	20.00	1.00	2.00	45.00	8.20	46.37	-5.04
4	4.00	10.00	3.00	1.00	43.11	-13.43	50.43	-14.26
5	4.00	5.00	2.00	3.00	45.00	1.02	48.24	0.85
6	2.00	20.00	3.00	3.00	39.24	-21.05	30.18	-23.63
7	2.00	5.00	1.00	1.00	40.23	6.60	33.42	3.16
8	6.00	10.00	1.00	3.00	52.60	9.95	50.32	-5.59
9	2.00	10.00	2.00	2.00	40.40	3.61	29.44	-3.61

*FP represents feed pressure, FS means feed speed, GP represents grinding pressure

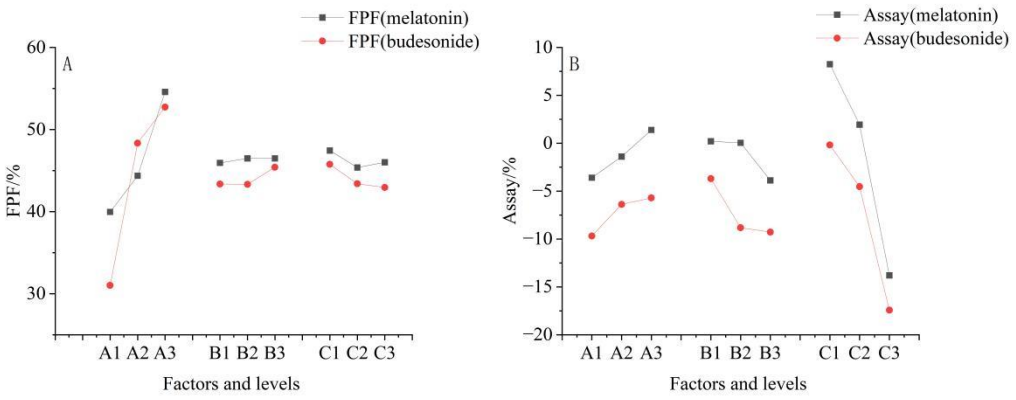

Figure 5. 6 Relationship between response and the three factors and levels.

Feed Pressure as the Key Factor for FPF

The orthogonal experiment revealed that feed pressure (A) exerted the most significant influence on the fine particle fraction (FPF) for both budesonide and melatonin among the three investigated factors (feed pressure, feed speed, and grinding pressure). The feed speed and grinding pressure did not exhibit a strong correlation with the FPF. Notably, increasing the feed pressure resulted in a higher FPF in this study. When the feed pressure was set to 6 bar, the FPF surpassed 50% for both budesonide and melatonin. This can be attributed to the combined effects of entrainment velocity (drawing powder into the milling chamber) and the impaction force associated with higher feed pressure.

Balancing Grinding Pressure and Drug Loss

While increasing the grinding pressure has the potential to enhance FPF, it can also lead to a higher loss of fine drug particles, as indicated by the lower drug concentration observed with increased grinding pressure in Table 5.6. This can counteract the benefits of an improved FPF for drug delivery. The effect of grinding pressure (C) on drug content was statistically significant (P=0.048 for melatonin and P=0.038 for budesonide), with higher pressure resulting in lower drug concentration as shown in Table 5.7. This translates to a reduction in the total emitted dose owing to the loss of fine drug particles.

The impact of the grinding pressure differed between the two drugs. Melatonin exhibited negligible loss at lower grinding pressures, whereas the budesonide concentration fell below 90% in most experiments (Table 5.6). This suggests that a larger portion of fine budesonide particles escaped the mixture during air jet mixing than fine lactose particles. Additionally, the cohesive properties of

budesonide caused the mixture to solidify and adhere to the milling chamber walls after prolonged mixing and a high feed speed. This phenomenon significantly influenced the drug concentration, making feed speed a secondary but impactful factor.

Table 5. 8 Analysis of variance for air jet mixing (n=3)

Sources of variation	Freedom (N)	FPF (melatonin) Sum of squares	Mean square	F	Significance difference	FPF (budesonide) Sum of squares	Mean square	F	Significance difference
modified model	6	344.788a	57.465	17.669	0.055	814.091a	135.682	28.915	0.034
intercept	1	19295.062	19295.062	5932.723	0.000	17451.291	17451.291	3719.046	0.000
A	2	337.563	168.782	51.896	**0.019**	791.968	395.984	84.388	**0.012**
B	2	6.644	3.322	1.021	0.495	13.646	6.823	1.454	0.407
C	2	0.580	0.290	0.089	0.918	8.476	4.238	0.903	0.525
error	2	6.505	3.252			9.385	4.692		
total variation	9	19646.354				18274.766			
modified total variation	8	351.292				823.476			
a. R-square = 0.981 (Adjusted-R-square = 0.926)						a. R-square = 0.989(Adjusted-R-square = 0.954)			
		Assay (melatonin)				Assay (budesonide)			
modified model	6	845.980a	140.997	7.262	0.126	583.247	97.208	9.947	0.094
intercept	1	13.250	13.250	0.682	0.496	474.804	474.804	48.584	0.020
A	2	37.513	18.756	0.966	0.509	27.245	13.623	1.394	0.418
B	2	32.117	16.058	0.827	0.547	57.553	28.777	2.945	0.254
C	2	776.351	388.175	19.992	**0.048**	498.448	249.224	25.501	**0.038**
error	2	38.833	19.416			19.546	9.773		
total variation	9	898.063				1077.597			
modified total variation	8	884.813				602.793			
a. R-square =0.956 (Adjusted-R-square = 0.824)						a. R-square = 0.979(Adjusted-R-square = 0.915)			

Prioritizing Drug Content for Melatonin

For the melatonin mixture, a lower feed speed is recommended, despite its insignificant influence on the FPF. This process is designed to minimize fine drug loss, considering that even at a feed speed of 20 g/min, the drug content can exceed 95%. When formulating cohesive drugs into agglomerates, careful consideration should be given to the potential for fine drug losses.

Optimizing Agglomerate Formulation for High FPF and Drug Content

To achieve a balance between the high emitted dose (ED) and fine particle fraction (FPF), further experiments were conducted for the melatonin formulation to achieve superior fine particle delivery. These experiments evaluated the impact of feed pressures (2, 4, and 6 bar) at a constant grinding pressure of 1 bar on mixture properties, agglomerate morphology, and aerodynamic performance. The melatonin formulations were designated as MA2, MA4, and MA6. Similarly, budesonide formulations were labelled as BA2, BA4, and BA6.

5.3.6 Mixture properties and agglomerate particle morphology

The morphology of the mixed samples was analysed using scanning electron microscopy (SEM), whereas light microscopy was employed to examine individual agglomerate particles (Figure 5.7). At a feed pressure of 2 bar, cohesive particles formed random aggregates both internally within the mixture and externally on the surface of the melatonin and budesonide agglomerates (Figure 5.7-A1, A2). Increasing the feed pressure from 2 to 4 bar resulted in a more uniform distribution of fine particles within the melatonin sample and reduced the formation of irregular small agglomerates. Notably, it was only when a feed pressure of 6 bar was reached that highly dispersed mixtures became evident for budesonide. Thus, higher feed pressures promoted greater homogeneity in the mixtures, as observed under light microscopy (Figure 5.7-B,-C). Both light microscopy and SEM images revealed that agglomerate particles displayed spherical shapes with smooth surfaces when subjected to mixing pressures exceeding 2 bar.

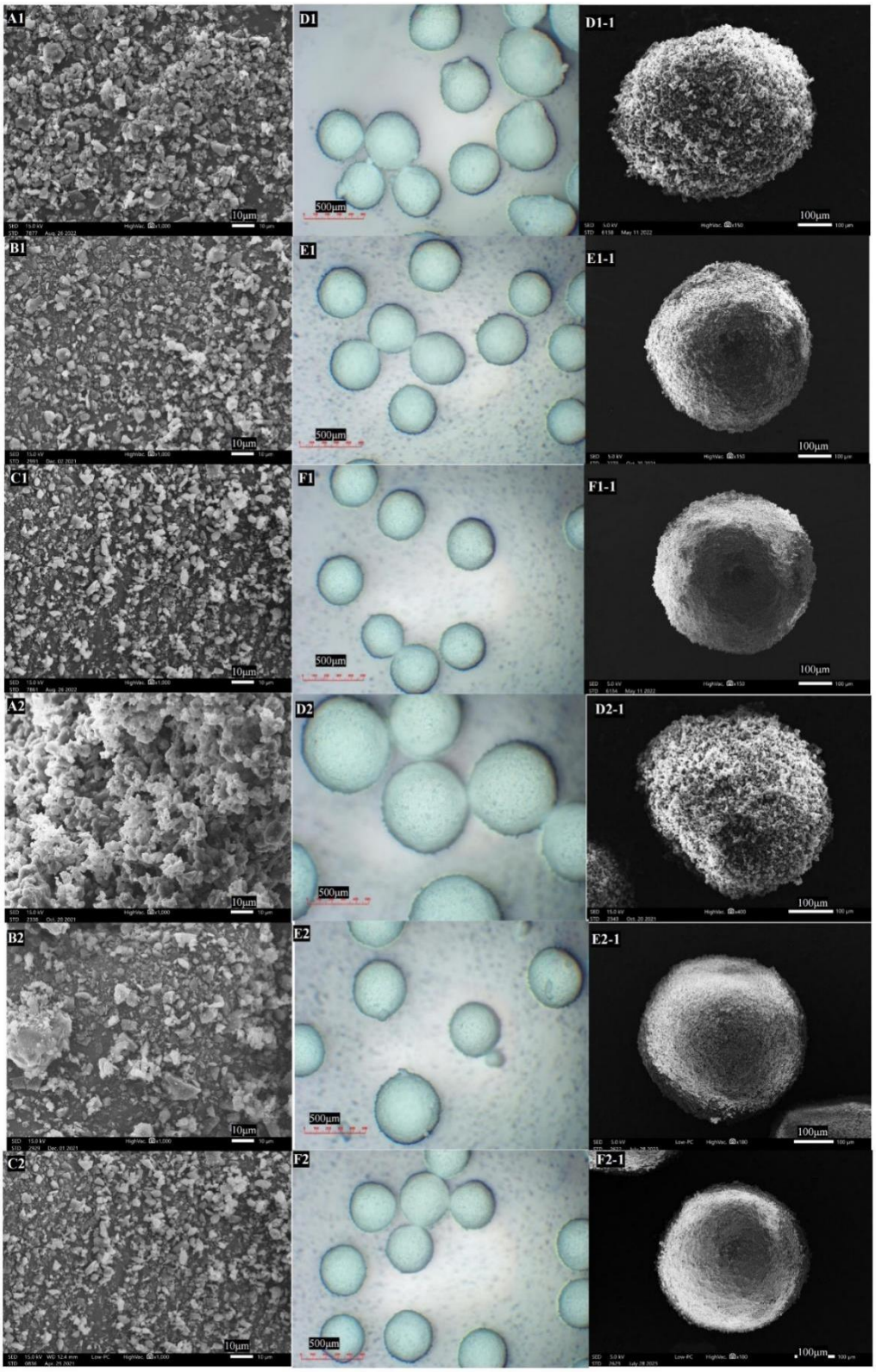

Figure 5. 7 The SEM morphology of the mixture at different mixing pressures (A-2 bar, B-4 bar, and C-6 bar, magnification 1,000×), light microscopy of agglomerates (D-2 bar, E-4 bar, and F-6 bar, magnification 50×), and SEM images of agglomerates (D-1: 2 bar, E-1: 4 bar, and F-1: 6 bar, magnification 150×). A1-F1 represents the melatonin agglomerate formulation and A2-F2 represents the budesonide agglomerate formulation.

The agglomerate particles were categorised into narrower size ranges to

investigate their impact on the delivery dose. As the mixing pressure increased from 2 bar to 6 bar, the weight-based ratio of agglomerates in the 350-500 µm size fraction to those in the 200-350 µm size fraction decreased from approximately 3:1 to 1:1 for melatonin agglomerate formulation and from 6.4:1 to 1.2:1 for the budesonide formulation. Notably, a higher mixing pressure resulted in reduced variability in the agglomeration size distribution, as evidenced by the error bars in Figure 5.8-C.

When delivered through the dosing unit of the Turbuhaler® device (Figure 5.8-D, -E and -F for melatonin formulations, Figure 5.8-F, -H and -I for budesonide formulations), metering doses primarily relied on the size fractions of agglomerates. Formulations with larger agglomerates prepared at lower mixing pressures led to voids within the dosing units and, consequently, lower loads; conversely, a higher mixing pressure facilitated a more uniform distribution of size fractions, allowing for nearly full loading of powder mass within the dosing unit and ensuring consistent delivery doses (Figure 5.8-F and I).

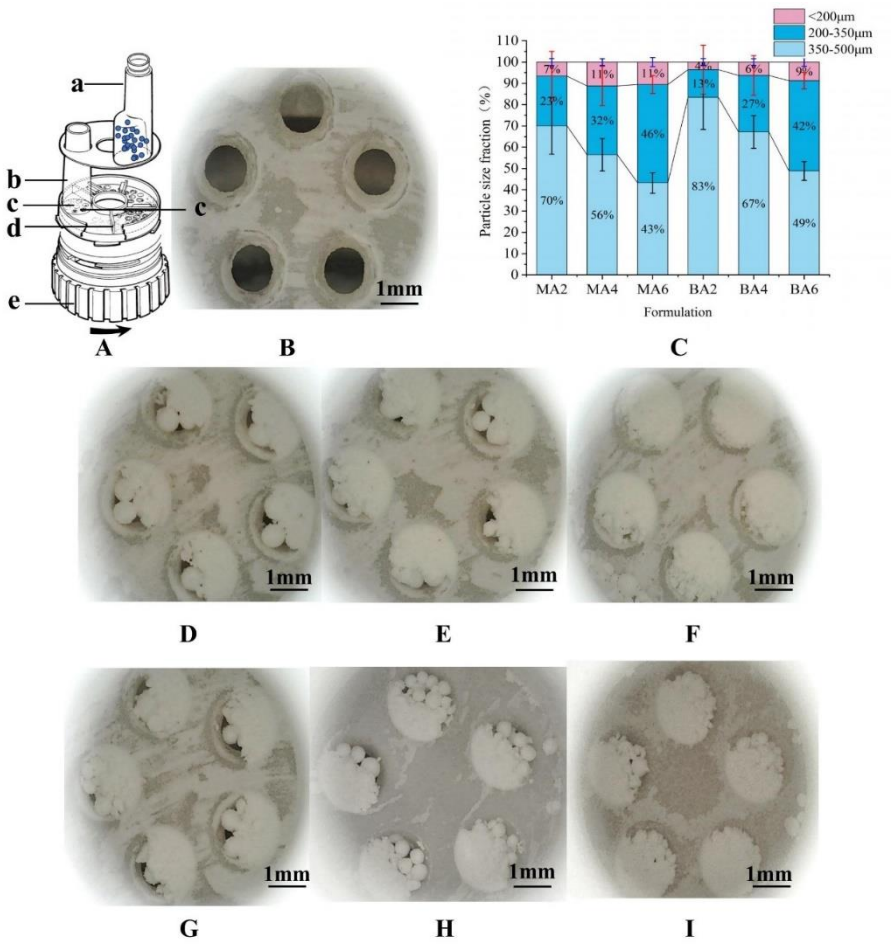

Figure 5. 8 A: Schematic of Turbuhaler® (a. reservoir for agglomerate particles, b. inhalation channel, c. dosing unit, d. plastic scraper, e. dosing wheel); B: Optical microscope of the dosing unit; C: Size fraction based on the weight of the agglomerate formulation; D, E and F illustrate the dose loading of melatonin formulations MA2, MA4 and MA6, G, H, and I illustrate the dose loading of budesonide formulations BA2, BA4 and BA6 respectively.

When mixing pressure was increased and milling pressure kept low, a sufficient mixing effect was observed resulting in a uniform mixture for the preparation of agglomerate formulation, meanwhile, powder clogging was also avoided in milling chamber. Specifically, when the mixing pressure was low, the low shear force acted on the particles, and particle collision and adhesion in the air stream resulted in a larger particle size distribution (MA2 and BA2). When the mixing pressure increased, a larger shear force led to violent collision, reducing the possibility of particle adhesion to achieve a uniform mixture morphology of both formulations.

5.3.7 In vitro aerosolization performance

The in vitro aerosolisation performance of the agglomerate formulations is illustrated in Figure 5.9 and Table 4. As the mixing pressure increased, the ED

improved with reduced deviation. It was postulated that both the mixing pressure and size fraction ratio could potentially influence the ED and its deviation. To investigate this hypothesis, experiments were conducted by sieving and adjusting different ratios of 355-500 µm and 200-355 µm agglomerate particles from the BA2 and BA6 formulations in Turbuhaler®. Figure 5.8 demonstrated that for each formulation (MA2, MA6, BA2, and BA6), the ED exhibited enhancement with decreased deviation as the proportion values declined until reaching a plateau at a size fraction ratio of approximately 1.5:1. Further reduction in the fraction ratio from 1:2 to 1:3 resulted in fluctuating ED values, with larger deviations of approximately 85% for melatonin and approximately 80% for budesonide. The overall delivery dose of the melatonin formulation was higher than that of the budesonide formulation because of the reduced loss of fine API particles in the melatonin mixture during air jet mixing. These findings indicated a similar trend for both formulations, highlighting that the optimal delivery dose with lower deviation relied heavily on achieving an even distribution of large and small agglomerate particles.

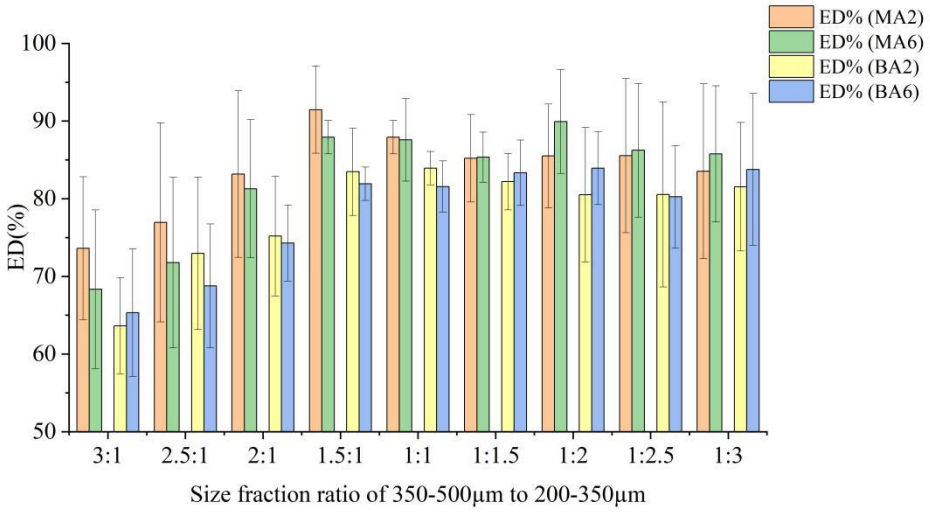

Figure 5. 9 Investigation of agglomerate size fraction ratio on ED with BA2 and BA6 formulations

A higher mixing pressure contributed to nearly equal size fractions of large and small agglomerate particles, resulting in an improved emitted dose (ED) and reduced deviation. As previously suggested by Wetterlin (Wetterlin, 1988), the delivery dose in the reservoir inhaler device is metered based on the volume.

Therefore, it is important to maintain uniform and constant void spaces among agglomerate particles during each loading action to ensure minimal variation in the delivery dose. Thus, optimising the balance of the particle-size fractions is crucial.

A lower deviation was observed when the ratio of the 350-500μm to 200-350μm size fractions ranged from 1.5:1 to 1:2, which was validated by analysing the corresponding error bars. Additionally, larger agglomerates possess greater mass and cohesion forces, making them more susceptible to gravity and requiring a higher drag force from the airflow for dispersion. Consequently, larger agglomerates face difficulties in releasing and being entrained by airflow. Hence, an increase in the size fraction ratio from 1:1 to 3:1 results in a decrease in ED.

The aerosolisation performance was also influenced by mixing pressure, as indicated in Table 5.8. There were significant increases in the emitted dose (ED) and fine particle fraction (FPF) for both formulations from 2 bar to 6 bar, followed by a declining trend in mass median aerodynamic diameter (MMAD), suggesting superior deagglomeration and dispersion at elevated mixing pressures after the high shear mixing process. Increasing the mixing pressure led to a significant reduction in drug deposition in the artificial throat and an enhancement in FPF, particularly evident through the increased deposition observed in later stages of the Next Generation Impactor (NGI).

Figure 5.10 demonstrated a declining trend of deposition in the artificial throat and an improvement from stage 3 to stage 6 for both formulations. However, there was a contrasting observation regarding deposition in the pre-separator for melatonin and budesonide formulations, as decreased deposition suggested better dispersion for the budesonide formulation at higher mixing pressures.

Table 5. 9 Aerodynamic properties of melatonin agglomerate formulation.

		ED/%	FPD/μg	FPF/%	MMAD/μm	GSD
Melatonin	MA2	75.8±12.8	62.0±12.4	40.8±2.7	2.7±0.2	1.8±0.1
	MA4	82.5±9.2	82.4±3.2	49.9±0.9	2.5±0.2	1.8±0.0
	MA6	88.9±2.9	93.3±3.8	52.6±1.6	2.3±0.1	1.8±0.0
Budesonide	BA2	71.6±0.4	36.9±1.5	32.2±1.2	3.2±0.1	1.8±0.1
	BA4	73.5±0.8	50.9±1.6	43.3±1.0	2.5±0.0	1.8±0.0
	BA6	85.4±2.4	70.1±1.2	51.4±0.5	2.3±0.1	1.8±0.0

ED = emitted dose; FPD = fine particle dose; FPF = fine particle fraction; GSD = geometric standard deviation; MMAD = mass median aerodynamic diameter; Data are represented as mean ± SD (n = 3).

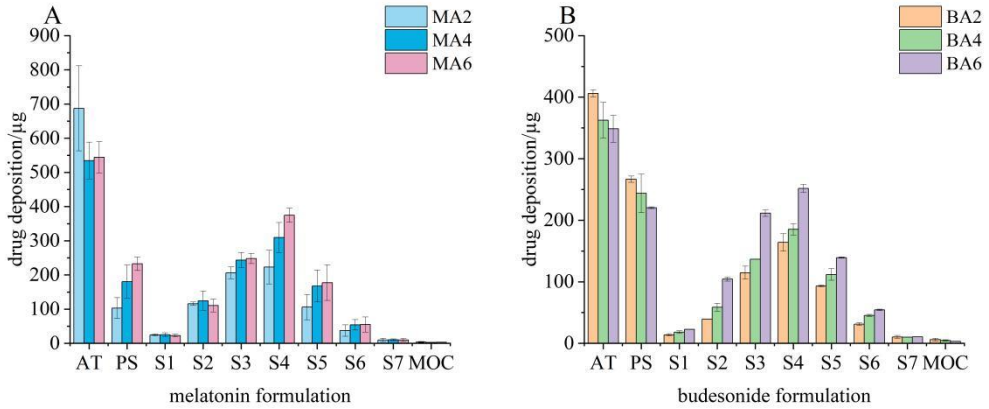

Figure 5. 10 The comparative analysis of the deposition pattern between melatonin(A) and budesonide(B) agglomerate formulations

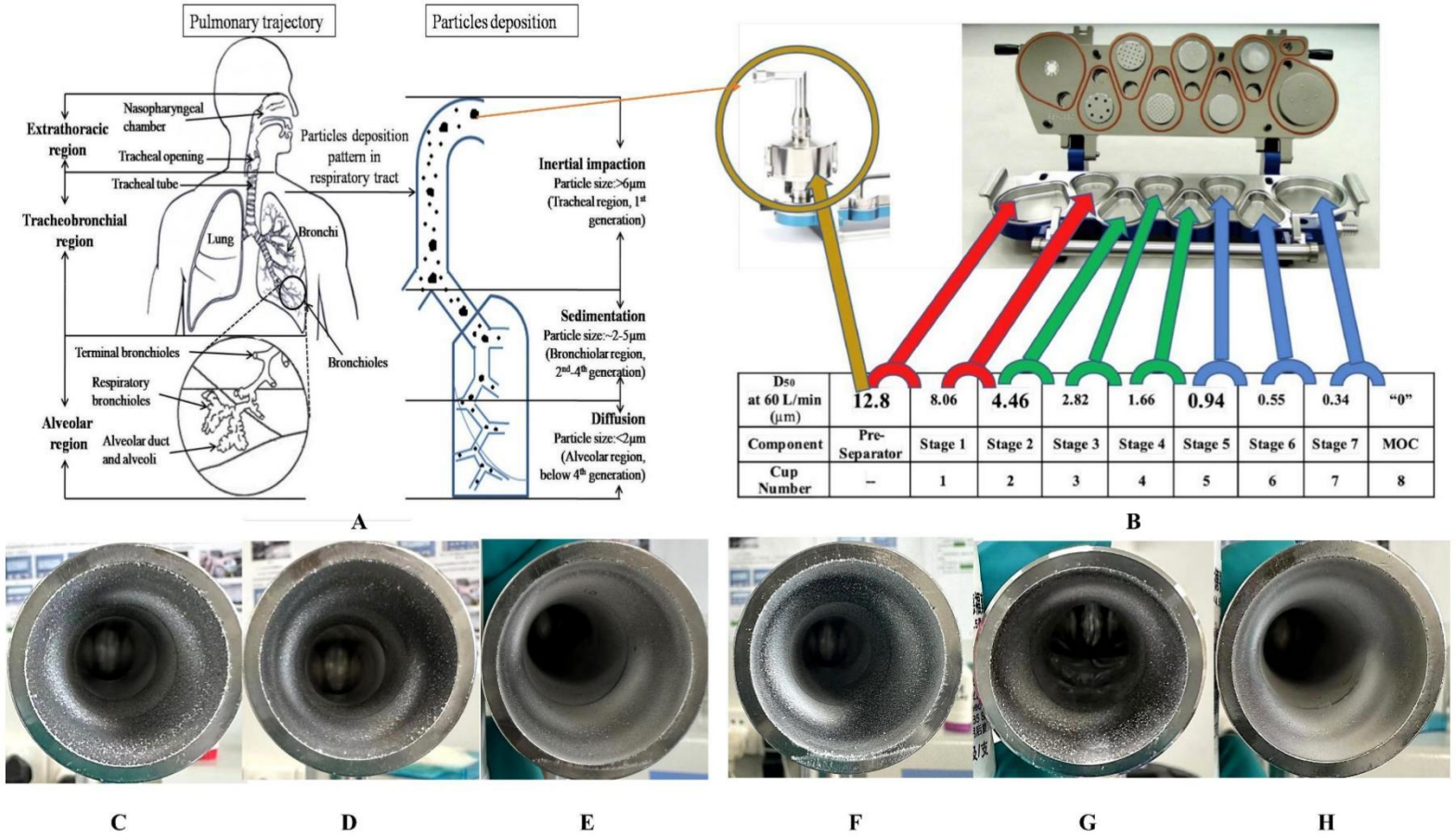

D_{50} at 60 L/min (μm)	12.8	8.06	4.46	2.82	1.66	0.94	0.55	0.34	"0"
Component	Pre-Separator	Stage 1	Stage 2	Stage 3	Stage 4	Stage 5	Stage 6	Stage 7	MOC
Cup Number	–	1	2	3	4	5	6	7	8

Figure 5. 11 A: Pulmonary tract and size-dependent deposition of particles in the respiratory tract(Chaurasiya and Zhao, 2021); B: Cutoff aerodynamic diameter for stages of NGI (US Pharmacopoeia 32); C, D, and E illustrate the particle deposition of melatonin formulations (MA2, MA4, and MA6) in the artificial throat; F, G, and H illustrate the particle deposition of budesonide formulations (BA2, BA4, and BA6) in artificial throats.

This phenomenon can be attributed to a reduction in the deposition within the artificial throat, as depicted in Figure 5.11, where aggregates larger than 12.8μm tend to deposit. However, with increasing mixing pressure, there was a gradual decrease in the number of larger-sized clusters and an increase in the number of fine particles. Notably, when using a mixing pressure of 2 bar for both formulations, inferior deagglomeration of coarse particles was observed, whereas fine particles dominated at a mixing pressure of 6 bar. Given that lactose constituted a significant proportion of the formulation, elevated mixing pressures could potentially reduce inter-particle cohesive forces between the drug and lactose and consequently enhance aerosolisation performance.

5.3.8 Mechanistic investigation of the de-agglomeration process in agglomerate formulations

To comprehend the de-agglomeration behaviour of the agglomerate formulation under varying mixing pressures, the impact of the flow rate on aerosolisation was assessed using a Turbuhaler® within a flow rate range of 30-120 L/min. The distribution density versus flow rate charts in Figure 5.12 and Figure 5.13 for melatonin and budesonide formulations, respectively, reveal distinct deagglomeration patterns, particularly at lower flow rates. By characterising the effect of mixing pressure on the alterations in the agglomerate structure through a series of flow rates, it becomes evident that deagglomeration varies across different sites within the Turbuhaler device.

Melatonin Formulation:

For the melatonin formulation from air jet mixing with a feed pressure of 2 bar, the particle size distribution was bimodal at lower flow rates of 30 and 45 L/min and exhibited a shoulder at approximately 35 μm, indicating that the collision between the agglomerate and the interior wall of the device failed to achieve complete deagglomeration. However, when the mixing pressure was 4 bar and 6 bar, mono-modal distributions were observed at flow rates of 30-120 L/min, and size distributions larger than 20μm showed a decreasing trend when the mixing

pressure increased.

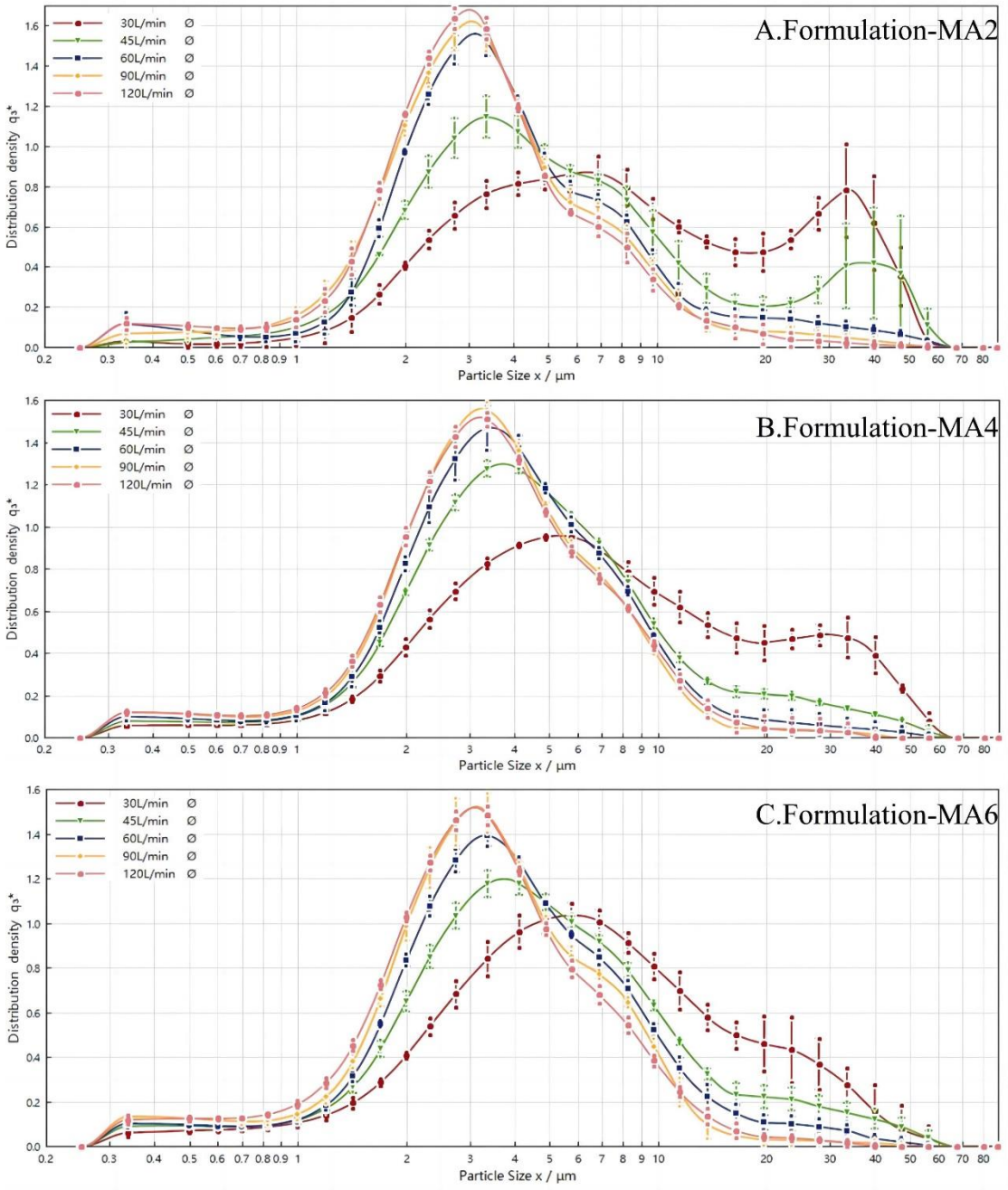

Figure 5. 12 Released particle size distribution profiles of melatonin formulations dispersed from Turbuhaler® at 30-120 L/min. *. distribution density q^3 represents the probability density function of a certain particle size and was derived with PAQXOS® software (Sympatec GmbH, Clausthal-Zellerfeld, Germany)

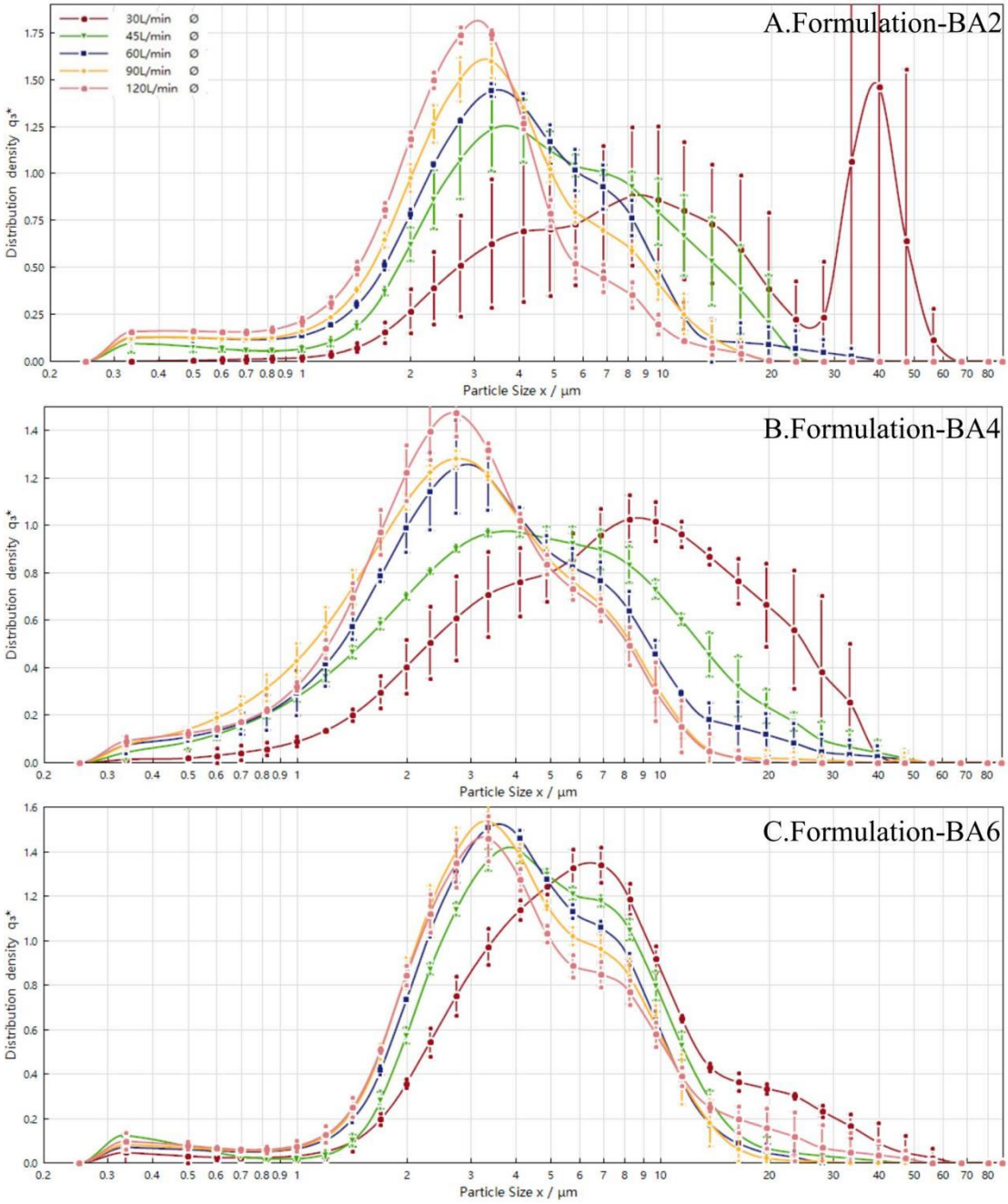

Figure 5. 13 Released particle size distribution profiles of budesonide formulations dispersed from Turbuhaler® at 30-120 L/min.

Budesonide formulation

The deagglomeration state of the budesonide formulation revealed a different particle size distribution pattern. First, a bimodal distribution with a large deviation was observed in the formulation produced at 2 bar mixing pressure at low air flow rates of 30 and 45 L/min and 30, 45, and 60 L/min, respectively. At a lower mixing speed of 300rpm, there was evidence of some small clusters with sizes of approximately 10µm at an air flow rate of 30 L/min with a larger density

distribution deviation. Second, the formulation with a mixing speed of 300rpm demonstrated a mono-modal distribution profile and a lower density distribution deviation when the flow rate exceeded 30 L/min.

Relative Deagglomeration and Airflow Rate

The results in Figure 5.14 demonstrate distinct variations in the relative de-agglomeration behaviour of both formulations under different flow rates. In brief, the relative de-agglomeration was determined by comparing the cumulative particle size of aerosolized powder less than 5.4 μm (obtained through laser diffraction particle sizing of the aerosol plume and representing the inhalable range) with the total availability of particles within that size range (measured by laser diffraction particle sizing of the powder dispersed under compressed air). Both agglomerate formulations exhibited an increase in relative de-agglomeration as the air flow rate increased. However, for formulations produced at a mixing pressure of 2 bar, there was a rapid rise in relative de-agglomeration for melatonin formulation at low air flow rates, which then plateaued at 90 L/min with a value around 88.1±3.7%. In contrast, the budesonide formulation showed a slower increase in relative de-agglomeration with increasing airflow rate, reaching approximately 80.0±3.9% at 90 L/min. Generally, both formulations produced at mixing pressures of 4 bar and 6 bar displayed similar levels of relative deagglomeration when subjected to airflow rates above 60 L/min.

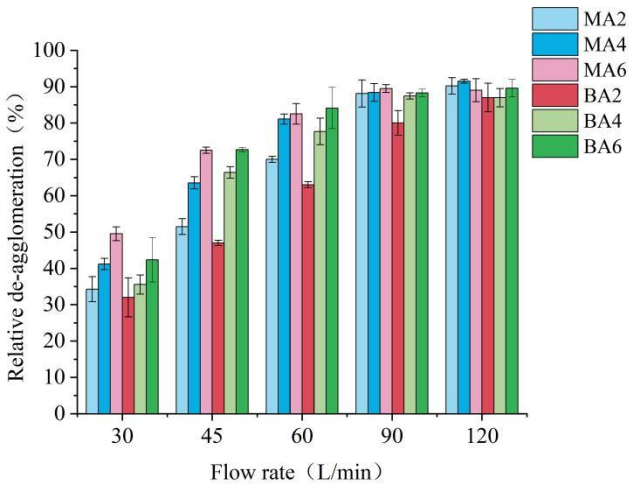

Figure 5. 14 Relative de-agglomeration behavior of agglomerate formulations at different flow

rates

To mathematically represent the relationship between the relative deagglomeration and airflow rate, the data were fitted using a previously reported 3-parameter sigmoidal equation (Behara et al., 2011). This method, described in the methods section (2.4.1.10 Deagglomeration evaluation), employs nonlinear least-squares regression. One key parameter obtained from this model is "x_0", which represents the airflow rate at which 50% of the maximum relative deagglomeration occurs. Table 5.9 summarizes the fitting statistics for each formulation. As shown in Figure 5.15, the sigmoidal equation effectively modelled the deagglomeration profiles for most formulations, with R-squared values exceeding 0.99. These parameters effectively captured the deagglomeration behaviour of each formulation and revealed the relationship between the mixing pressure, deagglomeration, and fine particle fraction (FPF). Notably, a clear inverse correlation between FPF and x_0 was observed in Figure 5.16.

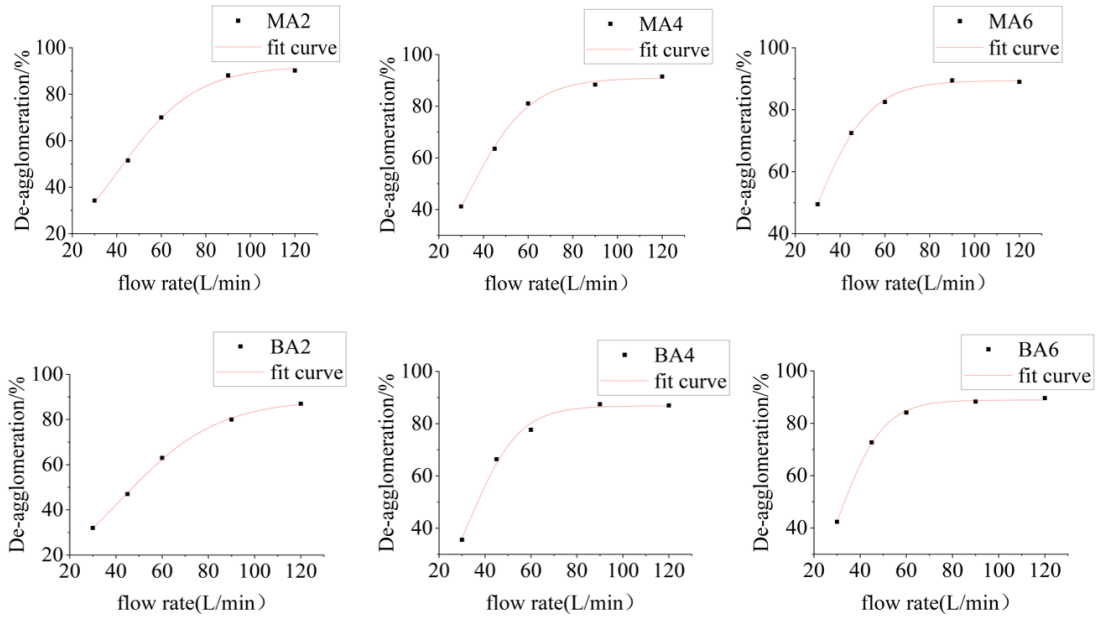

Figure 5. 15 Non-linear least squares regression on the profile of relative de-agglomeration versus flow rate

Table 5. 10 Non-linear fitting of the relative de-agglomeration versus flow rate profile for agglomerate formulation and the corresponding FPF

Formulation	X_0 (L/min)	R^2	FPF (%)

MA2	39.9 ± 0.9	0.996	40.8±2.7
MA4	32.8 ± 0.7	0.995	49.9±0.9
MA6	27.1 ± 0.5	0.997	52.6±1.6
BA2	42.0 ± 0.6	0.998	32.2±1.2
BA4	33.5 ± 1.0	0.988	43.3±1.0
BA6	30.8 ± 0.3	0.998	51.4±0.5

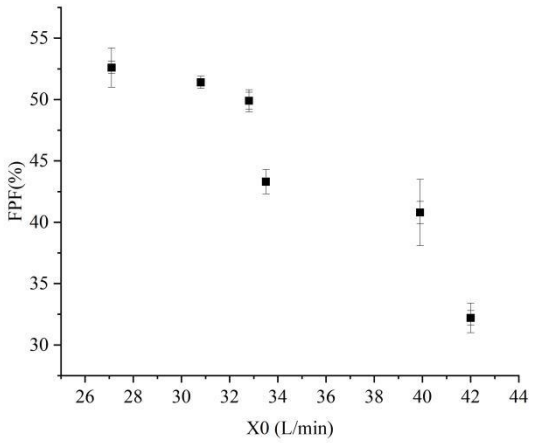

Figure 5. 16 Correlation of X0 with FPF of agglomerate formulation of melatonin and budesonide

The NGI, with its defined stages and flow rates, provides a standardized method for characterizing the aerodynamic particle size distribution (APSD) of inhaled particles. Laser diffraction, with its ability to rapidly measure particle size distributions over a wide range, complements the NGI by providing further insights into the particle size characteristics of the formulation.

The Next Generation Impactor (NGI) is a sophisticated tool designed to simulate real-life inhalation conditions and assess the potential pulmonary deposition of drugs delivered via dry powder inhalers (DPIs). It achieves this by replicating the aerodynamic principles governing particle deposition in the human respiratory tract. The NGI consists of a series of progressively smaller stages, each designed to capture particles of specific aerodynamic diameters. As the aerosolized drug particles are drawn through the NGI at a controlled flow rate (typically corresponding to human inhalation rates, e.g., 30-90 L/min), they encounter stages with decreasing cut-off diameters. Particles with sufficient inertia are

deposited on each stage, while smaller particles remain suspended in the airflow and are collected on subsequent stages or a final filter. This staged separation closely mirrors the deposition patterns observed in the human respiratory tract, where larger particles are deposited in the upper airways, and smaller particles reach the deeper lung regions.

Additionally, the NGI accounts for real-life inhalation dynamics by incorporating flow rate variability, which is critical for simulating different patient inhalation profiles. By adjusting the flow rate, the NGI can replicate the varying inhalation strengths of patients, providing a more accurate prediction of drug deposition under real-world conditions. Furthermore, the NGI's design minimizes particle bounce and re-entrainment, ensuring that the collected particle distribution reflects true deposition behavior. This makes the NGI an invaluable tool for optimizing DPI formulations and predicting their performance in clinical settings. However, it is crucial to acknowledge the limitations of these techniques in simulating real-life inhalation conditions.

- **Limitations:**

Simplified Respiratory Tract Model: The NGI, while a valuable tool, simplifies the complex geometry and physiological processes of the human respiratory tract. It does not account for factors such as:

Turbulence: The turbulent airflow within human airways, which can significantly influence particle deposition.

Lack of Physiological Relevance: The NGI does not incorporate physiological factors such as mucociliary clearance, which play a crucial role in particle transport and removal from the lungs**.**

Laser Diffraction Limitations:

Assumption of Spherical Particles: Laser diffraction techniques often assume spherical particle shapes. Deviations from sphericity, such as those observed with irregularly shaped particles, can significantly impact the accuracy of size measurements.

Limited Information on Particle Morphology: Laser diffraction primarily provides information about particle size. It does not provide detailed information about particle morphology (e.g., shape, surface roughness), which can significantly influence aerodynamic behavior and deposition.

Impact on Drug Delivery

Figure 5.16 demonstrates that deagglomeration (as represented by x_0) is inversely correlated with the mixing pressure. The formulations produced at 2 bar (MA2 and BA2) contained larger clusters owing to the presence of significant mass and cohesive forces. These forces increase the gravitational force, leading to premature deposition in the throat region. Consequently, a higher airflow rate was required to disperse these clusters, resulting in the high drug deposition on the artificial throat surface observed for these formulations. As the flow rate increased, these larger clusters fragmented into smaller particles, which eventually disappeared at 90 L/min.

In contrast, formulations produced at higher mixing pressures (4 bar and 6 bar) exhibited smaller particle size fractions. This reduces the gravitational forces, allowing for the entrainment and dispersion of agglomerates at lower airflow rates. This ultimately leads to more efficient transport of drug particles to the lungs, where deagglomeration can occur due to bronchial airflow, facilitating the deposition of the active pharmaceutical ingredient (API) in the lungs. The observed unimodal distributions with smaller particle sizes in the profiles from to 4-6 bar further support this notion, indicating improved aerosolisation performance with increasing mixing pressure.

The NGI, with its defined stages and flow rates, provides a standardized method for characterizing the aerodynamic particle size distribution (APSD) of inhaled particles. Laser diffraction, with its ability to rapidly measure particle size distributions over a wide range, complements the NGI by providing further insights into the particle size characteristics of the formulation.

However, it is crucial to acknowledge the limitations of these techniques in

simulating real-life inhalation conditions.

- **NGI Limitations:**
    - **Simplified Respiratory Tract Model:** The NGI, while a valuable tool, simplifies the complex geometry and physiological processes of the human respiratory tract. It does not account for factors such as:
        - **Turbulence:** The turbulent airflow within the human airways, which can significantly influence particle deposition.
        - **Particle-wall interactions:** Interactions between inhaled particles and the airway walls, which can affect deposition patterns.
        - **Physiological factors:** Factors such as breathing rate, tidal volume, and airway resistance, which vary between individuals and can significantly impact particle deposition.
    - **Lack of Physiological Relevance:** The NGI does not incorporate physiological factors such as mucociliary clearance, which play a crucial role in particle transport and removal from the lungs.
- **Laser Diffraction Limitations:**
    - **Assumption of Spherical Particles:** Laser diffraction techniques often assume spherical particle shapes. Deviations from sphericity, such as those observed with irregularly shaped particles, can significantly impact the accuracy of size measurements.
    - **Limited Information on Particle Morphology:** Laser diffraction primarily provides information about particle size. It does not provide detailed information about particle morphology (e.g., shape, surface roughness), which can significantly influence aerodynamic behavior and deposition.

Despite these limitations, the NGI and laser diffraction remain valuable tools for characterizing the aerodynamic properties of inhaled particles

5.4. Discussion

In a previous study, the disparity between high-shear and low-shear mixers in the preparation of carrier-based dry powder mixtures was investigated (Rudén et al., 2019). By assessing the bulk powder, fluidisation, and aerosolisation properties of the powder blends, it was demonstrated that high-shear blends significantly enhance the Fine Particle Fraction (FPF). This enhancement may be attributed to alterations in the bulk powder properties owing to the generation of fine particles in situ, leading to improved fluidisation properties.

Ward and Schultz explored the co-micronisation of drug substances with fine lactose using jet milling as an efficient and straightforward approach to formulate inhalable powders, particularly for initially highly cohesive drug substances(Ward and Schultz, 1995b). However, inappropriate micronisation processes result in disproportionate loss of fine drug and lactose particles, leading to heterogeneous drug concentrations in the mixture. This inhomogeneity adversely affects the uniformity of the delivered doses during inhalation therapy.

Our study revealed that high-shear mixing of fine materials at high speeds led to stronger adhesion between the drug and lactose, resulting in a higher proportion of cohesive aggregates and, consequently, lower emitted doses and FPF. The optimal aerodynamic performance of the agglomerate formulation was achieved through a combination of a higher feed pressure to generate sufficient mixing effects and a lower milling pressure to prevent powder clogging in the milling cavity, resulting in a uniform mixture.

The formulation of DPI agglomerates typically involves micronised drugs or a blend with finely dispersed lactose particles, aiming for particle sizes comparable to those of the active pharmaceutical ingredient (API). The extent of inter-particle detachment during inhalation plays a crucial role in determining the effectiveness of drug delivery to the lungs (de Boer et al., 2004). The inter-

particulate forces within the powder formulation can be influenced by the method and intensity of mixing (Alyami et al., 2017). Despite their significance, the impact of mixing approaches on binary adhesive mixtures for agglomerate formulations has been largely overlooked and warrants detailed exploration. In this study, a combination of high shear and air jet mixing with various parameters was employed to establish the relationships among the agglomerate morphology, blend state, and formulation dispersibility(Lau et al., 2017b).

High shear mixing was an alternative to the low shear blending process with the advantage of reducing the mixing time and improving the dispersion of fine material in the coarse particle bed (Vanarase et al., 2013). It was found in this study that when a mixing speed from 300rpm to 1200rpm was used, there was no significant effect on the mixture homogeneity and particle size distribution. However, SEM observation of the mixture exhibited a nonhomogeneous powder structure with small aggregates when a lower mixing speed was applied, and fragments adhered to the surface of the final agglomerate formulation particles, even though combination with air jet mixing was carried out at lower air pressure. This was not observed in the air-jet mixing process. Therefore, this interesting observation might be related to the formation of drug-lactose agglomerates upon blending with high intensity, which is known to undergo a rapid initial agglomeration by impact with other particles and the mixing vessel walls, and this rapid initial agglomeration increases with the mixing speed(You et al., 2021). It is known that small agglomerates may also be formed during the agglomeration process, in which the fragments attach to larger agglomerate particles and are reduced in size but increase in mechanical strength by inter-particle collisions (Tamadondar et al., 2019). Changes in the size fraction of the agglomerate particles after spheroidisation provided information about the powder structure with increasing mixing speed. For the budesonide mixture, both the bulk and tapped densities showed insignificant changes at different mixing speeds; however, there was an increasing trend for the melatonin formulation,

indicating the significant effect of mixing on the alteration of powder structure and the subsequent particle agglomeration process. Moreover, because budesonide is more cohesive in nature than melatonin and accounts for 20% of the mixture, the higher interactive forces also contribute to the difference in powder density properties. Thus, the size fraction(>500μm) of the budesonide agglomerate formulation accounted for a higher proportion at all mixing speeds, resulting in a lower emitted dose compared to the melatonin formulation. Therefore, a high shear mixing process could exert sufficient energy input to homogenise the cohesive mixture and break up the smaller aggregates to facilitate dosing.

Further aerodynamic deposition patterns suggested that the effects of mixing speed on fine particle delivery might be related to these structures. It is conceivable that for the 300rpm and 600rpm formulations examined in this study, there was sufficient deagglomeration due to the lower mechanical strength of the agglomerate, and a relatively higher FPF was observed, whereas 1200rpm may have been too intensive, resulting in poor deagglomeration of drug-fines agglomerates through the device with a lower FPF. Such a hypothesis, however, can be proven by the higher deposition in the pre-separator. Therefore, consideration must be given to further mitigate the interparticle forces formed with various mixing intensities and to maintain a balance between the content uniformity of the API and good dispersion of the mixture(Zhang et al., 2024).

The air jet mixing process is a highly efficient manufacturing technique that offers an alternative approach to the conventional high shear mixing process, resulting in reduced mixing time and improved dispersion for agglomerate formulations (Giry et al., 2006). By increasing the mixing pressure while maintaining a low milling pressure, a significant enhancement in the mixing effect was observed. This not only ensured the uniformity of the mixture, but also prevented powder clogging in the milling chamber. Specifically, a higher mixing pressure led to an increased shear force of the air flow, causing intense

collisions between the powder particles and reducing the particle adhesion. Consequently, a uniform mixture morphology of melatonin and budesonide was achieved, without any clusters attached to the final agglomerate particles. The relationship between the size fraction of the agglomerate particles below and above 350μm and the mixing pressure was further explored, indicating a strong correlation. However, it is important to consider balancing the loss of fine particles, especially API, in formulations with higher fine particle delivery resulting from increased mixing pressure to ensure the desired drug concentration. It has been suggested that an appropriate mixing pressure effectively achieves a homogeneous mixture and enhances the dispersion of clusters in agglomerate formulations, despite the cohesive nature of the fine particles. Ultimately, air jet mixing not only improves dose delivery, but also enhances fine particle delivery.

The pulmonary delivery processes of DPIs are divided into four stages: (i) fluidisation and dispersion of DPIs within the inhaler device, (ii)de-agglomeration of DPIs, (iii) transportation of DPIs through the oropharynx and throat, and (iv) deposition of APIs in the lung(Cui et al., 2022). Deagglomeration characterisation using laser diffraction equipped with the INHALER™ technology can simulate the first three stages and predict the final DPI deposition efficiency. When exposed to varying inhalation airflow rates, the drag force acting on agglomerates changes. This in turn influences the extent of airflow entrainment and de-agglomeration (Chew and Chan, 2001, Nguyen et al., 2014, van Wachem et al., 2020). The formulations produced at elevated mixing pressures had lower X_0 values for both melatonin and budesonide. This indicates superior de-agglomeration and aerosolisation performance. Notably, the proportion of clusters exceeding 12 μm emitted from the device decreased with increasing mixing pressure, mirroring the trend observed for the overall agglomerate particle size distribution. Cohesive agglomerate formulations exhibit complex particle interactions. These interactions depend not only on the inherent variability of single particle-particle events based on size, but also on the number

and type of contacts with neighbouring particles and the spectrum of surface energies presented on each particle's surface (Pinson et al., 1998). Particle orientation within the powder bed further influences how particles are held together, leading to microscale non-homogeneity. Different mixing methods can be used to create network domains with varying tensile strengths. These variations are related to the size of interacting particles, work of cohesion between contacting particles, and packing fraction in different areas of the powder bed (Kendall and Stainton, 2001). As a result, when exposed to dispersive forces, entrainment and relative de-agglomeration are expected to occur differently, depending on the cohesive structure of the powder bed (Nguyen et al., 2014, van Wachem et al., 2020).

Based on the above, the relative de-agglomeration versus air flow rate profile used in conjunction with the FPF provided a deep understanding of the cohesive powder structure and the mechanism that agglomerate break-up was not step-wise since collisions in device would cause progressive break-up into fractions such as half, quarter, etc., and would resulted in a decrease in the position of the larger mode with increased air flow rates under different mixing condition(Breuer and Khalifa, 2019), it is likely that the mixing process induced different powder structure to be subjective to different extent of impaction and/or aerodynamic drag force.

5.5. Conclusions

This study demonstrated that combining high shear mixing with air jet mixing offers a significant strategy for optimising dry powder inhaler (DPI) formulations. Air jet mixing employed subsequent to high shear mixing yielded superior results in two key aspects: improved aerosol performance and a more favourable agglomerate size distribution. Compared to high shear mixing alone, air jet mixing fostered a more uniform mixture with fewer aggregates. This translates to a notably enhanced emitted dose and fine particle fraction (FPF). These improvements are directly attributable to the specific agglomerate size

distribution achieved and the facilitated de-agglomeration during inhalation owing to the incorporation of air jet mixing.

This study underscores the importance of in vitro techniques, such as relative deagglomeration profiles, for comprehensively characterising DPI formulations. We demonstrated the potential of these techniques to evaluate the influence of the processing parameters on the performance of agglomerate DPI formulations. These findings provide valuable insights into advancements in both DPI formulation design and mixing techniques. Further research is warranted to delve deeper into the intricate interactions suggested by this study. This includes employing advanced techniques to examine the trends observed for various drugs, blending methods, and aerosolisation conditions. In addition, investigating the behaviour of ternary formulations with varying drug concentrations is of significant interest. By fostering a comprehensive understanding of these factors, researchers can achieve rapid optimisation of DPI performance during development, ultimately leading to improved clinical outcomes in patients who rely on DPI therapy.

Chapter 6. Continuous particle agglomeration via vibration and mechanical dry coating technique for enhanced aerodynamic performance

6.1 introduction

Spherical agglomerates can be used as powder formulations for inhalation owing to their superior flowability to handle compared to micronised powder and improved fine particle dispersion. However, budesonide and melatonin exhibit distinct cohesion/adhesion properties as studied in Chapter 4 and 5, drug loss/adhesion during spheroidization were potential obstacles from a therapeutic and continuous industrial production point of view. Fine particle agglomeration relies on the inherent cohesive forces of the particles. During spheroidisation in a coating pan, these forces cause the formation of small primary aggregates. These aggregates then grow larger in a layer-by-layer fashion as additional fine particles adhere to their surfaces(Seiphoori et al., 2020). The resulting larger agglomerates are essentially fractal structures composed of smaller interconnected primary aggregates bonded by cohesive forces, typically van der Waals forces.

As spheroidisation progressed, the weight of the agglomerate bed compressed the particles, increasing their packing density and contact with each other. This densification process manifests differently depending on the material properties:

- **Enhanced Mechanical Strength:** For cohesive materials, increased interparticle contact translates into stronger and more robust agglomerates.
- **Fragmentation:** For less cohesive powders, continued spheroidisation can lead to the breakage of larger agglomerates into smaller fragments.

The conventional spheroidisation process often achieves good sphericity and flowability for the soft agglomerates produced. However, this extended processing time introduces some limitations (Hartmann, 2008):

- **Uncontrolled Mechanical Strength:** The prolonged processing can result in agglomerates with unpredictable mechanical properties.
- **Broad Size distribution:** This process may also lead to a wide range of agglomerate sizes within the final product.

Both issues can hinder the efficiency of deagglomeration and fine particle dispersion during inhalation. Insufficient deagglomeration within the lungs can lead to improper penetration of the powder dosage to the bronchial region, potentially compromising drug delivery (Le et al., 2012).

To address the challenges associated with conventional production methods, alternative techniques, such as particle agglomeration under ultrasonic vibration and resonant acoustic mixing, offer promising solutions. These techniques enable the continuous production of well-defined agglomerate formulations with efficient deagglomeration and fine-particle dispersion properties. Ultrasonic vibration has emerged as a valuable tool for controlled agglomeration of fine particles, particularly those with diameters of 2.5 μm or less (Riera et al., 2015). This technique leverages high-intensity aerial ultrasonic waves to induce targeted vibrations within the particle population. These vibrations promote interparticle collisions, ultimately facilitating the formation of agglomerates (Garbarienė et al., 2021). A critical advantage of ultrasonic vibration is its ability to generate agglomerates with inherently loose microstructures, which significantly enhances their dispersibility. During the spheroidisation process within the coating pan (Figure 6-1A, B), the spherical agglomerates underwent continuous rotation and sliding motion from the bottom of the pan. Notably, the ultrasonic vibration waves were effectively transmitted to these agglomerates, inducing low-amplitude vibrations within the constituent smaller aggregates (Figure 6-1C, D). This induced vibration weakens or even minimises the contact points between the smaller aggregates.

Consequently, ultrasonic vibration facilitates the formation of agglomerates composed of finer particles and smaller mechanically weaker sub-aggregates

(Nakai et al., 2016). This specific characteristic offers a distinct advantage for budesonide, a drug known for its propensity to adhere to the interior walls of rotating vessels. By mitigating inter-aggregate bonding forces, ultrasonic vibration has the potential to significantly reduce this adhesion issue.

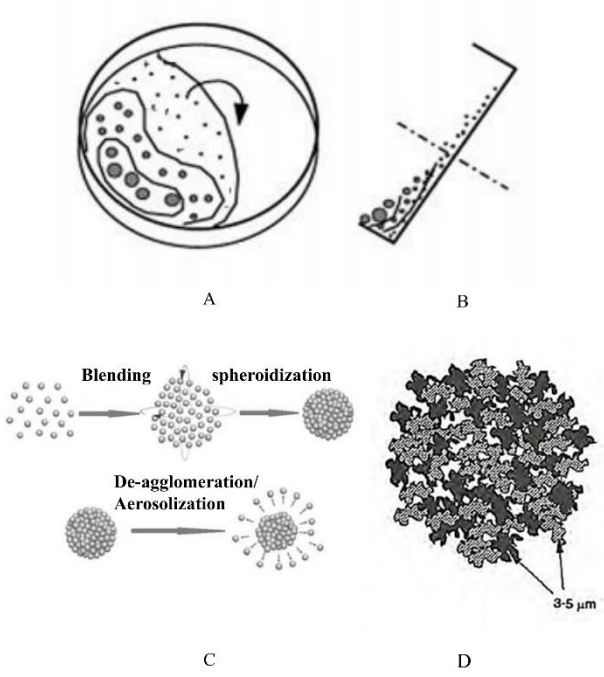

Figure 6. 1 Schematic of (A) front view and (B) side view of particle agglomeration under ultrasonic vibration (ZHENG, 2012). (C) Principle of particle agglomeration, and (D) schematic of individual agglomerate.

Achieving continuous particle agglomeration of melatonin and fine lactose presented a unique challenge owing to the inherently low cohesive nature of the drug particles. To overcome this limitation and facilitate efficient adhesion and agglomeration under high acceleration forces, this investigation focused on optimising the mixing and pre-agglomeration stages.

Resonant acoustic mixing (RAM) has emerged as a promising technique owing to its ability to induce a micro-mixing effect throughout the entire mixture. This effect, achieved through low-frequency acoustic vibration, results in the movement and collision of bulk particles with their neighbours (Osorio and Muzzio, 2015). A key advantage of RAM is the absence of mixing dead zones, which ensures an even distribution of shear force throughout the mixing vessel.

During the RAM process, the system is maintained at its resonant frequency, facilitating efficient energy transfer from the machine to the powder material (Knoop et al., 2016). This transferred energy promotes the adherence of API particles to lactose particles or to each other via van der Waals interactions (Abiona et al., 2022b). Additionally, fluidisation and random collision of larger aggregates contribute to the formation of smaller clusters, ultimately leading to the desired final agglomerates (Osorio et al., 2016).

For cohesive drugs, such as budesonide, achieving optimal mechanical properties within agglomerates during spheroidisation is critical. As demonstrated by Kendall and Stainton, the mechanical strength of agglomerates directly correlates with the cohesion between individual particles(Kendall and Stainton, 2001). Mechanical dry coating decreases the inter-particle force or minimises the contact area between the drug particles (Zhou et al., 2010a).This technique utilises controlled shear and compression forces to coat the ternary component (such as magnesium stearate) onto fine lactose particles (Morton, 2006). The process involves subjecting particles to a combination of impaction and compression as they are forced between the edge of the press head and the chamber wall. The high-speed rotation facilitates exposure and intense coating of ternary components on lactose surfaces (Zhou et al., 2010c).

Combined Approach: Vibration and Mechanical Dry Coating with Force Control agents

This chapter investigates the use of ultrasonic and resonant acoustic vibrations to produce spherical agglomerates of budesonide and melatonin. Incomplete deagglomeration can lead to fragments affecting the patient's mouth and throat, potentially causing local and systemic side effects. To address these challenges, this study explored the incorporation of a mechanical dry coating with force control agents during the vibration process. This combined approach has the potential to improve the respirable fraction of the final formulation, ensuring

optimal drug delivery to the targeted lung regions, and potentially leading to enhanced therapeutic outcomes for various respiratory conditions.

6.2. Methods

6.2.1 Production of agglomerate formulation by ultrasonic vibration

Budesonide and melatonin were first micronised using a spiral air jet mill with micronisation and a feed pressure of 8 bar to obtain a D_{90} value of less than 5 µm. The lactose mixture was then blended with micronised APIs (4:1, w/w) in a cyclomixer at a mixing speed of 300 rpm for 30 min. The obtained mixture was then pre-agglomerated using a vibration feeder before being transferred to a rotary drum agglomerator. The power supply of the vibration feeder was set at 160V and 80 Hz, respectively. The agglomerates were smoothed and strengthened at 60 rpm for 10 min at predetermined power inputs of 0 W, 100 W, 200 W and 400 W.

6.2.2 Investigation of particle agglomeration with acoustic mixer

6.2.2.1 The pre-study of grids on agglomerate particle size distribution

To evaluate the effect of grids on the agglomerate particle size distribution during acoustic mixing, 50 g batches of binary mixture (20%w/w APIs) were prepared in a pre-study without and with single- or double-layer grids under different gravitational accelerations, the grids were braided with molybdenum wire (0.1 mm in diameter), and pre-assembled in the centre of the mixing container before oscillation, as shown in Fig 6.2. The acoustic mixing was operated at accelerations (g=9.8 m/s^2) of 60 g, 70 g, and 80 g for 10 min at a frequency of approximately 60 Hz, as previously reported(Tanaka et al., 2016). Agglomerate particles were produced as described in Section 2.2.4.3. The experimental design is presented in Table 6.1.

Table 6. 1 Experimental design to determine the effects of grids in resonant acoustic mixer.

Sample ID	Acceleration (g)	Grids	Mixing time
F1	60		
F2	70	No grid	
F3	80		
F4	60		
F5	70	Single layer	10min
F6	80		
F7	60		
F8	70	Double layer	
F9	80		

6.2.2.2 Optimization for particle agglomeration with acoustic mixer

Building on the pre-study findings, the optimisation phase with a batch size of 500g involved preparing formulations using double-layer grids within the same production method. This approach facilitated a more in-depth investigation of the impact of these grids on various key properties, such as the bulk properties of powder mixtures, agglomerate morphology, mechanical strength, and aerodynamic behaviour at different flow rates.

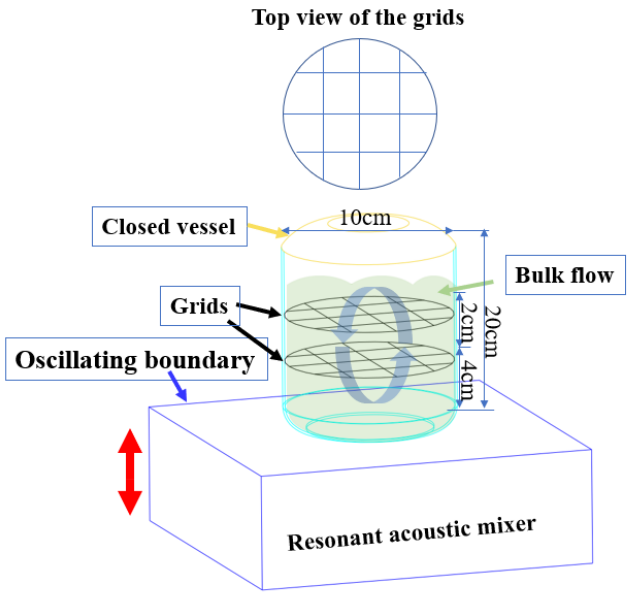

Figure 6. 2 Schematic of RAM mixing with grids for particle agglomeration.

Melatonin and lactose (Inhalac 70, MEGGLE GmbH & Co. KG) were micronised using an air jet mill, as described in Chapter 4, at identical milling and feeding pressures of 5 bar. It is well documented that micronisation can

introduce amorphous content to material surfaces, necessitating a conditioning step (Briggner et al., 1994).

Pre-agglomeration and Spheroidization

After blending with a resonant acoustic mixer (RAM) (Ramixers G500, Shenzhen Ramixers Technology Co., LTD) at varying intensity levels, the pre-agglomerated powder mixture was sieved again to break down the large aggregates. Spheroidisation was then performed using a RO-TAP® test sieve shaker (RX-29, HAVER & BOECKER OHG, Germany) with eccentric oscillation at 150 rpm for 5 min. A combination of 500 μm and 350 μm mesh screens was used on the sieve shaker, which employed a horizontal circular motion with tapping. A tapping motion (100 taps per minute) was applied for 1 min to force the agglomerates through the mesh screens and onto the rotating pan, where the spherical agglomerates were classified.

Post-agglomeration Treatment

Following the agglomeration process, the resulting agglomerates were placed inside a chamber set at 25°C and 50% RH for 2 h to dissipate the static charge before further analysis.

6.2.3 Intensive mechanical dry coating

Mechanical dry coating using Magnesium Stearate (MgSt) was employed to reduce the cohesive forces of lactose particles because of the inherently hydrophobic nature of the drug materials. This process involved coating only lactose and not the drug itself.

Coating Procedure

- Approximately 50 g samples of lactose were blended with varying weight by weight (w/w) ratios of MgSt (0%, 0.5%, 1%, and 3%) in a cyclomixer (IM-0.1/1, HOSOKAWA MICRO B.V.) at 300 rpm for 10 min. The samples were designated M1, M2, M3, and M4, corresponding to the respective MgSt concentrations.

- After blending, the lactose-MgSt mixtures were transferred to the cylindrical chamber of the mortar grinder.
- The dry coating process was conducted for 30 min at a rotational speed of 120 rpm. This process aimed to coat MgSt particles onto the surface of lactose particles (Zhou et al., 2010b).

6.2.4 Particle size distribution

The particle size distributions of the materials before and after size reduction were determined using a HELOS laser diffractometer (Sympatec GmbH, Clausthal-Zellerfeld, Germany). Before the measurement, the dispersion pressure was set at 3.5 bar. The R2 lens (measuring range 0.45-87.5 µm) was utilized with an optical concentration of 0.5%-5%. The obtained data were analyzed with the PAQXOS® software (version 5.0, Sympatec GmbH, Clausthal-Zellerfeld, Germany). The particle size distribution was expressed as D_{10}, D_{50}, and D_{90} with the mean and standard deviation (SD) from three measurements.

6.2.5 Density properties of powder mixture

To understand the mechanical behaviour of agglomerates, researchers often build models that represent their structure and properties at a larger macroscopic scale (Kendall and Stainton, 2001). These models consider the attractive forces between fine particle surfaces that lead to adhesion, and ultimately, the formation of agglomerates containing hundreds of individual particles. Interestingly, such models predict that these agglomerates can exhibit porosity, elasticity, and strength comparable to those expected for much smaller micrometer-sized agglomerates.

As the adhesive forces between particles increase, the overall strength of the agglomerate is also expected to increase (Puri et al., 2019). However, this strength often shows an inverse relationship with the particle size. In theory, a perfectly formed flaw-free agglomerate composed of very small particles is surprisingly strong. Imperfections and cracks within the agglomerate structure inevitably reduce their actual strength.

Characterizing Agglomerate Strength and Density

The mechanical strength (σ) of an agglomerate particle is a key parameter used to characterise the de-agglomeration behaviour of an agglomerate formulation(Das et al., 2013). The mechanical strength depends on the packing fraction which is related to the tapped density of the powder mixture. Because the mass ratio of lactose to budesonide was fixed, the packing fraction could be considered proportional to the tapped density.

- **Bulk density:** The bulk density (ρ_b) of the powder was determined according to the USP-NF-35 standard. This method involved gently weighing a known volume (10 ml) of powder in a cylinder and dividing the weight by the volume to obtain the density in g/cm³.
- **Tapped density:** The tapped density (ρ_t was measured using an automatic tapper (Powder Tester®, PT-X, Hosokawa Micron (Shanghai) Powder Machinery Co. Ltd) following the USP-NF-35 standard. This method involves tapping a 10 ml cylinder containing the powder for 5 min at a rate of 250 taps per minute. Three replicate measurements were conducted for each powder sample.
- **True density:** The true densities of lactose and budesonide were 1.545 and 1.271 g/cm³, respectively (Kaialy et al., 2011a).

6.2.6. Assessment of surface energy (SE)

A surface energy analyser (SEA, Surface Measurement Systems Ltd., London, United Kingdom) was used to assess the specific surface area (SSA) and surface energy (SE) of the mixed samples, as previously reported(Mangal et al., 2019a). A 150±15 mg sample was weighed into pre-silanised glass columns (4 mm inner diameter × 30 mm length) without excessive tapping to avoid consolidation. Both ends of the columns were loosely filled with pre-silanised glass wool to avoid powder movement. Prior to the measurements, preconditioning of the column was conducted with 0% RH and 10 cm^3 /min nitrogen carrier gas flow for 60 min.

The surface energy consists of a dispersive component and a specific Lewis acid-base component. An alkane series of octane to undecane served as nonpolar probes to calculate the dispersive component; chloroform and ethyl acetate were used as polar probes to predict the Lewis acid-base component(Kondor et al., 2015). The surface energy was measured at a surface coverage of 0.05 p/p_0 (where p is the partial pressure and p_0 is the saturation vapor pressure). The measurement conditions were set to 0% RH and 30 °C, with a carrier gas flow of 10 cm3 /min. Raw data processing was conducted using SEA Analysis Software (Surface Measurement Systems Ltd.). SE calculations were based on the Dorris and Gray approach as previously described(Shi et al., 2011). Each powder sample was measured in triplicates.

6.2.7. Agglomerate size and morphology characterization

The Turbuhaler® dosing unit operates on the basis of volumetric principles. It incorporated a circular disc positioned at the base of the drug reservoir, featuring an array of strategically placed conical holes (further elaborated in Chapter 4). During dose actuation, a plastic scraper positioned above each conical hole shepherds the agglomerates into a dosing unit with a high degree of reproducibility upon rotation of the dosing wheel(Basheti et al., 2013). This mechanism ensures the consistent and accurate delivery of medication with each inhalation manoeuvre.

Significance of Particle Size Distribution:

To achieve consistent and precise dosing, the agglomerate formulation requires a well-defined distribution of particle sizes, each exhibiting distinct flow properties. This heterogeneity plays a critical role in effectively filling the voids within the dosing unit during the metering process. This, in turn, minimises potential variations in the delivered dose, as outlined in previous literature (Wetterlin, 1988).

Agglomerate characterisation techniques

- **Digital Optical Microscopy:** This technique is employed to analyze the diameter and morphology (shape) of the individual agglomerates. High-resolution images (3664 × 2748 pixels) were captured at a magnification of 5x under reflected light. Subsequent image analysis software (size analyser V5.30), compliant with ISO 9276-6 standards, calculated the equivalent circle diameter and sphericity (a measure of roundness) for each agglomerate.
- **Scanning Electron Microscopy (SEM) with Energy-Dispersive X-ray Analysis (EDX):** The SEM (SEM, JCM-7000; JEOL, Japan) provided high-resolution, magnified images of the agglomerate morphology, enabling a detailed assessment of their surface characteristics. Additionally, EDX functionality facilitated elemental analysis, specifically quantifying the presence and distribution of Magnesium Stearate (MgSt) within the formulated mixture. Prior to the SEM analysis, the samples were subjected to the following treatment:
    1. The agglomerates were meticulously mounted onto a carbon tape for optimal imaging.
    2. A gold Smart Coater (DII-29030SCTR) is applied to enhance the sample's conductivity, ensuring clear and accurate image acquisition (with an electrical current of 3 A for 2 minutes to conduct the gold sputter coating process at 0.67 Pa with working distance of 12.5 mm).
    3. Imaging was conducted at an acceleration voltage of 15 kV.

By combining these techniques, a comprehensive understanding of the size, shape, and elemental composition of engineered agglomerates was achieved. This information is crucial for optimising the performance of the Turbuhaler® inhaler and ensuring consistent targeted drug delivery to the lungs.

6.2.8 Aerodynamic assessment

The aerodynamic performance of agglomerate formulation was characterized with Next Generation impactor (NGI). A flow rate of 60.0 L/min (±5%) was set

with a pressure drop of 4 kPa using a vacuum pump (HCP 5 Copley Scientific Ltd, UK) to allow 4 L of air through the inhaler within 4s in each measurement. The flow rate and suction time were controlled using a flow meter (DFM2; Copley Scientific, UK).

Spherical agglomerates of approximately 150 mg were initially weighed and filled into Turbuhaler® (the capacity of the dose chamber was approximately 1 mg per auction). API and lactose deposited in the mouthpiece and at different NGI stages were rinsed with the eluent phase and determined using API and lactose quantification methods.

To avoid particle bouncing and shifting to later NGI stages during deposition, 0.5% (w/v) silicone oil in n-hexane solution was used to pre-coat the impactor stages before measurement. The Emitted Dose (ED), Fine Particle Fraction (FPF), and fine particle dose (FPD) were calculated from the measured API content in each stage. (FPD and FPF are the mass and percentage of drug with an aerodynamic diameter between 0.5 and 5 μm, respectively, calculated as the ratio to the ED).

6.2.9 Dissolution of aerosolized particles

Following aerosolisation within the Turbuhaler®, particles deposited at a specific stage (stage 4) of the Next Generation Impactor (NGI) are isolated for further analysis.

Targeted Particle Collection:

- A specialised filter (RC55, Whatman®) with a defined diameter (4.7 cm) and pore size (0.45μm) was strategically placed within the NGI at stage 4 during the airflow simulation (60 L/min).
- The anticipated amount of deposited powder was estimated based on NGI experiments.

Sample Retrieval and Dissolution Test Setup:

- After the simulated inhalation process, the filter containing the deposited particles was carefully extracted from the NGI stage 4.

- A Transdermal diffusion cell system pre-warmed to 37°C was used for the dissolution test.
- The receptor chamber of the system was filled with 20 ml of pre-warmed dissolution medium (0.5% v/v tween-80 solution) and continuously stirred using a magnetic stirrer.
- The filter, acting as a diffusion membrane, was positioned at the bottom of a Transwell insert within the receptor chamber and secured by a clip to prevent medium leakage. This configuration allowed the dissolution medium to interact with the particles on the filter (Figure 6.3).

Dissolution Testing Procedure:

- At predetermined intervals (0, 10, 20, 30, 45, 60, 90, and 120 min), a small volume (0.5 mL) of dissolution medium was collected from the receptor chamber.
- To maintain a consistent volume, the collected medium was immediately replaced with an equal volume of fresh pre-warmed medium.
- The experiment was conducted in triplicate, and the results were expressed as the percentage of drug dissolved at each time point relative to the total amount of drug on the filter.

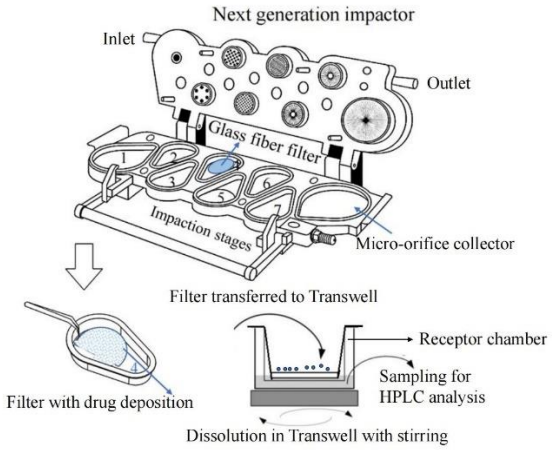

Figure 6. 3 Schematic of the in vitro dissolution of aerosolised particles.

6.2.10 Mechanical strength measurement

To determine the mechanical strength of the individual spherical agglomerates, a micromanipulation technique was utilised based on previously established methods in Section 3.3.2.10 (Zhang et al., 2022).

Ensuring Measurement Accuracy:

- **Force Transducer Calibration:** Prior to measurement, the force transducer was meticulously calibrated, adhering to the recommended protocol outlined by Yan (2008). This calibration step guaranteed the accuracy of the acquired force data.

Sample Preparation and Selection:

- **Size Fraction Sieving:** Agglomerate particles were sieved to obtain a specific size range of interest. In this case, only particles between 355 and 500 µm were chosen for further analysis.
- **Random Sample Selection:** Twenty agglomerates within the chosen size range were randomly selected to constitute a representative sample set for testing.

Micromanipulation Measurement Process:

- **Positioning the Sample:** The chosen agglomerate particles were carefully positioned on a glass plate using a view camera for precise manipulation.
- **Force Application and Rupture:** A force probe connected to a high-precision force transducer (Model 406A, Aurora Scientific Inc., Canada) was used to compress the soft agglomerate. The compression speed was precisely controlled at a preset rate of 1 µm/s. This process continued until the agglomerate ruptured under the applied force.
- **Data Acquisition:** The voltage signal transmitted from the force transducer was continuously recorded throughout the compression test using a data-acquisition system (PC-100, NARISHIGE Science Instrument LAB, Japan). These data were subsequently used to calculate the rupture force.

- **Deformation Measurement:** The deformation at the point of rupture, quantified by the diametric compressive displacement, was directly determined from the recorded voltage versus time curve.

Data Analysis and Controlled Environment:

- **Strength Analysis Software:** The acquired data were meticulously analysed using specialised Micro-Particle Strength Analysis software (v2.1.x, Micromanipulation and Microencapsulation Research Group (μCAP)). This software streamlines the calculation of the key mechanical properties.
- **Temperature Control:** All measurements were conducted in a strictly controlled temperature environment maintained at 20 ± 2°C. A consistent temperature minimises the potential variations in the measured strength values.

6.2.11 Deagglomeration and dispersion behavior characterization

De-agglomeration occurred when the agglomerates were exposed to impaction or shear force induced by air flow through the inhaler device. To explore the impact of vibration on the deagglomeration behaviour of the formulated particles. Dry dispersion laser diffraction was employed as the primary assessment technique (Jaffari et al., 2013).

Experimental Setup and Process:

- **Sample Preparation and Loading:** Soft agglomerates (5 mg) were carefully loaded into the testing tube of a Sympatec HELOS/RODOS laser diffractometer equipped with an R2 lens (detection range: 0.45-87.5 μm).
- **Dispersion Pressure Variation:** To evaluate deagglomeration characteristics, a series of dispersion pressure (DP) settings are manually applied, ranging from 0.2 bar to 4.0 bar. This range effectively assesses the dispersibility of the agglomerates without introducing the complexities associated with the inhaler device.

- **Measurement Initiation and Termination:** The laser diffraction measurement commences when the optical concentration (Ø) surpasses 0.5% and ceases once Ø falls below 0.3%. This ensured reliable data acquisition within an optimal concentration range.
- **Triplicate Measurements:** The entire measurement process was meticulously repeated three times at each designated dispersion pressure to enhance data robustness.

Data Analysis and Interpretation:

- **Median Particle Size (D_x):** The D_x (µm) is the median particle size (D_{50}) at each dispersion pressure (0.2-4.0bar).
- **Fully Deagglomerated Size (DH):** DH represents the D_{50} value (µm) obtained at the highest dispersion pressure (4.0 bar), which is considered to be in a fully deagglomerated state.
- **Degree of Deagglomeration (DA):** The DA value (Equation 2) reflects the extent of deagglomeration at each pressure level. A higher DA indicates a superior deagglomeration behaviour.

$$DA = \frac{DH}{D_x} \qquad \text{Equation (2)}$$

- **Graphical Representation:** The calculated DAs were subsequently plotted against the corresponding dispersion pressures to visualise the deagglomeration profile of the formulated agglomerates. This plot offers valuable insights into the influence of ultrasonic vibration on the ease with which agglomerates break down into smaller particles under applied pressure.

To further investigate how the combination of mechanical dry coating and vibration for agglomeration techniques influences the fine particle dispersion profile within a Turbuhaler® inhaler, a specially modified Sympatec HELOS instrument was prepared to facilitate real-time monitoring of these profiles(Cui et al., 2022).

Modular Setup for Simulated Inhalation:

- The analysis utilised a modular Sympatec HELOS system specifically designed for this purpose. This setup incorporated three key components:
    - An inhaler device adapter specifically designed for Turbuhaler® inhaler.
    - An artificial throats that mimic the human throat environment.
    - A pre-separator that simulates the bronchi bifurcation within the lungs.
- The artificial throat selectively captures particles with larger inertia, replicating their impact on the human throat during inhalation.
- Conversely, finer particles with lower inertia successfully navigated the artificial throat and were subsequently detected using the laser detector.

Measurement Parameters and Data Acquisition:

- **Trigger Levels:** Laser diffraction measurements (using an R2 lens) were initiated when the optical concentration (Ø) reached 1.0% and terminated when it fell below 0.5%.
- **Measurement Duration and Recording Interval:** Each measurement lasted for 4 s, with data meticulously recorded every 100 ms, at a constant airflow rate of 60 L/min.
- **Triplicate Measurements:** To ensure data reliability, each sample underwent the measurement process three times.

Data Analysis and Release Profile Generation:

- **PAQXOS® Software:** PAQXOS® software (Sympatec GmbH) was used for comprehensive data analysis.
- **Particle Release Calculation (Equation 3 and 4):** The software calculates the release amount of particles (R) at each 100 ms interval using Equations 3 and 4.

$$R = C_{opt} \times dQ_3 \qquad \text{Equation (3)}$$

where

dQ_3 represent the volume percentage of particles within a size range (%)

$dQ_3 = Q_3(D_{i1}) - Q_3(D_{i2})$ Equation (4)

Q3 (D_i) represents the ratio of total volume of particles that smaller than D_i to the total volume of all particles. D_i represented the instantaneous particle size measurement of every 100ms within 4s duration. The particle fraction between D_{10} of budesonide (D_{i2}=0.5µm) and D_{90} of lactose (D_{i1}=7µm) were captured during measurement.

- **Release Profile Generation:** The software generates a release amount profile (R) as a function of time (t). This profile visually depicts how the amount of released particles varies over the 4-second measurement duration. Key parameters extracted from this profile include:
    - R_{max}: The maximum release amount (%) achieved at a specific time point.
    - R_{AUC}: The total amount of particles (%) released throughout the entire measurement.
    - T_{max}: The time (min) it takes to reach the maximum release amount (Rmax).

Software for Visualisation:

The generated release amount profiles (R vs. t) were plotted and visualised using the Origin 2023b software (Origin Lab).

6.3. Results

6.3.1. Bulk properties of powder mixture after mechanical dry coating

As detailed in Table 6.2, the micronisation process successfully reduced the Active Pharmaceutical Ingredient (API) particles to an inhalable size range, with a D_{90} (particle diameter at which 90% of the particles are smaller) of 3.23 ± 0.15 µm. Micronized lactose particles, chosen for their role as a carrier material, had a larger D_{90} of 6.97 ± 0.62 µm compared to the MgSt (Magnesium Stearate)

particles (3.07 ± 0.05 µm). This difference in size ensured that lactose could be effectively coated with MgSt.

Importantly, the D_{90} values of the lactose-MgSt mixtures exhibited minimal changes with varying MgSt concentrations. This indicates that the mechanical dry coating process has a negligible impact on the size reduction of lactose particles. However, the surface area of lactose decreased after coating compared to that in the uncoated state. This suggests that the MgSt particles successfully occupied the high surface energy sites on the lactose surface, potentially reducing the inter-particle interactions and agglomeration tendencies.

Table 6. 2 Particle size and SSA of powder bulk properties

Formulation composition	Particle size (µm)			SSA (m^2 /g)
	D_{10}	D_{50}	D_{90}	
Budesonide	0.51±0.01	1.56±0.07	3.23±0.15	6.15±0.12
Melatonin	0.54±0.0	1.59±0.03	3.35±0.03	7.51±0.03
MgSt	0.50±0.01	1.43±0.04	3.07±0.05	8.66±0.15
Micronized Lactose	1.08±0.06	2.99±0.99	6.97±0.62	3.92±0.48
Lactose-0.5% MgSt	0.62±0.01	2.41±0.03	7.38±0.03	2.80±0.43
Lactose -1% MgSt	0.56±0.02	2.11±0.04	6.93±0.07	2.35±0.11
Lactose -3% MgSt	0.50±0.00	1.96±0.03	6.92±0.04	2.62±0.07

Scanning Electron Microscopy with Energy Dispersive X-Ray analysis (SEM-EDX) was employed to characterise the uniformity of the mechanical dry coating process, as illustrated in Figure 6.4. This technique allowed for the analysis of the elemental composition of the surface of the lactose-MgSt mixtures.

The measured molar fraction of magnesium (Mg) on the mixture surface, as shown in Table 6.3, exhibited good agreement with the values calculated from the stoichiometry of the coating process. This suggests minimal or negligible loss of MgSt during the dry coating process, indicating successful and uniform coating of the lactose particles.

Table 6. 3 Elemental analysis (EA) of mixture after mechanical dry coating with EDX

MgSt	Atom type	C	O	Mg
0.5%	* MoF, sto	50.45	49.53	0.02
	MoF, EDX	46.66±0.20	53.31±0.39	0.03±0.01
1%	MoF, sto	50.63	49.32	0.04

3%	MoF, EDX	47.16±0.20	52.79±0.39	0.05±0.01
	MoF, sto	51.84	48.04	0.12
	MoF, EDX	48.72±0.20	51.13±0.38	0.15±0.01

*Molar fractions (MoF) are expressed in % and calculated from stoichiometry (sto) and EDX.

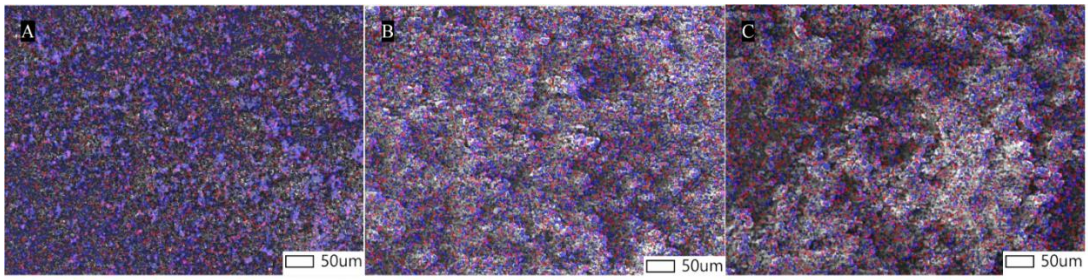

Figure 6. 4 SEM-EDX image of mechanical dry coating with different concentrations of magnesium stearate (A: 0.5%, B: 1% and C: 3%. Red represents magnesium element and the blue represents oxygen element)

6.3.2 Production of budesonide agglomerate formulation with ultrasonic vibration

6.3.2.1 Bulk properties of agglomerate formulation

Ultrasonic vibration offers several advantages for creating inhalable dry powder formulations. As shown in Figure 6.5 and Table 6.4, optical microscopy revealed that vibration contributed to both a smaller agglomerate size and higher sphericity. This was further confirmed by scanning electron microscopy (SEM) analysis in Fig 6.5 (F1-H1). With vibration, the agglomerate surface exhibits a looser structure with evenly packed individual particles, indicating better dispersion of fine particles upon inhalation. In contrast, formulations without vibration had a surface covered with clumped and interlocked aggregates. Ultrasonic vibration also improves the drug content within the agglomerates by reducing powder adherence during processing.

Micromanipulation measurements demonstrate that ultrasonic vibration progressively reduces the rupture force of the agglomerates, from 5.3 ± 0.5 mN to 0.8 ± 0.2 mN as the power level increases from 0 W to 400 W. However, the rupture deformation remained within 10%, classifying them as elastic particles (Paul et al., 2014). This elasticity ensures that they can withstand the filling and

packing processes of the manufacturing process without significant structural damage.

Although ultrasonic vibration weakened the agglomerates, the process maintained sufficient mechanical stability, particularly at a power level of 200 W. This stability is suitable for pharmaceutical manufacturing, as evidenced by the comparable rupture force (0.8 ± 0.2 mN) to commercially available Turbuhaler® inhaler particles (1.69 ± 0.47 mN, n=20).

Table 6. 4 Properties of soft agglomerates under varied ultrasonic power

Power/Watt	F1-0W	F2-100W	F3-200W	F4-400W
X_{EQPC} (mean ±SD)/ μm	563.8±79.4	552.2±75.6	424.3±46.3	379.6±88.3
Sphericity (mean ±SD)	0.8±0.0	0.9±0.0	0.9±0.0	0.9±0.0
Drug content/%	81.6±1.0	95.0±2.2	98.9 ±0.6	98.6±3.1
Rupture force/mN	5.3±0.5	4.5±0.8	3.6±1.6	0.8±0.2
Rupture Deformation （%）	4.3 ±1.2	5.2±1.1	4.7±0.9	3.6±1.1

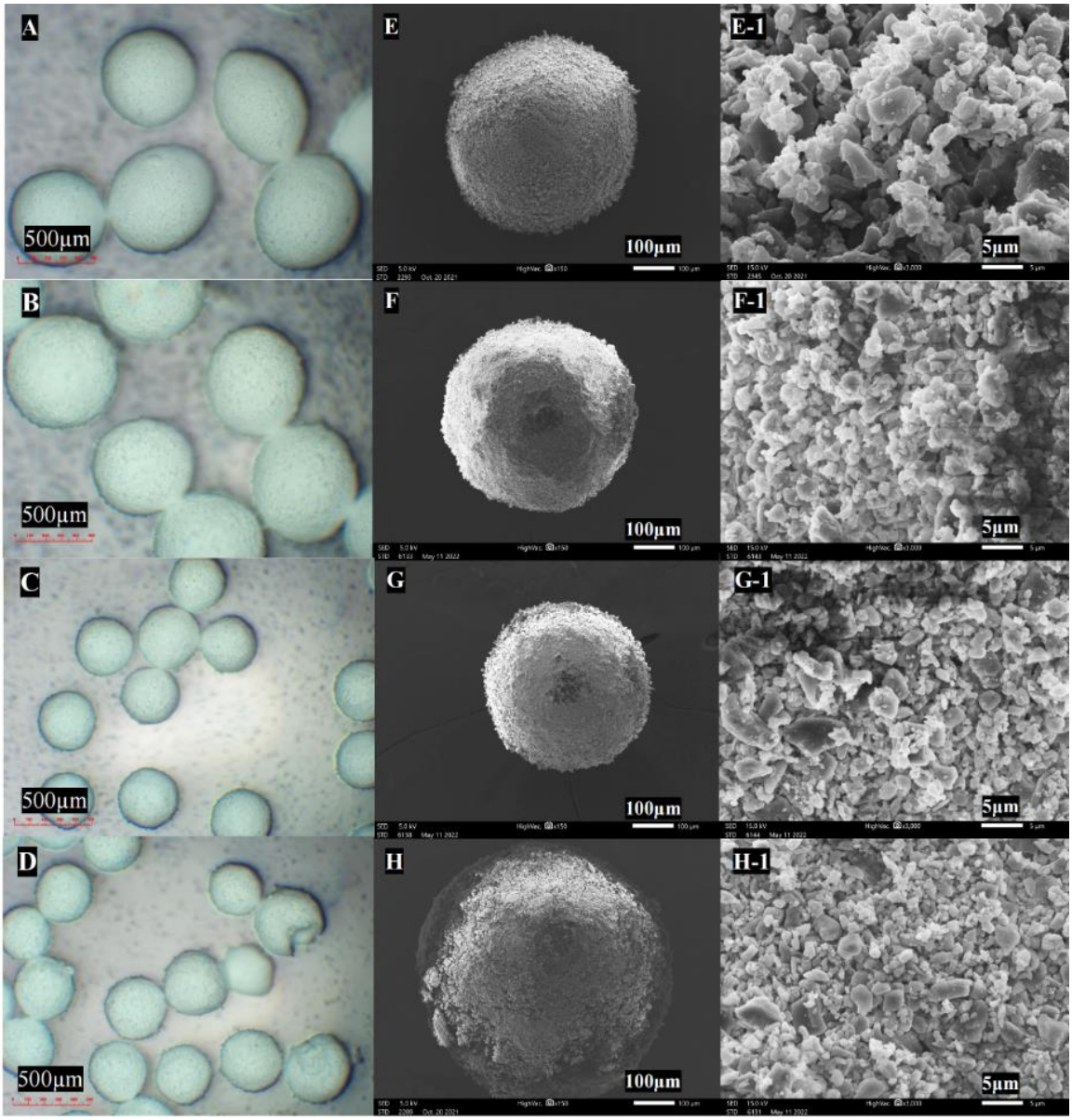

Figure 6. 5 Light microscope images of agglomerates under ultrasonic vibration (A: 0 W, B: 100 W, C: 200 W, and D: 400 W); SEM images of agglomerates and corresponding surfaces (E and E-1:0 W, F and F-1: 100 W, G and G-1: 200 W, H and H-1: 400 W (magnification of microscope for agglomerate:50×; SEM for agglomerate: 150×, for surface: 3000×).

6.3.2.2 In vitro aerosolization performance

The aerosolisation performance of the formulation was significantly improved with ultrasonic vibration, as shown in Table 6.5. While the Emitted Dose (ED) for both budesonide and lactose increased slightly across the tested power range (0 W to 400 W), the Fine Particle Fraction (FPF) exhibited a substantial increase. Budesonide FPF jumped from 36.2 ± 3.0% to 53.2 ± 4.1%, and lactose FPF rose from 31.8 ± 4.1% to 52.5 ± 4.6%. This indicates that a greater proportion of drug

particles falls within the ideal size range for efficient inhalation and lung deposition. Figure 6.6 further strengthens this observation by illustrating the aerosol deposition profile across the Next Generation Impactor (NGI) stages. The data revealed a clear trend; stages 4, 5, and 6 (representing the lung region) showed significantly higher deposition for formulations treated with ultrasonic vibration. Conversely, deposition in the artificial throat and pre-separator (simulating the upper airways) was noticeably reduced after vibration treatment. These findings collectively suggest that ultrasonic vibration effectively breaks down agglomerates into finer particles. This translates into a more inhalable formulation with improved targeting of the medication to the intended lung regions, potentially leading to enhanced therapeutic benefits.

Table 6. 5 Aerodynamic properties of formulation prepared with vary vibration intensity (n = 3)

	F1-0W	F2-100W	F3-200W	F4-400W
Budesonide				
ED/%	78.7±4.6	81.6±2.3	82.2±1.9	82.7±1.7
FPD/μg	57.0 ±6.2	73.5±10.4	80.3±6.6	88.8±5.2
FPF/%	36.2±3.0	45.0±5.6	48.8±2.8	53.2 ±4.1
MMAD/μm	2.7±0.1	2.6±0.1	2.5±0.0	2.4±0.2
GSD	1.8 ±0.0	1.7±0.0	1.7±0.1	1.8±0.1
Lactose				
ED/%	64.5±6.7	78.8±2.3	86.0±2.9	84.5±4.0
FPD/μg	164.1±27.4	230.4±13.8	306.1±12.1	355.1±18.2
FPF/%	31.8±4.1	36.6±1.3	45.2±0.8	52.5±4.6
MMAD/μm	2.7±0.1	2.6±0.1	2.5±0.0	2.4±0.2
GSD	1.8 ±0.0	1.7±0.0	1.7±0.1	1.8±0.1

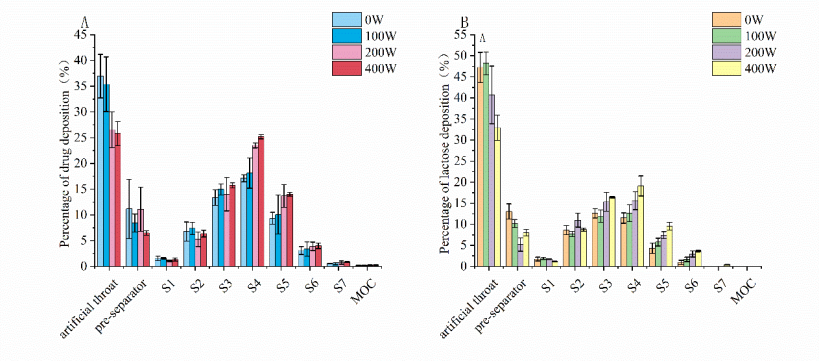

Figure 6. 6 Aerodynamic deposition profile of (A)budesonide and (B)lactose under ultrasonic vibration

6.3.2.3 Production of ternary budesonide formulation with combination of mechanical coating and ultrasonic vibration

The bulk properties of the mixture after mixing with budesonide were measured and are listed in Table 6.6. All formulations had a lower SD (<2%) in terms of drug content, and could be considered excellent and suitable inhalable blends (Sebti et al., 2007). The tapped density of the mixtures increased as the powders were mechanically dry coated, but did not show any further increase with increasing MgSt concentration. However, the surface energy decreased significantly to 99.3 ± 2.1 mJ/m^2 when 3% MgSt was incorporated, which can be compared to the 315.0 ± 8.0 mJ/m^2 without mechanical dry-coating. Therefore, although the increase in the packing fraction could be related to an exponential increase in the mechanical strength of the powder agglomerates (Das et al., 2013), the substantial reductions in the powder surface energy offset this increasing trend.

Table 6. 6 Overview results of bulk properties for the mixture (n = 3).

Mixture	**M1-0%**	**M2-0.5%**	**M3-1%**	**M4-3%**
Drug content (%)	99.0 ± 0.6	99.4 ± 0.5	100.6 ± 1.2	104.3 ± 1.5
Bulk density (g/mL)	0.22 ± 0.01	0.26 ± 0.01	0.26 ± 0.03	0.25 ± 0.01
Tapped density (g/mL)	0.35 ± 0.01	0.45 ± 0.02	0.45 ± 0.02	0.46 ± 0.02
Total surface energy , γ_s^T (mJ/m^2)	315.0 ± 8.0	253.0 ± 6.3	125.9 ± 2.9	99.3 ± 2.1

Building on the established understanding that magnesium stearate enhances aerosol performance in DPIs(Kumar et al., 2022), this study investigates the effects of mechanical dry coating, with and without the addition of ultrasonic vibration (200 W power input), on spherical agglomerate properties and aerodynamic deposition.

Table 6.7 highlights that combining ultrasonic vibration with mechanical dry coating resulted in a generally improved drug content. However, the mean diameter and rupture force of the agglomerates decreased compared with those obtained using mechanical dry coating alone.

Table 6. 7 Agglomerates bulk properties and aerodynamic performance (n = 3) for formulations with different preparation methods.

Spheroidization without ultrasonic vibration			Spheroidization with ultrasonic vibration		
F5-0.5%MgSt	F6-1%MgSt	F7-3%MgSt	F8-0.5%MgSt	F9-1%MgSt	F10-3%MgSt

X_{EQPC}/μm	489.7±86.6	452.6±75.5	389.0±61.3	428.0±34.3	408.4±26.1	364.7±23.7
Rupture force/mN	4.5±0.8	3.9±0.7	3.6±0.6	2.6±0.4	2.2±0.2	1.8±0.1
Drug content/%	87.8±1.2	96.2 ±0.9	97.7±0.2	98.6±3.1	101.3±1.3	98.6±3.1
ED/%	83.5±6.3	90.2±5.9	93.4±0.9	93.5±1.8	92.9 ±5.3	95.8±3.9
FPD/μg	79.3±7.1	92.3±11.0	102.9±13.9	118.7±11.6	132.0±5.2	136.7±5.1
FPF/%	47.2±5.8	51.4±4.2	55.1±6.9	63.4±5.1	71.1±1.3	71.4±1.7
MMAD/μm	2.5±0.2	2.5±0.2	2.3±0.3	2.2±0.1	2.2±0.2	2.1±0.2
GSD	1.8±0.0	1.8 ±0.1	1.7 ±0.1	1.7±0.0	1.7±0.0	1.7±0.0

ED = emitted dose; FPD = fine particle dose; FPF = fine particle fraction; GSD = geometric standard deviation; MMAD = mass median aerodynamic diameter; Data are represented as mean ± SD

Table 6.7 and Figure 6.8 illustrated the impact of various formulation techniques on the aerodynamic properties of inhalable dry powder formulations, directly influencing their drug delivery efficiency. This study focused on mechanical dry coating, ultrasonic vibration (200 W), and a combined approach to evaluate their effects on the emitted dose (ED), fine particle fraction (FPF), and particle deposition profile.

Emitted dose and residual aggregate:

The analysis revealed a higher ED associated with mechanically dry coating compared to ultrasonic vibration alone. Figure 6.7 suggests a potential explanation: fewer residual aggregates within the metering hole after dry coating likely facilitated smoother powder release during inhalation. Interestingly, the combined approach yielded an even greater improvement in ED, indicating a synergistic effect for optimal powder flow.

Fine Particle Fraction and Magnesium Stearate Concentration:

Both mechanical dry coating and ultrasonic vibration demonstrated a general improvement in the FPF, particularly at elevated magnesium stearate (MgSt) concentrations. However, the most significant enhancement was observed using the combined method. Notably, this approach achieved a remarkable FPF plateau of 71.1 ± 1.3% with a 1% MgSt coating. This signifies the superior ability of the combined method to generate fine particles that are ideally suited for deep lung deposition, potentially leading to enhanced drug delivery to the target site.

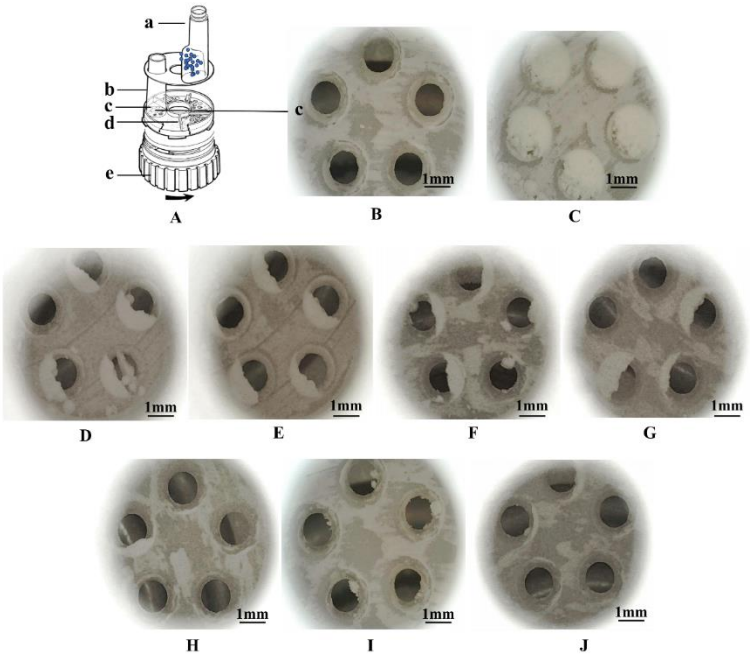

Figure 6. 7 Schematic of the Turbuhaler ® in disassembled form (A), dosing unit (B) and after metering (C): a) mouthpiece with spiral channel, b) reservoir for agglomerate, c) inhalation channel, d) dosing holes, e) scraper, f) dosing wheel(Wetterlin, 1988); the images D to G illustrate the residual in dosing unit after inhalation for ultrasonic powers of 0 W to 400 W, respectively. Images H to J illustrate the mechanical dry coating with 0.5% to 3% MgSt.

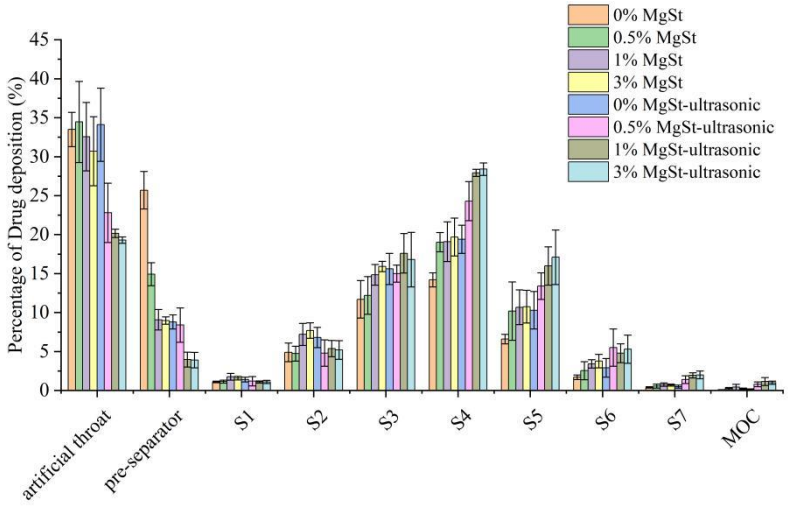

Figure 6. 8 Aerodynamic particle size distribution of soft agglomerate with different concentration of MgSt addition in formulation and spheroidization, (n=3)

Detailed Assessment of Deagglomeration and Dispersion:

Figure 6.8 provides a more in-depth analysis of the influence of the chosen production methods on deagglomeration and dispersion during inhalation. The following key trends were observed:

- **Reduced Upper Airway Deposition:** The combined method exhibited a significant reduction in deposition within both the artificial throat and the pre-separator, which simulated the upper airways. In contrast, mechanically dry coating alone demonstrated reduced deposition in the pre-separator. This suggests that the combined approach produces particles with a lower propensity to become trapped in the throat or upper airways, potentially minimising unwanted side effects.
- **Enhanced Lung Deposition:** The combined method also facilitated greater deposition of fine particles, particularly in stages 4 to 7 of the Next Generation Impactor (NGI). These stages represent the lower regions of the lung, indicating that the particles produced by the combined method are more likely to reach their intended target site for optimal drug delivery.

6.3.2.4 Deagglomeration and dispersion of agglomerate formulation

Impact of Ultrasonic Power on Deagglomeration:

Figure 6.9 reveals the distinct deagglomeration behaviours associated with different ultrasonic power levels. The median particle size (D_{50}) after deagglomeration decreased as the ultrasonic power increases from 0 W to 200 W at various dispersion pressures. However, a further increase to 400 W did not result in any additional reduction. The de-agglomeration profile (DA vs. dispersion pressure) indicates a trend of increasing relative deagglomeration with higher ultrasonic power. This suggests variations in the cohesive properties and mechanical strength of formulations produced at different power settings.

For instance, at a low dispersion pressure of 0.2 bar, the non-vibrated formulation exhibited a low DA value (0.50), implying a significant portion remained agglomerated. This translates to a lower FPF during inhalation as previously reported (Jaffari et al., 2013). In contrast, DA value of 0.66 is achieved with 400 W vibration, indicating a greater proportion of

deagglomerated particles available for inhalation, potentially leading to improved FPF.

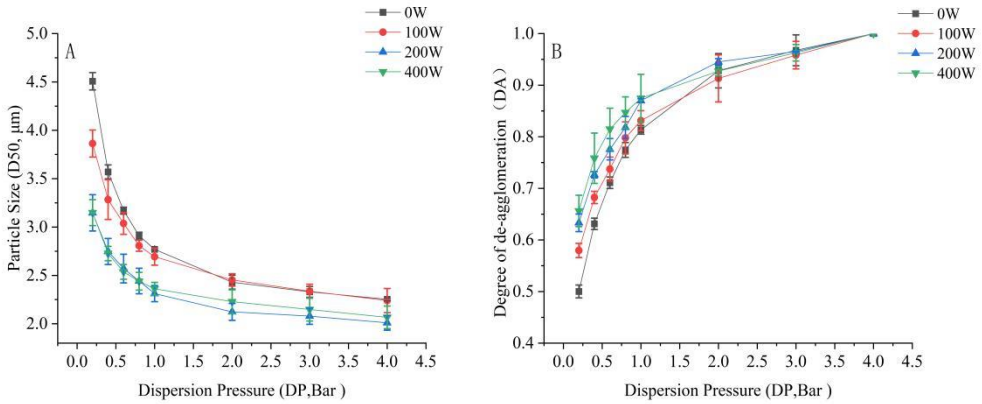

Figure 6. 9 Deagglomeration performance of formulations with ultrasonic vibration: (A) Particle size versus dispersion pressure curve and (B) de-agglomeration profiles for agglomerates, (n=3)

Fine Particle Dispersion Analysis:

Fig 6.10 delves deeper into the effects of mechanical dry coating (individual) and its combination with ultrasonic vibration on the fluidisation and dispersion process within a Dry Powder Inhaler (DPI). Both methods demonstrate a similar trend: the amount of fine particles released initially increases and then plateaus with increasing MgSt concentration.

- The formulations with 0.5% and 1% MgSt exhibited approximately 1.5- and 2-fold increases in the maximum release amount (R_{max}), respectively, compared to the formulation without MgSt.
- However, no significant difference in the total release amount (R_{AUC}) is observed between the 1% and 3% MgSt formulations.

Overall, formulations produced with the combined approach (mechanical dry coating + ultrasonic vibration) exhibited shorter T_{max} (time to reach maximum release) and higher RAUC than those using only mechanical dry coating at equivalent MgSt concentrations. These findings suggest that the combination method not only promotes efficient deagglomeration but also facilitates faster entrainment of fine particles by airflow during inhalation.

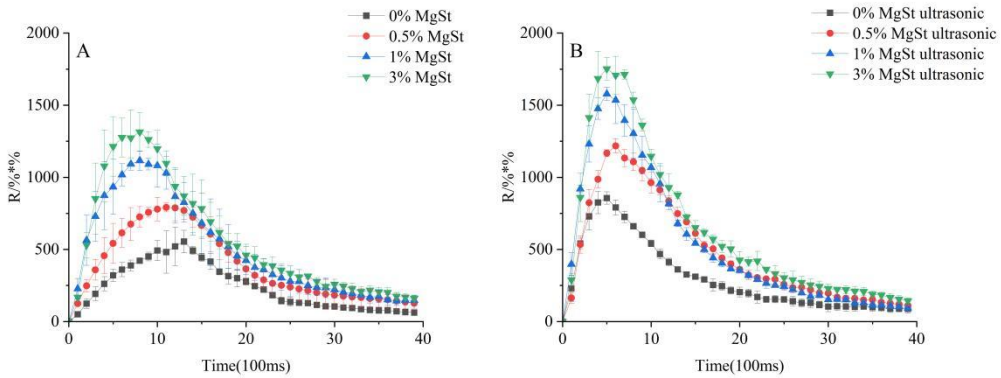

Figure 6. 10 Release profile of formulations with individual mechanically dry coating (A) and combination with ultrasonic vibration (B). R_{max} represents the maximum of release amount at T_{max}; T_{max} represents the time to R_{max}, R_{AUC} is the total release amount.

6.3.2.5 Dissolution evaluation of aerosolized particles

The interplay between deposition and dissolution in budesonide dry powder inhaler (DPI) formulations was explored, with a particular focus on the role of ultrasonic vibration. The inherent hydrophobicity of budesonide necessitates careful consideration of formulation techniques, as strategies that enhance deposition may inadvertently hinder dissolution and ultimately reduce bioavailability.

Balancing Deposition and Dissolution Challenges

Previous research (Kumar et al., 2022) has established that mechanical dry coating with magnesium stearate (MgSt) effectively improves the fine particle deposition of budesonide within the lungs. However, this approach can also influence the dissolution rate of aerosolised drug particles in the lung epithelium, which is a critical step for optimal drug absorption. Figure 6.11 demonstrates the impact of production methods (mechanical dry coating alone vs. combined with ultrasonic vibration) on the dissolution profile of budesonide formulations containing varying MgSt concentrations.

Key Observations:

- **Overall similar trends:** Both production methods exhibited a generally comparable trend in terms of dissolution, suggesting that ultrasonic

vibration does not significantly alter the fundamental dissolution behaviour of budesonide.

- **Faster Dissolution with Vibration:** Interestingly, formulations produced with ultrasonic vibration displayed a slightly faster dissolution rate than those solely relying on mechanical dry coating. This observed difference could be attributed to the enhanced particle interaction with the dissolution medium due to ultrasonic treatment.
- **Impact of MgSt Concentration:** The MgSt concentration also plays a crucial role:
    - **1% MgSt:** Regardless of the production method, formulations containing 1% MgSt achieved a plateau of complete dissolution within 120 min.
    - **5% MgSt:** When a higher MgSt concentration (5%) was employed, formulations produced with mechanically dry coating alone exhibited a markedly slower dissolution rate, with incomplete dissolution at approximately 85%.
    - **Improved Dissolution with Combined Approach:** Conversely, the combined approach of mechanical dry coating and ultrasonic vibration facilitates complete dissolution even at this higher MgSt level.

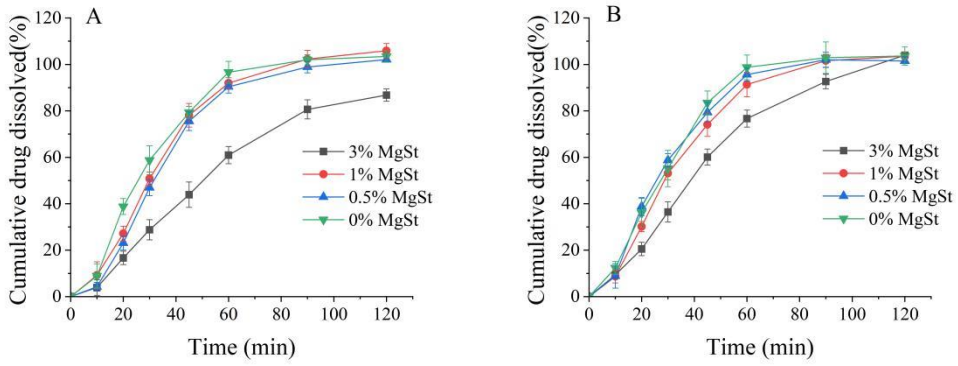

Figure 6. 11 Dissolution of aerosolized drug particles from agglomerates obtained with mechanical dry coating individually(A) and in combination with ultrasonic vibration(B).(n=6)

6.3.3 Production of agglomerate formulation via acoustic

vibration

6.3.3.1 The pre-study of grids on agglomerate particle size distribution

The influence of the mixing acceleration (60 g, 70 g, and 80 g) and grid presence on the size distribution is depicted in Figure 6.12. Without grids, significantly larger particles dominated, with over 40% exceeding 500 µm at 60 g of acceleration. Increasing the acceleration offered a minimal improvement for this size fraction.

The grid application dramatically reduced the large particle fraction (>500 µm) to below 10% when double layers were used. Conversely, the total quantity within the 350-500 µm and 200-350 µm ranges increased with higher acoustic energy inputs (70 g and 80 g) (probability valve $p<0.05$). Notably, for these higher acceleration levels, the smaller size fraction (200-350 µm) approached that of the larger one (350-500 µm) ($p>0.05$). Interestingly, the fraction of particles smaller than 200 µm progressively decreases with increasing acceleration.

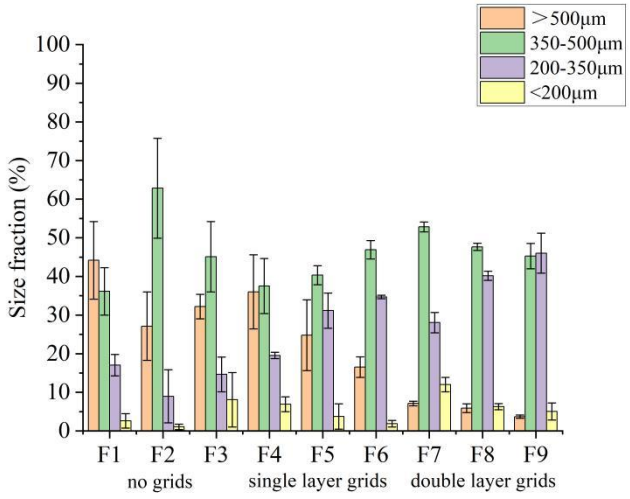

Figure 6. 12 Size fraction of agglomerates based on weight with/without grids at different accelerations.

Figure 6.13 illustrates the crucial role of the agglomerate size distribution in metering doses delivered from the Turbuhaler® device. Larger agglomerates

obtained without grids or with single-layer grids resulted in lower drug loads within the dosing chamber. This effect was attributed to the increased void volume within the dosing units as the particle size increased. In contrast, a higher acoustic mixing intensity promotes a specific size distribution, leading to uniform powder filling with minimal voids in the dosing chamber, and consequently, consistent delivery doses.

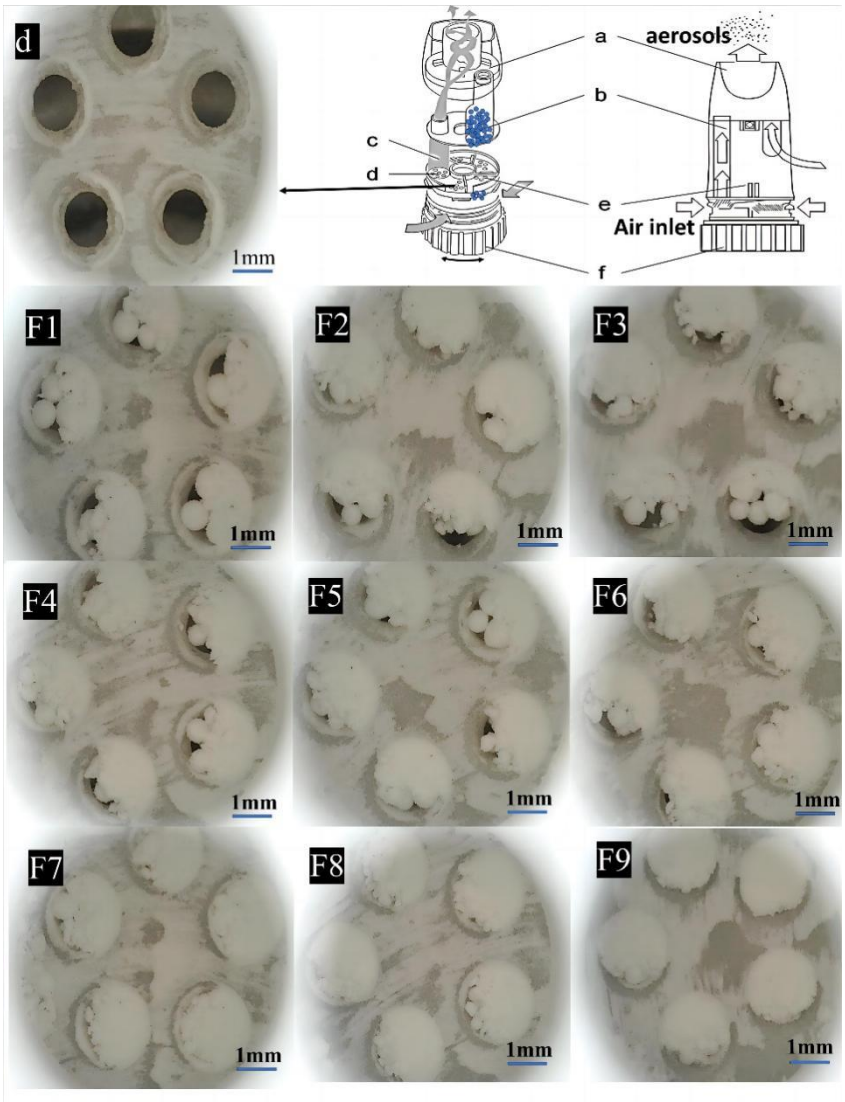

Figure 6. 13 Schematic of the Turbuhaler ® in disassembled form (top-left) and cross-section (top-right): a) mouthpiece with spiral channel, b) reservoir for agglomerate, c) inhalation channel, d) dosing holes after emptying of a dose, e) scraper, f) dosing wheel(Wetterlin, 1988); the bottom images illustrate the dose loading during inhalation.

6.3.3.2 Powder bulk property analysis

Table 6.8 highlights that the bulk density remained relatively unchanged across all formulations and accelerations, with minimal variation. However, the tapped density displayed a significant increase (approximately 10%) for mixtures prepared with double-layer grids compared with those without, at each corresponding acceleration level. This suggests that RAM with grids effectively modifies the powder structure by reducing the porosity. Additionally, the tapped density exhibited a gradual increase with increasing acceleration regardless of the grid presence. This indicates that a homogeneous mixture can be achieved using RAM at different accelerations. Notably, the experiment demonstrates excellent mixing performance with the resonant acoustic mixer for all acceleration levels (60–80 g) within a 10-minute timeframe. Furthermore, the grids did not influence the homogeneity of the blends.

Table 6. 8 Summary results of density property and assay.

	Without grids			With grids		
	F1-60g	F2-70g	F3-80g	F7-60g	F8-70g	F9-80g
Bulk density (g/cm^3)	0.21±0.01	0.21±0.01	0.23±0.03	0.24±0.03	0.25±0.04	0.25±0.01
Tapped density (g/cm^3)	0.30±0.01	0.31±0.02	0.33±0.02	0.33±0.03	0.34±0.01	0.37±0.01
Packing fraction	20.47±0.75	21.39±1.42	22.81±1.07	22.62±0.34	23.60±0.11	25.78±0.41
Percentage of target (%)	98.60±3.06	101.32±1.28	99.49±1.94	100.55±1.24	99.94±1.37	99.38±0.50

Fig 6.14 visually represents the tapped density distribution after a specified number of taps. A powder bed with a higher packing fraction exhibited better consolidation than that with a lower packing fraction. This difference in the powder structure leads to variations in the packing behaviour during vibration. The tapped density of the mixtures prepared at 70 g and 80 g accelerations suggests a higher packing fraction than that at 60 g. This implies a greater degree of consolidation and particle collision with the grids during acoustic mixing, which ultimately results in smaller particle clusters.

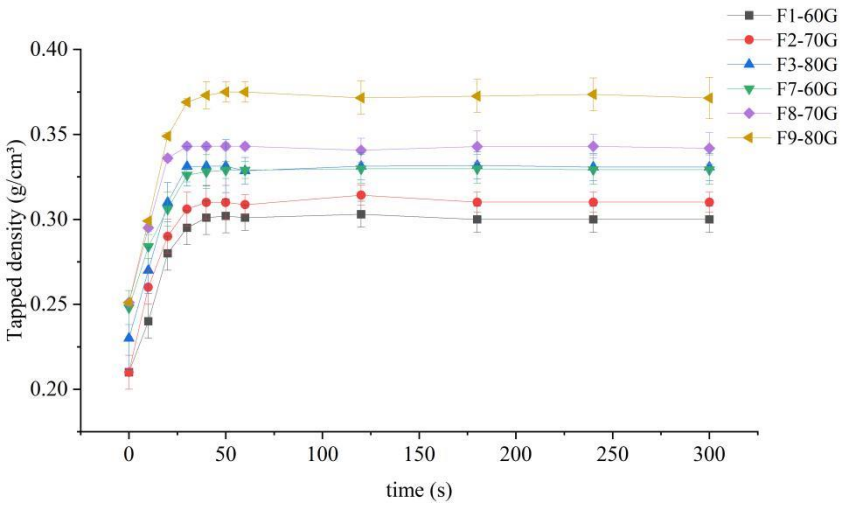

Figure 6. 14 Tapped density curves of formulations without/with grids at different accelerations.

6.3.3.3 Agglomerate morphology and mechanical properties

Effect of Acoustic Mixing Intensity

Scanning electron microscopy (SEM) revealed distinct variations in the agglomerate morphology depending on the applied acceleration during acoustic mixing.

- **Without Grids:** Agglomerates formed without grids exhibited a lower degree of sphericity and a surface covered with clusters, hindering consistent dosing from the Turbuhaler® chamber.
- **With Grids:** Spherical agglomerates with tightly packed structures were observed at high accelerations (70g and 80 g). However, the 60 g setting yielded loosely compacted and porous agglomerates with surface cracks. This suggests insufficient powder coalescence due to the lower packing fraction at this intensity.

Density and Mechanical Properties:

Table 6.9 highlights the influence of acoustic mixing intensity on both agglomerate density and mechanical properties:

- **Density:** agglomerate density progressively increases with higher acceleration levels.

- **Rupture Force:** The average rupture force of the agglomerates prepared at 80 g was nearly double that of those formed at 60 g, indicating greater mechanical strength.
- **Rupture Deformation:** All formulations exhibited a rupture deformation below 10%, classifying them as elastic particles(Paul et al., 2014).
- **Rupture Tension:** Formulations prepared at 70 g and 80 g displayed a two-fold increase in rupture tension compared with 60 g, signifying enhanced elasticity.

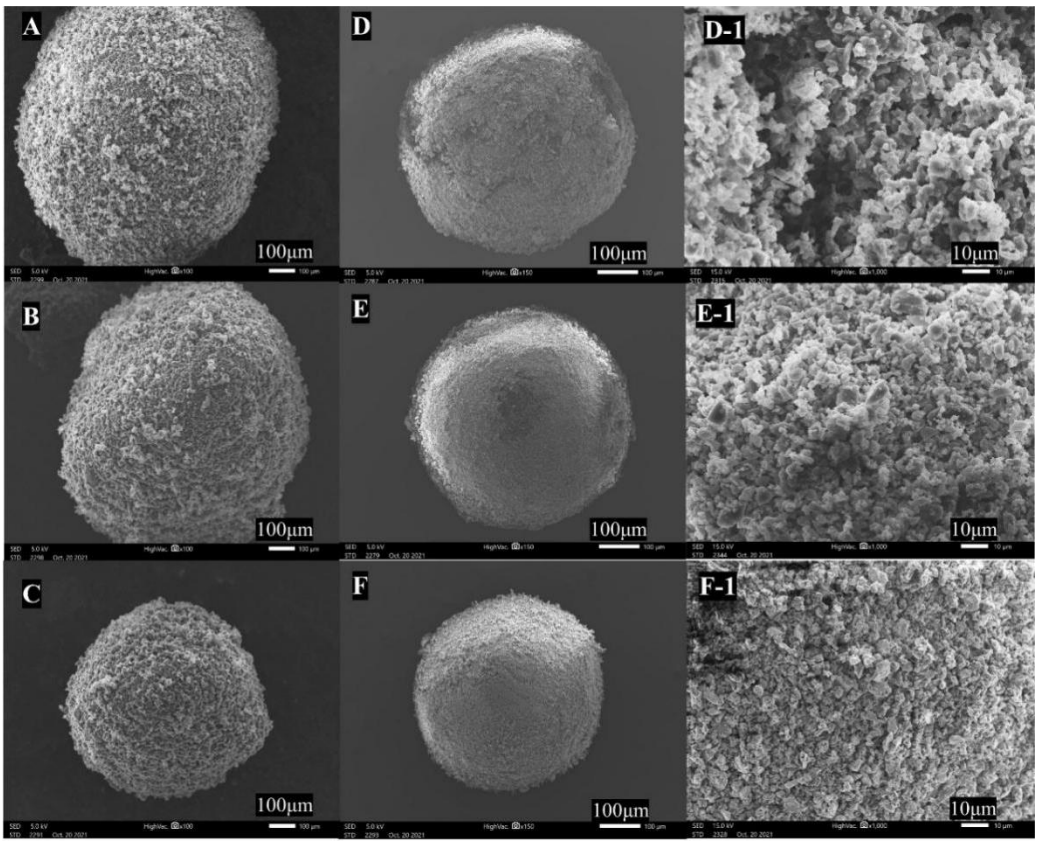

Figure 6. 15 SEM image of agglomerate particles and surface morphology mixed without grids at magnification 100 × (A: 60g, B: 70g, and C: 80g,) and with double layer grids (D, D-1 for 60g, E, E-1 for 70g and F, F-1 for 80g) at magnifications of 150 × and 1000 ×, respectively.

Mechanical Stability and Pharmaceutical Suitability:

These findings suggest that acoustic mixing with double-layer grids at higher intensities (70g and 80g) generates mechanically stable agglomerates with

desirable elastic properties. This aligns well with the requirements of pharmaceutical manufacturing. Additionally, the rupture force values were comparable to those measured in commercially available Turbuhaler® inhalers (e.g. PULMICORT Turbuhaler®), further supporting the suitability of this approach.

Optimising the acoustic mixing intensity during agglomeration plays a crucial role in shaping the morphology, size distribution, and mechanical properties of DPI formulations. Utilising double-layer grids at higher accelerations (70 g and 80 g) promotes the formation of spherical, densely packed agglomerates with enhanced mechanical strength and elasticity. These characteristics ensure consistent and efficient drug delivery from the Turbuhaler® inhalers, potentially leading to improved patient outcomes.

Table 6. 9 Summary results of agglomerate density and mechanical property

	Bulk density / (g/cm^3)	Rupture force / (mN)	Rupture Deformation/ (%)	Rupture Tension/(μN/μm）
F7	0.28±0.01	0.94±0.56	3.03±1.19	0.0020±0.0010
F8	0.31±0.00	1.51±0.50	4.96±2.55	0.0048±0.0029
F9	0.35±0.03	2.06±0.56	4.35±1.00	0.0040±0.0016
Turbuhaler®	0.34±0.00	1.83±0.83	4.33±1.27	0.0037±0.0014

6.3.3.4. Aerodynamic assessment

Impact on Deposition Pattern:

Figure 6.16 reveals the most significant differences in deposition patterns across stages 3-5 of the NGI:

- **Increased Acceleration, Increased Lung Deposition:** At a flow rate of 60 L/min, drug deposition in stages 4 and 5 (representing the lower lung regions) improved by nearly 50% when the acceleration increased from 60 g to 70 g. Further improvements were observed at 80 g, with an additional increase in deposition during stages 3 and 4.
- **Enhanced Flow Rate Independence:** With decrease in airflow rate (from 60 L/min to 30 L/min), the FPF of the 60 g formulation decreased significantly (from 40.8% to 24.2%). However, formulations prepared at 70 g and 80 g exhibited a much smaller FPF decrease of approximately

20%. Similarly, at a higher flow rate of 90 L/min, the FPF of the formulations prepared at 70 g and 80 g remained comparable.

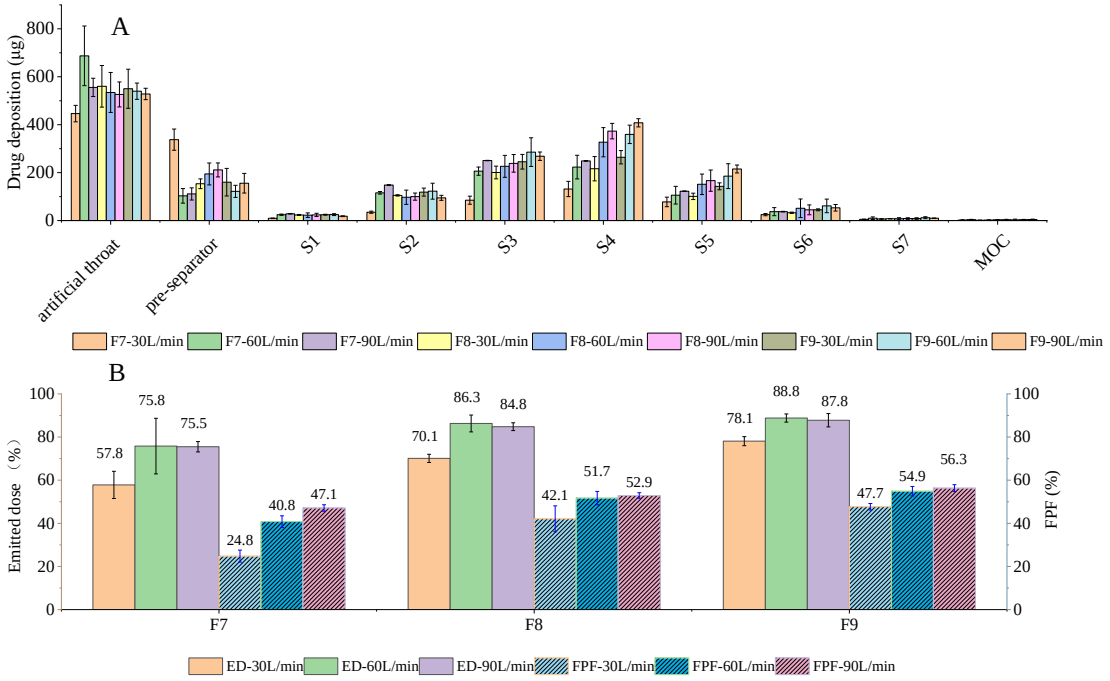

Figure 6. 16 Amount of drug deposited at each stage of NGI at different flow rates (A) and effect of flow rate on aerosol performance of formulations from different accelerations (B)

These observations suggest that a higher acoustic mixing intensity promotes superior deagglomeration, leading to a greater proportion of drug particles reaching the lower regions of the lungs. Additionally, formulations prepared at higher intensities displayed a reduced dependence on airflow rate, indicating a more consistent deposition behaviour across different inhalation profiles. This translates to potentially reliable drug delivery for patients with varying lung function.

The acoustic mixing intensity is a critical factor for optimising the aerodynamic performance of DPI formulations. Higher intensity settings (70 g and 80 g) promoted improved lung deposition, enhanced flow rate independence, and potentially more reliable drug delivery for patients with diverse inhalation capabilities.

6.3.3.5 De-agglomeration characterization of agglomerate

formulation

Fig 6.17 and Fig 6.18 illustrate the influence of acoustic mixing intensity on the deagglomeration behaviour of dry powder inhaler (DPI) formulations. Deagglomeration, the process of separating larger aggregates into inhalable particles, is critical for efficient drug delivery through inhalation(Das et al., 2013, Chen et al., 2013, Jaffari et al., 2013).

Impact of Acceleration on Deagglomeration

The level of acceleration applied during acoustic mixing significantly affected the observed deagglomeration behaviour.

- **60 g Acceleration:** At low airflow rates (30 and 45 L/min), the frequency versus particle size profile exhibited a bimodal distribution. This suggests the presence of persistent clusters of approximately 30-40 μm and incomplete dispersion at these lower flow rates. However, at higher flow rates (60-120 L/min), a shoulder appeared at approximately 6-8 μm, indicating some degree of deagglomeration.
- **Higher Accelerations (70 g and 80 g):** A distinct pattern emerges with increased acceleration.
    - **70g:** A broader size distribution was observed at 30 L/min, suggesting ongoing deagglomeration. This transitioned to a mono-modal distribution at higher flow rates (45 L/min and above), indicating a more complete particle separation.
    - **80g:** The most consistent deagglomeration behaviour was observed across all flow rates. This suggests a more homogeneous powder structure at the microscopic level, likely owing to fewer variations in particle interactions and surface energies.

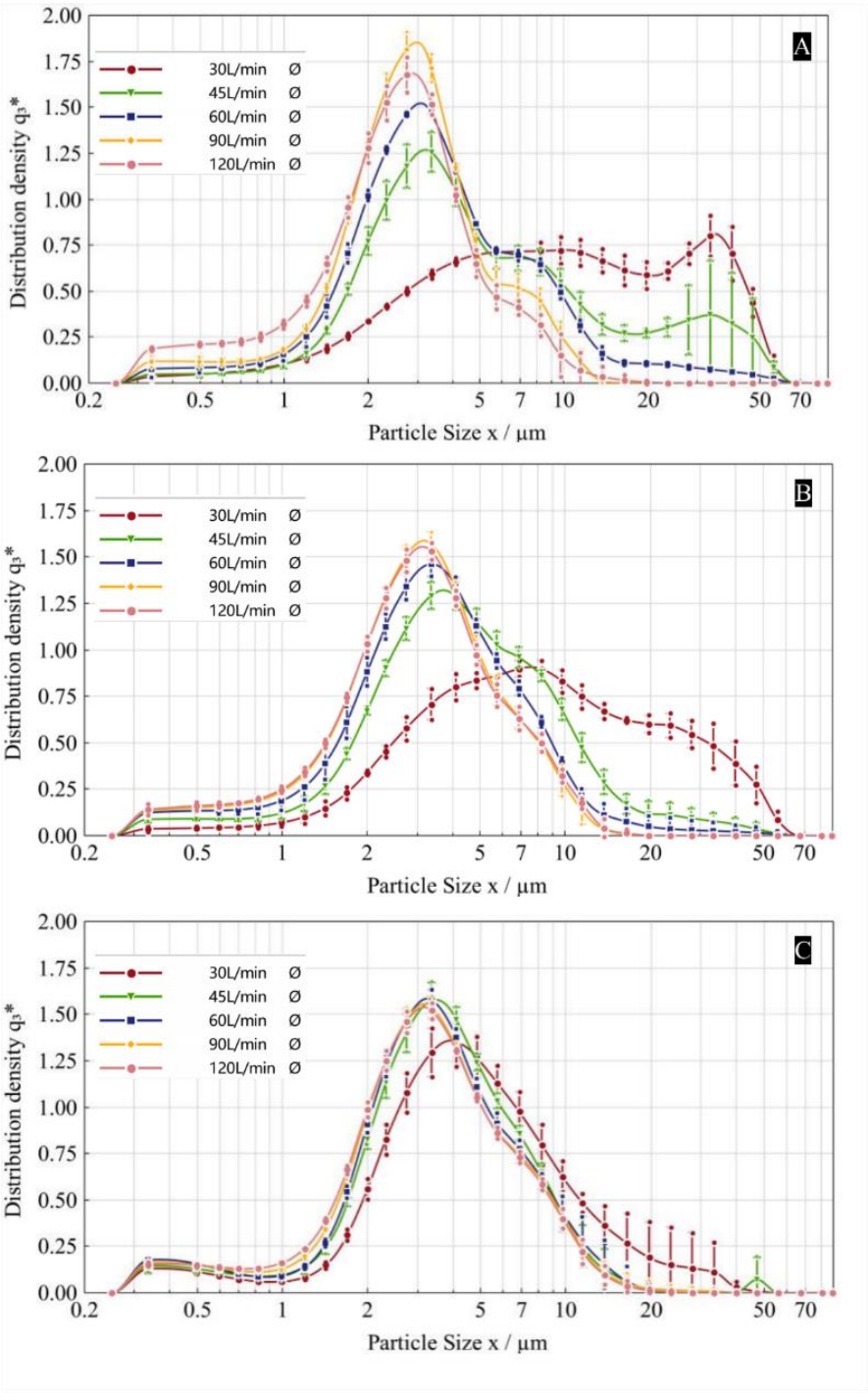

Figure 6. 17 Particle size distributions of formulations produced with double layer grids at various accelerations (A: 60 g, B: 70 g, and C: 80 g) dispersed from Turbuhaler® at 30–120 L/min.

*. distribution density q^3 represents the probability density function of a certain particle size and was derived with PAQXOS® software (Sympatec GmbH, Clausthal-Zellerfeld, Germany)

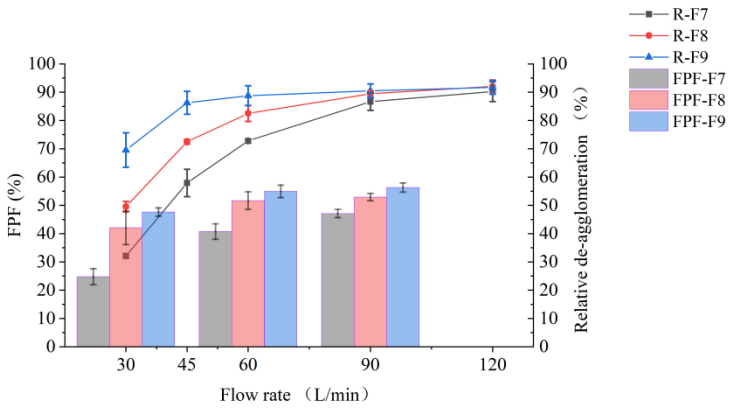

Figure 6. 18 Relative de-agglomeration (R) and FPF of formulations utilising different accelerations at different airflow rates.

Relative Deagglomeration and Flow Rate

Figure 6.18 depicts the relationship between relative deagglomeration and airflow rate for formulations prepared at different intensities. The key observations include the following.

- **Positive Correlation:** Formulations mixed at higher accelerations exhibit a greater degree of relative deagglomeration at lower airflow rates than those prepared at lower accelerations. For instance, the 80 g formulation achieved a significantly higher relative deagglomeration of 69.56 ± 6.09% at 30 L/min, compared to only 41.12 ± 1.56% for the 60 g formulation.
- **Convergence at Higher Flow Rates:** At higher flow rates (90 and 120 L/min), all formulations exhibited a similar deagglomeration pattern, reaching a plateau at approximately 90%.

Correlation with FPF: The trend observed in the relative deagglomeration (R) strongly correlates with the fine particle fraction (FPF) at different flow rates. This implies that a higher degree of deagglomeration directly translates into a greater proportion of particles within the optimal size range for efficient inhalation.

The acoustic mixing intensity is a critical factor influencing the deagglomeration behaviour in DPI formulations. Higher intensity settings (70 g and 80 g) promoted more efficient particle breakdown, particularly at lower airflow rates.

This translates to a higher FPF and potentially improved drug delivery efficiency across a wide range of inhalation profiles.

6.3.3.6 Production of ternary melatonin formulation with combination of mechanical dry coating and acoustic vibration

Building on the success of ultrasonic vibration spheroidisation, which achieved a significantly higher Fine Particle Fraction (FPF) and minimal impact on dissolution with a 1% Magnesium Stearate (MgSt) coating (as shown in previous studies), this study investigated the application of the same MgSt concentration in a ternary melatonin formulation produced via acoustic vibration.

***In vitro* aerosolization performance**

The results confirmed the substantial influence of the MgSt coating on the aerosolisation performance of the melatonin formulation. Data from Table 6.10 and Figure 6.19 demonstrate a significant reduction in drug deposition within the artificial throat, simulating the oropharyngeal region. This decrease was accompanied by a concomitant improvement in the FPF, suggesting a more targeted delivery profile with a greater proportion of drug particles reaching the lungs and less unwanted deposition in the upper respiratory tract.

Table 6. 10 Aerosol properties of melatonin formulations with and without MgSt dry coating

	ED/%	FPD/μg	FPF/%	MMAD/μm	GSD
0% MgSt	88.8±4.5	48.2±2.3	54.9±5.8	2.3±0.1	1.7±0.1
1% MgSt	99.2±1.9	70.6±2.4	71.6±3.1	2.0±0.1	1.7±0.0

ED = emitted dose; FPD = fine particle dose; FPF = fine particle fraction; GSD = geometric standard deviation; MMAD = mass median aerodynamic diameter; Data are presented as mean ± SD (n = 3).

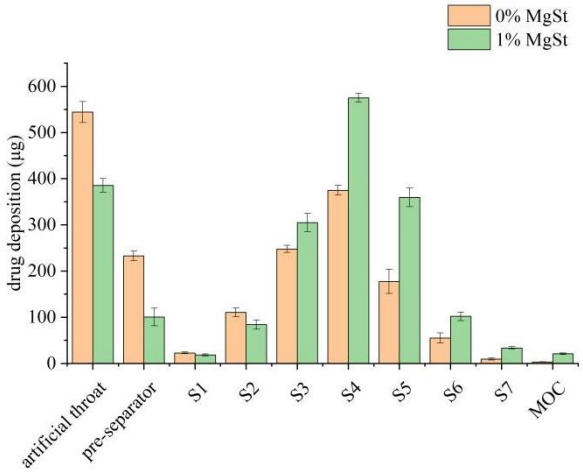

Figure 6. 19 Aerodynamic particle size distribution of melatonin agglomerates with/without mechanical dry coating

De-agglomeration characterization

Figure 6.20 illustrates the relative de-agglomeration efficiency of the ternary formulations at different flow rates. Notably, formulations containing fine lactose, treated with mechanical dry coating, exhibited significantly higher de-agglomeration levels. At a flow rate of 30 L/min, these formulations achieved a de-agglomeration level of 75.3%, with the maximum observed at 60 L/min.

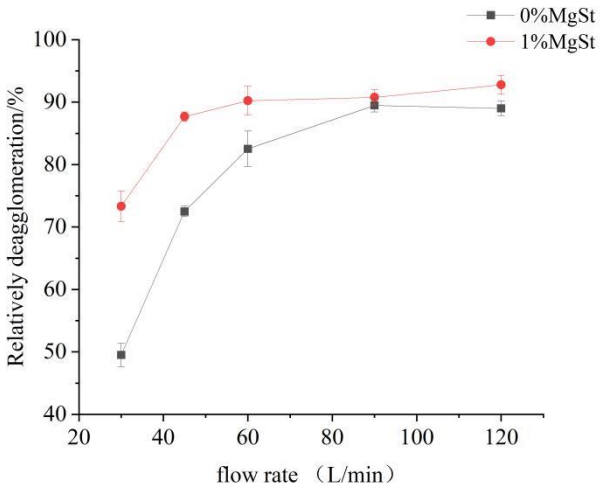

Figure 6. 20 Relative de-agglomeration behavior of melatonin formulation with/without mechanical dry coating

This phenomenon can be attributed to the efficient coating of MgSt onto lactose particles via mechanofusion, leading to a decrease in their surface energy (Zhou et al., 2013a). Since lactose is a major component of the formulation, this surface

modification significantly reduces inter-particle cohesive forces, ultimately enhancing aerosolisation performance (Zhou et al., 2010b).

6.4 Discussion

Spherical agglomerate formulations are initially formed using a rotary drum agglomerator, which compacts and collides with the micronised powder particles. However, the traditional method has certain limitations. First, it yields an uncontrollable size distribution with larger agglomerates, hindering precise metering in devices such as Turbuhaler® (Trofast, 1996a, Wetterlin, 1988). Second, self-weight-induced compaction during spheroidisation increases the mechanical strength of agglomerates, making deagglomeration and dispersion in the lungs difficult(Trofast, 1996a). This requires repeated sieving for size control, rendering the process unsuitable for continuous production.

Recent research has explored alternative methods such as twin-screw extruders and vibrating chutes with speakers. While these approaches aim for continuous production, vibration is not uniformly transferred throughout the chute, leading to inconsistent particle strength and size distribution (Etschmann and Scherliess, 2022).

This study presents a significant advancement by combining mechanical dry coating with ultrasonic and acoustic vibrations for budesonide and melatonin. This novel approach has several advantages:

1. **Continuous Production:** The process enables the continuous generation of uniformly sized agglomerate particles.
2. **Improved aerosolisation:** The lower mechanical strength of spherical agglomerates facilitates deagglomeration and reduces fine particle interaction forces, leading to enhanced aerosolisation performance.
3. **Optimised Deposition:** The reduced fine particle fraction and minimised interaction forces translate to improved aerosol performance and less deposition in the upper airways, favouring deposition in the target area (lungs) and reducing unwanted deposition in the throat.

Ultrasonic Vibration

Ultrasonic waves exhibit a size-dependent effect, inducing significant vibrations in micronised particles while minimally impacting larger particles (Riera et al., 2015). This targeted approach fosters collisions between fine particles, resulting in the formation of agglomerates with a weaker mechanical structure compared with conventional spheroidisation techniques(Riera et al., 2015). Unlike traditional methods, where weight-induced compaction occurs, ultrasonic waves prevent excessive compression, yielding loosely bound aggregates.

Conventional ultrasonic agglomeration setups suffer from uneven transmission of vibrations owing to metal connections(Priyadarshi et al., 2021). A water bath was used to address these "dead zones" by ensuring the uniform exposure of ultrasonic waves throughout the powder bed. This approach yielded highly uniform, near-spherical agglomerates with sphericity exceeding 0.9, which is a critical factor for accurate and consistent dosing during manufacturing(Etschmann and Scherliess, 2022).

Optimizing Dispersibility: Balancing Strength and Flexibility

Ultrasonic vibration enhances the aerosolisation performance of drug formulations by reducing their mechanical strength while preserving their elasticity. This delicate balance is quantified using two key metrics: rupture force and rupture deformation (Adi et al., 2011b). The observed increase in the "dispersibility area" (DA) at lower dispersion pressures signifies this improved balance, facilitating easier deagglomeration within the inhaler device (Jaffari et al., 2013).

Relevance to Inhaler Functionality: Dispersing with Minimal Force

The shear stress encountered within an inhaler is roughly equivalent to a dispersing pressure of 0.1 bar(Shekunov et al., 2003). This pressure is sufficient to assess deagglomeration behaviour at lower pressures and serves as a reliable indicator of the overall dispersibility within the inhaler(Friebel et al., 2012). Conversely, formulations lacking ultrasonic treatment require a higher dispersing

force to overcome the stronger interparticle interactions, reflected in their lower "fine particle fraction" (FPF).

Reduced Throat Deposition for Targeted Lung Delivery

The benefits of ultrasonic vibrations extend beyond the creation of dispersible particles. As illustrated in Figure 6, it significantly reduced the deposition of the active pharmaceutical ingredient (API) in the throat and upper airways. This phenomenon can be attributed to two factors:

- **Smaller Aggregates, Enhanced Detachment:** Larger, more inertial aggregates tend to trap drug particles, leading to premature deposition in the initial stages of the inhaler. Conversely, the smaller aggregates produced via ultrasonication readily deagglomerate upon colliding with the inhaler walls, releasing drug particles for deeper lung penetration (Kinnunen et al., 2015).
- **Improved Lactose Deposition:** Ultrasonic treatment also promoted better deposition of fine lactose particles. This likely results from reduced interparticle forces, allowing more fine particles to detach during deagglomeration. These fine lactose particles can act as carriers for the drug or co-deposit with drug particles, ultimately improving overall lung delivery efficiency.

Acoustic vibration

To realize continuous particle agglomeration, Resonance Acoustic Mixing (RAM) technology is a versatile powder processing technique to create superior agglomerate formulations for less cohesive drug particles. Prior research has established RAM as a highly effective method for efficiently blending powders that exhibit poor mixing characteristics(Tanaka et al., 2016). In this study, RAM with grids was employed to facilitate the mixing and pre-agglomeration of dry powders before the final particle formation. The primary aim was to generate well-structured finer aggregates that readily broke down and dispersed into fine particles within the inhaler to realise a continuous particle agglomeration process.

Particle Interactions and the Role of RAM

During RAM, the small size distribution of both the active pharmaceutical ingredient (API) and lactose carrier particles renders gravity a negligible force. Particle behaviour is primarily governed by interparticle attraction forces, leading to adhesion and subsequent aggregate formation(Gosens et al., 2010). These aggregates may then be influenced by a combination of vibration, gravity, and inertia, with larger aggregates being less susceptible to adhesion because of their increased size.

The van der Waals interactions play a critical role in the adhesion between the fine API and lactose particles(LaMarche et al., 2017). This interaction is size-dependent, with finer particles exhibiting a greater tendency to adhere to each other than larger aggregates. RAM, with its low-frequency acoustic vibrations, induces a micro-mixing effect throughout the mixture, promoting bulk particle movement and interparticle collisions (Osorio and Muzzio, 2015). This uniform distribution of the shear force eliminates areas where mixing is incomplete (dead zones), ensuring a well-homogenised mixture(Kumar et al., 2022).

Impact of Vibration Intensity and Grids on Agglomerates

This study investigated the influence of vibration intensity and grids on the tapped density (packing density) of mixtures, which reflects the interaction forces between particles and small aggregates. A lower acceleration (60 g) without grids or with single-layer grids resulted in less frequent collisions between aggregates and, consequently, a non-uniform distribution of mechanical strength (Das et al., 2013). A lower vibration intensity also led to loosely packed aggregates with surface cracks, as observed in the scanning electron microscopy (SEM) images (Figure 5 D-1).

In contrast, a higher vibration intensity yielded a higher tapped density, indicating the formation of finer aggregates with less void space (Figure 5 E-1 and F-1). This translates to a preferred size distribution with a high degree of

sphericity and smooth surfaces, which is ideal for a consistent emitted dose during inhalation.

Enhanced Aerosol Performance through RAM

Higher acceleration during RAM processing resulted in significant improvements in aerosol performance. Acoustic mixing with grids facilitated the superior dispersion and fluidisation of the agglomerates. Consistent drug deposition across various airflow rates is crucial for clinical application. Uneven dispersion can lead to side effects or reduced therapeutic efficacy, particularly in patients with varying lung functions (Skloot, 2017).

The aerodynamic characteristics of agglomerate formulations were compared at different airflow rates. The formulation processed at higher acceleration exhibited a higher emitted dose and less variation in the fine particle fraction (FPF) compared with the lower acceleration group. This can be attributed to the reduced agglomerate entrainment with higher acceleration mixing and enhanced deagglomeration within the inhaler device. Grids used in conjunction with higher acceleration yielded agglomerate particles with nearly identical emitted dose (ED) and FPF values across different flow rates.

Particle Size Distribution and Aerodynamic Behavior

Laser diffraction analysis of de-agglomerated particles under varying flow rates provided further insight into their aerodynamic behaviour. A better dispersion of aggregates translates to a higher FPF. However, airflow rates below a certain threshold may be insufficient to fully deagglomerate large or strong particles, resulting in lower FPF(Tong et al., 2013). This correlation between aerosolised particle size distribution and aerodynamic deposition patterns highlights the importance of the agglomerate structure in inhalation performance(Breuer and Khalifa, 2019). The formulation processed at 60 g exhibited a larger particle size fraction at low flow rates, indicating the presence of incompletely deagglomerated particles and a lower FPF. A higher vibration intensity led to a

decrease or even disappearance of this larger particle fraction, correlating well with the observed increase in the FPF.

Synergistic Action

The combination of mechanically dry coating of ternary components with both ultrasonic and acoustic vibrations for particle agglomeration further improved the aerosol performance of the agglomerate formulation. This study leverages the well-established connection between the agglomerate strength and interparticle cohesion (Kendall and Stainton, 2001). A mortar grinder with precisely controlled pressure was employed to generate frictional forces during the dry coating process (Zhou et al., 2010c). This technique modifies the surface characteristics of the powder mixture, effectively reducing the intrinsic cohesive forces, particularly those associated with fine lactose, which is the main cause of cohesion (Pfeffer et al., 2001, Yang et al., 2019, Yang et al., 2015). The success of this approach was confirmed by Inverse Gas Chromatography (IGC) results (Williams, 2015), which showed a substantial decrease in cohesion after mechanically dry coating.

Synergy with Vibration for Enhanced Cohesion Reduction:

While mechanical dry coating offers significant benefits, the introduction of ultrasonic and acoustic vibrations creates a synergistic effect. The exact mechanisms require further investigation, but vibrations likely disrupt particle packing or create additional frictional forces during dry coating. This disrupts the interparticle interactions within the powder mixture, leading to a deeper reduction in cohesive forces compared to mechanical dry coating alone, as illustrated by the reduction in deposition in the early stage of NGI.

Performance Benefits from Synergy:

The synergy between the mechanical dry coating and ultrasonic/acoustic vibration facilitates "bursting inhalation", which is the rapid release of high-concentration aerosol clouds. This translates into several benefits for both budesonide and melatonin formulations.

Improved Delivery for Budesonide:

- **Enhanced Fine Particle Release:** A positive correlation exists between increased Magnesium Stearate (MgSt) concentration and improved fine particle release of budesonide. This aligns with the observed increase in the Fine Particle Fraction (FPF) and decrease in the rupture force, both signifying better dispersion and easier inhalation.
- **Reduced Residue and Efficient Delivery:** A significant increase in the Emitted Dose (ED) suggests that less powder residue remains in the inhaler after use. This, combined with the improved FPF, indicates more efficient drug delivery to the target site within the lungs.

Effective Dispersion for Melatonin:

- **Increased Deagglomeration:** The method led to a significant increase in the relative deagglomeration percentage for melatonin, indicating a more effective dispersion compared to traditional methods. This effect was even more pronounced at different airflow rates (30 L/min and 60 L/min).
- **Reduced Deposition and Targeted Delivery:** There was a significant reduction in drug particle deposition in the upper airways (artificial throat and pre-separator stages). This, along with improved FPF, suggests more targeted delivery of the medication to the desired location in the lungs.

Consideration for Dissolution: A Balancing Act

Although the combination of mechanical dry coating with ultrasonic and acoustic vibration effectively reduces interparticle cohesion, this synergy presents a potential challenge for dissolution.

Dissolution Studies and MgSt:

A key consideration is the impact of the MgSt concentration on the dissolution rate. Previous studies (Nokhodchi et al., 2009) have suggested that the hydrophobic properties of MgSt can slow wetting and decrease drug dissolution. This study employed a dissolution test using an artificial membrane that mimicked the lung surface (Sonvico et al., 2021, Floroiu et al., 2018).

Interestingly, only the 3% MgSt formulation with mechanical dry coating exhibited a significantly reduced dissolution rate.

Balancing Dispersion and Dissolution:

The superior dispersion achieved with vibration likely plays a crucial role, as reported in the literature (La Zara et al., 2021, Price et al., 2020), which leads to increased deposition of fine particles on the membrane, facilitating faster wetting upon contact with the medium. This observation suggests a balance between the dispersion and the ability of MgSt to hinder dissolution. At lower MgSt concentrations (1%), the thin coating on the lactose surface may be insufficient to significantly impact water penetration and slow down dissolution, even for highly insoluble drugs, such as budesonide. (Kumar et al., 2022).

Conclusion:

This study demonstrates the potential of combining mechanical dry coating with ultrasonic and acoustic vibration for superior dry powder inhaler (DPI) agglomerate formulations. Although Turbuhaler® can effectively deliver 1 mg of soft agglomerates per inhalation, which is sufficient for most inhaled corticosteroids (van Aalderen and Sprikkelman, 2011, Jain, 2003), further research is needed to optimise delivery for different drug applications and investigate the impact of varying drug-to-lactose ratios to achieve the required dose strength for diverse clinical indications.

Expanding Formulation Options:

Beyond optimising the drug-to-lactose ratios, exploring different ternary components for mechanically dry coating holds promise. The introduction of these additional components could further reduce interparticle interactions, potentially leading to even more effective DPI formulations. Evaluating a wider range of ternary components could ultimately optimise the agglomerate formulation system used with the Turbuhaler®, maximising aerosolisation while minimising side effects.

Chapter 7. Conclusions

Overall Conclusion

This thesis evaluated the potential of soft agglomerate formulations for efficient pulmonary drug delivery. Soft agglomerates, developed for both local and systemic inhaled therapies, were produced with varying proportions of fine lactose, making them suitable for clinical trials due to their adjustable dose strengths. A brief overview of the three main chapters were as follows:

Chapter 4 focused on the production of soft lactose agglomerates. Micronized lactose with surface modifications was processed using a vibration bowl feeder and rotating pan to create agglomerates with optimal roundness, flowability, and distribution for Turbuhaler dispersion. This approach enhanced metering dose consistency and enabled automated filling processes.

Chapter 5 explored the optimization of dry powder inhaler (DPI) formulations through the combination of high shear and air jet mixing. This method resulted in improved aerosol performance and agglomerate size distribution compared to high shear mixing alone. The enhanced emitted dose and fine particle fraction (FPF) were attributed to the uniform mixture and facilitated de-agglomeration during inhalation.

Chapter 6 investigated the synergistic effect of mechanical dry coating combined with ultrasonic and acoustic vibration on DPI agglomerate formulations. This approach effectively reduced interparticle forces, leading to a rapid release of high-concentration aerosol clouds. The improved aerosol performance was demonstrated for both budesonide and melatonin formulations.

Key Findings and Contribution to New Knowledge:

This comprehensive study has elucidated the critical role of fine lactose properties and processing techniques in achieving optimal performance for dry powder inhaler (DPI) agglomerate formulations. The findings underscore the paramount importance of precise control over fine lactose particle size and shape

for superior particle agglomeration. This, in turn, leads to desired dosing behavior, efficient deagglomeration within the lungs, and ultimately, effective delivery of fine drug particles. Additionally, the study demonstrates the potential for tailoring vibration parameters during processing to manipulate the size distribution of agglomerates, impacting their dosing function for formulations containing multiple active pharmaceutical ingredients (APIs).

1.Fine lactose properties are critical for optimal DPI performance

The study underscores the critical role of fine lactose characteristics, such as particle size and shape, in achieving optimal performance for DPI formulations. Precise control over these properties is essential for superior particle agglomeration and drug delivery efficiency.

By elucidating the impact of particle size and shape on agglomeration and performance, the study provides a strong foundation for optimizing DPI formulations based on lactose characteristics.

2.Modified lactose surfaces enhance stability

The study explores the potential benefits of modifying amorphous lactose surfaces with specific temperature and humidity to enhance formulation stability. This approach has the potential to improve the shelf life and efficacy of DPI medications, particularly for drugs that are sensitive to degradation.

3.Synergistic mixing improves morphology and delivery

The research highlights the synergistic effects of high shear mixing and air jet mixing in improving the morphology of agglomerate particles. This synergistic approach leads to enhanced fine particle delivery and a more uniform mixture with fewer aggregates, ultimately contributing to more effective drug delivery.

4.Processing techniques impact agglomeration and performance

The research demonstrates the significant influence of processing techniques on agglomerate properties and, consequently, DPI performance. Vibration parameters can be tailored to manipulate the size distribution of agglomerates, catering to the specific requirements of formulations containing multiple active

pharmaceutical ingredients (APIs).

This finding opens new avenues for developing DPI formulations with targeted characteristics for specific drug delivery requirements.

5.Highlights the importance of in vitro characterization techniques

The importance of in vitro techniques for product characterization is further emphasized by the study's findings on the relative deagglomeration behavior. These techniques offer invaluable tools for evaluating the impact of processing parameters on the performance of agglomerate DPI formulations.

Future Work

This research serves as a springboard for further exploration into the complexities of agglomerate formulation design and processing. Some key areas for future investigation are as follows:

- **Deeper Investigation of Processing Interactions:** A more granular investigation is warranted to understand the combined effects of mixing techniques (e.g. high shear mixing, air jet mixing, and potentially others) and aerosolisation conditions on agglomerate size, morphology, and deagglomeration behaviour across a wider spectrum of drugs. This could involve advanced techniques for examining trends in various drug types, blending methods, and aerosolisation settings.
- **Ternary Formulations:** Exploring the behaviour of ternary formulations by incorporating additional components beyond lactose and the drug is of particular interest. The introduction of these components holds promise for potentially reducing interparticle interactions and leading to even more effective DPI formulations. Evaluating a broader range of ternary components could ultimately optimize the agglomerate formulation system used with the Turbuhaler® device, maximizing aerosolization efficiency while minimizing side effects.

  Given the unique properties of budesonide (a corticosteroid) and melatonin (a lipophilic hormone), the following classes of compounds

were considered as potential candidate components for ternary mixtures in dry powder inhalers (DPIs), along with their rationale:

Other Hormonal Agents:

Rationale: Incorporating other hormones with complementary or synergistic effects to budesonide and melatonin could offer enhanced therapeutic benefits.

Potential Candidates:

Cortisol: Another glucocorticoid with anti-inflammatory properties.

Progesterone: Possesses anti-inflammatory and immunomodulatory effects.

Thyroxine (T4): May have potential synergistic effects with budesonide and melatonin in regulating various physiological processes.

Potential Candidates:

Vitamin C (ascorbic acid): A well-known antioxidant with potential to enhance the stability of budesonide and melatonin.

Vitamin E (alpha-tocopherol): A lipid-soluble antioxidant that may provide protection for melatonin.

Cholesterol:

Rationale: Cholesterol can modulate membrane fluidity and may enhance the permeation of lipophilic compounds like melatonin across biological membranes.

- **Delivery Optimisation:** Further research is needed to explore how this approach can be adapted for the delivery of drugs with varying potencies that require different dose strengths for diverse clinical applications. This may involve the optimisation of the drug-to-lactose ratio within the formulation for targeted delivery.

Mechanical dry coating optimisation: While the study demonstrates the promise of mechanical dry coating with ultrasonic and acoustic vibration, further

research is needed to investigate the impact of varying drug-to-lactose ratios and their effect on achieving the desired dose strength for different clinical needs.

By delving deeper into these areas, researchers can gain a more comprehensive understanding of the interplay between the processing parameters, lactose properties, and drug characteristics. This knowledge will ultimately pave the way for the rapid development of more effective and efficient DPI formulations, significantly improving treatment outcomes and quality of life in patients who rely on inhalation therapies.

Limitations and Future Directions:

This study, while providing valuable insights into the development of novel DPI formulations, encountered several limitations that should be acknowledged and addressed in future research:

- **Reproducibility of Agglomeration:** Achieving consistent and reproducible agglomerate size and morphology across different batches proved challenging. This highlights the need for further optimization of process parameters and the implementation of robust quality control measures to ensure consistent product quality.
- **Scale-up Challenges:** The agglomeration process was conducted on a laboratory scale. Scaling up the process for large-scale manufacturing may present challenges in maintaining consistent agglomerate properties and ensuring uniform product quality. Further investigations are required to optimize the process for scale-up production.
- **Limited In Vivo Studies:** This study primarily focused on in vitro characterization of the developed formulations. Further in vivo studies in animal models are necessary to evaluate the efficacy and safety of these formulations in vivo and to correlate in vitro performance with in vivo deposition and therapeutic outcomes.
- **Focus on a Limited Number of Excipients:** The study explored a limited number of excipients. A more comprehensive investigation of

different excipient combinations and their impact on formulation properties and drug delivery would be beneficial.

- **Influence of Patient Factors:** The study did not investigate the impact of patient factors, such as inhalation technique and respiratory rate, on drug delivery from the developed formulations.

Future Research Directions:

- **Investigate alternative agglomeration techniques:** Explore alternative techniques such as fluidized bed agglomeration and spray congealing to improve process control and scalability.
- **Develop novel excipient systems:** Investigate the use of novel excipients, such as polymers with tailored properties, to enhance formulation stability and improve drug delivery.
- **Conduct in vivo studies:** Evaluate the efficacy and safety of the developed formulations in animal models and, ultimately, in human clinical trials.
- **Develop robust quality control measures:** Implement robust quality control measures to ensure consistent product quality and minimize batch-to-batch variability.
- **Investigate the influence of patient factors:** Conduct studies to assess the impact of patient factors, such as inhalation technique and respiratory rate, on drug delivery from the developed formulations.

By addressing these limitations and pursuing the outlined future research directions, we can further advance the development of innovative and effective DPI formulations for improved patient outcomes.

LIST OF PUBLICATIONS

Journals:

1. Qingzhen Zhang, Zheng Wang, Philip Hall, Particle agglomeration via resonant acoustic mixer for dry powder inhalation,Chemical Engineering Research and Design, Volume 203, 2024, Pages 253-262,

2. Zhang, Q., Kou, S., Cui, Y., Dong, J., Ye, Y., Wang, Y., Lu, R., Li, X., Nie, Y., Shi, K., Chen, F., Hall, P., Chen, X., Wang, Z., & Jiang, X. (2024). Ternary Dry Powder Agglomerate Inhalation Formulation of Melatonin With Air Jet Mixing to Improve In Vitro And In Vivo Performance. Journal of pharmaceutical sciences, 113(2), 434–444. https://doi.org/10.1016/j.xphs.2023.11.016

3. Zhang, Q., Wang, Z., Shi, K., Zhou, H., Wei, X., & Hall, P. (2023). Improving Inhalation Performance with Particle Agglomeration via Combining Mechanical Dry Coating and Ultrasonic Vibration. Pharmaceutics, 16(1), 68. https://doi.org/10.3390/pharmaceutics16010068

Conference paper:

1. Qingzhen Zhang, Zheng Wang, Philip Hall, Yan Zhao, &Bin Dong, Minimal amounts of sodium chloride combined with leucine improve aerosol performance of spray-dried vardenafil powders for inhalation. Drug Delivery to the Lungs, Volume 34, 2023

2. Qingzhen Zhang, Zheng Wang, Philip Hall, Particle agglomeration via resonant acoustic mixer for dry powder inhalation. 10th International Granulation Workshop -Granulation Conference

Bibliography

.

ABDO, R. W., SAADI, N., HIJAZI, N. I. & SULEIMAN, Y. A. 2020. Quality control and testing evaluation of pharmaceutical aerosols. *Drug Delivery Systems***,** 579-614.

ABHIJIT KADAM1*, M. P. 2017. Modal Analysis of Vibratory Bowl Feeder Machine. *International Journal on Recent Technologies in Mechanical and Electrical Engineering (IJRMEE),* 4.

ABIONA, O., WYATT, D., KONER, J. & MOHAMMED, A. 2022a. The Optimisation of Carrier Selection in Dry Powder Inhaler Formulation and the Role of Surface Energetics. *Biomedicines,* 10.

ABIONA, O., WYATT, D., KONER, J. & MOHAMMED, A. 2022b. The Optimisation of Carrier Selection in Dry Powder Inhaler Formulation and the Role of Surface Energetics. *Biomedicines,* 10**,** 2707.

ADAMI, R., RUSSO, P., AMANTE, C., DE SORICELLIS, C., DELLA PORTA, G., REVERCHON, E. & DEL GAUDIO, P. 2022. Supercritical Antisolvent Technique for the Production of Breathable Naringin Powder. *Pharmaceutics,* 14**,** 1623.

ADI, S., ADI, H., CHAN, H.-K., FINLAY, W., TONG, Z., YANG, R. & YU, A. 2011a. Agglomerate strength and dispersion of pharmaceutical powders. *Journal of Aerosol Science - J AEROSOL SCI,* 42**,** 285-294.

ADI, S., ADI, H., CHAN, H.-K., FINLAY, W. H., TONG, Z., YANG, R. & YU, A. 2011b. Agglomerate strength and dispersion of pharmaceutical powders. *Journal of Aerosol Science,* 42**,** 285-294.

AGNEW, J. E., SUTTON, P. P., PAVIA, D. & CLARKE, S. W. 1986. Radioaerosol assessment of mucociliary clearance: towards definition of a normal range. *Br J Radiol,* 59**,** 147-51.

ALYAMI, H., DAHMASH, E., BOWEN, J. & MOHAMMED, A. R. 2017. An investigation into the effects of excipient particle size, blending techniques and processing parameters on the homogeneity and content uniformity of a blend containing low-dose model drug. *PLoS One,* 12**,** e0178772.

AMMARI, W. G., MOHAMMAD, M. K. & TAYYEM, R. F. 2019. The impact of patients' real-life environmental temperature and humidity use conditions of tiotropium dry powder inhaler on its aerosol emission characteristics. *European Journal of Pharmaceutical Sciences,* 133**,** 137-144.

ARNOLD, W. 2014. Force Modulation in Atomic Force Microscopy. *In:* BHUSHAN, B. (ed.) *Encyclopedia of Nanotechnology.* Dordrecht: Springer Netherlands.

BADAL, M., PAZESH, S., NORDGREN, N., SCHULEIT, M., RUTLAND, M., ALDERBORN, G. & MILLQVIST-FUREBY, A. 2017. Milling induced amorphisation and recrystallization of α-lactose monohydrate. *International Journal of Pharmaceutics,* 537.

BALOIRA, A., ABAD, A., FUSTER, A., GARCÍA RIVERO, J. L., GARCÍA-SIDRO, P., MÁRQUEZ-MARTÍN, E., PALOP, M., SOLER, N., VELASCO, J. L. &

GONZÁLEZ-TORRALBA, F. 2021. Lung Deposition and Inspiratory Flow Rate in Patients with Chronic Obstructive Pulmonary Disease Using Different Inhalation Devices: A Systematic Literature Review and Expert Opinion. *Int J Chron Obstruct Pulmon Dis,* 16**,** 1021-1033.

BASHETI, I., BOSNIC-ANTICEVICH, S., ARMOUR, C. & REDDEL, H. 2013. Checklists for Powder Inhaler Technique: A Review and Recommendations. *Respiratory care,* 59**,** 1140-1154.

BEGAT, P., MORTON, D., SHUR, J., KIPPAX, P., STANIFORTH, J. & PRICE, R. 2009a. The Role of Force Control Agents in High-Dose Dry Powder Inhaler Formulations. *Journal of pharmaceutical sciences,* 98**,** 2770-83.

BEGAT, P., MORTON, D. A. V., SHUR, J., KIPPAX, P., STANIFORTH, J. N. & PRICE, R. 2009b. The Role of Force Control Agents in High-Dose Dry Powder Inhaler Formulations. *Journal of Pharmaceutical Sciences,* 98**,** 2770-2783.

BEGAT, P., PRICE, R., HARRIS, H., MORTON, D. A. V. & STANIFORTH, J. N. 2005. The Influence of Force Control Agents on the Cohesive-Adhesive Balance in Dry Powder Inhaler Formulations. *KONA Powder and Particle Journal,* 23**,** 109-121.

BEHARA, S. R. B., LARSON, I., KIPPAX, P., MORTON, D. A. V. & STEWART, P. 2011. An approach to characterising the cohesive behaviour of powders using a flow titration aerosolisation based methodology. *Chemical Engineering Science,* 66**,** 1640-1648.

BENKE, E., FARKAS, Á., SZABÓ-RÉVÉSZ, P. & AMBRUS, R. 2020. Development of an Innovative, Carrier-Based Dry Powder Inhalation Formulation Containing Spray-Dried Meloxicam Potassium to Improve the In Vitro and In Silico Aerodynamic Properties. *Pharmaceutics,* 12.

BERKENFELD, K., LAMPRECHT, A. & MCCONVILLE, J. T. 2015. Devices for dry powder drug delivery to the lung. *AAPS PharmSciTech,* 16**,** 479-490.

BREUER, M. & KHALIFA, A. 2019. Refinement of breakup models for compact powder agglomerates exposed to turbulent flows considering relevant time scales. *Computers & Fluids,* 194**,** 104315.

BRIGGNER, L.-E., BUCKTON, G., BYSTROM, K. & DARCY, P. 1994. The use of isothermal microcalorimetry in the study of changes in crystallinity induced during the processing of powders. *International Journal of Pharmaceutics,* 105**,** 125-135.

BRODKA-PFEIFFER, K., HÄUSLER, H., GRASS, P. & LANGGUTH, P. 2003. Conditioning following powder micronization: influence on particle growth of salbutamol sulfate. *Drug Dev Ind Pharm,* 29**,** 1077-84.

BRUM, J. & BURNETT, D. 2011. Quantification of surface amorphous content using dispersive surface energy: the concept of effective amorphous surface area. *AAPS PharmSciTech,* 12**,** 887-92.

BUND, R. K. & PANDIT, A. B. 2007. Sonocrystallization: effect on lactose recovery and crystal habit. *Ultrason Sonochem,* 14**,** 143-52.

BUNDGAARD, A., BACH-MORTENSEN, N. & SCHMIDT, A. 1982. The effect of sodium cromoglycate delivered by Spinhaler and by pressurized aerosol on

exercise-induced asthma in children. *Clin Allergy,* 12**,** 601-5.

BUNGERT, N., KOBLER, M. & SCHERLIEß, R. 2021. Surface energy considerations in ternary powder blends for inhalation. *International Journal of Pharmaceutics,* 609**,** 121189.

BUSTAMANTE-MARIN, X. M. & OSTROWSKI, L. E. 2017. Cilia and Mucociliary Clearance. *Cold Spring Harbor perspectives in biology,* 9**,** a028241.

CHAN, J. G. Y., WONG, J., ZHOU, Q. T., LEUNG, S. S. Y. & CHAN, H.-K. 2014. Advances in device and formulation technologies for pulmonary drug delivery. *AAPS PharmSciTech,* 15**,** 882-897.

CHAURASIYA, B. & ZHAO, Y.-Y. 2021. Dry Powder for Pulmonary Delivery: A Comprehensive Review. *Pharmaceutics* [Online], 13.

CHEN, J., WANG, J., ULRICH, J., YIN, Q. & XUE, L. 2008. Effect of Solvent on the Crystal Structure and Habit of Hydrocortisone. *Crystal Growth & Design,* 8**,** 1490-1494.

CHEN, L., HENG, R.-L., DELELE, M. A., CAI, J., DU, D.-Z. & OPARA, U. L. 2013. Investigation of dry powder aerosolization mechanisms in different channel designs. *International Journal of Pharmaceutics,* 457**,** 143-149.

CHEW, N. Y. & CHAN, H. K. 2001. Use of solid corrugated particles to enhance powder aerosol performance. *Pharm Res,* 18**,** 1570-7.

CHONG, R. H. E., JONES, B. E., DÍEZ, F., BIRCHALL, J. C. & COULMAN, S. A. 2016. Evaluating the sensitivity, reproducibility and flexibility of a method to test hard shell capsules intended for use in dry powder inhalers. *International Journal of Pharmaceutics,* 500**,** 316-325.

COATES, M. S., FLETCHER, D. F., CHAN, H.-K. & RAPER, J. A. 2005. The Role of Capsule on the Performance of a Dry Powder Inhaler Using Computational and Experimental Analyses. *Pharmaceutical Research,* 22**,** 923-932.

CUI, Y., HUANG, Y., ZHANG, X., LU, X., XUE, J., WANG, G., HU, P., YUE, X., ZHAO, Z., PAN, X. & WU, C. 2022. A real-time and modular approach for quick detection and mechanism exploration of DPIs with different carrier particle sizes. *Acta Pharm Sin B,* 12**,** 437-450.

DAHMASH, E. Z. & MOHAMMED, A. R. 2015. Functionalised particles using dry powder coating in pharmaceutical drug delivery: promises and challenges. *Expert Opinion on Drug Delivery,* 12**,** 1867-1879.

DAS, S., LARSON, I., YOUNG, P. & STEWART, P. 2009. Surface energy changes and their relationship with the dispersibility of salmeterol xinafoate powders for inhalation after storage at high RH. *European Journal of Pharmaceutical Sciences,* 38**,** 347-354.

DAS, S. C., BEHARA, S. R. B., BULITTA, J. B., MORTON, D. A. V., LARSON, I. & STEWART, P. J. 2012. Powder Strength Distributions for Understanding De-agglomeration of Lactose Powders. *Pharmaceutical Research,* 29**,** 2926-2935.

DAS, S. C., BEHARA, S. R. B., MORTON, D. A. V., LARSON, I. & STEWART, P. J. 2013. Importance of particle size and shape on the tensile strength distribution and de-agglomeration of cohesive powders. *Powder Technology,* 249**,**

297-303.
DAS, S. C., ZHOU, Q., MORTON, D. A. V., LARSON, I. & STEWART, P. J. 2011. Use of surface energy distributions by inverse gas chromatography to understand mechanofusion processing and functionality of lactose coated with magnesium stearate. *European Journal of Pharmaceutical Sciences,* 43**,** 325-333.
DAVIES, M., BRINDLEY, A., CHEN, X., MARLOW, M., DOUGHTY, S. W., SHRUBB, I. & ROBERTS, C. J. 2005. Characterization of drug particle surface energetics and young's modulus by atomic force microscopy and inverse gas chromatography. *Pharm Res,* 22**,** 1158-66.
DE BOER, A. H., HAGEDOORN, P., GJALTEMA, D., GOEDE, J., KUSSENDRAGER, K. D. & FRIJLINK, H. W. 2003. Air classifier technology (ACT) in dry powder inhalation. Part 2. The effect of lactose carrier surface properties on the drug-to-carrier interaction in adhesive mixtures for inhalation. *Int J Pharm,* 260**,** 201-16.
DE BOER, A. H., HAGEDOORN, P., GJALTEMA, D., LAMBREGTS, D., IRNGARTINGER, M. & FRIJLINK, H. W. 2004. The mode of drug particle detachment from carrier crystals in an air classifier-based inhaler. *Pharm Res,* 21**,** 2167-74.
DE BOER, A. H., HAGEDOORN, P., HOPPENTOCHT, M., BUTTINI, F., GRASMEIJER, F. & FRIJLINK, H. W. 2017. Dry powder inhalation: past, present and future. *Expert Opinion on Drug Delivery,* 14**,** 499-512.
DEPASQUALE, R., LEE, S. L., SALUJA, B., SHUR, J. & PRICE, R. 2015. The Influence of Secondary Processing on the Structural Relaxation Dynamics of Fluticasone Propionate. *AAPS PharmSciTech,* 16**,** 589-600.
DJOKIĆ, M., DJURIŠ, J., SOLOMUN, L., KACHRIMANIS, K., DJURIĆ, Z. & IBRIĆ, S. 2014. The influence of spiral jet-milling on the physicochemical properties of carbamazepine form III crystals: Quality by design approach. *Chemical Engineering Research and Design,* 92**,** 500-508.
DU, M., KALIA, N., FRUMENTO, G., CHEN, F. & ZHANG, Z. 2017. Biomechanical properties of human T cells in the process of activation based on diametric compression by micromanipulation. *Med Eng Phys,* 40**,** 20-27.
DUNST, P., BORNMANN, P., HEMSEL, T. & SEXTRO, W. 2018. Vibration-Assisted Handling of Dry Fine Powders. *Actuators,* 7**,** 18.
EBNESAJJAD, S. 2016. Introduction to Plastics. *In:* BAUR, E., RUHRBERG, K. & WOISHNIS, W. (eds.) *Chemical Resistance of Engineering Thermoplastics*. William Andrew Publishing.
ENDRES, S. C., CIACCHI, L. C. & MÄDLER, L. 2021. A review of contact force models between nanoparticles in agglomerates, aggregates, and films. *Journal of Aerosol Science,* 153**,** 105719.
ERIKSSON, J., SJÖGREN, E., LENNERNÄS, H. & THÖRN, H. 2020. Drug Absorption Parameters Obtained Using the Isolated Perfused Rat Lung Model Are Predictive of Rat In Vivo Lung Absorption. *Aaps j,* 22**,** 71.
ESHEL, G., LEVY, G. J., MINGELGRIN, U. & SINGER, M. J. 2004. Critical Evaluation of the Use of Laser Diffraction for Particle-Size Distribution Analysis. *Soil*

Science Society of America Journal, 68**,** 736-743.

ETSCHMANN, C. & SCHERLIESS, R. 2022. Formulation of rifampicin softpellets for high dose delivery to the lungs with a novel high dose dry powder inhaler. *Int J Pharm,* 617**,** 121606.

FANG, L., YAN, Y., AGARWAL, O., YAO, S., SEPPALA, J. E. & KANG, S. H. 2020. Effects of Environmental Temperature and Humidity on the Geometry and Strength of Polycarbonate Specimens Prepared by Fused Filament Fabrication. *Materials (Basel, Switzerland),* 13**,** 4414.

FAULHAMMER, E., WAHL, V., ZELLNITZ, S., KHINAST, J. G. & PAUDEL, A. 2015. Carrier-based dry powder inhalation: Impact of carrier modification on capsule filling processability and in vitro aerodynamic performance. *Int J Pharm,* 491**,** 231-42.

FLAMENT, M.-P., LETERME, P. & GAYOT, A. 2004. The influence of carrier roughness on adhesion, content uniformity and the in vitro deposition of terbutaline sulphate from dry powder inhalers. *International journal of pharmaceutics,* 275**,** 201-9.

FLOROIU, A., KLEIN, M., KRÄMER, J. & LEHR, C. M. 2018. Towards Standardized Dissolution Techniques for In Vitro Performance Testing of Dry Powder Inhalers. *Dissolution Technologies,* 25**,** 6-18.

FRIEBEL, C., STECKEL, H. & MÜLLER, B. W. 2012. Rational design of a dry powder inhaler: device design and optimisation. *J Pharm Pharmacol,* 64**,** 1303-15.

FUSSELL, A. L., GRASMEIJER, F., FRIJLINK, H. W., DE BOER, A. H. & OFFERHAUS, H. L. 2014. CARS microscopy as a tool for studying the distribution of micronised drugs in adhesive mixtures for inhalation. *Journal of Raman Spectroscopy,* 45**,** 495-500.

GAO, H., HAMMER, T., ZHANG, X., HE, W., XU, G. & WANG, J. 2020. Quantifying respiratory tract deposition of airborne graphene nanoplatelets: The impact of plate-like shape and folded structure. *medRxiv***,** 2020.08.28.20183608.

GARBARIENĖ, I., DUDOITIS, V., ULEVIČIUS, V., PLAU Š KAITĖ-ŠUKIENĖ, K., KILIKEVIČIUS, A., MATIJOŠIUS, J., RIMKUS, A., KILIKEVIČIENĖ, K., VAINORIUS, D., MAKNICKAS, A., BORODINAS, S. & BYČENKIENĖ, S. 2021. Application of Acoustic Agglomeration Technology to Improve the Removal of Submicron Particles from Vehicle Exhaust. *Symmetry,* 13**,** 1200.

GARNIER, S., PETIT, S., MALLET, F., PETIT, M. N., DANY, L., COSTE, S., LEFEBVRE, J. & COQUEREL, G. 2008. Influence of ageing, grinding and preheating on the thermal behaviour of α-lactose monohydrate. *International journal of pharmaceutics,* 361**,** 131-40.

GHORI, M. & CONWAY, B. 2018. Triboelectrification of Pharmaceutical Powders: A Critical Review.

GIRY, K., PÉAN, J. M., GIRAUD, L., MARSAS, S., ROLLAND, H. & WÜTHRICH, P. 2006. Drug/lactose co-micronization by jet milling to improve aerosolization properties of a powder for inhalation. *Int J Pharm,* 321**,** 162-6.

GOMBÁS, Á., SZABÓ-RÉVÉSZ, P., KATA, M., REGDON, G. & ISTVÁN, E. 2002. Quantitative Determination of Crystallinity of α-Lactose Monohydrate by

DSC. *Journal of Thermal Analysis and Calorimetry,* 68**,** 503-510.
GONDA, I. 2004. Particulate Interactions in Dry Powder Formulations for Inhalation. *Journal of Controlled Release - J CONTROL RELEASE,* 96**,** 509-509.
GOSENS, I., POST, J. A., DE LA FONTEYNE, L. J., JANSEN, E. H., GEUS, J. W., CASSEE, F. R. & DE JONG, W. H. 2010. Impact of agglomeration state of nano- and submicron sized gold particles on pulmonary inflammation. *Part Fibre Toxicol,* 7**,** 37.
GRANT, A. C., WALKER, R., HAMILTON, M. & GARRILL, K. 2015. The ELLIPTA® Dry Powder Inhaler: Design, Functionality, In Vitro Dosing Performance and Critical Task Compliance by Patients and Caregivers. *Journal of aerosol medicine and pulmonary drug delivery,* 28**,** 474-485.
GRASMEIJER, F., GRASMEIJER, N., HAGEDOORN, P., FRIJLINK, H. & DE BOER, A. 2015. Recent advances in the fundamental understanding of adhesive mixtures for inhalation. *Current pharmaceutical design,* 21.
GRASMEIJER, F., LEXMOND, A. J., VAN DEN NOORT, M., HAGEDOORN, P., HICKEY, A. J., FRIJLINK, H. W. & DE BOER, A. H. 2014. New Mechanisms to Explain the Effects of Added Lactose Fines on the Dispersion Performance of Adhesive Mixtures for Inhalation. *PLOS ONE,* 9**,** e87825.
GU, Z., LI, S., ZHANG, F. & WANG, S. 2016. Understanding Surface Adhesion in Nature: A Peeling Model. *Advanced Science,* 3**,** 1500327.
GUENETTE, E., BARRETT, A., KRAUS, D., BRODY, R., HARDING, L. & MAGEE, G. 2009. Understanding the effect of lactose particle size on the properties of DPI formulations using experimental design. *International Journal of Pharmaceutics,* 380**,** 80-88.
HAIKARAINEN, J., SELROOS, O., LÖYTÄNÄ, T., METSÄRINNE, S., HAPPONEN, A. & RYTILÄ, P. 2017. Budesonide/Formoterol Easyhaler®: Performance Under Simulated Real-Life Conditions. *Pulmonary Therapy,* 3**,** 125-138.
HARTMANN, T. 2008. *Agglomeration feiner Pulver: ein neues Verfahren zur Softpellet-Produktion.* PhD thesis, Kiel University.
HASSAN, M. S. & LAU, R. 2010. Effect of particle formulation on dry powder inhalation efficiency. *Curr Pharm Des,* 16**,** 2377-87.
HASSAN, M. S. & LAU, R. W. 2009. Effect of particle shape on dry particle inhalation: study of flowability, aerosolization, and deposition properties. *AAPS PharmSciTech,* 10**,** 1252-62.
HAWARE, R. V., VINJAMURI, B. P., SARKAR, A., STEFIK, M. & STAGNER, W. C. 2018. Deciphering magnesium stearate thermotropic behavior. *International Journal of Pharmaceutics,* 548**,** 314-324.
HE, J. & NOVOSSELOV, I. V. 2017. Design and Evaluation of an Aerodynamic Focusing Micro-Well Aerosol Collector. *Aerosol science and technology : the journal of the American Association for Aerosol Research,* 51**,** 1016-1026.
HEINSON, W. R., CHAKRABARTI, A. & SORENSEN, C. M. 2014. Crossover from spherical particle Mie scattering to circular aperture diffraction. *Journal of the Optical Society of America A,* 31**,** 2362-2364.

HICKEY, A. J., MANSOUR, H. M., TELKO, M. J., XU, Z., SMYTH, H. D. C., MULDER, T., MCLEAN, R., LANGRIDGE, J. & PAPADOPOULOS, D. 2007. Physical Characterization of Component Particles Included in Dry Powder Inhalers. I. Strategy Review and Static Characteristics. *Journal of Pharmaceutical Sciences,* 96**,** 1282-1301.

HIRSCHBERG, C., JENSEN, N. S., BOETKER, J., MADSEN, A. Ø., KÄÄRIÄINEN, T. O., KÄÄRIÄINEN, M.-L., HOPPU, P., GEORGE, S. M., MURTOMAA, M., SUN, C. C., RISBO, J. & RANTANEN, J. 2019. Improving Powder Characteristics by Surface Modification Using Atomic Layer Deposition. *Organic Process Research & Development,* 23**,** 2362-2368.

HOE, S., YOUNG, P. M. & TRAINI, D. 2011. Aerosol Tribocharging and its Relation to the Deposition of Oxis™ Turbuhaler® in the Electrical Next Generation Impactor. *Journal of Pharmaceutical Sciences,* 100**,** 5270-5280.

HOMMA, Y. 2001. III–V Growth, In Situ Observation by Scanning Electron Microscopy of. *In:* BUSCHOW, K. H. J., CAHN, R. W., FLEMINGS, M. C., ILSCHNER, B., KRAMER, E. J., MAHAJAN, S. & VEYSSIÈRE, P. (eds.) *Encyclopedia of Materials: Science and Technology.* Oxford: Elsevier.

HOPPENTOCHT, M., HAGEDOORN, P., FRIJLINK, H. W. & DE BOER, A. H. 2014. Technological and practical challenges of dry powder inhalers and formulations. *Advanced Drug Delivery Reviews,* 75**,** 18-31.

HUA, J.-L., YE, X.-F., DU, C.-L., XIE, N., ZHANG, J.-Q., LI, M. & ZHANG, J. 2021. Optimizing inhalation therapy in the aspect of peak inhalation flow rate in patients with chronic obstructive pulmonary disease or asthma. *BMC Pulmonary Medicine,* 21**,** 302.

HUPPERTZ, T. & GAZI, I. 2016. Lactose in dairy ingredients: Effect on processing and storage stability¹. *Journal of Dairy Science,* 99**,** 6842-6851.

IKEGAMI, K., KAWASHIMA, Y., TAKEUCHI, H., YAMAMOTO, H., MIMURA, K., MOMOSE, D.-I. & OUCHI, K. 2003. A new spherically agglomerated drug composite system with lactose for dry powder inhalation. *Advanced Powder Technology,* 14**,** 215-229.

ISLAM, N., STEWART, P., LARSON, I. & HARTLEY, P. 2005. Surface roughness contribution to the adhesion force distribution of salmeterol xinafoate on lactose carriers by atomic force microscopy. *J Pharm Sci,* 94**,** 1500-11.

IVANISEVIC, I., MCCLURG, R. B. & SCHIELDS, P. J. Uses of X-Ray Powder Diffraction In the Pharmaceutical Industry. *Pharmaceutical Sciences Encyclopedia.*

IVANOVA, V., GARBUZENKO, O. B., REUHL, K. R., REIMER, D. C., POZHAROV, V. P. & MINKO, T. 2013. Inhalation treatment of pulmonary fibrosis by liposomal prostaglandin E2. *European journal of pharmaceutics and biopharmaceutics : official journal of Arbeitsgemeinschaft fur Pharmazeutische Verfahrenstechnik e.V,* 84**,** 335-344.

JAAFAR-MAALEJ, C., ANDRIEU, V., ELAISSARI, A. & FESSI, H. 2009. Assessment methods of inhaled aerosols: technical aspects and applications. *Expert Opin Drug Deliv,* 6**,** 941-59.

JAFFARI, S., FORBES, B., COLLINS, E., BARLOW, D. J., MARTIN, G. P. & MURNANE, D. 2013. Rapid characterisation of the inherent dispersibility of respirable powders using dry dispersion laser diffraction. *Int J Pharm,* 447**,** 124-31.

JAIN, S. 2003. Inhaled steroids are associated with cataracts. *Thorax,* 58**,** 1026.

JALLO, L. J., CHEN, Y., BOWEN, J., ETZLER, F. & DAVE, R. 2011. Prediction of Inter-particle Adhesion Force from Surface Energy and Surface Roughness. *Journal of Adhesion Science and Technology,* 25**,** 367-384.

JANSON, C., LÖÖF, T., TELG, G., STRATELIS, G. & NILSSON, F. 2016. Difference in resistance to humidity between commonly used dry powder inhalers: an in vitro study. *npj Primary Care Respiratory Medicine,* 26**,** 16053.

JANSSEN, P. H. M., BISHARAT, L. M. N. & BASTIAANSEN, M. 2023a. Complexities related to the amorphous content of lactose carriers. *International Journal of Pharmaceutics: X,* 6**,** 100216.

JANSSEN, P. H. M., BISHARAT, L. M. N. & BASTIAANSEN, M. 2023b. Complexities related to the amorphous content of lactose carriers. *Int J Pharm X,* 6**,** 100216.

JETZER, M. W., SCHNEIDER, M., MORRICAL, B. D. & IMANIDIS, G. 2018a. Investigations on the Mechanism of Magnesium Stearate to Modify Aerosol Performance in Dry Powder Inhaled Formulations. *Journal of Pharmaceutical Sciences,* 107**,** 984-998.

JETZER, M. W., SCHNEIDER, M., MORRICAL, B. D. & IMANIDIS, G. 2018b. Investigations on the Mechanism of Magnesium Stearate to Modify Aerosol Performance in Dry Powder Inhaled Formulations. *J Pharm Sci,* 107**,** 984-998.

JOARDDER, M. U. H., BOSUNIA, M. H., HASAN, M. M., ANANNO, A. A. & KARIM, A. 2024. Significance of Glass Transition Temperature of Food Material in Selecting Drying Condition: An In-Depth Analysis. *Food Reviews International,* 40**,** 952-973.

JONES, M., SANTO, J., YAKUB, B., DENNISON, M., MASTER, H. & BUCKTON, G. 2010. The relationship between drug concentration, mixing time, blending order and ternary dry powder inhalation performance. *International journal of pharmaceutics,* 391**,** 137-47.

KADAM, A. 2017. Modal Analysis of Vibratory Bowl Feeder Machine. *International Journal on Recent Technologies in Mechanical and Electrical Engineering (IJRMEE),* 4**,** 5-10.

KAIALY, W., MARTIN, G. P., TICEHURST, M. D., ROYALL, P., MOHAMMAD, M. A., MURPHY, J. & NOKHODCHI, A. 2011a. Characterisation and deposition studies of recrystallised lactose from binary mixtures of ethanol/butanol for improved drug delivery from dry powder inhalers. *Aaps j,* 13**,** 30-43.

KAIALY, W., MARTIN, G. P., TICEHURST, M. D., ROYALL, P., MOHAMMAD, M. A., MURPHY, J. & NOKHODCHI, A. 2011b. Characterisation and Deposition Studies of Recrystallised Lactose from Binary Mixtures of Ethanol/Butanol for Improved Drug Delivery from Dry Powder Inhalers. *The AAPS Journal,* 13**,** 30-43.

KAIALY, W. & NOKHODCHI, A. 2013. Engineered mannitol ternary additives improve dispersion of lactose-salbutamol sulphate dry powder inhalations. *The AAPS journal,* 15**,** 728-743.

KAMRANIAN MARNANI, A., BÜCK, A., ANTONYUK, S., VAN WACHEM, B., THÉVENIN, D. & TOMAS, J. 2019. The Effect of Very Cohesive Ultra-Fine Particles in Mixtures on Compression, Consolidation, and Fluidization. *Processes,* 7**,** 439.

KENDALL, K. & STAINTON, C. 2001. Adhesion and aggregation of fine particles. *Powder Technology,* 121**,** 223-229.

KHALILI, S. F., GHANBARZADEH, S., NOKHODCHI, A. & HAMISHEHKAR, H. 2018. The effect of different coating materials on the prevention of powder bounce in the next generation impactor. *Research in pharmaceutical sciences,* 13**,** 283-287.

KHOEI, A. R., MASTERS, I. & GETHIN, D. T. 2002. Design optimisation of aluminium recycling processes using Taguchi technique. *Journal of Materials Processing Technology,* 127**,** 96-106.

KINNUNEN, H., HEBBINK, G., PETERS, H., HUCK, D., MAKEIN, L. & PRICE, R. 2015. Extrinsic lactose fines improve dry powder inhaler formulation performance of a cohesive batch of budesonide via agglomerate formation and consequential co-deposition. *Int J Pharm,* 478**,** 53-59.

KINNUNEN, H., HEBBINK, G., PETERS, H., SHUR, J. & PRICE, R. 2014. An investigation into the effect of fine lactose particles on the fluidization behaviour and aerosolization performance of carrier-based dry powder inhaler formulations. *AAPS PharmSciTech,* 15**,** 898-909.

KNOOP, C., TODOROVA, Z., TOMAS, J. & FRITSCHING, U. 2016. Agglomerate fragmentation in high-intensity acoustic standing wave fields. *Powder Technology,* 291**,** 214-222.

KONDOR, A., QUELLET, C. & DALLOS, A. 2015. Surface characterization of standard cotton fibres and determination of adsorption isotherms of fragrances by IGC. *Surface and Interface Analysis,* 47.

KOU, X., CHAN, L. W., SUN, C. C. & HENG, P. W. S. 2017. Preparation of slab-shaped lactose carrier particles for dry powder inhalers by air jet milling. *Asian Journal of Pharmaceutical Sciences,* 12**,** 59-65.

KULASINSKI, K., KETEN, S., CHURAKOV, S. V., GUYER, R., CARMELIET, J. & DEROME, D. 2014. Molecular Mechanism of Moisture-Induced Transition in Amorphous Cellulose. *ACS Macro Letters,* 3**,** 1037-1040.

KUMAR, V., SETHI, B., YANEZ, E., LEUNG, D. H., GHANWATKAR, Y. Y., CHEONG, J., TSO, J., NARANG, A. S., NAGAPUDI, K. & MAHATO, R. I. 2022. Effect of magnesium stearate surface coating method on the aerosol performance and permeability of micronized fluticasone propionate. *International Journal of Pharmaceutics,* 615**,** 121470.

LA ZARA, D., SUN, F., ZHANG, F., FRANEK, F., BALOGH SIVARS, K., HORNDAHL, J., BATES, S., BRÄNNSTRÖM, M., EWING, P., QUAYLE, M. J., PETERSSON, G., FOLESTAD, S. & VAN OMMEN, J. R. 2021. Controlled Pulmonary Delivery of

Carrier-Free Budesonide Dry Powder by Atomic Layer Deposition. *ACS Nano,* 15**,** 6684-6698.

LABIRIS, N. R. & DOLOVICH, M. B. 2003. Pulmonary drug delivery. Part I: physiological factors affecting therapeutic effectiveness of aerosolized medications. *British journal of clinical pharmacology,* 56**,** 588-599.

LAMARCHE, C. Q., LEADLEY, S., LIU, P., KELLOGG, K. M. & HRENYA, C. M. 2017. Method of quantifying surface roughness for accurate adhesive force predictions. *Chemical Engineering Science,* 158**,** 140-153.

LAMEŠIĆ, D., PLANINŠEK, O., LAVRIČ, Z. & ILIĆ, I. 2017. Spherical agglomerates of lactose with enhanced mechanical properties. *Int J Pharm,* 516**,** 247-257.

LANE, E. A. & MOSS, H. B. 1985. Pharmacokinetics of melatonin in man: first pass hepatic metabolism. *J Clin Endocrinol Metab,* 61**,** 1214-6.

LAU, M., YOUNG, P. M. & TRAINI, D. 2017a. Co-milled API-lactose systems for inhalation therapy: impact of magnesium stearate on physico-chemical stability and aerosolization performance. *Drug Development and Industrial Pharmacy,* 43**,** 980-988.

LAU, M., YOUNG, P. M. & TRAINI, D. 2017b. Investigation into the Manufacture and Properties of Inhalable High-Dose Dry Powders Produced by Comilling API and Lactose with Magnesium Stearate. *AAPS PharmSciTech,* 18**,** 2248-2259.

LE, V. N., ROBINS, E. & FLAMENT, M. P. 2012. Agglomerate behaviour of fluticasone propionate within dry powder inhaler formulations. *Eur J Pharm Biopharm,* 80**,** 596-603.

LECHUGA-BALLESTEROS, D., MILLER, D. P. & ZHANG, J. 2002. Residual water in amorphous solids: Measurement and effects on stability. *In:* LEVINE, H. & LEVINE, H. (eds.) *Amorphous Food and Pharmaceutical Systems.* The Royal Society of Chemistry.

LEE, S. L., ADAMS, W. P., LI, B. V., CONNER, D. P., CHOWDHURY, B. A. & YU, L. X. 2009. In Vitro Considerations to Support Bioequivalence of Locally Acting Drugs in Dry Powder Inhalers for Lung Diseases. *The AAPS Journal,* 11**,** 414-423.

LEUNG, C. M. S., TONG, Z., ZHOU, Q. T., CHAN, J. G. Y., TANG, P., SUN, S., YANG, R. & CHAN, H. K. 2016. Understanding the Different Effects of Inhaler Design on the Aerosol Performance of Drug-Only and Carrier-Based DPI Formulations. Part 1: Grid Structure. *Aaps j,* 18**,** 1159-1167.

LI, M., WILKINSON, D. & PATCHIGOLLA, K. 2005. Comparison of Particle Size Distributions Measured Using Different Techniques. *Particulate Science and Technology,* 23**,** 265-284.

LISTIOHADI, Y., HOURIGAN, J., SLEIGH, R. & STEELE, R. 2009. Thermal analysis of amorphous lactose and α-lactose monohydrate. *Dairy Science & Technology - DAIRY SCI TECHNOL,* 89**,** 43-67.

LISTIOHADI, Y. D., HOURIGAN, J., SLEIGH, R. & STEELE, R. J. 2005. Role of amorphous lactose in the caking of α-lactose monohydrate powders. *Australian Journal of Dairy Technology,* 60**,** 19-32.

LIU, L., LABANI, N., CECON, E. & JOCKERS, R. 2019. Melatonin Target Proteins: Too

Many or Not Enough? *Frontiers in Endocrinology,* 10.

LOH, Z. H., SAMANTA, A. K. & SIA HENG, P. W. 2015. Overview of milling techniques for improving the solubility of poorly water-soluble drugs. *Asian Journal of Pharmaceutical Sciences,* 10**,** 255-274.

LOUEY, M. & STEWART, P. 2002. Particle Interactions Involved in Aerosol Dispersion of Ternary Interactive Mixtures. *Pharmaceutical research,* 19**,** 1524-31.

LOUEY, M. D., VAN OORT, M. & HICKEY, A. J. 2004. Aerosol Dispersion of Respirable Particles in Narrow Size Distributions Produced by Jet-Milling and Spray-Drying Techniques. *Pharmaceutical Research,* 21**,** 1200-1206.

LV, L., CHEN, Y. & ZHAO, B. 2024. Pathogen shape: Implication on pathogenicity via respiratory deposition. *Environment International,* 191**,** 108978.

MACDONALD, R., ROWE, D., MARTIN, E. & GORRINGE, L. 2016. The spiral jet mill cut size equation. *Powder Technology,* 299**,** 26-40.

MAGHSOODI, M. 2015. Role of solvents in improvement of dissolution rate of drugs: crystal habit and crystal agglomeration. *Advanced pharmaceutical bulletin,* 5**,** 13-18.

MAJD, F. & NICKERSON, T. A. 1976. Effect of alcohols on lactose solubility. *J Dairy Sci,* 59**,** 1025-32.

MANGAL, S., PARK, H., NOUR, R., SHETTY, N., CAVALLARO, A., ZEMLYANOV, D., THALBERG, K., PURI, V., NICHOLAS, M., NARANG, A. S. & ZHOU, Q. 2019a. Correlations between surface composition and aerosolization of jet-milled dry powder inhaler formulations with pharmaceutical lubricants. *International Journal of Pharmaceutics,* 568**,** 118504.

MANGAL, S., PARK, H., NOUR, R., SHETTY, N., CAVALLARO, A., ZEMLYANOV, D., THALBERG, K., PURI, V., NICHOLAS, M., NARANG, A. S. & ZHOU, Q. T. 2019b. Correlations between surface composition and aerosolization of jet-milled dry powder inhaler formulations with pharmaceutical lubricants. *Int J Pharm,* 568**,** 118504.

MANNINO, G., PERNICI, C., SERIO, G., GENTILE, C. & BERTEA, C. M. 2021. Melatonin and Phytomelatonin: Chemistry, Biosynthesis, Metabolism, Distribution and Bioactivity in Plants and Animals—An Overview. *International Journal of Molecular Sciences,* 22**,** 9996.

MARTI, O. 1999. *AFM Instrumentation and Tips. In: Handbook of Micro/Nanotribology, 2nd edn., ed*, B. Bushan (CRC, Boca Raton)

MAY, S., JENSEN, B., WEILER, C., WOLKENHAUER, M., SCHNEIDER, M. & LEHR, C. M. 2014. Dissolution testing of powders for inhalation: influence of particle deposition and modeling of dissolution profiles. *Pharm Res,* 31**,** 3211-24.

MERKUS, H. G. 2009. Laser Diffraction. *In:* MERKUS, H. G. (ed.) *Particle Size Measurements: Fundamentals, Practice, Quality.* Dordrecht: Springer Netherlands.

MIRZA, S., MIROSHNYK, I., HEINÄMÄKI, J., ANTIKAINEN, O., RANTANEN, J., VUORELA, P., VUORELA, H. & YLIRUUSI, J. 2009. Crystal morphology engineering of pharmaceutical solids: tabletting performance enhancement.

AAPS PharmSciTech, 10**,** 113-119.

MITCHELL, J. & NAGEL, M. 2004. Particle Size Analysis of Aerosols from Medicinal Inhalers. *KONA Powder and Particle Journal,* 22**,** 32-65.

MOHAMMADI-JAM, S. & WATERS, K. E. 2014. Inverse gas chromatography applications: A review. *Advances in Colloid and Interface Science,* 212**,** 21-44.

MORT, J. 2003. Polymers, Electronic Properties. *In:* MEYERS, R. A. (ed.) *Encyclopedia of Physical Science and Technology (Third Edition).* New York: Academic Press.

MORTON, D. 2006. *Dry powder inhaler formulations comprising surface-modified particles with anti-adherent additives*. EP2174653B1.

MUCHÃO, F. P. & SILVA FILHO, L. V. R. F. D. 2010. Avanços na inaloterapia em pediatria. *Jornal de Pediatria,* 86**,** 367-376.

NAIK, S., MUKHERJEE, R. & CHAUDHURI, B. 2016. Triboelectrification: A review of experimental and mechanistic modeling approaches with a special focus on pharmaceutical powders. *International Journal of Pharmaceutics,* 510**,** 375-385.

NAKAI, T., ASAMI, T. & MIURA, H. 2016. Convergence of intense aerial acoustic waves radiated by a rectangular transverse vibrating plate. *Japanese Journal of Applied Physics,* 55**,** 07KE09.

NGUYEN, D., RASMUSON, A., THALBERG, K. & NIKLASSON BJO¨RN, I. 2014. Numerical modelling of breakage and adhesion of loose fine-particle agglomerates. *Chemical Engineering Science,* 116**,** 91-98.

NICHOLS, S. C., MITCHELL, J. P., SHELTON, C. M. & ROBERTS, D. L. 2013. Good Cascade Impactor Practice (GCIP) and Considerations for "In-Use" Specifications. *AAPS PharmSciTech,* 14**,** 375-390.

NOKHODCHI, A., OKWUDARUE, O. N., VALIZADEH, H. & MOMIN, M. N. 2009. Cogrinding as a tool to produce sustained release behavior for theophylline particles containing magnesium stearate. *AAPS PharmSciTech,* 10**,** 1243-51.

NUGENT, C., YIU, G., SONG, S. & CARACTA, C. 2018. The pharmacokinetics, safety, and tolerability of single, high-strength doses of fluticasone propionate and fluticasone propionate/salmeterol delivered via a novel multidose dry powder inhaler in adolescents and adults with persistent asthma. *Journal of Asthma,* 55**,** 898-906.

ORTIGOZA, M. B., MOBINI, C. L., ROCHA, H. L., BARTLETT, S., LOOMIS, C. A. & WEISER, J. N. 2023. Targeting host sialic acids in the upper respiratory tract with a broadly-acting neuraminidase to inhibit influenza virus transmission. *bioRxiv*.

OSORIO, J. G., HERNÁNDEZ, E., ROMAÑACH, R. J. & MUZZIO, F. J. 2016. Characterization of resonant acoustic mixing using near-infrared chemical imaging. *Powder Technology,* 297**,** 349-356.

OSORIO, J. G. & MUZZIO, F. J. 2015. Evaluation of resonant acoustic mixing performance. *Powder Technology,* 278**,** 46-56.

OUABBAS, Y., DODDS, J., GALET, L., CHAMAYOU, A. & BARON, M. 2009. Particle–particle coating in a cyclomix impact mixer. *Powder Technology,* 189**,** 245-252.

PATWA, A. & SHAH, A. 2015. Anatomy and physiology of respiratory system relevant to anaesthesia. *Indian Journal of Anaesthesia,* 59.

PAUL, J., ROMEIS, S., TOMAS, J. & PEUKERT, W. 2014. A review of models for single particle compression and their application to silica microspheres. *Advanced Powder Technology,* 25**,** 136-153.

PENG, T., LIN, S., NIU, B., WANG, X., HUANG, Y., ZHANG, X., LI, G., PAN, X. & WU, C. 2016. Influence of physical properties of carrier on the performance of dry powder inhalers. *Acta Pharmaceutica Sinica B,* 6**,** 308-318.

PFEFFER, R., DAVE, R. N., WEI, D. & RAMLAKHAN, M. 2001. Synthesis of engineered particulates with tailored properties using dry particle coating. *Powder Technology,* 117**,** 40-67.

PILCER, G., WAUTHOZ, N. & AMIGHI, K. 2012. Lactose characteristics and the generation of the aerosol. *Adv Drug Deliv Rev,* 64**,** 233-56.

PINSON, D., ZOU, R. P., YU, A. B., ZULLI, P. & MCCARTHY, M. J. 1998. Coordination number of binary mixtures of spheres. *Journal of Physics D: Applied Physics,* 31**,** 457.

PRICE, R., SHUR, J., GANLEY, W., FARIAS, G., FOTAKI, N., CONTI, D. S., DELVADIA, R., ABSAR, M., SALUJA, B. & LEE, S. 2020. Development of an Aerosol Dose Collection Apparatus for In Vitro Dissolution Measurements of Orally Inhaled Drug Products. *Aaps j,* 22**,** 47.

PRICE R, S. J., WOODCOCK D, YOUNG PM. 2004. *Delivery device for a dry powder aerosol*.

PRIYADARSHI, A., KHAVARI, M., SUBROTO, T., PRENTICE, P., PERICLEOUS, K., ESKIN, D., DURODOLA, J. & TZANAKIS, I. 2021. Mechanisms of ultrasonic de-agglomeration of oxides through in-situ high-speed observations and acoustic measurements. *Ultrasonics Sonochemistry,* 79**,** 105792.

PULIVENDALA, G., BALE, S. & GODUGU, C. 2020. Inhalation of sustained release microparticles for the targeted treatment of respiratory diseases. *Drug Deliv Transl Res,* 10**,** 339-353.

PURI, V., SHUR, J. & NARANG, A. S. 2019. Elucidating Molecular- and Particle-Level Changes during the Annealing of a Micronized Crystalline Drug. *Molecular Pharmaceutics,* 16**,** 4339-4351.

QUALICAPS. CAPSULE-BASED DRY POWDER INHALERS, AN OPTIMAL SOLUTION FOR DIFFERENT INSPIRATIONAL RATES. 2016.

QUINLAN, L., MORTON, D. & ZHOU, Q. 2015. Particle Engineering Via Mechanical Dry Coating in the Design of Pharmaceutical Solid Dosage Forms. *Current pharmaceutical design,* 21.

RIERA, E., GONZÁLEZ-GOMEZ, I., RODRÍGUEZ, G. & GALLEGO-JUÁREZ, J. A. 2015. Ultrasonic agglomeration and preconditioning of aerosol particles for environmental and other applications. *In:* GALLEGO-JUÁREZ, J. A. & GRAFF, K. F. (eds.) *Power Ultrasonics.* Oxford: Woodhead Publishing.

ROJAS, J. R., CRUCHAGA, M. A., CELENTANO, D. J., GANAOUI, M. E. & PATEYRON, B. 2010. Numerical Forecast of the Melting and Thermal Histories of Particles Injected in a Plasma Jet. *Eprint Arxiv*.

RUDAWSKA, A. & JACNIACKA, E. 2018. Evaluating uncertainty of surface free energy measurement by the van Oss-Chaudhury-Good method. *International Journal of Adhesion and Adhesives,* 82**,** 139-145.

RUDÉN, J., VAJDI, A., FRENNING, G., BRAMER, T., THALBERG, K. & ALDERBORN, G. 2019. *Comparison Between High-and Low-shear Mixers in the Formation of Adhesive Mixtures for Dry Powder Inhalers*.

RUSSO, P., BUTTINI, F., SONVICO, F., BETTINI, R., MASSIMO, G., SACCHETTI, C., COLOMBO, P. & SANTI, P. 2004. Chimeral agglomerates of microparticles for the administration of caffeine nasal powders. *Journal of Drug Delivery Science and Technology,* 14**,** 449-454.

SAHNI, E., YAU, R. & CHAUDHURI, B. 2011. Understanding granular mixing to enhance coating performance in a pan coater: Experiments and simulations. *Powder Technology,* 205**,** 231-241.

SANKHLA, A. M., PATEL, K. M., MAKHESANA, M. A., GIASIN, K., PIMENOV, D. Y., WOJCIECHOWSKI, S. & KHANNA, N. 2022. Effect of mixing method and particle size on hardness and compressive strength of aluminium based metal matrix composite prepared through powder metallurgy route. *Journal of Materials Research and Technology,* 18**,** 282-292.

SARANGI, S., THALBERG, K. & FRENNING, G. 2021. Effect of carrier size and mechanical properties on adhesive unit stability for inhalation: A numerical study. *Powder Technology,* 390**,** 230-239.

SEBTI, T., VANDERBIST, F. & AMIGHI, K. 2007. Evaluation of the content homogeneity and dispersion properties of fluticasone DPI compositions. *Journal of Drug Delivery Science and Technology,* 17**,** 223-229.

SEIPHOORI, A., MA, X. G., ARRATIA, P. E. & JEROLMACK, D. J. 2020. Formation of stable aggregates by fluid-assembled solid bridges. *Proc Natl Acad Sci U S A,* 117**,** 3375-3381.

SHAH, B., KAKUMANU, V. K. & BANSAL, A. K. 2006. Analytical techniques for quantification of amorphous/crystalline phases in pharmaceutical solids. *Journal of Pharmaceutical Sciences,* 95**,** 1641-1665.

SHAHIN, H. I. & CHABLANI, L. 2023. A comprehensive overview of dry powder inhalers for pulmonary drug delivery: Challenges, advances, optimization techniques, and applications. *Journal of Drug Delivery Science and Technology,* 84**,** 104553.

SHAWKY, M. 2016. *A Study on Synthesis and Characterization of Some (I -IV -VI) Groups Compounds for Solar Cells Energy Application.* Master Degree, Menoufiya University.

SHEKUNOV, B. Y., FEELEY, J. C., CHOW, A. H. L., TONG, H. H. Y. & YORK, P. 2003. Aerosolisation behaviour of micronised and supercritically-processed powders. *Journal of Aerosol Science,* 34**,** 553-568.

SHI, B., WANG, Y. & JIA, L. 2011. Comparison of Dorris-Gray and Schultz methods

for the calculation of surface dispersive free energy by inverse gas chromatography. *J Chromatogr A,* 1218**,** 860-2.

SHUR, J., PRICE, R., LEWIS, D., YOUNG, P. M., WOOLLAM, G., SINGH, D. & EDGE, S. 2016. From single excipients to dual excipient platforms in dry powder inhaler products. *International Journal of Pharmaceutics,* 514**,** 374-383.

SIMON, A., AMARO, M. I., CABRAL, L. M., HEALY, A. M. & DE SOUSA, V. P. 2016. Development of a novel dry powder inhalation formulation for the delivery of rivastigmine hydrogen tartrate. *International Journal of Pharmaceutics,* 501**,** 124-138.

SKLOOT, G. S. 2017. The Effects of Aging on Lung Structure and Function. *Clin Geriatr Med,* 33**,** 447-457.

SMITH, I. J. & PARRY-BILLINGS, M. 2003. The inhalers of the future? A review of dry powder devices on the market today. *Pulmonary Pharmacology & Therapeutics,* 16**,** 79-95.

SON YJ, M. D., WEERS JG 2021a. Optimizing Spray-Dried Porous Particles for High Dose Delivery with a Portable Dry Powder Inhaler. *Pharmaceutics*.

SON YJ, M. D., WEERS JG 2021b. Optimizing Spray-Dried Porous Particles for High Dose Delivery with a Portable Dry Powder Inhaler. *Pharmaceutics,* 9**,** 1528.

SONVICO, F., CHIERICI, V., VARACCA, G., QUARTA, E., D'ANGELO, D., FORBES, B. & BUTTINI, F. 2021. RespiCellTM: An Innovative Dissolution Apparatus for Inhaled Products. *Pharmaceutics,* 13**,** 1541.

STANKOVIC-BRANDL, M., ZELLNITZ, S., WIRNSBERGER, P., KOBLER, M. & PAUDEL, A. 2021. The Influence of Relative Humidity and Storage Conditions on the Physico-chemical Properties of Inhalation Grade Fine Lactose. *AAPS PharmSciTech,* 23**,** 1.

SYSTEMS, S. M. 2022. *Automated Dynamic Water Vapor Sorption Analyzer* [Online]. Surface Measurement Systems. Available: https://surfacemeasurementsystems.com/wp-content/uploads/2022/10/DVS-Adventure-brochure.pdf [Accessed 2024].

TAMADONDAR, M., DE MARTÍN, L. & RASMUSON, A. 2019. Agglomerate Breakage and Adhesion upon Impact with Complex-Shaped Particles. *AIChE Journal,* 65.

TANAKA, R., TAKAHASHI, N., NAKAMURA, Y., HATTORI, Y., ASHIZAWA, K. & OTSUKA, M. 2016. Verification of the mixing processes of the active pharmaceutical ingredient, excipient and lubricant in a pharmaceutical formulation using a resonant acoustic mixing technology. *RSC Advances,* 6**,** 87049-87057.

THAKRAL, N. K., ZANON, R. L., KELLY, R. C. & THAKRAL, S. 2018. Applications of Powder X-Ray Diffraction in Small Molecule Pharmaceuticals: Achievements and Aspirations. *J Pharm Sci,* 107**,** 2969-2982.

TIDKE., V. N., R.M., S. M. M. V. A. A. S. S. R. & TIGOTE 2021. A REVIEW ON MECHANICAL MICRONIZATION:A TOOL FOR INCREASING SOLUBILITY. *International Journal of Emerging Technologies and Innovative Research,* Vol.8**,** 278-291.

TOBYN, M., STANIFORTH, J. N., MORTON, D., HARMER, Q. & NEWTON, M. E. 2004. Active and intelligent inhaler device development. *Int J Pharm,* 277**,** 31-7.

TOMLINSON, H. S., CORLETT, S. A., ALLEN, M. B. & CHRYSTYN, H. 2005. Assessment of different methods of inhalation from salbutamol metered dose inhalers by urinary drug excretion and methacholine challenge. *British journal of clinical pharmacology,* 60**,** 605-610.

TONG, Z. B., ZHENG, B., YANG, R. Y., YU, A. B. & CHAN, H. K. 2013. CFD-DEM investigation of the dispersion mechanisms in commercial dry powder inhalers. *Powder Technology,* 240**,** 19-24.

TROFAST, E., FALK, J 1996a. *Agglomeration of finely divided powders* US-5551489-A.

TROFAST, E. A. C., FALK, ERIK J. 1996b. *Agglomeration of finely divided powders*. US5551489 (A).

TSUDA, A., HENRY, F. S. & BUTLER, J. P. 2013. Particle transport and deposition: basic physics of particle kinetics. *Comprehensive Physiology,* 3**,** 1437-1471.

TSUDA, A. & VENKATA, N. K. 2016. The role of natural processes and surface energy of inhaled engineered nanoparticles on aggregation and corona formation. *NanoImpact,* 2**,** 38-44.

VAN AALDEREN, W. M. C. & SPRIKKELMAN, A. B. 2011. Inhaled corticosteroids in childhood asthma: the story continues. *European Journal of Pediatrics,* 170**,** 709-718.

VAN WACHEM, B., THALBERG, K., NGUYEN, D., MARTIN DE JUAN, L., REMMELGAS, J. & NIKLASSON-BJORN, I. 2020. Analysis, modelling and simulation of the fragmentation of agglomerates. *Chemical Engineering Science,* 227**,** 115944.

VANARASE, A. U., OSORIO, J. G. & MUZZIO, F. J. 2013. Effects of powder flow properties and shear environment on the performance of continuous mixing of pharmaceutical powders. *Powder Technology,* 246**,** 63-72.

VANDENBERG, A. & WILLE, K. 2018. Evaluation of resonance acoustic mixing technology using ultra high performance concrete. *Construction and Building Materials,* 164**,** 716-730.

WARD, G. H. & SCHULTZ, R. K. 1995a. Process-Induced Crystallinity Changes in Albuterol Sulfate and Its Effect on Powder Physical Stability. *Pharmaceutical Research,* 12**,** 773-779.

WARD, G. H. & SCHULTZ, R. K. 1995b. Process-induced crystallinity changes in albuterol sulfate and its effect on powder physical stability. *Pharm Res,* 12**,** 773-9.

WEERS, J. G. & MILLER, D. P. 2015. Formulation Design of Dry Powders for Inhalation. *Journal of Pharmaceutical Sciences,* 104**,** 3259-3288.

WEGENER, T., HEDENSTRÖM, H. & MELANDER, B. 1992. Rapid onset of action of inhaled formoterol in asthmatic patients. *Chest,* 102**,** 535-8.

WEISS, C., MCLOUGHLIN, P., & CATHCART, H 2015. Characterisation of dry powder inhaler formulations using atomic force microscopy. *International journal of pharmaceutics*.

WETTERLIN, K. 1988. Turbuhaler: a new powder inhaler for administration of drugs to the airways. *Pharm Res,* 5**,** 506-8.

WILLIAMS, D. R. 2015. Particle engineering in pharmaceutical solids processing: surface energy considerations. *Curr Pharm Des,* 21**,** 2677-94.

WILLIAMS, R. L., ADAMS, W. P., POOCHIKIAN, G. & HAUCK, W. W. 2002. Content Uniformity and Dose Uniformity: Current Approaches, Statistical Analyses, and Presentation of an Alternative Approach, with Special Reference to Oral Inhalation and Nasal Drug Products. *Pharmaceutical Research,* 19**,** 359-366.

YAN, Y. 2008. *Rheological Properties of Non-Newtonian Fluids under Confinement.* PhD Thesis, University of Birmingham, UK.

YANG, M.-S., KANG, J.-H., KIM, D.-W. & PARK, C.-W. 2023. Recent developments in dry powder inhalation (DPI) formulations for lung-targeted drug delivery. *Journal of Pharmaceutical Investigation*.

YANG, Q., MA, Y. & ZHU, J. 2015. Applying a novel electrostatic dry powder coating technology to pellets. *European journal of pharmaceutics and biopharmaceutics,* 97**,** 118-124.

YANG, Q., YUAN, F., XU, L., YAN, Q., YANG, Y., WU, D., GUO, F. & YANG, G. 2019. An update of moisture barrier coating for drug delivery. *Pharmaceutics,* 11**,** 436.

YOU, Y., GUO, J., LV, X., WU, S., LI, Y., TANG, K. & YU, Y. 2021. Numerical Simulation of Particle Mixing Behavior in High Speed Shear Mixer and Cylinder Mixer. *ISIJ International,* 61**,** 2059-2065.

YOUNG, P. M., PRICE, R., TOBYN, M. J., BUTTRUM, M. & DEY, F. 2004. The influence of relative humidity on the cohesion properties of micronized drugs used in inhalation therapy. *J Pharm Sci,* 93**,** 753-61.

ZENG, X., MARTIN, G. & MARRIOTT, C. 2000a. *Particulate Interactions in Dry Powder Formulation for Inhalation*.

ZENG, X. M., MARTIN, G. P., TEE, S.-K., GHOUSH, A. A. & MARRIOTT, C. 1999. Effects of particle size and adding sequence of fine lactose on the deposition of salbutamol sulphate from a dry powder formulation. *International Journal of Pharmaceutics,* 182**,** 133-144.

ZENG, X. M., PANDHAL, K. H. & MARTIN, G. P. 2000b. The influence of lactose carrier on the content homogeneity and dispersibility of beclomethasone dipropionate from dry powder aerosols. *Int J Pharm,* 197**,** 41-52.

ZHANG, H., TAN, X., ZHANG, Z., YANG, X., WANG, L., LI, M., SHI, D., LI, Y., LI, J., LI, Z. & LIAO, X. 2023. Targeted Antibiotics for Lower Respiratory Tract Infection with Corynebacterium striatum. *Infect Drug Resist,* 16**,** 2019-2028.

ZHANG, Q., KOU, S., CUI, Y., DONG, J., YE, Y., WANG, Y., LU, R., LI, X., NIE, Y., SHI, K., CHEN, F., HALL, P., CHEN, X., WANG, Z. & JIANG, X. 2024. Ternary Dry Powder Agglomerate Inhalation Formulation of Melatonin With Air Jet Mixing to Improve In Vitro And In Vivo Performance. *Journal of Pharmaceutical Sciences,* 113**,** 434-444.

ZHANG, X., CUI, Y., LIANG, R., WANG, G., YUE, X., ZHAO, Z., HUANG, Z., HUANG, Y.,

GENG, J., PAN, X. & WU, C. 2020. Novel approach for real-time monitoring of carrier-based DPIs delivery process via pulmonary route based on modular modified Sympatec HELOS. *Acta Pharmaceutica Sinica B,* 10**,** 1331-1346.

ZHANG, Z., HE, Y. & ZHANG, Z. 2022. Micromanipulation and Automatic Data Analysis to Determine the Mechanical Strength of Microparticles. *Micromachines (Basel),* 13.

ZHANG, Z., STENSON, J. D. & THOMAS, C. R. 2009. Chapter 2 Micromanipulation in Mechanical Characterisation of Single Particles. *In:* LI, J. (ed.) *Advances in Chemical Engineering.* Academic Press.

ZHENG, B. W. 2012. *COMPUTER SIMULATION OF POWDER DISPERSION IN COMMERCIAL PHARMACEUTICAL INHALERS.* MASTER DEGREE, UNSW.

ZHENG, Z., LEUNG, S. S. Y. & GUPTA, R. 2021. Flow and Particle Modelling of Dry Powder Inhalers: Methodologies, Recent Development and Emerging Applications. *Pharmaceutics,* 13**,** 189.

ZHOU, Q., ARMSTRONG, B., LARSON, I., STEWART, P. J. & MORTON, D. A. 2010a. Effect of host particle size on the modification of powder flow behaviours for lactose monohydrate following dry coating. *Dairy Science & Technology,* 90**,** 237-251.

ZHOU, Q., QUINLAN, L., LARSON, I., STEWART, P. & MORTON, D. 2010b. Improving aerosolization of drug powders by reducing powder intrinsic cohesion via a mechanical dry coating approach. *International journal of pharmaceutics,* 394**,** 50-9.

ZHOU, Q. T., QU, L., GENGENBACH, T., LARSON, I., STEWART, P. J. & MORTON, D. A. 2013a. Effect of surface coating with magnesium stearate via mechanical dry powder coating approach on the aerosol performance of micronized drug powders from dry powder inhalers. *AAPS PharmSciTech,* 14**,** 38-44.

ZHOU, Q. T., QU, L., LARSON, I., STEWART, P. J. & MORTON, D. A. 2010c. Improving aerosolization of drug powders by reducing powder intrinsic cohesion via a mechanical dry coating approach. *Int J Pharm,* 394**,** 50-9.

ZHOU, Q. T., QU, L., LARSON, I., STEWART, P. J. & MORTON, D. A. V. 2010d. Improving aerosolization of drug powders by reducing powder intrinsic cohesion via a mechanical dry coating approach. *International Journal of Pharmaceutics,* 394**,** 50-59.

ZHOU, Q. T., TONG, Z., TANG, P., CITTERIO, M., YANG, R. & CHAN, H.-K. 2013b. Effect of Device Design on the Aerosolization of a Carrier-Based Dry Powder Inhaler—a Case Study on Aerolizer® Foradile®. *The AAPS Journal,* 15**,** 511-522.